DEVELOPMENT OF NOVEL COMBINATION STRATEGIES FOR THE TREATMENT OF PANCREATIC CANCER

Abdulfattah Yahya M Alhazmi

A thesis presented in fulfilment of the requirements for the degree of Doctor of Philosophy

December 2020

Strathclyde Institute of Pharmacy and Biomedical Sciences

University of Strathclyde, Glasgow, UK

DECLARATION BY RESEARCHER

I hereby certify that this research is entirely my own work, except where specifically indicated, and has not been taken from the work of others save and to the extent that such work has been cited and acknowledged within the text of my work.

This thesis is the result of the author's original research. It has been composed by the author and has not been previously submitted for examination that has led to the award of a degree.

SIGNED: 

PRINT NAME: Abdulfattah Yahya M Alhazmi

DATE: **17 December 2020**

ABSTRACT

Pancreatic cancer represents the seventh leading cause of cancer mortality globally, and despite the advances in cancer therapy over the last two decades, its prognosis is still poor with the survival rate among patients with pancreatic cancer for five years being less than 5%. This can be attributed to late-stage diagnosis, tumour heterogeneity, early metastasis, high local recurrence risk and resistance to conventional chemotherapy.

The current single agent or combination-based therapy approaches for pancreatic cancer have either failed to improve the overall survival or offered a marginal improvement as well as increasing the accompanied adverse events. Therefore, this project investigated, for the first time, novel triple combinations treatment schedules utilising the gold standard current treatment of gemcitabine plus the repurposed tyrosine kinase inhibitors (sunitinib or pazopanib) plus external beam radiation in pancreatic cancer cell lines *in vitro* and *in vivo*. We hypothesised that these novel combination strategies would improve anti-tumour efficacy in pancreatic cancer models compared to single or double combination therapies.

Our novel combination strategies with lower doses of gemcitabine, sunitinib, and XBR, resulted in greater anticancer efficacy than either treatment alone. The concurrent administration of gemcitabine with sunitinib when administered after radiation (three-treatment schedule 2 combination), showed a synergistic effect and was found to be the most effective combination strategy in our models.

Furthermore, our three-treatment combination in an *in vivo* pancreatic cancer nude mouse xenograft model, was the only combination approach able to shrink the tumours while other treatment strategies only delayed the xenografted pancreatic cancer tumour growth. Of note, all mice in this treatment group were euthanised two days before the end of the experiment (day 18) because of 20% weight loss relative to the initial body weight.

Altogether, our findings in this project offer a promising approach for treating pancreatic ductal adenocarcinoma in the clinic. Furthermore, lowering doses of all three agents is warranted to decrease the unfavourable side effects while maintaining anti-tumour activity.

ACKNOWLEDGEMENTS

I would like to thank my supervisor, Dr Marie Boyd for her academic help and support throughout the project. I am very grateful for not only her advice and feedback but also for her continuous encouragement, enthusiasm and kindness throughout the four years of this project. I will never forget her support in the most difficult days I needed her in. She was always close, ready, and happy for providing unlimited help. This project would not be possible without her supervision and guidance. Many thanks to her and I will be in her debt forever!

I would also like to extend sincere thanks to my second supervisor Professor Alexander Mullen and my assessor Dr Alison Thomson for their helpful feedback and revising my academic reports and thesis.

I will not forget the great effort exerted by members of the Biological Procedures Unit (BPU) to operate the animal study (*in vivo*) at a professional level; without their help, the in vivo would not be possible. Thanks to all of them, namely, Lee Wheeler, Carol Whitehouse, Kevin O'Halloran, Peter Conte, Brian Leiper, and Linda Horan. I also thank Dr Annette Sorensen and Agata Strunzova for their great help in the animal study.

I would like also to thank all members in our research group, Dr Annette, Dr Mohammed, Dr Khalid, DR David, Dr Reem, and Dr Issraa for their help and guidance throughout the lab work of this project.

Special and sincere thanks to Dr Mohammed Alshammari for teaching me the laboratory basics; and to Domenica McBride for looking after my cells while I was away and for her kind good-bye-card she left on my desk when she left us.

I also would like to thank my friends outside of SIPBS, Abdulrahman Qaisi and Hassan Almassoudi, who never stopped supporting and encouraging me throughout the period of study.

I would also like to submit my sincere thanks to the government of Saudi Arabia represented by the Saudi Arabian Cultural Bureau in London and Umm Al-Qura University for the financial support and fully sponsorship of my PhD study.

Finally, and most importantly, massive thanks to my father and my mother for their unwavering support and affection throughout my whole life. Moreover, sincere and eternal thanks to my wife (Areej Alhazmi) and my children (Jood, Joory, and Ahmed) who without their love, support, encouragement, and patience this project would not be possible. Thanks to my brothers and sisters for believing in me and for always making me smile through the darkest days throughout this project. I owe so much to my whole family for continuous and unconditional support and encouragement throughout these years.

TABLE OF CONTENTS

DECLARATION BY RESEARCHER ..... **II**

ABSTRACT ..... **III**

ACKNOWLEDGEMENTS ..... **V**

Table of Contents ..... **VII**

LIST OF TABLES ..... **XIII**

LIST OF EQUATIONS ..... **XIV**

LIST OF FIGURES ..... **XV**

LIST OF ABBREVIATIONS ..... **XIX**

CHAPTER 1: INTRODUCTION **1**

1.1 Introduction to cancer **1**

1.1.1 Statistics of cancer 1

1.1.2 Biology of cancer 5

1.1.3 Hallmarks of cancer and enabling characteristics 6

1.2 Pancreatic cancer **7**

1.2.1 Anatomy and physiology of the pancreas 7

1.2.2 Types of pancreatic cancer 7

1.2.3 Epidemiology of pancreatic cancer 8

1.2.4 Pancreatic cancer pathogenesis 9

1.2.4.1 Somatic alterations 10

1.2.4.2 Germline alterations and mutations 12

1.2.5 Staging of pancreatic cancer 13

1.2.6 Risk factors of pancreatic cancer 16

1.2.6.1 Non-modifiable risk factors 16

1.2.6.2 Modifiable risk factors 20

1.2.7 Clinical presentation, signs, and symptoms of pancreatic cancer 22

1.3 Current treatment approaches for pancreatic cancer 23

1.3.1 Surgery 23

1.3.1.1 Role of laparoscopy 24

1.3.1.2 Surgical management 24

1.3.2 Radiotherapy.....27

1.3.2.1 Radiation induced DNA double strand breaks and repair mechanisms 30

1.3.3 Gemcitabine as a single agent 31

1.3.3.1 Side effects of gemcitabine 33

1.3.3.2 Gemcitabine resistance in pancreatic cancer 35

1.3.4 Gemcitabine in combination with radiotherapy 39

1.3.5 Gemcitabine in combination with conventional chemotherapy.....40

1.3.6 Gemcitabine in combination with molecular-targeted therapy.....43

1.4 Targeted molecular therapy of cancer 45

1.4.1 Monoclonal antibodies 45

1.4.2 Tyrosine kinase inhibitors.....46

1.4.2.1 Clinical indications of sunitinib and pazopanib.....48

1.4.2.2 Mechanism of action and molecular targets of sunitinib and pazopanib 49

1.4.2.3 Side effects of sunitinib and pazopanib 53

1.5 Repurposing of drugs..... 53

1.6 Research aims and objectives 57

CHAPTER 2: MATERIALS AND METHODS..... 59

2.1 Cell lines and culture conditions 59

2.2 Cell passaging, thawing, and freezing 60

2.3 Cell doubling time 61

2.4 Treatment of pancreatic cancer cell lines 62

2.4.1 Treatment of cells with a single therapy 62

2.4.2 Treatment of control cells 62

2.4.3 Treatment of cells with XBR 63

2.4.4 Treatment of cells with combination therapies 63

2.5 Cell viability assay 65

2.6 Clonogenic survival assay 67

2.7 Combination index analysis 69

2.8 Linear quadratic analysis 71

2.9 Dose enhancement factor (DEF) 73

2.10 Cell cycle analysis 74

2.11 Annexin V apoptosis detection assay 75

2.12 DNA damage γ-H_2AX detection analysis 80

2.13 *In vivo* experiment 82

2.13.1 Experimental Animals 82

2.13.2 Tumour Xenografts 82

2.13.3 Tumour Therapy 83

2.13.4 Tumour growth inhibition and delay 85

2.14 Statistical analysis 86

CHAPTER 3: Cytotoxicity evaluation of single chemotherapy on pancreatic cancer cells *in vitro* 88

3.1 Introduction 88

3.2 Aims 89

3.3 Results 90

3.3.1 Cell viability of PANC-1 and MIA PaCa-2 cells following 24-hour treatment with anti-cancer agents 90

3.3.1.1 Cell viability of PANC-1 and MIA PaCa-2 cells following 24-hour treatment with gemcitabine 90

3.3.1.2 Cell viability of PANC-1 and MIA PaCa-2 cells following 24-hour treatment with sunitinib 91

3.3.1.3 Cell viability of PANC-1 and MIA PaCa-2 cells following 24-hour treatment with pazopanib 92

3.3.2 Clonogenic survival assay of PANC-1 and MIA PaCa-2 cells following 24 treatment with anti-cancer agents 95

3.3.2.1 Clonogenic survival assay of PANC-1 and MIA PaCa-2 cells following 24-hour treatment with gemcitabine 95

3.3.2.2 Clonogenic survival assay of PANC-1 and MIA PaCa-2 cells following 24-hour treatment with sunitinib 96

3.3.2.3 Clonogenic survival assay of PANC-1 and MIA PaCa-2 cells following 24-hour treatment with pazopanib 97

3.3.3 PANC-1 and MIA PaCa-2 doubling time.....100

3.3.4 Cell viability of PANC-1 and MIA PaCa-2 cells following 48-hour treatment with anti-cancer agents 102

3.3.4.1 Cell viability of PANC-1 and MIA PaCa-2 cells following 48-hour treatment with gemcitabine 102

3.3.4.2 Cell viability of PANC-1 and MIA PaCa-2 cells following 48-hour treatment with sunitinib 103

3.3.4.3 Cell viability of PANC-1 and MIA PaCa-2 cells following 48-hour treatment with pazopanib 103

3.3.5 Clonogenic survival assay of PANC-1 and MIA PaCa-2 cells following 48 treatment with anti-cancer agents 107

3.3.5.1 Clonogenic survival assay of PANC-1 and MIA PaCa-2 cells following 48-hour treatment with gemcitabine 107

3.3.5.2 Clonogenic survival assay of PANC-1 and MIA PaCa-2 cells following 48-hour treatment with sunitinib 108

3.3.5.3 Clonogenic survival assay of PANC-1 and MIA PaCa-2 cells following 48-hour treatment with pazopanib 109

3.3.6 Generating combination schedules based on single-agent curves 112

3.4 Discussion 114

CHAPTER 4: Cytotoxicity evaluation of combination therapy on pancreatic cancer cells *in vitro*..... 120

4.1 Introduction 120

4.2 Aims 121

4.3 Results 121

4.3.1 Cytotoxicity and mechanistic studies of gemcitabine, TKI, or XBR as single treatment in pancreatic cancer cells *in vitro*.....122

4.3.1.1 Cytotoxicity assessment of gemcitabine, TKI, and XBR in pancreatic cancer cells by clonogenic assay 122

4.3.1.2 The effect of single cytotoxic agents on the induction and repair of DNA damage measured by γ-H_2AX in pancreatic cancer cells 129

4.3.1.3 Analysis of the cell cycle progression of pancreatic cancer cells following exposure to single cytotoxic agents 136

4.3.1.4 The effect of single cytotoxic agents on the induction of apoptosis measured by Annexin V assay in pancreatic cancer cells 146

4.3.2 Cytotoxicity and mechanistic studies of gemcitabine and TKI as two-drug combination treatment in pancreatic cancer cells *in vitro*.....153

4.3.2.1 Assessment of cytotoxic effects of gemcitabine in combination with TKI on PANC-1 and MIA PaCa-2 cells by clonogenic assay, combination index analysis, and DEF.....154

4.3.2.2 The effect of two-drug combination treatments on the induction and repair of DNA damage measured by γ-H_2AX in pancreatic cancer cells 171

4.3.2.3 Analysis of the cell cycle progression of pancreatic cancer cells following two-drug combination treatment 176

4.3.2.4 The effect of two-drug combination treatments on the induction of apoptosis measured by Annexin V assay in pancreatic cancer cells ..186

4.3.3 Cytotoxicity and mechanistic studies of gemcitabine, sunitinib, and XBR as three-treatment combination in pancreatic cancer cells *in vitro* 192

4.3.3.1 Assessment of cytotoxic effects of gemcitabine plus sunitinib in combination with XBR on PANC-1 and MIA PaCa-2 cells by clonogenic assay and combination index analysis 192

4.3.3.2 The effect of three-treatment combination on the induction and repair of DNA damage measured by γ-H_2AX in pancreatic cancer cells 198

4.3.3.3 Analysis of the cell cycle progression of pancreatic cancer cells following three-treatment combination.....205

4.3.3.4 The effect of three-treatment combination on the induction of apoptosis measured by Annexin V assay in pancreatic cancer cells ..215

4.4 Discussion 222

4.4.1 Gemcitabine.....224

4.4.2 Sunitinib 228

4.4.3 Pazopanib.....232

4.4.4 Gemcitabine plus sunitinib 233

4.4.5 Gemcitabine plus sunitinib plus XBR.....238

CHAPTER 5: In vivo efficacy of gemcitabine, sunitinib, or XBR as single treatment or in combination in nude mice xenografts comprised of PANC-1 pancreatic cancer cells 242

5.1 Introduction 242

5.2 Aims 243

5.3 Results 243

5.4 Discussion 254

CHAPTER 6: General discussion, conclusion, and future work..... 265

APPENDICES..... 269

Appendix A Using gemcitabine in cancer animal models. 269

REFERENCES 271

LIST OF TABLES

Table 1.1 TNM classification for the staging of pancreatic cancer. 15

Table 1.2 Case-control studies showing the risk of pancreatic cancer in patients with chronic pancreatitis. 20

Table 1.3 Growth factor expression in pancreatic cancer cell lines. 52

Table 3.1 IC_{50} of the tested anti-cancer drugs following 24 hours of exposure (in μM), determined by Alamar Blue® assay. 94

Table 3.2 IC_{50} of the tested anti-cancer drugs following 24 hours of exposure (in μM), determined by clonogenic assay. 99

Table 3.3 IC50 of the tested anti-cancer drugs following 48 hours of exposure (in μM), determined by Alamar Blue® assay. 106

Table 3.4 IC_{50} of the tested anti-cancer drugs following 48 hours of exposure (in μM), determined by clonogenic assay. 111

Table 3.5 Generated doses of drugs to be used in combination therapy on PANC-1 and MIA PaCa-2 cells in μM. 113

Table 5.1 Relative tumour growth amongst the treatment groups on the last day of the experiment (day 20). 248

Table 5.2 Time to two-fold increase in tumour volumes, tumour growth inhibition (%TGI), and the growth delay in PANC-1 xenografts after 20 days of treatment. 250

LIST OF EQUATIONS

Equation 2.1 61
Equation 2.2 67
Equation 2.3 68
Equation 2.4 69
Equation 2.5 70
Equation 2.6 70
Equation 2.7 70
Equation 2.8 71
Equation 2.9 72
Equation 2.10 73
Equation 2.11 74
Equation 2.12 85
Equation 2.13 86

LIST OF FIGURES

Figure 1.1 Five-year relative survival rates for all stages of cancer during the period between 2007 and 2013. 4

Figure 1.2 Anatomy of pancreas, sites of pancreatic cancer, and pancreaticoduodenectomy (Whipple) surgical procedure. Adapted from navigatepancreaticcancer.com (website). 26

Figure 1.3 Molecular targets and mechanism of anti-tumour effects of sunitinib and pazopanib. 51

Figure 1.4 Schematic representation of the steps involved in *de novo* drug discovery process vs. drug repurposing. 56

Figure 2.1 Flow diagram illustrates the treatment schedules of two-drug combination therapy of gemcitane and sunitinib used in the study. 64

Figure 2.2 Stages of apoptosis after detection with FITC-Annexin V assay (Original figure). 79

Figure 2.3 Doses of gemcitabine and sunitinib used in previous *in vivo* studies (mg/kg/week). 84

Figure 3.1 Effect of cytotoxic therapy on cell viability of PANC-1 and MIA PaCa-2 cell lines following to 24-hour treatment exposure. 93

Figure 3.2 Effect of cytotoxic therapy on survival fraction of PANC-1 and MIA PaCa-2 cell lines following to 24-hour treatment exposure. 98

Figure 3.3 Growth curve and doubling time for pancreatic cancer cell lines. 101

Figure 3.4 Effect of cytotoxic therapy on cell viability of PANC-1 and MIA PaCa-2 cell lines following to 48-hour treatment exposure. 105

Figure 3.5 Effect of cytotoxic therapy on survival fraction of PANC-1 and MIA PaCa-2 cell lines following to 48-hour treatment exposure. 110

Figure 4.1 Effect of cytotoxic treatment on survival fraction of PANC-1 and MIA PaCa-2 cell lines following to 48-hour treatment exposure. 126

Figure 4.2 Clonogenic survival of PANC-1 and MIA PaCa-2 cells exposed to XBR from 0-6 Gy fitted to the linear-quadratic model. 128

Figure 4.3 The effect of single cytotoxic agents on the induction and repair of DNA damage measured by γ-H2AX in PANC-1 cells. 132

Figure 4.4 The effect of single cytotoxic agents on the induction and repair of DNA damage measured by γ-H2AX in MIA PaCa-2 cells. 135

Figure 4.5 Effect of gemcitabine, sunitinib, or XBR as a single treatment on the cell cycle progression of PANC-1 cells. 140

Figure 4.6 Effect of gemcitabine, sunitinib, or XBR as a single treatment on the cell cycle progression of MIA PaCa-2 cells. 145

Figure 4.7 The effect of single cytotoxic agents on apoptosis induction of PANC-1 cells..... 149

Figure 4.8 The effect of single cytotoxic agents on apoptosis induction of MIA PaCa-2 cells..... 152

Figure 4.9 Effect of gemcitabine and sunitinib as single or combination chemotherapy on survival of PANC-1 and MIA PaCa-2 cell lines. 157

Figure 4.10 Combination index (CI) analysis of the combined effect of gemcitabine and sunitinib on clonogenic survival of PANC-1 and MIA PaCa-2 cells. 159

Figure 4.11 Sunitinib sensitises pancreatic cancer cells to gemcitabine. 162

Figure 4.12 Gemcitabine sensitises pancreatic cancer cells to sunitinib. 163

Figure 4.13 Effect of gemcitabine and pazopanib as single or combination chemotherapy on survival of PANC-1 and MIA PaCa-2 cell lines. 166

Figure 4.14 Combination index (CI) analysis of the combined effect of gemcitabine and pazopanib on clonogenic survival of PANC-1 and MIA PaCa-2 cells. 168

Figure 4.15 Pazopanib decreases the sensitivity of pancreatic cancer cells to gemcitabine..... 170

Figure 4.16 The effect of gemcitabine and sunitinib as two-drug combination treatments on the induction and repair of DNA damage measured by γ-H2AX in PANC-1 cells. 173

Figure 4.17 The effect of two-drug combination treatments on the induction and repair of DNA damage measured by γ-H2AX in MIA PaCa-2 cells. 175

Figure 4.18 Effect of gemcitabine and sunitinib as a double combination treatment on the cell cycle progression of PANC-1 cells. 180

Figure 4.19 Effect of cytotoxic agents as double combination treatment on cell cycle progression of MIA PaCa-2 cells. 185

Figure 4.20 The effect of two-drug combination treatments on apoptosis induction of PANC-1 cells..... 188

Figure 4.21 The effect of two-drug combination treatments on apoptosis induction of MIA PaCa-2 cells. 191

Figure 4.22 Effect of gemcitabine plus sunitinib as two-drug concurrent combination alone or in combination with XBR on the survival of PANC-1 and MIA PaCa-2 cell lines. 195

Figure 4.23 Combination index (CI) analysis of the combined effect of gemcitabine plus sunitinib as a single drug with XBR on clonogenic survival of PANC-1 and MIA PaCa-2 cells..... 197

Figure 4.24 The effect of three-treatment combination on the induction and repair of DNA damage measured by γ-H2AX in PANC-1 cells. 201

Figure 4.25 The effect of three-treatment combination on the induction and repair of DNA damage measured by γ-H2AX in MIA PaCa-2 cells. 204

Figure 4.26 Effect of cytotoxic agents as three-treatment combination on cell cycle progression of PANC-1 cells. 209

Figure 4.27 Effect of cytotoxic agents as three-treatment combination on cell cycle progression of MIA PaCa-2 cells. 214

Figure 4.28 The effect of three-treatment combination on apoptosis induction of PANC-1 cells..... 218

Figure 4.29 The effect of three-treatment combination on apoptosis induction of MIA PaCa-2 cells. 221

Figure 5.1 Effect of gemcitabine, sunitinib, or XBR alone or in combination on the growth of PANC-1 xenografts (A). 246

Figure 5.2 The average of the area under the tumour volume curves of each mouse over the experimental time amongst the six treatment groups..... 253

LIST OF ABBREVIATIONS

3D-CRT	3D conformal radiotherapy
5-FU	5-fluorouracil
ANOVA	Analysis of variance
ATCC	American Type Culture Collection
BCR-ABL	Breakpoint cluster region-Abelson oncogene
BMI	Body mass index
BRCA1	Breast cancer tumour suppressor gene
BRCA2	Germline breast cancer gene 2
CA	California, United States
c-FMS	Transmembrane glycoprotein receptor tyrosine kinase
CI	Confidence interval
CP	Chronic pancreatitis
CRUK	Cancer Research UK
CSC	Cancer stem cell
CSF	Colony-stimulating factor
DEF	Dose enhancement factor
DM	Diabetes mellitus
DMEM	Dulbecco’s modified eagle’s medium
DMSO	Dimethyl sulfoxide
DNA	Deoxyribonucleic acid
EDTA	Ethylenediamine triacetic acid
EGFR	Endothelial growth factor receptor
EGTA	Ethylene glycol tetraacetic acid

EMA	The European Medicines Agency
EMDR	Environment-mediated drug resistance
EU	European Union
FACS	Fluorescence-activated cell sorting
FAMMM	Familial atypical multiple mole melanoma syndrome
FBS	Foetal bovine serum
FCS	Foetal calf serum
FDA	The American Food and Drug Administration
FGFR	Fibroblast growth factor receptor
FITC	Fluorescein isothiocyanate
FLT3	FMS-related tyrosine Kinase-3
FNA	Fine needle aspiration
GDNF	Glial cell-line derived neurotrophic factor receptor
Gem	Gemcitabine
Gy	Gray (radiation unit)
H_2AX	Histone family member X
hCNT	Human concentrative nucleoside transporters
hENT	Human equilibrative nucleoside transporters
HER	Human Epidermal Growth Factor Receptor
HR	Hazards ratio
HR	Homologous recombination
HS	Hillslope of the response curve
IARC	International Agency for Research on Cancer
IMRT	Intensity-modulated radiotherapy

IR	Ionising radiation
KIT	Stem cell factor receptor
LCK	Interleukin (IL)-2 receptor inducible T-cell kinase
LDH	Lactate dehydrogenase
MAPK	Mitogen-activated protein kinase
MEK	Mitogen-activated extracellular signal-regulated kinase
MIA PaCa-2	Pancreatic ductal adenocarcinoma cell line
MPACT	Metastatic pancreatic ductal adenocarcinoma clinical trial
mRNA	Messenger ribonucleic acid
NA	Not achieved
NADH	Nicotinamide adenine dinucleotide plus hydrogen
NADPH	Nicotinamide adenine dinucleotide phosphate hydrogen
NF-kB	Nuclear factor-kappa B
NHEJ	Non-homologous end joining
NICE	The National Institute for Health and Care Excellence
nM	nanomolar
NSCLC	Non-small cell lung cancer
OR	Odds ratio
OS	Overall survival
P	*p*-value
PALB2	Partner and localizer of BRCA2
PANC-1	Pancreatic adenocarcinoma cell line
Paz	Pazopanib
PBS	Phosphate buffered saline

PC	Pancreatic cancer
PDGF	Platelet-derived growth factor
PDGFR	Platelet-derived growth factor receptor
PEFG	Cisplatin, epirubicin, 5-FU and gemcitabine regimen
PFS	progression-free survival
PI	Propidium iodide
PI3K	Phosphoinositide 3-kinase
PMSF	Phenylmethanesulfonylfluoride
PS	Phospholipid phosphatidylserine
QALY	Quality-adjusted life-year
RET	Rearranged during transfection proto-oncogene
ROS	Reactive oxygen species
RPM	Revolutions per minute
RR	Relative risk
Sch. 1	Schedule 1 of combination; gemcitabine is applied first
Sch. 2	Schedule 2 of combination; gemcitabine is applied last
Sch. 3	Schedule 3 of combination; concurrent therapy
SEM	Standard error of the mean
SF	Survival fraction
SMC	The Scottish Medicines Consortium
Sun	Sunitinib
TKI	Tyrosine kinase inhibitor
TNM	Tumour node metastasis (Cancer staging system)
TP53	Tumour suppressor gene

UK	United Kingdom
USA	United States of America
VEGFR	Vascular endothelial growth factor receptor
vs.	Versus
WHO	World Health Organisation
WT	Wild-type
XBR	External beam radiation
µM	Micromolar

CHAPTER 1: INTRODUCTION

1.1 Introduction to cancer

1.1.1 Statistics of cancer

Cancer is considered one of the major health issues in the world and among the leading causes of morbidity and mortality in the United Kingdom (UK) and worldwide (Siegel, Miller and Jemal, 2016). It is recognised as the cause of one in four of all deaths within the UK (Cancer Research UK, no date d), and the estimated lifetime risk of cancer is 50% for males, and 45% for females born after 1960 in the UK (Cancer Research UK, no date c). According to the most recent global cancer statistics 2018 (Globocan website), there was an estimation of 18.1 million new cancer cases, and 9.6 million cancer deaths in 2018 (Bray *et al.*, 2018). The World Health Organisation (WHO) estimated a 70% increase in new cases of cancer over the next two decades (World Health Organisation, 2016). Furthermore, the annual cancer cases and mortality are expected to increase to 22 million new cases and 11.2 million cancer-related deaths by 2025 (World Health Organization, 2014). The increasing cancer burden can be attributed to several factors, including population growth, ageing, and the changing prevalence of certain causes of cancer linked to social and economic development (Bray *et al.*, 2018). Even though cancer therapy has been the focus of considerable research effort in recent years, the death rate caused by cancer is projected to continue increasing to reach above

13 million deaths in 2030 (Ferlay *et al.*, 2010) due to limited access to timely diagnosis and treatment in several countries (Bray *et al.*, 2018).

In the UK, approximately 363,000 people were diagnosed with cancer (185,000 males and 178,000 females) in 2016, which equates to approximately 990 new cases per day and a new case every two minutes (Cancer Research UK, no date b). Furthermore, the incidence rates for cancer in the UK increased by 25% between 1979–1981 and 2007–2009, with only 50% of people diagnosed with cancer surviving for more than 10 years. In 2016, there were around 164,000 deaths from cancer in the UK, demonstrating the urgency for significant improvements in cancer therapy to reduce the number of deaths (Cancer Research UK, no date b).

Different types of cancers respond variably to the available cancer therapies that have been developed over the last decade. For example, mortality rates for breast cancer decreased by 22% in the UK between 2006 and 2016 (Cancer Research UK, no date a), whereas the mortality rates of pancreatic cancer increased by 6% over the same period of time (Cancer Research UK, no date d). Moreover, the mortality from pancreatic cancer in the Europe Union (EU) is predicted to increase by 25% in 2025, to be the third leading cause of death from cancer after lung and colorectal cancers (Ferlay, Partensky and Bray, 2016). Finally, it was reported that the 5-year relative survival rates for all stages cancers during the period between 2007 and 2013 was highest for prostate cancer (99%), melanoma of the skin (92%), and female breast cancer

(90%) and lowest for cancers of the pancreas (8%), lung (18%), and liver (18%) (Siegel, Miller and Jemal, 2018) (Figure 1.1).

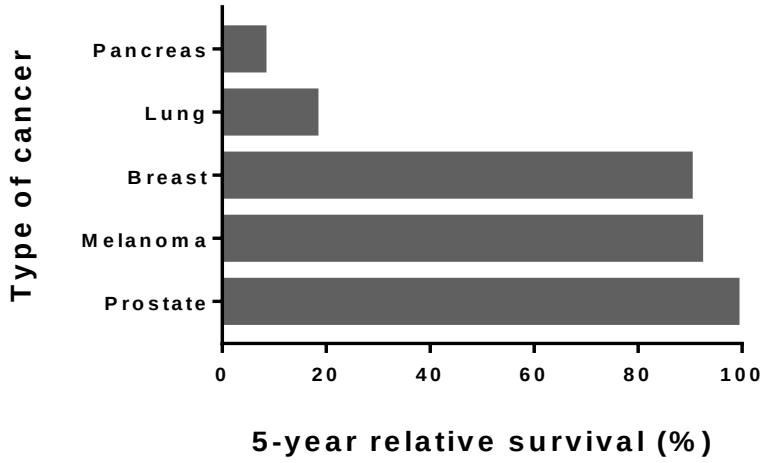

Figure 1.1 Five-year relative survival rates for all stages of cancer during the period between 2007 and 2013. Adapted from Siegel *et al.* (Siegel, Miller and Jemal, 2018)**.**

1.1.2 Biology of cancer

Cancer is a genetic disease that is characterised by abnormal patterns of gene expression which occur as a consequence of corruption or mutations in the cellular DNA of cells (Harrington, 2016). Two main classes of genes are responsible for the genesis of cancer; oncogenes and tumour suppressor genes (Vogelstein and Kinzler, 2004). Both gene classes have an essential function in growth, survival, and death of normal cells (Harrington, 2016). Mutations within these genes can cause activation of oncogenes or suppression of tumour suppressor genes an accumulation of which will result in uncontrolled cell proliferation (Vogelstein and Kinzler, 2004).

Oncogenes, which cause uncontrolled cell division and spread, are the mutated versions of the normal cellular genes (proto-oncogenes) that control cell proliferation and survival. They are activated in numerous pathways to cause cancers; three of them are the most common. One route to tumourigenesis is the via mutation of proto-oncogenes which leads to enhanced activity or altered biological function (Pellegata *et al.*, 1994). The second pathway is through gene amplification (an increase in the number of normal genes) leading to an increased amount of normal protein. The N-MYC oncogene in neuroblastoma is a good example of this activation pathway (Seeger *et al.*, 1985). The third activation pathway is through translocation of part of the DNA sequence from its normal chromosomal position (locus) to a new position (usually on a different chromosome) resulting in a generation of a novel fusion protein with enhanced biological activity; one example is the

BCR-ABL genes in chronic myeloid leukaemia (Harrington, 2016). Accumulation of one or more of these mutations over a long time may eventually lead to cancer.

Tumour suppressor genes are normal cellular genes that act to inhibit cell proliferation and survival and they are involved in controlling cell cycle progression and programmed cell death (apoptosis). The function of these genes is to arrest the progression of the cell cycle in order to carry out DNA repair, preventing mutations from being passed on to daughter cells (Harrington, 2016). CDKN2A and TP53 are the most frequently altered tumour suppressor gene in pancreatic cancer (Foo and Wang, 2017).

1.1.3 Hallmarks of cancer and enabling characteristics

In 2000, Hanahan and Weinberg (Hanahan and Weinberg, 2000) described six fundamental hallmarks of cancers that can largely explain their malignant behaviour. They are, briefly: maintaining replicative potential, avoiding programmed cell death, evading growth suppressors, growth factor independence or self-sufficiency, angiogenesis, and metastasis. These hallmarks were updated in 2011 through the addition of two emerging hallmarks (reprogramming energy metabolism, and evading immune destruction) and two enabling characteristics (genomic instability, and inflammation) (Hanahan and Weinberg, 2011).

1.2 Pancreatic cancer

1.2.1 Anatomy and physiology of the pancreas

The pancreas is a flat, pear-shaped gland located behind and below the stomach. It is about 6 inches long in an adult and less than two inches wide (Slack, 1995). The pancreas has two main types of cells, exocrine and endocrine cells. Most of the cells in the pancreas are exocrine cells and form the exocrine glands and ducts. Exocrine cells produce and release pancreatic enzymes that are released into the intestine to help the digestion of fat, carbohydrates, and protein in foods (Slack, 1995). Endocrine cells represent a small percentage of the cells in the pancreas and they are arranged in clusters called the islets of Langerhans. The main role of these cells is releasing insulin and glucagon hormones into the bloodstream to control blood sugar levels (Jennings *et al.*, 2015).

1.2.2 Types of pancreatic cancer

The exocrine cells and endocrine cells of the pancreas form different types of pancreatic tumours. Exocrine and endocrine cancers are completely different from each other in terms of risk factors, signs and symptoms, diagnostic tests, prognosis, and treatment approaches (American Cancer Society, no date). Ductal adenocarcinoma is the most common cancerous tumour of the pancreas as it accounts for 95% of all pancreatic cancers (Canadian Cancer Society, no date). Other and less common exocrine cancers include acinar cell carcinomas, squamous cell carcinomas, adenosquamous carcinomas, signet

ring cell carcinomas, pleomorphic adenocarcinomas (also called giant cell or sarcomatoid carcinoma), microadenocarcinomas, pancreatoblastomas, and oncocytic carcinomas (American Cancer Society, no date; Canadian Cancer Society, no date). Tumours of the endocrine pancreas (called neuroendocrine tumours) are uncommon and represent less than 5% of all pancreatic cancers (Jennings *et al.*, 2015). Subtypes of neuroendocrine tumours are usually named for the type of hormones the tumour cells make, such as gastrinomas, insulinomas, glucagonomas, and somatostatinomas (Jennings *et al.*, 2015).

1.2.3 Epidemiology of pancreatic cancer

Pancreatic ductal adenocarcinoma (hereafter referred to as pancreatic cancer), although relatively uncommon, represents the seventh leading cause of cancer mortality globally, as it is responsible for about 432,000 deaths per year (Bray *et al.*, 2018). In 2018, there were around 459,000 new cases of pancreatic cancer worldwide (Bray *et al.*, 2018). The incidence of pancreatic cancer appears to be rising in western countries over the past 35 years (Sakorafas, Tsiotou and Tsiotos, 2000). The highest incidence of pancreatic cancer was reported in Northern Europe and North America and was 3 to 4 times higher than rates seen in tropical countries (M. P. Curado *et al.*, 2007; Bray *et al.*, 2018). Based on data obtained from the surveillance epidemiology and end results (SEER) database, the incidence rate of PC is 12.4 and 10.9 per 100,000 men and women per year, respectively (Yellu, Kamireddy and Olowokure, 2018). In the UK, incidence rates of pancreatic cancer have increased by 16% over the last ten years, with a slightly larger increase in

females (18%) than in males (11%) (Cancer Research UK, no date d). In addition, pancreatic cancer was the tenth most common cancer in the UK (Keane *et al.*, 2014), accounting for 3% of all new cancer cases, hence about 10,000 people were diagnosed with pancreatic cancer in 2016 (50% males, and 50% females), which equates to approximately 27 cases diagnosed every day (Cancer Research UK, no date d). The crude incidence rate reveals that there are 18.8 new pancreatic cancer cases for every 100,000 males in the UK, and 16.5 for every 100,000 females. Almost half (47%) of cases were diagnosed in people aged 75 and above. The survival rate for ten years or more for those patients with pancreatic cancer was less than 1% in England and Wales between 2010 and 2011 (Cancer Research UK, no date d) and for five years is less than 5% (Keane *et al.*, 2014). In 2016, there were 9,263 deaths from pancreatic cancer in the UK (Cancer Research UK, no date d).

1.2.4 Pancreatic cancer pathogenesis

The molecular pathogenesis of pancreatic cancer has been extensively investigated in the last few decades (Mimeault *et al.*, 2005). Pancreatic cancer is fundamentally initiated and progressed by the accumulation of mutations in oncogenes (activation) and tumour suppressor genes (inactivation) (Mimeault *et al.*, 2005; Sarkar, Banerjee and Li, 2007; Foo and Wang, 2017). These mutations can be acquired (somatic mutations), or inherited (germline mutations) (Foo and Wang, 2017). Pancreatic cancer caused by somatic mutations or germline mutations is called sporadic or familial pancreatic cancer, respectively.

1.2.4.1 Somatic alterations

Whole exome sequencing has revealed that the genetic landscape of pancreatic cancer is dominated by approximately 48 somatic alterations in the genes KRAS, CDKN2A, TP53 and SMAD4 (also known as DPC4) (Jones *et al.*, 2008; Biankin *et al.*, 2012; Waddell *et al.*, 2015; Witkiewicz *et al.*, 2015).

KRAS is the most frequently altered oncogene in pancreatic cancer and is activated in approximately 95% of pancreatic tumours (Makohon-Moore and Iacobuzio-Donahue, 2016; Foo and Wang, 2017). RAS is located at chromosome 12p and encodes a member of the RAS family of guanosine triphosphate (GTP) binding protein that is vital to several cell signalling pathways, including the ERK, and AKT pathways. These pathways mediate many cellular functions, including proliferation, cell survival and cytoskeletal remodelling (Saiki and Horii, 2014; Makohon-Moore and Iacobuzio-Donahue, 2016; Foo and Wang, 2017). Point mutations in the KRAS oncogene lead to the generation of a constitutively active form of RAS. The constitutively activated RAS binds to GTP and sends uncontrolled growth stimulation signals to downstream signalling cascades, promoting uncontrolled cell growth (Sarkar, Banerjee and Li, 2007). Furthermore, KRAS amplification occurs together with the oncogenic mutation in approximately 4% of pancreatic cancers (Waddell *et al.*, 2015). BRAF, the signalling mediator immediately downstream of KRAS, is also mutated or amplified in a mutually exclusive manner from KRAS in 3–4% of cases (Makohon-Moore and Iacobuzio-Donahue, 2016).

CDKN2A is the most frequently altered tumour suppressor gene in pancreatic cancer (Foo and Wang, 2017). Inactivation of CDKN2A is detected in 95 % of pancreatic cancers (Jones *et al.*, 2008) and is thought to promote unrestricted cell proliferation (Foo and Wang, 2017). This gene, which is located on chromosome 9p, encodes two tumour suppressor proteins, $p16^{INK4A}$ and $p19^{ARF}$, which are involved in cell cycle regulation (Makohon-Moore and Iacobuzio-Donahue, 2016; Foo and Wang, 2017; Idachaba *et al.*, 2019) at the G1/S checkpoint by inhibiting the cyclin D/CDK4/6 complex, which in turn inhibits RB phosphorylation (Wood, Adsay and Hruban, 2013). In addition to DNA alteration, CDKN2A inactivation can be accomplished through several different mechanisms; such as epigenetic silencing via aberrant hypermethylation (Omura *et al.*, 2008), or homozygous deletion, inactivating mutation in one allele accompanied by loss of the other allele (Saiki and Horii, 2014).

TP53 is the second most frequently altered tumour suppressor gene and is inactivated in 75% to 85% of pancreatic cancer cases (Jones *et al.*, 2008; Makohon-Moore and Iacobuzio-Donahue, 2016). This gene is located on chromosome 17p, and it encodes the tumour suppressor protein P53, which plays an important role in cellular stress responses in damaged cells by activating DNA repair, inducing growth arrest, and triggering apoptosis (Saiki and Horii, 2014; Foo and Wang, 2017) through regulation of the G1/S checkpoint and maintenance of G2/M arrest (Vogelstein, Lane and Levine, 2000). Functional loss of the TP53 protein enables bypassing of cell cycle

checkpoints leading to enhanced cell survival and division in the presence of DNA damage (Saiki and Horii, 2014).

SMAD4 is a tumour suppressor gene on chromosome 18q (Hahn *et al.*, 1996; Foo and Wang, 2017) and is inactivated in approximately 55% of pancreatic cancers, either by homozygous deletion (30%) or by an intragenic mutation in association with loss of the second copy (25%) (Hahn *et al.*, 1996). The SMAD4 protein is a crucial co-transcription factor and mediator of the transforming growth factor-β (TGFβ) canonical signalling pathway for cellular growth, differentiation and maintenance of tissue homeostasis (Shi and Massagué, 2003; Makohon-Moore and Iacobuzio-Donahue, 2016). SMAD4 alterations are linked to poor prognosis and metastatic disease (Blackford *et al.*, 2009).

1.2.4.2 Germline alterations and mutations

Approximately 10% of pancreatic cancer cases have a familial basis (Shi, Hruban and Klein, 2009). Cohort and case-control studies have demonstrated that those with a family history of pancreatic cancer have a 1.9 to 13-fold increased risk of developing the disease (Ghadirian *et al.*, 1991; Schenk *et al.*, 2001; Jacobs *et al.*, 2010). The genetic basis for more than 80% of familial pancreatic cancer remains unknown (Hruban *et al.*, 2010). Several germline genetic syndromes have been linked to an increased risk of pancreatic cancer (Foo and Wang, 2017).

Germline breast cancer gene 2 (BRCA2) and Partner and localizer of BRCA2 (PALB2) (also called FANCN) mutations are associated with a significantly elevated lifetime risk for pancreatic cancer (Goggins *et al.*, 1996; Slater *et al.*, 2010; Lowery *et al.*, 2011). Besides, germline mutations in CDKN2A cause familial atypical multiple mole melanoma (FAMMM) syndrome, which results in a 38-fold increased risk of pancreatic cancer (De Snoo *et al.*, 2008). Moreover, germline mutations in cationic trypsinogen gene (PRSS1) and serine protease inhibitor, Kazal type 1 (SPINK1) have been linked to hereditary pancreatitis in young patients (Whitcomb *et al.*, 1996), which results in a 58-fold increased risk of pancreatic cancer (Lowenfels *et al.*, 1997). Furthermore, germline mutations in the ataxia-telangiectasia mutated gene (ATM), which encodes a protein involved in cell cycle regulation and the DNA damage response, have been detected in approximately 2 % of familial pancreatic cancer cases (Roberts *et al.*, 2012). Finally, Peutz-Jeghers syndrome (PJS) is associated with an increased risk of pancreatic cancer as a consequence of the development of gastrointestinal hamartomas and pigmented macules on the lips, and buccal mucosa (Foo and Wang, 2017). Germline mutations in Serine/threonine kinase 11 (STK11) (also known as liver kinase B1, LKB1) explain 80 % of PJS cases (Giardiello *et al.*, 1987).

1.2.5 Staging of pancreatic cancer

The stage of pancreatic cancer can be defined as the extent of the disease at the time of diagnosis. It is an important factor in determining treatment options and predicting a patient's prognosis. The American Joint Committee on Cancer

(AJCC) TNM system is the most common system used to stage cancers of the pancreas. The tumour (T) stage describes the size of the primary tumour; the node (N) stage describes the spread to nearby lymph nodes, and the metastasis (M) indicates whether cancer has metastasized to other organs of the body. Numbers or letters appear after T, N, and M to provide more details about each of these factors. Higher numbers mean the cancer is more advanced (Tamm *et al.*, 2003). A complete TNM classification of pancreatic cancer staging is shown in Table 1.1.

About 85% of pancreatic cancer cases are diagnosed as a non-resectable disease at the first diagnosis, either for having locally advanced (40%; 5 to 7 months OS) or metastatic disease (45%; 3 to 6 months OS) (Rivera *et al.*, 2009). The remaining 15% of cases have resectable tumours with 15 to 20 months median OS. However, there is a local or systemic recurrent disease in about 75% of the resected cases with a median OS of 3 to 5 months (Rivera *et al.*, 2009). The main reason for late diagnosis of pancreatic cancer could be the lack of specific cost-effective and reliable screening tests in people who have no symptoms of the disease (Sellam *et al.*, 2015).

Table 1.1 TNM classification for the staging of pancreatic cancer. Adapted from the American Cancer Society (American Cancer Society, no date).

Stage	Stage grouping	Stage description
0	Tis, N0, M0	The tumour is confined to the top layers of pancreatic duct cells and has not invaded deeper tissues. It has not spread outside of the pancreas. These tumours are sometimes referred to as pancreatic carcinoma in situ or pancreatic intraepithelial neoplasia III (PanIn III).
IA	T1, N0, M0	The tumour is confined to the pancreas and is 2 cm across or smaller (T1). The cancer has not spread to nearby lymph nodes (N0) or distant sites (M0).
IB	T2, N0, M0	The tumour is confined to the pancreas and is larger than 2 cm across (T2). The cancer has not spread to nearby lymph nodes (N0) or distant sites (M0).
IIA	T3, N0, M0	The tumour is growing outside the pancreas but not into major blood vessels or nerves (T3). The cancer has not spread to nearby lymph nodes (N0) or distant sites (M0).
IIB	T1-T3, N1, M0	The tumour is either confined to the pancreas or growing outside the pancreas but not into major blood vessels or nerves (T1-T3). The cancer has spread to nearby lymph nodes (N1) but not to distant sites (M0).
III	T4, Any N, M0	The tumour is growing outside the pancreas and into nearby major blood vessels or nerves (T4). The cancer may or may not have spread to nearby lymph nodes (Any N). It has not spread to distant sites (M0).
IV	Any T, Any N, M1	The cancer has spread to distant sites (M1).

1.2.6 Risk factors of pancreatic cancer

The risk factors for pancreatic cancer can be categorised into non-modifiable and modifiable risk factors (Lowenfels and Maisonneuve, 2002).

1.2.6.1 Non-modifiable risk factors

A. Age

Pancreatic cancer incidence is strongly related to age (Cancer Research UK, no date d). Pancreatic cancer is rare in the first decade of life and its incidence rates increase after age 30 and peaks in the seventh and eighth decade of life in both males and females (Midha, Chawla and Garg, 2016). Several studies acknowledged this strong association between the incidence of pancreatic cancer and age in the UK. For example, Keane and his colleagues conducted a study to examine the influence of socio-demographic and geographic factors on the incidence of pancreatic cancer utilising a large database of 562 UK general practices provided to The Health Improvement Network from 1st January 2000 and 31st December 2010 (Keane *et al.*, 2014). Among 3284 pancreatic cancer patients included in this study, it was reported that the adjusted incidence rate ratio of pancreatic cancer, after accounting for gender and time period, was 4.3 (95% CI 3.84 - 4.81; p <0.001) times higher in patients aged 70–79 and 5.88 (95%CI 5.24 - 6.61; p <0.001) times higher in those aged 80–89, compared to those aged 50–59. Moreover, around 47% of diagnosed

cases of pancreatic cancer between 2011 and 2013 were in patients aged 75 and over (Cancer Research UK, no date d).

B. Gender

Pancreatic cancer is approximately 30% more common in men than women. The overall age-adjusted incidence rate for pancreatic cancer is 10.9 per 100,000 for women and 13.9 per 100,000 for men (Midha, Chawla and Garg, 2016). The gender-specific hormonal risk factors for a causal role in susceptibility to pancreatic cancer have been evaluated in several studies (Fernandez *et al.*, 1995; Duell *et al.*, 2009; Wahi *et al.*, 2009). In a large systematic review of 371 articles to investigate the possible relationship between three reproductive factors and the risk of pancreatic cancer in women (Wahi *et al.*, 2009), authors concluded that reproductive factors are not associated with the development of pancreatic cancer in women. This suggests that the differences in pancreatic cancer rates between men and women may be attributed to environmental factors like smoking, or to undiscovered genetic factors influencing cancer incidence and mortality in males and females (Midha, Chawla and Garg, 2016).

C. Ethnicity

The race is a recognized risk factor for pancreatic cancer. In England, the incidence rate of pancreatic cancer in the period between 2002 and 2006 was significantly lower in Asian males, ranging from 4.6 to 8.6 per 100,000,

compared to rates in White males (10.2 to 10.7 per 100,000) and Black males (7.6 to 14.2 per 100,000). A similar pattern and incidence rates were reported for females. The Asian females had also a significantly lower incidence rate of pancreatic cancer (ranging from 2.9 to 5.9 per 100,000) than White (7.9 to 8.3 per 100,000) and Black (6.0 to 11.9 per 100,000) females (National Cancer Intelligence Network and Cancer Research UK, 2009). In the United States, African-Americans (Black people) have a significantly higher incidence rate of pancreatic cancer than Caucasians while the incidence is lowest in Asian Americans (Midha, Chawla and Garg, 2016). The higher incidence in African-Americans can be attributed to differences in modifiable risk factors such as diet, alcohol, smoking, and vitamin D insufficiency or race-specific genetic differences between these ethnic groups (Midha, Chawla and Garg, 2016).

D. Chronic pancreatitis

Chronic pancreatitis, which is a progressive inflammatory disease of the pancreas, is considered a major risk factor for pancreatic cancer (Raimondi *et al.*, 2010). Lowenfels and his colleagues in their historical review conducted in 1993, reported an increased risk of pancreatic cancer among patients with chronic pancreatitis with a standardized incidence ratio of 26.3 (Lowenfels *et al.*, 1993). Table 1.2 summarises several other case-control and cohort studies that interrogated the association between chronic pancreatitis and incidence of pancreatic cancers. These studies revealed that chronic pancreatitis is a risk factor for pancreatic cancer, though a few studies have reported either no association or much lower risk (Midha, Chawla and Garg, 2016).

E. Diabetes Mellitus

Diabetes Mellitus (DM) has been associated with an increased risk of pancreatic cancer (Midha, Chawla and Garg, 2016). In a population-based cohort study of 2122 patients aged 50 or above who developed pancreatic cancer within 3 years of meeting standardised criteria for DM, it was found that the risk of pancreatic cancer incidence is around eight-fold higher than the risk in a control population (OR 7.94, 95% CI 4.70-12.55) (Chari *et al.*, 2005). This risk increases significantly with longer duration of DM (Everhart, 1995). A meta-analysis of 17 case-control and 19 cohort or nested-case studies, including 9220 patients with pancreatic cancers (OR 1.82, 95% CI 1.66-1.89) (Huxley *et al.*, 2005) found that the risk of pancreatic cancer is significantly higher in patients with DM for 10 years while a recent large pooled case-control study including 8,305 cases and 13,987 controls (OR 1.30, 95% CI 1.03–1.63) (Bosetti *et al.*, 2014) identified an increased risk after 20 years or more. Recent studies suggested that insulin resistance, exposure to higher insulin concentrations and hyperglycaemia are also associated with increased risk of pancreatic cancer (Jee, 2005; Stocks *et al.*, 2009).

Table 1.2 Case-control studies showing the risk of pancreatic cancer in patients with chronic pancreatitis. Adapted from (Midha, Chawla and Garg, 2016). CP = Chronic Pancreatitis, RR=Relative Risk.

No	Author (Country)	Year	Cases (n)	Controls (n)	CP (cases)	CP (controls)	Comments
1	Fernandez *et al.* (Spain)	1995	362	1408	24	18	RR = 5.1(1.8–14.1)
2	Bansal *et al.* (USA)	1995	2639	7774	157	207	OR = 2.94 (2.19–3.94)
3	Moghaddam *et al.* (USA)	2007	808	808	60	6	OR: 10.9 (4.3–20.2
4	Gold *et al.* (USA)	1985	201	402	4	2	No significant association between PC and pancreatitis
5	Mack *et al.* (USA)	1986	490	490	5	2	RR = 5.0 (0.7–116.5)
6	Bueno De Mesquita *et al.* (Netherlands)	1992	176	487	1	4	No association RR = 0.86 (0.1–7.9)

1.2.6.2 Modifiable risk factors

A. Obesity

Obesity has been associated with pancreatic cancer (Midha, Chawla and Garg, 2016). A meta-analysis of 98 studies conducted in 18 countries to evaluate the association between obesity and 13 types of cancer including pancreatic cancer in men and women, reported increased pooled risk ratio in both obese men and women compared to those of normal weight [Men: RR 1.36; 95% CI 1.07 - 1.73, Women: RR 1.34; 95%CI 1.22 - 1.46] (Dobbins, Decorby and Choi, 2013). Similarly, another meta-analysis of 21 independent prospective studies involving 3,495,981 individuals and 8062 pancreatic cancer patients, demonstrated that the RR for cancer per 5 kg/m^2 increase in body mass index (BMI) was 1.16 (95%CI 1.06–1.17) in men and 1.10 (95% CI:

1.02–1.19) in women (Larsson, Orsini and Wolk, 2007). The association between obesity and increased risk of pancreatic cancer is not fully understood, but can be attributed to increased risk of diabetes, thrombosis, and other comorbid conditions associated with obesity (Li and Abbruzzese, 2010), or to yet undiscovered genetic factors (Feakins, 2016).

B. Smoking

Smoking is considered one of the most consistent and strongly associated risk factor associated with pancreatic cancer (Keane *et al.*, 2014) and it may be responsible for approximately 20% of pancreatic cancer cases (Iodice *et al.*, 2008). A meta-analysis of 82 studies conducted to assess the association between smoking and pancreatic cancer reported in published studies between 1950 and 2007, found the overall risk of pancreatic cancer for current smokers was 1.74 (95% CI 1.61–1.87) (Iodice *et al.*, 2008). It has been suggested that tobacco-specific nitrosamines (TSNAs) are possibly the responsible agents in tobacco that cause pancreatic cancer (Rivenson *et al.*, 1988; Preston-Martin, 1991).

C. Alcohol

Alcohol is a risk factor for pancreatic cancer because of its role in the aetiology of chronic pancreatitis and production of toxic metabolites, such as acetaldehyde, which are generated by ethanol metabolism (Midha, Chawla and Garg, 2016). A recent meta-analysis of 19 prospective studies, which

reported data from 4,211,129 individuals, concluded that low to moderate alcohol intake had little or no effect on the risk of pancreatic cancer, but high alcohol intake was associated with an increased risk of pancreatic cancer (RR 1.15; 95%CI: 1.06–1.25). The pooled analysis revealed that the risk was highest in patients with heavy liquor intake (RR, 1.43; 95% CI: 1.17–1.74) (Wang *et al.*, 2016).

1.2.7 Clinical presentation, signs, and symptoms of pancreatic cancer

The signs and symptoms of pancreatic cancer vary and depend on the location, size, and the stage of the tumour (Idachaba *et al.*, 2019). The tumours located at the head of the pancreas cause obstructive jaundice, caused by the biliary duct obstruction, and weight loss, which occurs as a result of steatorrhea and diarrhoea (Freelove and Walling, 2006). While tumours of the pancreas body and tail usually are accompanied by epigastric pain, vague abdominal symptoms also occur such as nausea, weight loss, and newly diagnosed diabetes (Kelsen *et al.*, 1997; Chari *et al.*, 2008; Dillhoff and Bloomston, 2018). The pain usually presents as a dull, deep pain, coming from the upper abdomen, radiating to the back, and may be exacerbated by eating or lying flat (Kelsen *et al.*, 1997; Freelove and Walling, 2006).

Obstruction of the bile duct causes jaundice with disproportionately increased levels of conjugated bilirubin and alkaline phosphatase in the blood. The urine is dark because of the high level of conjugated bilirubin and the absence of urobilinogen. The stool is pale because of the lack of stercobilinogen in the

bowel. As hepatic function becomes compromised, patients experience fatigue, anorexia, and bruising caused by loss of clotting factors. However, all early symptoms often are nonspecific and unrecognized; therefore, most pancreatic cancers are advanced at diagnosis (Freelove and Walling, 2006).

1.3 Current treatment approaches for pancreatic cancer

1.3.1 Surgery

Surgical resection is the cornerstone of therapy for long-term survival in patients with pancreatic cancer (Dillhoff and Bloomston, 2018). The 5-year survival rate has improved markedly to be between 10 and 15 per cent, compared to 5 per cent in the previous ten years, as reported in a retrospective study conducted on 113 patients who underwent surgical resection for pancreatic cancer between 1970 and 1992 (Sperti *et al.*, 1996). However, a minority of patients (less than 20%) have potentially resectable disease at the time of diagnosis (Sohn *et al.*, 2000; Dillhoff and Bloomston, 2018). The majority (>50%) of pancreatic cancers have metastasized at the onset of symptoms and at the time of diagnosis, or present with borderline resectable and unresectable locally advanced pancreatic cancer (30 to 40%) (Xia, Kim and Ahmad, 2018). The safest method of obtaining pathologic confirmation of malignancy before surgical resection is the fine needle aspiration (FNA) by endoscopic ultrasound (EUS) (Dillhoff and Bloomston, 2018).

For patients with painless jaundice or a newly diagnosed pancreas mass, cross-sectional imaging with intravenous contrast is mandatory for complete

staging and to stratify patients based on the primary tumour-vessel relationship to resectable, borderline resectable, unresectable, or metastatic disease (Dillhoff and Bloomston, 2018; Xia, Kim and Ahmad, 2018).

1.3.1.1 Role of laparoscopy

If the evaluation for the potential disease was not clear on cross-sectional imaging, laparoscopy has long been used as an alternative. It is useful for patients with findings on imaging that are suspicious for metastatic disease but not obviously metastatic and/or not amenable to confirmatory biopsy (Dillhoff and Bloomston, 2018). Laparoscopy is not widely used for determining local resectability because the evaluation of the mesenteric vasculature is not easily done with laparoscopy (Hennig *et al.*, 2002). For patients with metastatic disease discovered by laparoscopy, an unnecessary laparotomy is avoided, thus shortening hospital length of stay and allowing chemotherapy to be initiated sooner (Hashimoto *et al.*, 2015).

1.3.1.2 Surgical management

Nearly 70% of pancreatic cancers are located in the head of the pancreas with the remaining in the body and tail (Dillhoff and Bloomston, 2018). For tumours in the head of the pancreas, a pancreaticoduodenectomy (as known as Whipple procedure) is required. It has been the surgical procedure of choice for many years, and it was described by Whipple in his published paper in 1942 (Whipple, 1942). Advances in surgical technique have reduced the operative

mortality rate of patients undergoing pancreaticoduodenectomy to below 5 per cent in the 1990s (Yeo *et al.*, 1997).

Pylorus-preserving pancreaticoduodenectomy (PPPD) has been evaluated and compared to standard pancreaticoduodenectomy (Whipple procedure) in several randomized controlled trials (Tran *et al.*, 2004; Lin *et al.*, 2005; Seiler *et al.*, 2005). PPPD, which is a more conservative procedure, was introduced in an effort to prevent the long-term complications of dumping syndrome, bile reflux gastritis, and marginal ulcer which occur in Whipple procedure (Dillhoff and Bloomston, 2018). These trials have reported conflicting results, but most have not found statistically significant differences in overall and disease-free survival, overall morbidity and mortality, quality of life, blood loss, length of stay, operating time, resection margin status, or delayed gastric emptying between the two procedures (Tran *et al.*, 2004; Lin *et al.*, 2005; Seiler *et al.*, 2005).

On the other hand, pancreatectomy is a suitable choice for patients with tumours in the body and tail of the pancreas (Dillhoff and Bloomston, 2018). Splenectomy is also recommended for left-sided cancers (Dillhoff and Bloomston, 2018). Finally, it has been reported that lymph node status, which is involved in about 50 to 80% of cases, is an important predictor of survival in patients with pancreatic cancer; therefore, extended lymphadenectomy has been proposed in some practices (Dillhoff and Bloomston, 2018). However, several studies have revealed that extended lymphadenectomy was associated with higher complication rates without improvement in the quality

of life or overall survival (Yeo *et al.*, 2002; Riall *et al.*, 2005). Figure 1.2 illustrates anatomy of pancreas, sites of pancreatic cancer, and pancreaticoduodenectomy (Whipple) surgical procedure.

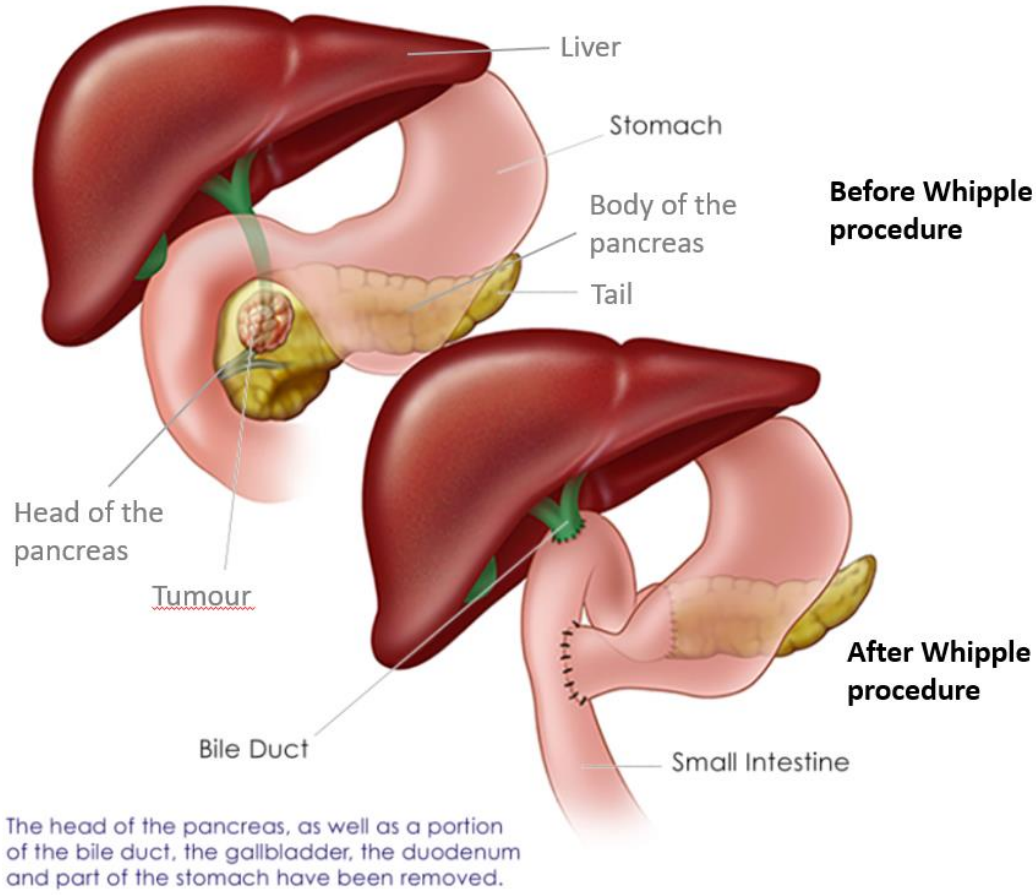

Figure 1.2 Anatomy of pancreas, sites of pancreatic cancer, and pancreaticoduodenectomy (Whipple) surgical procedure. Adapted from navigatepancreaticcancer.com (website).

1.3.2 Radiotherapy

Radiotherapy is an effective and widely used treatment modality for many tumours and about 50% of all cancer patients will receive radiation therapy during the illness as a part of their treatment either alone or in combination with surgery, immunotherapy, or chemotherapy (Delaney *et al.*, 2005; Ciric and Sersa, 2010). Radiotherapy is a highly cost-effective single modality treatment accounting about only 5% of the total cost of cancer care (Baskar *et al.*, 2012). Radiation can be delivered before surgery (neoadjuvant therapy) to shrink and downgrade the tumour with the goal of achieving a margin-free resection, or after surgery (adjuvant therapy), to destroy microscopic tumour cells that may have been left behind (Baskar *et al.*, 2012; Xia, Kim and Ahmad, 2018).

The most common approach of radiation therapy in the clinical setting is external beam radiation (XBR), in which high-energy rays delivered from outside the body to the location of the tumour (Baskar *et al.*, 2012). XBR is typically delivered in the form of X-ray photon beams using a linear accelerator (LINAC) which generates ionising radiation (IR). IR creates ions (electrically charged particles) and deposits energy in the cells of the tissues it passes through (Balagamwala *et al.*, 2013). The deposited high energy radiation causes DNA damage and, as is the goal of cancer therapy, cell death by either a direct interaction with cellular DNA, or indirectly by ionizing and exciting cellular water to form hydroxyl radical reactive oxygen species (ROS) which can interact with cellular DNA and intracellular macromolecular structures (Baskar *et al.*, 2012; Wang, Wang and Qian, 2018). DNA damage can be classified into double-strand breaks (DSBs) and single-strand breaks (SSBs).

DSBs are more toxic than SSBs in cancer as well as surrounding normal cells (Baskar *et al.*, 2012).

Conventional 2-dimensional (2D) radiation therapy, which uses rectangular fields based on 2D plain X-ray imaging, has several limitations. These limitations include delivering inadequate dosage to tumour cells, having inaccurate localization of tumour site, and lack of proper shielding to surrounding normal cells (Tribius and Bergelt, 2011). Due to these limitations, 2D XBR has largely been replaced by 3D conformal radiotherapy (3D-CRT) (Baskar *et al.*, 2012).

In 3D-CRT, each beam can be shaped around the target tumour site using a multi-leaf collimator (MLC). This allows radiation to conform to the exact tumour volume, and thus this approach permits substantially higher radiation doses to be delivered to the tumour (Bucci, Bevan and Roach III, 2005). However, this technique has not fully prevented radiation-induced cytotoxicity in the adjacent normal cells (Tribius and Bergelt, 2011).

Further advances to radiotherapy have been introduced by intensity-modulated radiotherapy (IMRT), which allows the oncologist to create irregular-shaped radiation doses that conform to the tumour whilst simultaneously avoiding critical organs (Veldeman *et al.*, 2008; Nakamura *et al.*, 2014). The intensity of the multiple beams can be modulated using advanced computer software (Baskar *et al.*, 2012). This allows the highest intensity radiation to be delivered to the gross tumour, with lower intensity radiation to the outer tumour edges, which limits the damage to surrounding

normal tissue and alleviates unequal dose deposition of radiation (Veldeman *et al.*, 2008; Baskar *et al.*, 2012).

When IMRT is delivered in 1–5 fractions and small beam apertures are utilized, this is considered stereotactic body radiation therapy (SBRT) (Rosati *et al.*, 2018). SBRT is a more modern technique that involves the delivery of higher doses of radiotherapy (≥5 Gy per fraction) within a shorter period of time (Franke *et al.*, 2015). Frequently, patients receiving SBRT are offered respiratory gating or taught the breath-holding technique to track or minimise tumour movement during treatment because the pancreas can move with respiration (Rosati *et al.*, 2018).

The evidence shows that compared to conventional chemoradiation, SBRT is effective in reducing tumour-related pain without affecting the quality of life (QoL) which enables SBRT to be integrated with systemic and targeted therapeutic interventions (Herman *et al.*, 2015; Rao *et al.*, 2016; Rosati *et al.*, 2018). SBRT is increasingly recognized as an important local treatment modality in pancreatic cancer, both in the neoadjuvant setting for resectable and borderline resectable disease (BRPC) and in the definitive setting for locally advanced disease (LAPC). Shorter courses of radiation therapy are thought to increase the biological equivalent dose (BED) that is delivered to the tumour, and have been proposed to decrease time away from systemic therapy and time to surgical resection (Rosati *et al.*, 2018). Finally, compared to pancreatic cancer patients who had lengthier courses of radiation therapy, the QoL outcomes of patients with shorter treatment courses were superior (Herman *et al.*, 2013).

Radiation therapy, although it has proven beneficial in most cancer therapy settings, carries several limitations and side effects. Unavoidable toxicity delivered to the surrounding normal cells, despite the significant advances in the precision of radiation therapy, remains an unresolved dilemma in radiotherapy (Löbrich and Kiefer, 2006). Furthermore, as a consequence of the damage to the normal cells and non-irradiated organs, short-term and delayed adverse effect and complications may occur, which can have long term detrimental effects on patients' quality of life (Al-Mefty *et al.*, 1990; Meershoek *et al.*, 2005). However, several studies have investigated toxicity associated with a different number of fractions (i.e., 3–5) of SBRT either alone or in combination with gemcitabine. It has been demonstrated that SBRT is well tolerated in terms of short- and long-term toxicity (Koong *et al.*, 2004; Schellenberg *et al.*, 2008, 2011; Pollom *et al.*, 2014). Finally, tumour resistance to radiotherapy remains a major problem in many cancerous tumours (Kim *et al.*, 2015).

1.3.2.1 Radiation induced DNA double strand breaks and repair mechanisms

Radiation damages DNA directly by deposition of energy and also indirectly by ionisation of water molecules, which generates hydroxyl radicals that interact with the DNA (Baskar *et al.*, 2012). In mammalian cells, the radiation-induced double-stranded DNA breaks are repaired mainly by non-homologous end joining (NHEJ) or homologous recombination (HR). The NHEJ is non-specific cell cycle

phase and considered as the main repair pathway for radiation-induced double strand DNA breaks (Lomax, Folkes and O'neill, 2013).

The NHEJ manages the repair of DSBs either induced by ionizing radiation or induced naturally which are initiated mainly, but not exclusively, in the G0 and G1 phases of the cell cycle (Bolderson *et al.*, 2009). Due to the lack of homologous DNA in the G0 and G1 phases of the cell cycle, NHEJ is a more error-prone form of repair due to its nature independent of DNA sequence symmetry (Bolderson *et al.*, 2009).

In contrast to NHEJ, HR DNA repair mechanism is active only in late S and G2/M phases of the cell cycle when homologous regions of DNA are abundant due to DNA replication (Bolderson *et al.*, 2009). The reliance of HR on regions of sequence homology makes this process significantly more precise and less likely to result in critical loss of genetic information (Hefferin and Tomkinson, 2005).

1.3.3 Gemcitabine as a single agent

Gemcitabine (2',2'-difluoro-2'-deoxycytidine) is a fluorine-substituted pyrimidine analogue antimetabolite (Plunkett *et al.*, 1996). Gemcitabine is transported and incorporated into DNA by a nucleoside transporter and catalytically converted to Gem- mono, di- and triphosphate by deoxycytidine kinase (Huang *et al.*, 1991). This triphosphate metabolite irreversibly blocks ribonucleotide reductase and DNA synthesis (Montano *et al.*, 2017), leading to stalling the DNA replication forks of cells in the S phase of the cell cycle (Hamed, Straubinger and Jusko, 2013), DNA strand breaks and disturbance

of DNA repair mechanisms (Affram *et al.*, 2015). This DNA damage consequently activates cell cycle checkpoints, induces S phase arrest (Kufe *et al.*, 1980; Huang *et al.*, 1991; Xie and Plunkett, 1995). The arrest permits time for DNA repair before the cell progresses through the cell cycle. Irreparable DNA damage can result in permanent cell cycle arrest, induction of apoptosis, or mitotic cell death caused by loss of genomic material (Liubavičiute *et al.*, 2015). Gemcitabine also activates TP53, a tumour suppressor gene, following its incorporation into DNA (Thottassery, 2006). This activation of the tumour suppressor gene results subsequently in G1 phase (Galmarini *et al.*, 2002) and S phase (Yong *et al.*, 2013; Ono, Basson and Ito, 2015) arrest, effective suppression of anti-apoptotic proteins, and a high degree of apoptosis (Galmarini *et al.*, 2002).

Gemcitabine was approved in 1996 by the FDA as the first-line therapy of locally advanced (non-resectable stage II or stage III) or metastatic (stage IV) pancreatic ductal adenocarcinoma (Barton-Burke, 1999). The NICE technology appraisal guidance [TA25] approved gemcitabine as an option for first-line chemotherapy for patients with advanced or metastatic adenocarcinoma of the pancreas in May 2001 (National Institute for Health and Care Excellence (NICE), 2001).

Gemcitabine (Gemzar®), as a single agent, is considered the gold standard and the historical first-line treatment for patients with pancreatic ductal adenocarcinomas (Sclafani *et al.*, 2015) although its clinical benefit remains marginal (Burris *et al.*, 1997). Gemcitabine's superiority in clinical trials as the

backbone chemotherapy for several types of cancer can be attributed to its positive impact on clinical benefit outcome measures and acceptable safety profile (Sclafani *et al.*, 2015). It has been found that the clinical benefit, in terms of combined assessment of pain, performance status, and weight compared to baseline, was observed in 23.8% of advanced pancreatic cancer patients randomised to gemcitabine (mean duration 18 weeks) compared to only 4.8% of patients randomised to 5-fluorouracil (5-FU) (mean duration 13 weeks) (n = 126; p = 0.02) (Burris *et al.*, 1997). A statistically significant advantage ($p = 0.002$) in median progression-free survival (PFS) (9 weeks and 4 weeks) and overall survival (OS) (5.65 months and 4.41 months) were observed for the gemcitabine group compared to 5-FU group, respectively. Furthermore, the probability of surviving at 1 year was 18% for patients randomised to gemcitabine and 2% for those randomised to 5-FU (Burris *et al.*, 1997). After this phase III trial, monotherapy with gemcitabine (30-min infusion) has been the standard treatment in patients with advanced pancreatic ductal adenocarcinoma for more than a decade (Rivera *et al.*, 2009).

1.3.3.1 Side effects of gemcitabine

Tonato *et al.* (Tonato, Mosconi and Martin, 1995) reviewed data from 790 patients who received gemcitabine for the treatment of a range of tumour types. The authors demonstrated that gemcitabine was remarkably well tolerated with few of the side-effects normally associated with cytotoxic agents. In particular, extensive myelosuppression is infrequent with modest WHO toxicity grades 3 and 4 for haemoglobin in 6.4% and 0.9% of patients,

respectively, leucocytes in 8.1% and 0.5%, neutrophils in 18.7% and 5.7%, and platelets in 6.4% and 0.9%. Nausea and vomiting were mild and hair loss was rare.

Similarly, in a multicentre phase II study of gemcitabine in 794 patients with inoperable non-small cell lung cancer (NSCLC) (Abratt *et al.*, 1994), researchers found that the majority of patients experienced mild nausea and vomiting which were easily managed with standard antiemetic drugs. Grades 3 and 4 nausea and vomiting occurred in only 5% and 0% of patients, respectively. Common side effects, not graded by WHO criteria, include transient mild flu-like symptoms, with lethargy and malaise. These tended not to be progressive and were of minimal clinical significance. Grade 1 elevation in liver transaminases occurred in approximately 33% of patients, but this was not an indication for dose reductions and was not progressive with further therapy. Finally, there was a low incidence of drug-related complications that required hospitalisation. Of 21 hospital admissions, nine were for intercurrent tumour complications, six were for blood transfusions, and three were due to sepsis (Abratt *et al.*, 1994). All three sepsis cases were not associated with neutropenia: one was for dehydration due to vomiting and inadequate oral intake, the second case was for the haemolytic uremic syndrome, and the last case was for the probable radiation-recall phenomenon (Abratt *et al.*, 1994). Radiation recall is an acute inflammatory reaction that can be triggered when chemotherapy agents are administered after radiotherapy (Burris and Hurtig, 2010). The patient with possible radiation-recall phenomenon had initially undergone surgical resection of the tumour followed by irradiation to 56 Gy,

five 2-Gy fractions per week. He developed sepsis after four cycles of gemcitabine (Abratt *et al.*, 1994).

1.3.3.2 Gemcitabine resistance in pancreatic cancer

Since the introduction of gemcitabine in 1996, only negligible improvement in prognosis and survival has been achieved for pancreatic cancer patients. This failure can be attributed mainly to gemcitabine resistance, which develops within weeks of initiation of chemotherapy. Therefore, it is necessary to understand the cellular mechanisms that regulate resistance to gemcitabine in order to improve treatment outcome (Binenbaum, Na'ara and Gil, 2015; Liu *et al.*, 2016). Modalities of gemcitabine resistance can be broadly categorised into either intrinsic to the cancer cell, or extrinsic, which influenced by the cancer microenvironment (Binenbaum, Na'ara and Gil, 2015).

1.3.3.2.1 Mechanisms of intrinsic resistance

Mechanisms of intrinsic resistance to gemcitabine can be generally classified into two subgroups. Firstly, mechanisms that interfere with drug transport, drug metabolism, or drug-induced DNA damage. Secondly, mechanisms that disrupt gemcitabine-induced apoptosis following DNA damage (Binenbaum, Na'ara and Gil, 2015).

Metabolism-based resistance:

Gemcitabine (difluoro deoxycytidine, dFdC) is phosphorylated inside the cell by deoxycytidine kinase (dCK) into dFdCMP, which is converted by other pyrimidine kinases to its active diphosphate and triphosphate derivatives, dFdCDP and dFdCTP (Mini *et al.*, 2006). Therefore, cellular deficiency of dCK, which has been demonstrated in pancreatic cancer (Kazuno *et al.*, 2005; Ohhashi *et al.*, 2008), is a major contributor to gemcitabine resistance *in vitro* and *in vivo*. Furthermore, upregulation of the dCK enzyme has also been shown to enhance gemcitabine cytotoxic efficacy in the pancreatic, biliary tract, and gastrointestinal cancers (Horii *et al.*, 2015).

Transport-based resistance:

Gemcitabine is infused and transported into cells through the human equilibrative (hENTs) and concentrative type (hCNTs) nucleoside transporters (Mini *et al.*, 2006). ENT1, CNT1 and CNT3 have often been related to gemcitabine resistance in humans, and have therefore been proposed as predictive markers for gemcitabine response in the clinical settings (Spratlin *et al.*, 2004; Giovannetti *et al.*, 2006; Bhutia *et al.*, 2011). The potential roles of these NTs have been demonstrated *in vitro*, when ENT1 knockout in NSCLC cells induced gemcitabine resistance, while its upregulation enhanced its cytotoxic activity (Achiwa *et al.*, 2004). Moreover, pathological specimens from ovarian cancer patients demonstrated that CNT1 is downregulated in cancer cells compared to the surrounding healthy cells (Hung *et al.*, 2015). Furthermore, in a systematic review of ten studies with 855 patients conducted to evaluate the potential predictive value of hENT1 expression in pancreatic

tumour cells in patients treated with gemcitabine, the authors demonstrated that patients with high expression of hENT1 had significantly longer OS compared to those with low expression of this cellular transporter (Nordh, Ansari and Andersson, 2014). It has also been reported that the matricellular protein cysteine-rich angiogenic inducer 61 (CYR61) can negatively regulate the nucleoside transporters hENT1 and hCNT3 (Hesler *et al.*, 2016). To overcome gemcitabine transport-based resistance, gemcitabine delivery into cancer cells by nano-particles has been found to be efficacious, *in vitro* and *in vivo*, in lung cancer cells (Hung *et al.*, 2015) and pancreatic cancer cells (Poon *et al.*, 2015). Although this success has been reported in pre-clinical studies, the probability of success of a nanoparticle drug progressing from pre-clinical proof-of-principle to commercial launch is about 6% (Cook *et al.*, 2014). The cost-effectiveness provided by the nanomedicine drug versus conventional therapy is a key consideration when adopting nanoparticle therapies (Hare *et al.*, 2017). Thus, the increased cost of nanoparticle systems can prevent them from being a principal treatment choice in the clinical setting (Hare *et al.*, 2017).

Pathways modulating-based resistance:

Although induction of DNA damage is the main mechanism of action of gemcitabine, the drug is also highly potent against confluent cells that are not in the S phase of the cell cycle (Kroep *et al.*, 2000). The tumour suppressor gene P53 is a modulator of gemcitabine efficacy. While both P53-mutated and WT cells display S-phase arrest in response to gemcitabine, only the WT cells display a G1 phase arrest, effective suppression of anti-apoptotic proteins

such as IAP or BCL-2, and a high degree of apoptosis (Galmarini *et al.*, 2002). As P53 mutations dominate the landscape of pancreatic cancer, gemcitabine resistance is an inherent trait of pancreatic cancer cells (Chen *et al.*, 2011). In addition, nuclear factor kappa B (NF-kB) is upregulated in P53-mutated pancreatic cancer cells in response to gemcitabine treatment, resulting in gemcitabine resistance (Arlt *et al.*, 2003). Moreover, hypoxia plays an important role in pancreatic cancer cells resistance to gemcitabine through the activation of PI3K/Akt/NF-kB signalling pathways that regulate cell proliferation, angiogenesis, and apoptosis (Yokoi and Fidler, 2004).

1.3.3.2.2 Mechanisms of extrinsic resistance

As well as its role in supporting tumour growth, progression, and metastasis, the pancreatic cancer microenvironment also induces drug resistance, in a process termed environment-mediated drug resistance (EMDR) (Binenbaum, Na'ara and Gil, 2015). Tumour stroma in pancreatic cancer plays an important role in tumour progression and EMDR (Binenbaum, Na'ara and Gil, 2015). Furthermore, overexpression of aldehyde dehydrogenase 1A1 (ALDH1A1), which is one of the characteristic features of tumour-initiating and/or cancer stem cell (CSC) properties in pancreatic cancer, plays an important in both intrinsic and acquired resistance to gemcitabine (Duong *et al.*, 2012, 2014).

Pancreatic cancer stem cells (PCSCs) contribute to tumour progression, metastasis, and resistance to common chemotherapy (Zhan *et al.*, 2015; Mallik and Karandish, 2016). Hong *et al.* (Hong *et al.*, 2009) reported that CD44 has a key role in gemcitabine resistance in PCSCs. Moreover, pancreatic cancer

cells characterized by CD44+CD24+ESA+ on their surface showed resistance to gemcitabine and radiotherapy (Lee, Dosch and Simeone, 2008).

1.3.4 Gemcitabine in combination with radiotherapy

Various studies have demonstrated the poor response rate of single-agent gemcitabine in the treatment of pancreatic cancer (Casper *et al.*, 1994; Carmichael *et al.*, 1996). While this response rate improves slightly when other systemic agents are used in combination with gemcitabine, toxicity is also increased without significant survival benefit (Louvet *et al.*, 2005; Reni *et al.*, 2005; Cunningham *et al.*, 2009; Colucci *et al.*, 2010). However, the addition of radiotherapy to gemcitabine was found to be beneficial with higher but tolerated toxicity levels (Sainato *et al.*, 2015). This combination ensures similar efficacy against pancreatic cancer with lower gemcitabine (Blackstock *et al.*, 2003; Magnino *et al.*, 2005; Evans *et al.*, 2008) or radiation (Sharma *et al.*, 2015) doses.

Nucleoside analogues, including gemcitabine, are among the most effective and most widely used agents to sensitize tumour cells to radiation treatment (i.e., radiosensitisers) (McGinn, Shewach and Lawrence, 1996). *In vitro*, It has been found that prolonged exposure to gemcitabine results in potent radiosensitisation of the colon (Shewach *et al.*, 1994), breast (Rockwell and Grindey, 1992), and pancreatic (Lawrence *et al.*, 1996) cancer cell lines.

A meta-analysis of 15 randomized controlled trials for the treatment of locally advanced pancreatic cancer in 1128 patients, revealed that chemoradiotherapy was superior in the 6-month and 12-month survival rates to the radiotherapy alone group or chemotherapy alone group (P = 0.0001 and P = 0.02, respectively), whereas the 18-month survival showed no significant difference (P = 0.23) (Chen *et al.*, 2013). However, the chemoradiotherapy group had significantly more grade 3-4 treatment-related haematologic and non-haematologic toxicities than the chemotherapy or radiotherapy alone groups (OR = 3.74 and 1.71; 95%CI 2.56-5.47 and 1.16-2.53, both $p < 0.01$) (Chen *et al.*, 2013). Therefore, triple therapy with the addition of TKI targeted therapy (sunitinib or pazopanib) to the chemoradiotherapy, utilising lower doses of each component, is hypothesised in this project to reduce the reported treatment-related adverse effects and improve treatment outcome in pancreatic cancer patients.

1.3.5 Gemcitabine in combination with conventional chemotherapy

In a recent literature review of the current treatment options for metastatic pancreatic cancer, Sclafani *et al.* (Sclafani *et al.*, 2015) summarised results from 13 phase III studies comparing combination chemotherapy versus single-agent gemcitabine for the first-line treatment of advanced pancreatic cancer. Briefly, they demonstrated that in nine studies out of 13 no improvement in OS (the primary endpoint of most studies) was found. These nine studies compared gemcitabine alone with the combination therapy of gemcitabine with 5FU (Berlin *et al.*, 2002), irinotecan (Rocha Lima *et al.*, 2004), oxaliplatin

(Louvet *et al.*, 2005; Poplin *et al.*, 2006), pemetrexed (multi-targeted antifolate) (Oettle *et al.*, 2005), cisplatin (Heinemann *et al.*, 2006; Colucci *et al.*, 2010), capecitabine (Herrmann *et al.*, 2007; Cunningham *et al.*, 2009).

Similar negative results were found from double-blind randomised control trials when gemcitabine alone was compared to combination therapy with the topoisomerase inhibitor (exatecan) (Abou-Alfa *et al.*, 2006), and the broad-spectrum matrix metalloproteinase inhibitor (marimasmat) (Bramhall *et al.*, 2002).

However, OS benefit was observed for combination treatments (with fluoropyrimidines and platinum agents) over single-agent gemcitabine in four meta-analyses and/or subgroup analyses restricted to patients with good performance status (Heinemann *et al.*, 2007, 2008; Sultana *et al.*, 2007; Cunningham *et al.*, 2009). In addition, combination chemotherapy with cisplatin, epirubicin, 5-FU and gemcitabine (PEFG regimen) demonstrated better outcomes over single-agent gemcitabine in terms of response rate (38.5% versus 8.5%, p = 0.0008), 4-month PFS (60% versus 28%, hazard ratio (HR) 0.46, p = 0.001; primary endpoint of the study) and OS (HR 0.65, p = 0.047) (Reni *et al.*, 2005). Nevertheless, this study had some limitations including the relatively small sample size (n = 99) and the choice of 4-months PFS (instead of OS) as the primary endpoint (Sclafani *et al.*, 2015).

Recently, the FDA and the EMA approved nab-paclitaxel (albumin-bound paclitaxel) as first-line therapy for advanced and metastatic pancreatic ductal

adenocarcinoma in combination with gemcitabine (Sclafani *et al.*, 2015). The Scottish Medicines Consortium (SMC) also approved this combination in February 2015 (UK and Pancreatic Cancer UK, 2016). The regulatory approval followed the results of the largest international, multicentre, randomised phase III metastatic pancreatic ductal adenocarcinoma trial (MPACT), which compared single-agent gemcitabine versus gemcitabine plus nab-paclitaxel (n = 861) (Von Hoff *et al.*, 2013). The combination therapy with gemcitabine plus nab-paclitaxel revealed a statistically significant clinical benefit over standard single-agent gemcitabine in terms of median OS (8.5 months versus 6.7 months, HR 0.72, p <0.0001) which was the primary endpoint of the study, median PFS (5.5 versus 3.7 months, HR 0.69, p <0.0001) and tumour response rate (23% versus 7%, p <0.001). The survival for one year (35% vs. 22%), two years (10% vs. 5%), and three years (4% vs. 0%) were estimated in the gemcitabine-nab-paclitaxel group versus the gemcitabine group, respectively (Matsuoka and Yashiro, 2016). Weekly treatment with this combination was generally well tolerated. The treatment-related grade ≥3 adverse events which occurred significantly more frequently in the combination group than in the gemcitabine-alone group were neutropenia (38% vs. 27%), Febrile neutropenia (3% vs. 1%), leukopenia (31% vs. 16%) fatigue (17% vs. 7%), and reversible peripheral neuropathy (17% vs. 1%). Interestingly, Krishna *et al.* (2015) (Krishna *et al.*, 2015), in a retrospective study, demonstrated that a bi-weekly (instead of weekly as in the MPACT trial) administration of gemcitabine and nab-paclitaxel may improve the toxicity profile and significantly reduce the costs of this combination treatment without affecting

the overall efficacy. Nevertheless, from an economic point of view, the National Institute for Health and Care Excellence (NICE), in the UK, recently stated that nab-paclitaxel did not fulfil their criteria for a cost-effective therapy as they found that nab-paclitaxel plus gemcitabine compared with gemcitabine alone would cost between £72,500 and £78,500 per quality-adjusted life-year (QALY) gained (Goldstein *et al.*, 2016).

1.3.6 Gemcitabine in combination with molecular-targeted therapy

To overcome resistance in pancreatic cancer, multiple targeted therapy agents have also been added to gemcitabine. For example, in a double-blind, placebo-controlled, international, phase III trial of 569 patients from 17 countries with locally advanced or metastatic pancreatic ductal adenocarcinoma, erlotinib (an oral HER1/EGFR tyrosine kinase inhibitor) in combination with gemcitabine (n= 285) was compared to gemcitabine with placebo alone (n = 284) (Moore *et al.*, 2007). It was reported that the overall survival (the primary endpoint in this study) was significantly prolonged with erlotinib plus gemcitabine (median 6.24 months) compared to gemcitabine with placebo (median 5.91 months) (HR 0.82; 95% CI 0.69 to 0.99; p= 0.038). This combination also associated with an improvement in one-year survival (23% *vs.* 17%; p = 0.023) and PFS (HR 0.77; 95% CI 0.64 to 0.92; p = 0.004). Although these findings were statistically significant, the overall survival advantage (approximately 10 days only) seems modest. However, as a consequence of this trial, the American Food and Drug Administration (FDA) and the European Medicines Agency (EMA) approved erlotinib in combination

with gemcitabine as first-line therapy for locally advanced or metastatic pancreatic cancer (Sclafani *et al.*, 2015).

Except for erlotinib, targeted therapies have largely failed to show a significant benefit in the treatment of pancreatic cancer when added to the standard single-agent chemotherapy, gemcitabine (Sclafani *et al.*, 2015). For example, despite the strong biological rationale for these combination strategies, targeting KRAS with tipifarnib (Van Cutsem *et al.*, 2004), MAPK with cetuximab (Philip *et al.*, 2010), MEK with selumetinib (Bodoky *et al.*, 2012) or trametinib (Infante *et al.*, 2014), and mTOR with everolimus (Wolpin *et al.*, 2009) in addition to single-agent gemcitabine failed to improve the outcome of locally advanced or metastatic pancreatic cancer patients compared to gemcitabine alone (n= 668 HR=1.03 p=0.75; n=745 HR=1.06 p=0.19; n=70 HR=1.03 p=0.92; n=160 HR=0.98 p=0.453, n=33 p>0.05, respectively).

Because of these marginal improvement and disappointing outcome from current single and combination therapy, this research project aimed to develop novel combination strategies for the treatment of pancreatic cancer. We examined the cytotoxicity of two tyrosine kinase inhibitors (TKI), sunitinib and pazopanib, for the first time, against PANC-1 and MIA PaCa-2 pancreatic cancer cell lines. Both are currently approved in the treatment of renal cell carcinoma (Motzer *et al.*, 2014), and in May 2011, the US FDA approved sunitinib for the treatment of progressive, well-differentiated pancreatic neuroendocrine tumours in patients with unresectable locally advanced or metastatic disease (Blumenthal *et al.*, 2012).

1.4 Targeted molecular therapy of cancer

Targeted molecular therapy is a form of personalized medical therapy designed to inhibit specific cellular signalling pathways involved in cancer growth, resistance, and metastasis (Shaib and El-Rayes, 2018). The therapy is personalized to meet each person's individual needs because cancer develops differently in everyone (*Targeted Molecular Therapy – Abramson Cancer Center*, no date). Potential advantages of targeted therapies over conventional cytotoxic therapies are improved safety profile due to selective inhibition of cancer-related pathways, which limits unnecessary damage to healthy cells, and enhanced cytotoxic activity (Danovi, Wong and Lemoine, 2008). The development of agents targeting specific tumour pathways including tyrosine kinases has been hypothesised as a promising approach for the treatment of pancreatic cancer (Gupta and El-Rayes, 2008).

Monoclonal antibodies against the epidermal growth factor receptor (such as cetuximab) or the vascular endothelial growth factor receptor (such as bevacizumab) and EGFR tyrosine kinase inhibitors (TKIs) (such as erlotinib and gefitinib) or VEGFR TKI (such as sunitinib and pazopanib) are currently utilised clinical examples for molecularly targeted cancer therapy.

1.4.1 Monoclonal antibodies

Cetuximab is the most frequent anti-EGFR antibody used against cancer (Borja-Cacho *et al.*, 2008). Because of its high affinity for the extracellular

domain, it limits the RAS/PI3K transduction signals (Borja-Cacho *et al.*, 2008). Cetuximab also enhances the synthesis of pro-apoptotic proteins and reduces angiogenesis by decreasing VEGF and IL-8 synthesis (Overholser *et al.*, 2000).

Bevacizumab is the only anti-VEGF antibody that has been used in clinical trials. It has been found that bevacizumab increased survival, response, and progression-free survival in patients with metastatic colorectal cancer (Cohen *et al.*, 2007). It also improves the response and survival in patients with breast cancer, NSCLC, and renal cell carcinoma (De Gramont and Van Cutsem, 2005).

However, both antibody agents, cetuximab and bevacizumab failed to show a significant benefit in the treatment of pancreatic cancer when added to the standard single-agent chemotherapy, gemcitabine (Kindler *et al.*, 2007; Philip *et al.*, 2010).

1.4.2 Tyrosine kinase inhibitors

Mutations in the KRAS pathway present in approximately 95% of patients with pancreatic cancer (Makohon-Moore and Iacobuzio-Donahue, 2016; Foo and Wang, 2017). This pathway contains several protein kinases of the RAF-family. RAF-1, the main RAS effector, activates Mitogen-Activated Protein Kinases / Extracellular-Signal Regulated Kinases (MAPK/ERK) by phosphorylation. Activated MAPK/ERK translocates into the nucleus and

enhances the expression of factors that control cell proliferation (Scaltriti and Baselga, 2006). Inhibition the activity of the tyrosine kinase domain shows promise in the treatment of cancer; thus TKIs were approved by FDA for treatment of patients with NSCLC, head and neck tumours, gastrointestinal stromal tumours, and more recently, pancreatic cancer (Borja-Cacho *et al.*, 2008). Erlotinib and gefitinib are anti-EGFR agents whilst sunitinib and pazopanib are Anti-VEGFR agents.

Sunitinib is an oral multitargeted inhibitor which inhibits various tyrosine kinases that have been implicated in tumour growth and angiogenesis, including VEGFRs, PDGFRs, stem cell factor receptor (KIT), and other RTKs (Mendel *et al.*, 2003; Yee *et al.*, 2004; Faivre *et al.*, 2007). Sunitinib was approved for the treatment of advanced renal cell carcinoma, imatinib-resistant gastrointestinal stromal tumour, and progressive, well-differentiated pancreatic neuroendocrine tumours (Raymond *et al.*, 2011; Sun *et al.*, 2014; Kulke *et al.*, 2017). Additionally, sunitinib is reported to have direct antiproliferative and apoptotic effects against various tumours, including esophagogastric cancer (Lyros *et al.*, 2010), pheochromocytoma tumour cells (Saito *et al.*, 2012), follicular thyroid cancer cells (Grosse *et al.*, 2014), transitional cell carcinoma (TCC) of the bladder (Ping, Wu and Yu, 2012) and medulloblastoma tumour cells (Yang *et al.*, 2010). Sunitinib is also reported to enhance tumour radiosensitivity in breast cancer (El Kaffas *et al.*, 2014), pancreatic cancer (Cuneo *et al.*, 2008), oesophageal adenocarcinoma (Kleibeuker, ten Hooven, Castricum, *et al.*, 2015), and colon cancer (Sun *et al.*, 2012).

However, as discussed in section 1.3.6, several classes of targeted therapies have been evaluated in pancreatic cancer in large randomized clinical trials and the results have been largely disappointing although these trials were supported by promising preclinical data and a reasonable molecular rationale (Shaib and El-Rayes, 2018). Despite the approval of EGFR TKI, erlotinib, in combination with gemcitabine for the treatment of pancreatic cancer, the disease prognosis has remained poor and overall and progress-free survival rates have not improved since the approval (Awasthi, Schwarz and Schwarz, 2011). Therefore, this research project aimed at developing novel combination strategies for the treatment of pancreatic cancer based on two multi-target anti-angiogenesis VEGFR tyrosine kinase inhibitors (TKI), sunitinib and, for the first time, pazopanib. The efficacy of these repurposed two agents in combination with radiochemotherapy has been examined *in vitro* and *in vivo.*

1.4.2.1 Clinical indications of sunitinib and pazopanib

Sunitinib and pazopanib are currently approved in the treatment of renal cell carcinoma (Motzer *et al.*, 2014). Furthermore, pazopanib was approved also for the treatment of sarcoma and sunitinib for the treatment of gastrointestinal tumours (Sorokin *et al.*, 2018). Moreover, in May 2011, the US FDA approved sunitinib for the treatment of progressive, well-differentiated pancreatic neuroendocrine tumours in patients with unresectable locally advanced or metastatic disease (Blumenthal *et al.*, 2012).

1.4.2.2 Mechanism of action and molecular targets of sunitinib and pazopanib

Both sunitinib and pazopanib inhibit angiogenesis through blocking the intracellular tyrosine kinase portion of the three VEGFR subtypes VEGFR-1, VEGFR-2 and VEGFR-3, and the two PDGFR subtypes PDGFR-α and PDGFR-β (Izzedine *et al.*, 2007; Sonpavde and Hutson, 2007). They also target the stem cell factor receptor (KIT) (Eaby-sandy, Grande and Viale, 2012). KIT is reported to be expressed in PANC-1 but not in MIA PaCa-2 pancreatic cancer cell lines (Yasuda *et al.*, 2006). Pharmacological studies demonstrated that sunitinib also targets the colony-stimulating factor 1 receptor (CSF-1R), FMS-related tyrosine Kinase-3 (FLT3), and glial cell line-derived neurotrophic factor receptor (GDNF) (Izzedine *et al.*, 2007; Eaby-sandy, Grande and Viale, 2012; Bisht, Feldmann and Brossart, 2013; Haas *et al.*, 2016), however, these receptors are not expressed in PANC-1 and MIA PaCa-2 pancreatic cancer cell lines (Table 1.3). Restriction enzyme analysis confirmed that Capan-2 and MIA PaCa-2 are heterozygous for the G691S RET allele, whereas AsPC-1 and PANC-1 cells are homozygous for the wild-type allele. Interestingly, whereas GDNF strikingly increased cell growth in Capan-2 and MIA PaCa-2 cells, the effect on AsPC-1 and PANC-1 cells was significantly less prominent ($p < 0.01$) (Sawai *et al.*, 2005). Pazopanib also targets the fibroblast growth factor receptor (FGFR) subtypes 1 and 3 (Keisner and Shah, 2011; Plummer *et al.*, 2013) and FGFR-2 (Ranieri *et al.*, 2014). These receptors were reported to be overexpressed in both PANC-1 and MIA PaCa-2 cell lines (Ishiwata *et al.*, 2012). Furthermore, pazopanib also targets

interleukin (IL)-2 receptor inducible T-cell kinase (LCK), and transmembrane glycoprotein receptor tyrosine kinase (c-FMS) (Keisner and Shah, 2011) but these are not expressed in PANC-1 and MIA PaCa-2 pancreatic cancer cells (Table 1.3).

Molecular targets and mechanism of anti-tumour effects of sunitinib and pazopanib are shown in Figure 1.3. The mechanism underlying anti-tumour efficacy of sunitinib and pazopanib can be classified as direct cytotoxic effects, anti-angiogenic effects (inhibition of new blood vessel formation), or vascular disruption of existing VEGF/VEGFR-dependant tumour blood vessels leading to central tumour cell necrosis (Faivre *et al.*, 2007).

Vascular endothelial growth factor (VEGF) and its receptors are overexpressed in human pancreatic ductal adenocarcinoma (Luo *et al.*, 2001). Platelet-derived growth factor (PDGF) receptors chain β is also found to be overexpressed in both cell lines, PANC-1 and MIA PaCa-2, of pancreatic cancer (Beauchamp *et al.*, 1990). Several growth factors are also overexpressed in pancreatic cancer, such as stem cell (Yasuda *et al.*, 2006) and fibroblast growth factors (Ishiwata *et al.*, 2012). A complete list of growth factors overexpressed in pancreatic cancer, categorised by the cell line, is shown in Table 1.3.

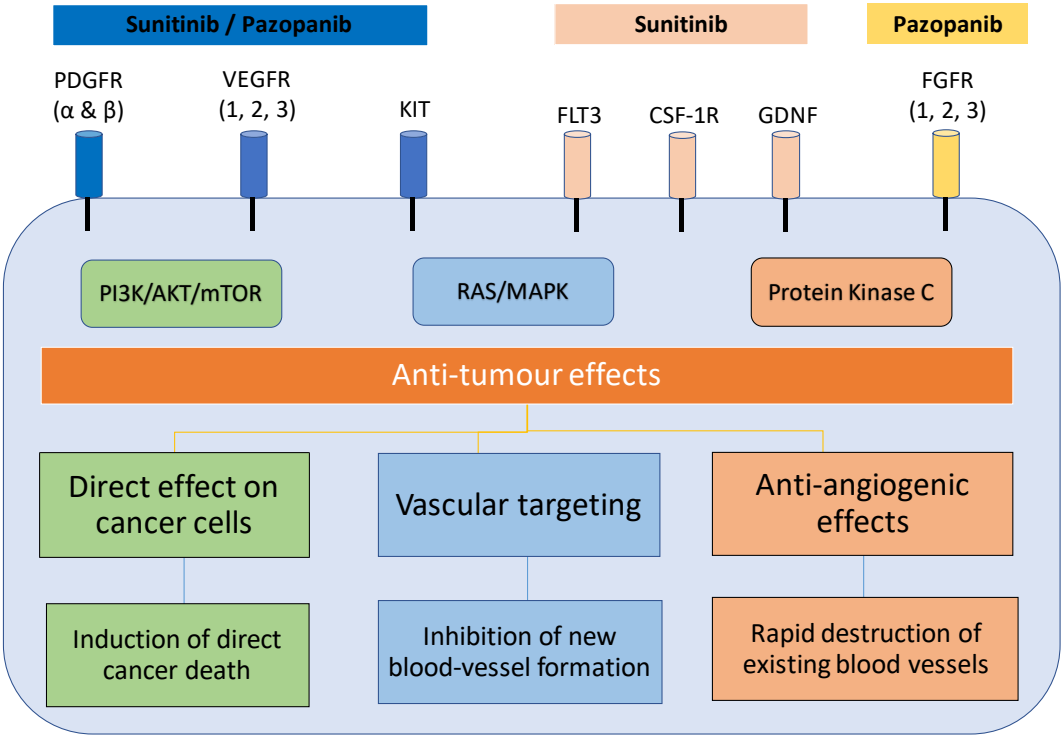

Figure 1.3 Molecular targets and mechanism of anti-tumour effects of sunitinib and pazopanib. Adapted from Faivre *et al.* (Faivre *et al.*, 2007). Both sunitinib and pazopanib target PDGFR, VEGFR, and KIT. Sunitinib targets FLT3, CSF-1R, and GDNF. Pazopanib targets FGFR. PDGFR, Platelet-derived growth factor receptor; VEGFR, Vascular endothelial growth factor receptor; KIT, Stem cell factor receptor; CSF-1R, colony-stimulating factor 1 receptor; FLT3, FMS-related tyrosine Kinase-3; GDNF, glial cell line-derived neurotrophic factor receptor; MAPK, mitogen-activated protein kinase; mTOR, mammalian target of rapamycin; PI3K, phosphatidylinositol 3-kinase; AKT, protein kinase B.

Table 1.3 Growth factor expression in pancreatic cancer cell lines.
PDAC = Pancreatic ductal adenocarcinoma; VEGFR= Vascular endothelial growth factor; KIT = Stem Cell Factor Receptor; FGFR = Fibroblast growth factor receptor; TGF = Transforming Growth Factor.

Growth factor expression in PDAC	Study reference	PANC-1	MIA PaCa-2
VEGFR-1& 2	(Luo *et al.*, 2001)	++	+
PDGFR-β	(Beauchamp *et al.*, 1990)	+	+
KIT	(Yasuda *et al.*, 2006)	+	-
FGFR-1 IIIc	(Ishiwata *et al.*, 2012)	++(15)	++(11)
FGFR-2 IIIc		+++ (50)	++(5.5)
FGFR-3 IIIc		+(1)	+++(30)
FGFR-4	(Ishiwata *et al.*, 2012)	+(1)	+(6.5)
TGF-α	(Beauchamp *et al.*, 1990; Ishiwata *et al.*, 2012)	+	++
TGF-β 1&3	(Beauchamp *et al.*, 1990; Ishiwata *et al.*, 2012)	+	+
TGF-β 2	(Beauchamp *et al.*, 1990)	+	-

1.4.2.3 Side effects of sunitinib and pazopanib

In a randomized, open-label, multi-countries, phase III trial conducted to compare the efficacy and safety between sunitinib and pazopanib as first-line treatment in 1,110 patients with metastatic renal-cell carcinoma, researchers found similar efficacy and different safety and quality of life profiles (Motzer *et al.*, 2013). Both groups had similar rates of dose reduction and drug discontinuation because of adverse events (Motzer *et al.*, 2013). Generally, the most common adverse events included diarrhoea, fatigue, hypertension, and nausea. Patients treated with sunitinib, as compared with those treated with pazopanib, had a higher incidence of fatigue (63% vs. 55%), the hand-foot syndrome (50% vs. 29%), and thrombocytopenia (78% vs. 41%). On the other hand, patients treated with pazopanib had a higher incidence of increased levels of alanine aminotransferase (60%, vs. 43% with sunitinib) (Motzer *et al.*, 2013). Hypothyroidism has been observed in patients received sunitinib in several studies (Desai *et al.*, 2006; Rini *et al.*, 2007).

1.5 Repurposing of drugs

Drug repurposing (also called drug repositioning, reprofiling or re-tasking) is an approach for assigning already known and/or approved drugs to new medical indications (Chakraborty and Trivedi, 2015). This strategy offers numerous advantages over developing an entirely new drug for a given indication. Firstly, the risk of failure is lower in the repurposed drug because it has already been found to be sufficiently safe in preclinical studies

(Pushpakom *et al.*, 2019). It has been demonstrated that almost 90% of the identified novel compounds fail in clinical trials, resulting in the rise of the pharmaceutical research and development cost (Gupta *et al.*, 2013). Secondly, the time frame for drug development can be reduced from 13-17 years for developing *de novo* drugs to 3-12 years for the repurposed drug (Ashburn and Thor, 2004). This is because most of the preclinical evaluation, safety assessment and, in most cases, formulation development already have been accomplished (Pushpakom *et al.*, 2019). Thirdly, this approach has substantial savings in preclinical and phase I and II costs (Chong and Sullivan Jr, 2007; Pushpakom *et al.*, 2019). The costs of bringing a repurposed drug to market have been estimated to be US$300 million on average, compared with an estimated ~$2–3 billion for a new chemical entity (Nosengo, 2016). Finally, repurposed drugs may reveal new targets and pathways that can be further explored and used in cancer therapy (Strittmatter, 2014; Pushpakom *et al.*, 2019). Figure 1.4 represents the steps involved in the *de novo* drug discovery process versus drug repurposing with the main features of both the processes.

There are numerous successful cases of drug repurposing. For example, repurposing of sildenafil citrate for erectile dysfunction, which was based on serendipity, is considered the most famous and the most successful repurposed drug, with worldwide sales totalling $2.05 billion in 2012 (Pushpakom *et al.*, 2019). Another successful example is repurposing raloxifene from osteoporosis to breast cancer in 2007, with worldwide sales of $237 million in 2015 (Pushpakom *et al.*, 2019).

Sunitinib and pazopanib were originally approved for the treatment of renal cell carcinoma (Motzer *et al.*, 2014). Following on from this indication, sunitinib was repurposed and obtained FDA approval for the treatment of progressive, well-differentiated pancreatic neuroendocrine tumours in patients with unresectable locally advanced or metastatic disease (Blumenthal *et al.*, 2012). Pazopanib was also repurposed and approved for the treatment of sarcoma (Sorokin *et al.*, 2018). Therefore, in the current project, both sunitinib and pazopanib were examined for their efficacy against pancreatic cancer *in vitro* and *in vivo*.

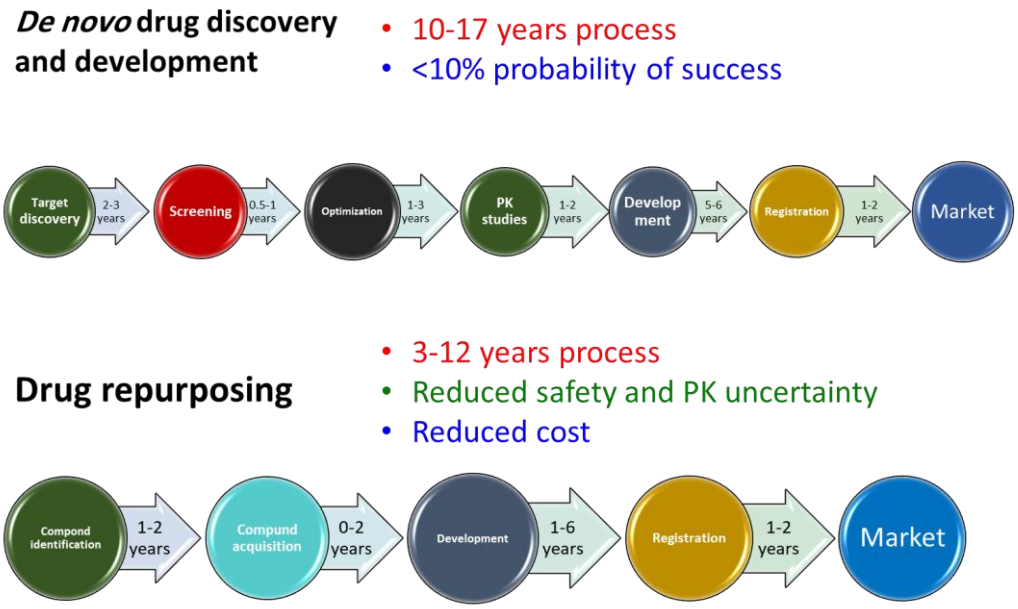

Figure 1.4 Schematic representation of the steps involved in *de novo* drug discovery process vs. drug repurposing. Adapted from Ashburn and Thor (Ashburn and Thor, 2004).

1.6 Research aims and objectives

Pancreatic cancer prognosis is still poor and despite the advances provided by combination therapies such as gemcitabine/erlotinib or gemcitabine/nab-paclitaxel, survival rates have barely improved. Further research focused on new combination strategies, incorporating the new targeted therapies, and identifying potential predictive factors of response are required to be able to offer effective tailored therapies to pancreatic cancer patients.

Therefore, we hypothesise that novel triple combinations and treatment schedule strategies of gemcitabine plus repurposed angiogenesis inhibitor (sunitinib or pazopanib) plus external beam radiation would improve cell kill in pancreatic cancer models compared to single or double conventional therapies. We also hypothesised that these combinations could have efficacy in the clinic. This hypothesis was based on the fact that multimodality combination therapy with lower therapeutic doses of each treatment may improve the disease outcome in two ways. Firstly, combination therapy may enhance the treatment efficacy through different mechanisms of cytotoxicity that ensure reaching higher numbers of cancer heterogeneous cells with different tyrosine kinase expression. Secondly, combination strategies may reduce the chance of pancreatic cancer cells resistance to radiochemotherapy, which was thought to be the major contributor to poor prognosis, and also was reported to be dose-dependent.

The specific aims of this study were:

I. To assess the cytotoxic efficacy of radiotherapy (XBR) and chemotherapy/targeted therapy (gemcitabine, sunitinib, and, for the first time, pazopanib) as single treatment on the viability and survival of pancreatic cancer cell lines *in vitro.*

II. To assess the cytotoxic efficacy of novel combination strategies on pancreatic cancer cell lines *in vitro.* This would be achieved through the evaluation of dose enhancement factors and radiochemosensitisation of cells following combination therapy, and assessment of synergism between those agents using the combination index analysis approach.

III. To explore the underlying mechanisms of cytotoxic action of these therapeutic approaches via conducting DNA damage and repair detection, cell cycle analysis, and apoptosis detection, mechanistic studies.

IV. To assess the cytotoxic efficacy of those therapeutic agents either as single or combination treatment on pancreatic cancer in the animal model (*in vivo*).

CHAPTER 2: MATERIALS AND METHODS

2.1 Cell lines and culture conditions

Two pancreatic cancer cell lines were utilised in this project (PANC-1 and MIA PaCa-2).

The human pancreatic carcinoma cell lines (PANC-1 and MIA PaCa-2) used in this study were both obtained from the American Type Culture Collection (ATCC®, Virginia, USA). The PANC-1 cell line was derived from a 56-year-old male with adenocarcinoma in the head of the pancreas which invaded the duodenal wall in 1973 (Lieber *et al.*, 1975), while the MIA PaCa-2 cell line was established in 1975 from tumour tissue of the pancreas obtained from a 65-year-old Caucasian male (Yunis, Arimura and Russin, 1977).

Both PANC-1 and MIA PaCa-2 cells were cultured and maintained in Dulbecco's modified eagle's medium (DMEM) cell growth medium, which was obtained from Gibco® (Paisley, UK), containing L-glutamine (300 mg/L) and 4.5 g/L D-Glucose, and supplemented with 10% (v/v) foetal bovine serum (FBS, LabTech® Int. Ltd, East Sussex, UK), 5% (v/v) of penicillin-streptomycin (10,000 µg/mL) solution (Gibco®, Paisley, UK), to prevent bacterial contamination, and 100 mM sodium pyruvate, to improve cell survival in culture (improves the cell's ability to metabolize glucose in the media to produce energy) (Gibco®, Paisley, UK).

Cell lines were cultured and maintained in 75 cm^3 culture flasks (Corning B.V, Buckinghamshire, UK) with growth medium at 37ºC ± 1ºC in a 5% ± 1% CO_2 air atmosphere until they reached 70-80% of cell confluence where the cells were further passaged.

2.2 Cell passaging, thawing, and freezing

Cells were passaged by removal of the existing cell growth medium, washing with 5 ml of phosphate-buffered saline (PBS) (Oxiod Limited, Hampshire, UK) and detachment using 3 ml of Accutase® solution (Sigma, UK). The cells were then incubated for 5 minutes at 5% CO_2 and 37°C to enhance dissociation from the flask. Once the cells had fully detached, 5 ml of a fresh growth medium was added to neutralise the Accutase®, and the cells in the suspension were disaggregated to a single-cell suspension using a 21-gauge needle and seeded into 75 cm^3 culture flasks containing 20 ml of fresh growth medium.

To freeze cells at -80 °C for later use, the cell suspension was centrifuged at 1400 revolutions per minute (RPM) for 5 minutes. The supernatant was fully removed, and the pellets were re-suspended in 1 ml of the freezing medium (growth medium + 10% (v/v) dimethyl sulfoxide (DMSO), and then transferred to cryovials (Thermo Fisher Scientific Inc, Surrey, UK) for storage in -80 °C. DMSO is added to prevent the formation of ice crystals and cells damage during the freezing process (Lovelock and Bishop, 1959) and reported to have

the advantage of more rapid penetration into most cells compared to glycerol (Meryman, 2007).

To thaw cells, cryovials were warmed at 37 °C, centrifuged at 1400 RPM for 5 minutes, and then the pellet was re-suspended in 5 mL fresh growth media. The cell solution was then transferred to either a 25 cm^3 or a 75 cm^3 flask, depending on cell concentration in cryovial, and incubated for 3 to 5 days at 37ºC and 5% CO_2 until the cells reached 70-80% confluence.

2.3 Cell doubling time

The time taken for the cell population of PANC-1and MIA PACA-2 cells to double during the exponential growth phase was determined to ensure that cancer cells duplicate at least for one time in the presence of cytotoxic agents. For both pancreatic cancer cell lines, 0.5×10^5 cells were seeded into each well of a 6-well plate in 3 mL of complete cell growth medium. After 24-hour incubation, the cells in the first well were washed with PBS, detached with Accutase® solution, disaggregated through a 21-gauge needle, and counted using a haemocytometer. One subsequent well was counted every 24 hours for a further 5 days. The time required for the cell population to double in the exponential growth phase (DT) was calculated using Equation 2.1.

$$\text{Doubling Time} = \text{Time B (hours)} - \text{Time A (hours)} \qquad \text{Equation 2.1}$$

Where; Time A = the time taken in hours for the cell population to reach, for example, 1×10^5 cells and Time B is the time taken in hours for the cell population to double to 2×10^5 cells.

2.4 Treatment of pancreatic cancer cell lines

Pancreatic cancer cell lines (PANC-1 and MIA PaCa-2) were treated in this project with a single chemotherapeutic agent, XBR, or a combination of two drugs with or without XBR.

2.4.1 Treatment of cells with a single therapy

Three therapeutic agents were utilised in this project: gemcitabine, sunitinib, and pazopanib. Stock solutions of 10 mM concentration of each drug were prepared by dissolving 2.63 mg of gemcitabine, 5.32 mg of sunitinib, or 4.37 mg of pazopanib in 1 ml of DMSO (Sigma-Aldrich®, Gillingham, UK), which were aliquoted in Eppendorf tubes in lower concentrations (100 µM) and stored at -20 °C to reduce freeze-thaw cycles and prevent contamination. To achieve the relevant working concentrations, serial dilutions from stock solutions were prepared in the appropriate fresh growth medium immediately prior to each experiment. Working stocks were discarded after each freeze-thaw cycle.

2.4.2 Treatment of control cells

Unless otherwise stated, cells in the untreated group control were maintained and incubated in DMEM growth medium containing DMSO, at the same final

concentration as the treatment of interest. The volume of DMSO to be added to the growth medium is calculated as 0.01% (v/v) for each 1 μM of the highest concentration of the drug in the experiment; this is because DMSO was used only to prepare the stock solution of 10 mM and all subsequent concentrations were diluted in the growth medium.

2.4.3 Treatment of cells with XBR

For irradiation treatment studies, the growth medium was removed from cells and replaced with 1 ml of fresh growth media prior to XBR exposure. Cells were exposed to increasing doses of XBR (0-6 Gray) using a Precision X-RAD 225 KeV X-Ray cabinet (North Branford, CT, USA), at a dose rate of 2.3 Gray/minute.

2.4.4 Treatment of cells with combination therapies

For *in vitro* experiments using combinations of two drugs, growth medium was removed from the cells and replaced with fresh media containing relevant concentrations of gemcitabine and/or one of the two tyrosine kinase inhibitors (TKIs), sunitinib or pazopanib. Combinations were evaluated using the following three treatment schedules: gemcitabine administered 48 hours before TKI (schedule 1), gemcitabine administered 48 hours after TKI (schedule 2), or gemcitabine administered simultaneously with TKI (schedule 3). Flow diagram (Figure 2.1) illustrates the treatment schedules of two-drug combination therapy (e.g. gemcitane and sunitinib).

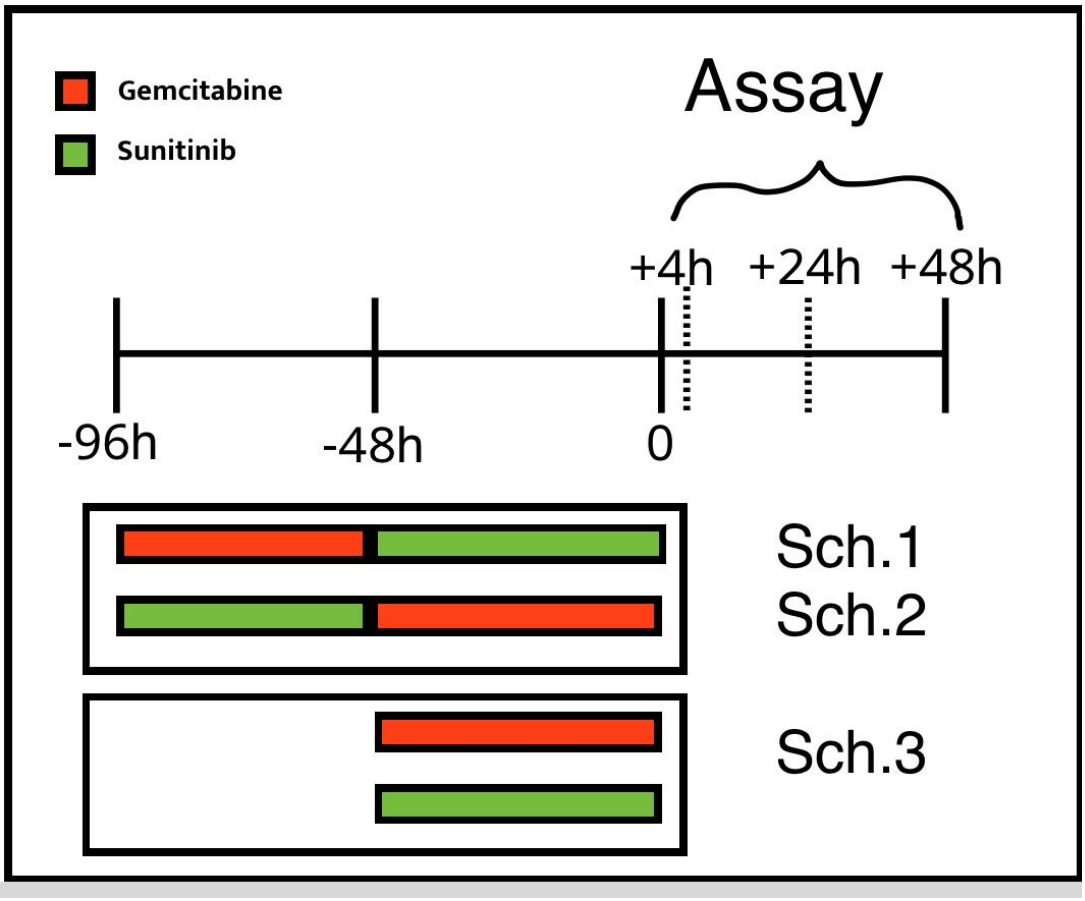

Figure 2.1 Flow diagram illustrates the treatment schedules of two-drug combination therapy of gemcitane and sunitinib used in the study.

Triple combinations of XBR and gemcitabine/sunitinib were also evaluated, using similar scheduling. Gemcitabine and sunitinib were administered simultaneously 48 hours before or after XBR (schedule 1 and schedule 2, respectively), or concurrently with XBR (schedule 3).

The concentrations for each drug used in combination studies were the IC_{50}, IC_{25}, and IC_{10}, which were obtained from the dose-response (inhibition) non-linear regression curve of single-agent cytotoxicity studies generated by GraphPad Prism® software (version 7.00), as described in GraphPad Prism's user manual (Motulsky, no date).

2.5 Cell viability assay

The cell viability assay, using AlamarBlue® solution is designed to quantitatively measure the viability of human and animal cell lines (Mosmann, 1983) and it has been widely used in cell viability and cytotoxicity experiments over the past 50 years (Rampersad, 2012). Cell viability can be spectrophotometrically measured when resazurin (a blue and non-fluorescent dye in its oxidized form) is reduced by the mitochondrial Nicotinamide adenine dinucleotide phosphate hydrogen (NADPH) dehydrogenase and Nicotinamide Adenine Dinucleotide plus Hydrogen (NADH) dehydrogenase enzymes to resorufin (a red and highly fluorescent dye) only in viable cells. Therefore, by measuring the changes in the fluorescence of the dye in the intracellular environment, the number of metabolic activity and therefore the number of viable cells can be detected (Bonnier, 2015).

The alamar blue assay was carried out to assess the cytotoxic effect of a range of concentrations of gemcitabine, sunitinib, and pazopanib on the viability of PANC-1 and MIA PaCa-2 cells. Based on the literature review, a wide range of doses of each drug (from 0.1 to 2000 μM for gemcitabine and from 0.1 to 200 μM for TKIs) was initially examined by the alamar blue assay in both cell lines. The final examined concentrations utilised ranged from 50 to 800 μM for gemcitabine and 1 to 40 μM for TKIs. Following counting using a haemocytometer (Jencons, UK), 3000 cells were seeded in each required well of a 96-well plate, and then incubated for 48 hours until 60-70% confluent. After removing the growth medium from the wells, cells were treated with 100 μL of already prepared serial drug concentrations (3 well per each concentration including control). After 24 or 48 hours of incubation at 37^{o}C, the treatment solution was replaced with the same amount (100 μL) of 10% of alamar blue solution (Life Technologies, Paisley, UK). Eight wells, which were left without cells, were filled with 100 μL AlamarBlue® solution as a background control. The plate was placed in the incubator for 3 hours before reading on a POLARstar® Omega (to read fluorescence from a microplate; BMG LABTECH®, Germany) at 560 nM excitation and 590 nM emission wavelength levels as previously described (O'brien *et al.*, 2000). The difference between the average fluorescence of treated and background wells was calculated and normalised to the untreated control cells in order to calculate the cell viability. The dose-response non-linear least squares curve with logarithmic treatment's concentration on the X-axis and the percentage of cell viability on the Y-axis was plotted, as described in GraphPad Prism's user manual (Motulsky, no

date), following the model represented by Equation 2.2, and IC_{50} values (the inhibitory concentration of treatment at which the cell viability decreased by 50%) were calculated using GraphPad Prism® software (version 7.00).

$$Y = \frac{100}{1 + 10^{(LogIC_{50} - X)\,.\,HS}} \qquad \text{Equation 2.2}$$

Where **X** represents the logarithm of treatment concentration which inhibits cell growth with ***Y*** percentage; and ***HS*** represents the hillslope of the response curve, obtained from GraphPad Prism software.

2.6 Clonogenic survival assay

Clonogenic assay or colony formation assay is an *in vitro* cell survival assay based on the ability of a single cell to undergo unlimited division and to form a colony, which is a cluster which consists of at least 50 cells (Franken *et al.*, 2006). It is considered the gold standard method to determine the effectiveness of ionizing radiation and other cytotoxic agents on the survival rate of cancer cells because it determines potentially lethal- and sublethal damage repair (Franken *et al.*, 2006).

PANC-1 or MIA PaCa-2 cells were seeded in 25 cm^3 flasks in 5 ml of growth medium and incubated for 48 to 72 hours at 37°C and 5% CO_2 atmosphere until 60-70% confluent. The growth medium was then removed, cells were

washed with PBS and then treated with serial concentrations of the appropriate drug solution in 5 mL of fresh growth medium and incubated for 24 or 48 hours.

After 24 or 48 hours of treatment with cytotoxic agents, a cell suspension was made by removing the medium, washing with PBS, detaching cells from the treatment flasks with Accutase® (Sigma, UK), and neutralising it with an equal amount of growth medium. Following counting using a haemocytometer, 300 cells from each treatment flask were seeded in three 60 mm Petri dishes (Sigma-Aldrich®, Gillingham, UK) containing 5 ml of fresh growth medium and incubated for 10-14 days at 37°C and 5% CO_2 to allow the formation of at least 50 colonies in the control dishes. The medium was then removed, and colonies were washed with PBS and fixed in pure methanol (VWR Chemicals®, Germany) for 10 minutes before staining with 10% Giemsa stain solution (VWR Chemicals®, Germany) for at least 40 minutes. Dishes were then washed with water and colonies were counted by the naked eye. The survival fraction (SF) was calculated by comparing the average number of colonies formed from the treated cells to that of untreated cells, as shown in the following Equation 2.3:

$$SF = \frac{Average\ number\ of\ colonies\ in\ treated\ celles}{Average\ number\ of\ colonies\ in\ untreated\ cells} \quad \text{Equation 2.3}$$

2.7 Combination index analysis

To assess the interaction and additive, synergistic, or antagonistic relationship between two agents which both were found to be cytotoxic as single treatment, the combination index analysis, which is a mathematical algorithm based on the median-effect principal and established by Chou and Talalay (Chou and Talalay, 1984), was performed using CalcuSyn® software.

The median effect of the treatment dose for each drug used in combination and for combination therapy itself was calculated as the proportion of cells affected by the treatment dose to cells population unaffected by the treatment dose using Equation 2.4.

$$F_a/F_u = (D/IC_{50})^m \qquad \text{Equation 2.4}$$

Where $\boldsymbol{F_a}$ is the fraction of the cell population affected; F_u is the fraction of the cell population unaffected by the dose ($\boldsymbol{D}$); $\boldsymbol{m}$ is the hill-slope of the curve, and $\boldsymbol{IC_{50}}$ is the dose that inhibited 50% of colony formation.

In order to plot the dose-effect curve in GraphPad Prism®, the previous equation was solved for $\boldsymbol{F_a}$ as shown in Equation 2.5.

$$F_a = \frac{D^m}{D^m + {IC_{50}}^m} \qquad \text{Equation 2.5}$$

The median-effect equation was then linearized to the logarithmic form (Equation 2.6) to convert it to a straight-line equation, where the coefficient $\boldsymbol{m}$ becomes the slope of the line.

$$\log F_a/F_u = m\log(D) - m\log(IC_{50}) \qquad \text{Equation 2.6}$$

IC50 was calculated from the x-intercept (log*IC50*) and the coefficient m (slope) was determined for each treatment from the previous equation, the dose of constituent drugs and the combination required to produce a set amount of toxicity was determined using Equation 2.7:

$$D = IC_{50}(F_a/F_u)^{1/m} \qquad \text{Equation 2.7}$$

The median effect plot gives the slope of each line, the *m* value, and the intercept of the dose-effect axis and the median-effect axis, which allows for an accurate IC_{50} measurement to be taken. The linear regression coefficient of the median effect plot for each drug or combination determines the suitability of the use of combination index analysis. If the median effect plot of the

constituent drugs is parallel, it is assumed that the modes of action of the constituent drugs are mutually exclusive and the effect of the combination can be described using Equation 2.8.

$$CI = \frac{(D)_1}{(D_x)_1} + \frac{(D)_2}{(D_x)_2} \qquad \text{Equation 2.8}$$

Where D is the dose of each constituent drug used in combination required to inhibit x percentage of cells, and D_x is the dose of each constituent drug required to inhibit x percentage of cells as a single agent and CI is the combination index, a value that describes the nature of the combination. A CI value of > 1.1 indicates infra-additivity (antagonism), a value between 0.9 and 1.1 indicates additivity, and a CI value < 0.9 indicates supra-additivity (synergism).

2.8 Linear quadratic analysis

To assess mathematically the ability of gemcitabine plus the TKI to sensitise pancreatic cancer cell lines (PANC-1 and MIA PaCa-2) to XBR, the experimental clonogenic survival data for cells exposed to XBR alone and in combination with gemcitabine plus sunitinib was fitted to the linear-quadratic model which describes the relationship between radiation dose and cell survival. For the ability to manage the experiment in terms of possible combination, these values together were treated for the purpose of the linear-

quadratic equation and combination index analysis as a single treatment, as has been previously reported for other triples (McCluskey *et al.*, 2012).

The most widely used model for cell survival is the linear-quadratic (LQ) model, and it was first used in 1942 by Lea and Catcheside (Lea *et al.*, 1942) to fit radiation-induced chromosome damage (Scheidegger *et al.*, 2013). This mathematical model is based on the observation that the logarithmic plot of the surviving cell fraction (*SF*) versus radiation dose (*D*) (Equation 2.9) can be described by a linear component (α coefficient) and a quadratic dose-dependent component (β coefficient) (Scheidegger *et al.*, 2013).

The linear component (α coefficient) represents the initial slope of the survival curve at low radiation doses, in which the cytotoxicity, resulted from the single-particle ionisation events, increases linearly with radiation dose. The quadratic component (β coefficient) describes the latter slope of the survival curve, in which the cytotoxicity, resulted from two independent ionisation events and accumulation of sub-lethal lesions, increases in proportion to the square of the dose (Barendsen, 1997; Franken *et al.*, 2001).

$$SF = e^{-(\alpha D + \beta D)} \qquad \text{Equation 2.9}$$

Where SF denotes the survival fraction at XBR dose (D). The α and β coefficients are the linear and the quadratic phases of the curve, respectively.

GraphPad Prism software, version 7.0, was used to fit the experimental clonogenic survival fractions to the linear-quadratic model (Equation 2.9) and to obtain the linear component (α coefficient) and the quadratic component (β coefficient) values.

Equation 2.10 was used to calculate the IC_{50} from the linear-quadratic survival curve of PANC-1 and MIA PaCa-2 cells after exposure to XBR alone or in combination with gemcitabine plus sunitinib (Chou and Talalay, 1984).

$$IC_{50} = \frac{-\alpha \pm \sqrt{(\alpha^2 - 4\,\beta \ln 0.5)}}{2\,\beta} \qquad \text{Equation 2.10}$$

2.9 Dose enhancement factor (DEF)

Sensitisation of pancreatic cancer cell lines to gemcitabine was assessed by co-administration of increasing concentrations of gemcitabine with fixed doses of sunitinib, pazopanib, or XBR. The survival fraction of the cells (as described in section 2.6) following the exposure to the combination of gemcitabine with the sensitizer (normalised to the survival fraction following gemcitabine alone) was compared to the effect of the survival fraction following the exposure to gemcitabine alone. The ratio between the IC_{50} of gemcitabine alone to the IC_{50} of gemcitabine in the presence of the sensitizer was calculated using Equation 2.11. The resultant ratio is described as a dose enhancement factor (Roeske *et al.*, 2007) or a sensitisation factor (Wang *et al.*, 2015).

$$DEF_{IC50} = \frac{IC_{50}\ [Gemcitabine\ alone]}{IC_{50}\ [Gemcitabine + Sensitiser)} \qquad \text{Equation 2.11}$$

2.10 Cell cycle analysis

The effect of gemcitabine, sunitinib, pazopanib, or XBR alone or in combination on the cell cycle progression of the pancreatic cancer cell lines was assessed with Fluorescence-Activated Cell Sorting (FACS) analysis. PANC-1 and MIA PaCa-2 cells were seeded at 1 × 10^5 cells in 25 cm^3 flasks and incubated for 48 hours until the exponential growth phase was reached (approximately 60-70% confluence). Cells then were exposed to XBR or treated with gemcitabine, sunitinib, or pazopanib as described in sections 2.4.1, 2.4.3, and 2.4.4. Following 48 hours of treatment, the growth medium containing treatment was decanted and replaced with drug-free fresh growth media and incubated for 4, 24, or 48 hours. These time-points after treatment cessation were chosen in order to allow cells to arrest and induce apoptosis (Ochs and Kaina, 2000). After that, cells were washed with PBS, detached using Accutase® solution (Sigma, UK), and centrifuged at 1400 RPM for 5 minutes. The supernatant was removed, and cells were washed with PBS and re-pelleted at 1400 RPM, for 5 minutes.

Cells were fixed in 3 ml of 70% ice-cold ethanol and incubated at 4^{o}C for at least 1 hour in the case of the same-day analysis or at -20^{o}C for later analysis. On the day of analysis, fixed cells were pelleted by centrifugation at 1400 RPM

for 5 minutes, ethanol supernatant was removed, and cells were re-suspended and centrifuged twice with 10 ml of cold PBS at 1400 RPM for 10 minutes. The PBS was then removed, and pellets were suspended in 250 µL distilled water containing 10 µg/mL propidium iodide (PI) (Sigma-Aldrich®, Gillingham, UK) to label DNA content and 50 µg/mL RNase (Sigma-Aldrich®, Gillingham, UK) to degrade the RNA and ensure only DNA, not RNA, is stained. Falcon tubes, which contained the cell suspension were incubated on ice in the dark for at least 1 hour before the cell cycle distribution was analysed in the FACSCanto machine (Becton Dickinson Systems, Cowley, UK) and data were analysed using BD CellQuest^{TM} Pro software (version 5.1.1). Three independent experiments were carried out with a minimum of 10,000 cells/sample and results presented as the percentage of cells in each phase of the cell cycle [mean ± standard deviation (SD)].

2.11 Annexin V apoptosis detection assay

Apoptosis is a programmed and a physiological cell death that plays an important role in tissue homeostasis (Van Engeland *et al.*, 1998). The imbalance between cell proliferation and apoptosis is one of the hallmarks of cancer (Hanahan and Weinberg, 2000). Understanding of the basic mechanisms that underlie apoptosis will enhance the treatment of cancer (Van Engeland *et al.*, 1998).

The FITC Annexin V assay was used to determine the percentage of cells within a population that were undergoing apoptosis. In the early stages of

apoptosis, several alterations occur at the cell membrane. One of these changes is the translocation of the membrane phospholipid phosphatidylserine (PS) from the inner side of the plasma membrane to the outer layer, by which PS becomes exposed at the external surface of the cell (Vermes *et al.*, 1995). Fluorescently FITC-labelled Annexin V, which is a calcium-dependent phospholipid-binding protein that has a high affinity for PS, is used to specifically target and identify cells in early apoptosis with exposed PS (Vermes *et al.*, 1995). Annexin V cannot bind to viable cells since the molecule is not able to penetrate the phospholipid bilayer, whereas, in the dead cells, the inner leaflet of the membrane, due to the loss of its integrity, is available for binding with Annexin V (Van Engeland *et al.*, 1998). Propidium iodide (PI), a membrane-impermeable DNA stain, is used to discriminate between dead and apoptotic cells. Viable cells with intact membranes exclude PI, whereas the membranes of dead and damaged cells are permeable to PI (Van Engeland *et al.*, 1998). Therefore, cells that stain negative for both FITC Annexin V and PI are alive and not undergoing measurable apoptosis. Cells that stain positive for FITC Annexin V and negative for PI are undergoing early apoptosis. Cells that stain positive for both FITC Annexin V and PI are in the end stage of apoptosis. Finally, cells that stain positive for PI and negative for FITC Annexin V are either undergoing necrosis or are already dead (Vermes *et al.*, 1995).

Pancreatic cancer cell lines (PANC-1 or MIA PaCa-2) were seeded at 1×10^5 cells in 25 cm^3 flasks and incubated for 48 hours until the exponential growth phase was reached (approximately 60-70% confluence). The cells were then

exposed to XBR or treated with increasing dosing of gemcitabine, sunitinib, or pazopanib as described in sections 2.4.1, 2.4.3, and 2.4.4. Following 48 hours of treatment, the growth medium containing treatment was replaced with drug-free fresh growth media, and cells were incubated at 37ºC and 5% CO_2 atmosphere for 4, 24, or 48 hours. These time-points after treatment cessation were chosen in order to allow cells to arrest and induce apoptosis (Ochs and Kaina, 2000). After that, cells were washed with PBS and detached from flask surface using Accutase® solution. The cell suspension was then centrifuged at 1400 RPM for 5 minutes. The supernatant was removed and cell pellets were washed twice with cold PBS and resuspended at a concentration of 1×10^6 cells/ml in 1X Annexin V binding buffer solution; 1 part of 10X Annexin V binding buffer (BD Bioscience, Oxford, UK) diluted in 9 parts of distilled water. 100 µL of each sample, containing 1×10^5 cells, was transferred to a FACs tube, gently vortexed, and incubated for 15 minutes at room temperature (25°C) in the dark with 5 µL of FITC Annexin V stain and 5 µL of PI (BD Bioscience, Oxford, UK). Three controls were also prepared to set up the analysis compensation and quadrants; unstained cells, cells stained with FITC Annexin V stain only, and cells stained with PI only. 400 µl of Annexin V staining buffer was then added to each sample. Flow cytometry analysis was performed within one hour using the BD FACSCanto analyser (Becton Dickinson Systems, Cowley, UK), with 10,000 events per sample measured. The percentage of apoptotic cells was the total count which resulted from the addition of the percentage of cells in early apoptosis (quadrant 2; with Annexin V positive and PI negative) and the percentage of cells in late apoptosis

(quadrant 3; with both positive staining for both FITC Annexin V and PI) (*see* Figure 2.2). The data were analysed using BD FACSDiva, V6.13 software. Data reported was an average of three independent experiments ± SD.

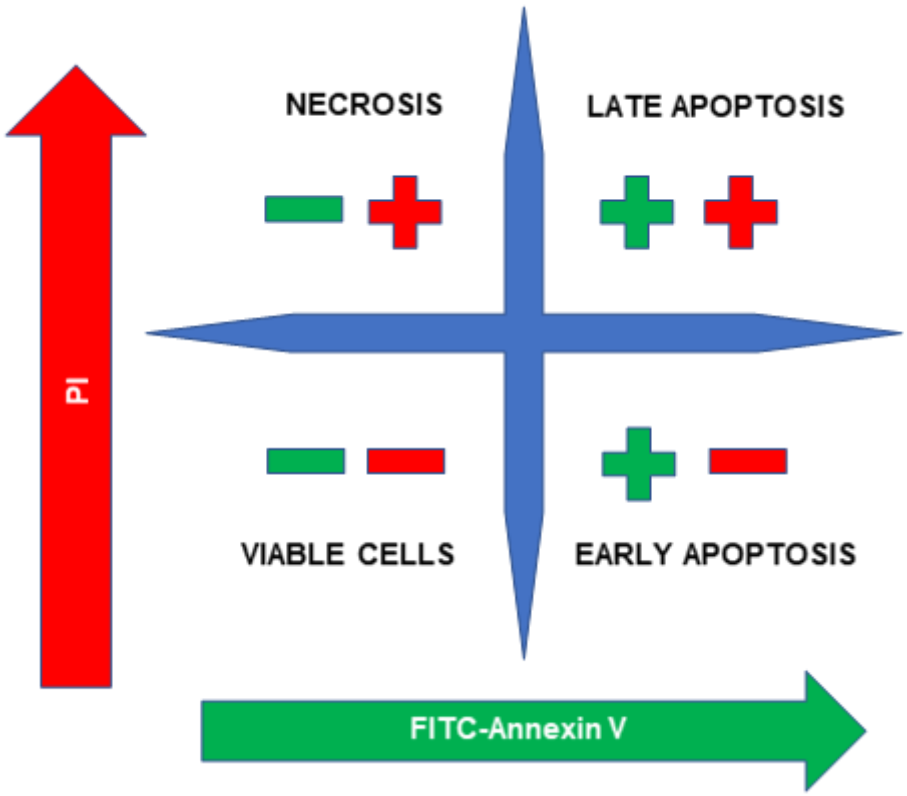

Figure 2.2 Stages of apoptosis after detection with FITC-Annexin V assay (Original figure).

2.12 DNA damage γ-H_2AX detection analysis

Histone (H_2AX) is a key factor protein in the repair process of damaged DNA (Kuo and Yang, 2008). When DNA double-stranded breaks (DSBs) damage occurs, H_2AX is phosphorylated on the 139th serine residue to form γ-H_2AX. This biomarker of DSBs DNA damage can be conjugated to an antibody (FITC-conjugated anti-phospho-histone H_2AX Ser139) and used in detection and visualization the magnitude of DSBs damage by flow cytometry. γ-H_2AX detection assay is more precise and sensitive to DSBs than the other techniques, such as a comet, pulse-field electrophoresis (2-D gel electrophoresis) and neutral elution assays (Kuo and Yang, 2008). H_2AX assay is used to assess both DNA damage initiation and its repair. Therefore, γ-H_2AX expression was measured at three time-points (4, 24, and 48 hours after treatment) to investigate the damage caused to the DNA and more important to explore if this damage was repaired. The less DNA repair the more cancer cell death and the more efficacy of the cytotoxic agent.

Pancreatic cancer cell lines (PANC-1 or MIA PaCa-2) were seeded at 1×10^5 cells in 25 cm^3 flasks and incubated for 48 hours until the exponential growth phase was reached (approximately 60-70% confluence). The cells were then exposed to XBR or treated with gemcitabine, sunitinib, or pazopanib as described in sections 2.4.1, 2.4.3, and 2.4.4. Following 48 hours of treatment, the growth medium containing the drug was replaced with drug-free fresh growth media and then cells incubated at 37^{o}C and 5% CO_2 atmosphere for 4,

24, or 48 hours. These time-points after treatment cessation were chosen to allow cells to arrest and induce apoptosis (Ochs and Kaina, 2000). Cells were then washed with PBS and detached from the flask surface using Accutase® solution. The cell suspension was pelleted in a centrifuge for 5 minutes at 1400 RPM and washed twice in PBS. The cells were then fixed in 500 µl of 4% paraformaldehyde for 20 minutes at 25°C. Cells were washed twice in PBS to remove the fixative solution and permeabilised by resuspension at a density of 2×10^6 cells/ml in 0.3% (V/V) Triton-X (Sigma-Aldrich®, UK) for 30 minutes. 50 µl of each sample was then re-suspended in 100 µl blocking buffer, containing 0.1% Triton-X and 0.5% bovine serum albumin (BSA; Sigma-Aldrich®, UK). The cell samples were then stained with 2 µl of 100 µg/ml FITC-conjugated anti-phospho-histone H_2AX (Ser139) antibody (Millipore®, Watford, UK) and incubated on ice for 20 minutes in the dark. Following the staining period, the excess antibody was washed in 500 µl of blocking buffer and re-centrifuged at 1400 RPM for 5 minutes. Finally, samples were re-suspended in 150 µl of FACs buffer (PBS containing 0.5% BSA), transferred to FACS tube and analysed within one hour using the BD FACSCanto analyser, with 10,000 events per sample measured. The data were analysed using BD FACSDiva, V6.13 software and reported as an average of three independent experiments ± SD, expressed as fold change in γ-H_2AX of treated samples normalised to untreated control.

2.13 *In vivo* experiment

2.13.1 Experimental Animals

Six-week-old female, congenitally athymic nude mice of strain MF1 nu/nu were obtained from Charles River PLC (Kent, United Kingdom). *In vivo* experiments were performed in accordance with the UK Coordinating Committee on Cancer Research guidelines for the welfare of animals in experimental neoplasia (Workman *et al.*, 1998). All work was carried out under Home Office project licence P164B98DA and following approval from the University of Strathclyde Ethics committee.

2.13.2 Tumour Xenografts

PANC-1 xenografts were established in nude mice by subcutaneous injection of 4×10^6 exponentially growing PANC-1 cells, freshly harvested at 60%–70% confluency. After 18 days, mice which harboured tumours of volume of approximately 65 mm^3 (5 × 5 millimetres in diameter) were randomised into six treatment groups of eight or nine mice each. This number was utilised as power calculations determined sample size of all groups totalling to 48 was required to detect a medium effect size of 0.54 with power (1-β) of 0.78 at 0.05 α level. Power study was conducted using G*Power Software, version 3.1 for Windows®.

2.13.3 Tumour Therapy

Control groups of mice received PBS (once a week, 100 µl by intraperitoneal injection) and the treatment experimental groups received gemcitabine (180 mg/kg dissolved in PBS, administered once a week, 100 µl by intraperitoneal injection) alone, sunitinib (40 mg/kg dissolved in PBS, administered daily, 250 µl by oral gavage) alone, XBR (5 Gy, single-dose at day 0, as described in section 2.4.3) alone, a concurrent combination of gemcitabine plus sunitinib, or triple therapy with single XBR dose administered at day 0 prior to concurrent combination of gemcitabine and sunitinib. Doses of gemcitabine and sunitinib were based on the median weekly doses (mg/kg) used in previous *in vivo* studies and shown in Figure 2.3. Appendix A shows a table summarises using gemcitabine in 16 published *in vivo* studies.

To monitor potential toxicity, body weight was measured three times weekly and experimental animals were evaluated for signs of distress using standard guidelines (Morton & Griffiths, 1985). In compliance with the project licence, mice whose xenografts diameter reached 16 mm in any direction or lost more than 20% of their initial body weight were euthanized.

Subcutaneous tumours were measured with digital Vernier callipers every two or three days after the treatment. On the assumption of ellipsoidal geometry (Graham and Freshney, 2000), diameter measurements were converted to an approximate volume using Equation 2.12.

A

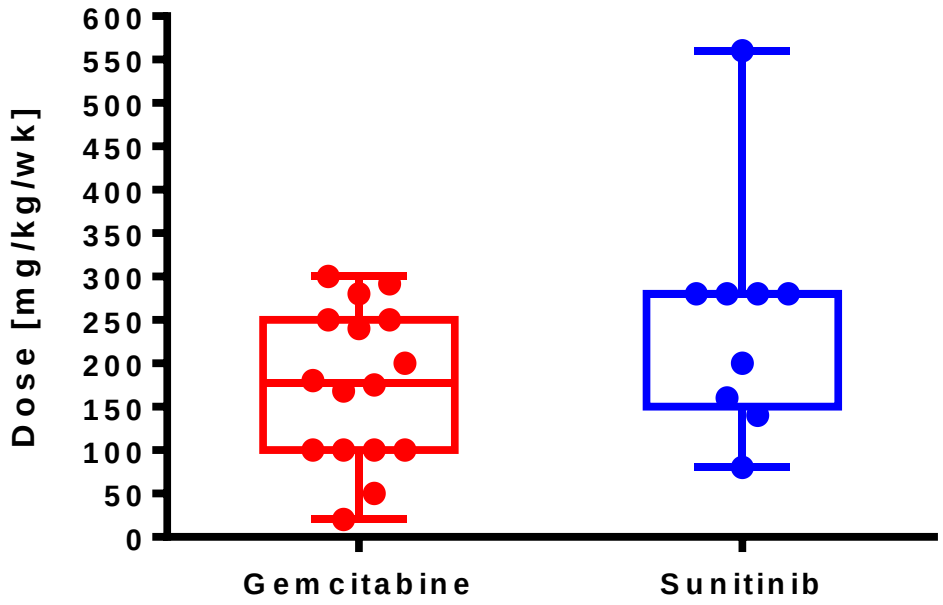

B

Descriptive analysis	Gemcitabine	Sunitinib
Number of studies	16	9
Minimum weekly dose	20.00	80.00
25% Percentile	100.0	150.0
Median weekly dose	**177.5**	**280.0**
75% Percentile	250.0	280.0
Maximum weekly dose	300.0	560.0
Mean weekly dose	175.3	251.1
Std. Deviation	88.91	137.5
Std. Error of Mean	22.23	45.84
Lower 95% CI of mean	127.9	145.4
Upper 95% CI of mean	222.7	356.8

Figure 2.3 Doses of gemcitabine and sunitinib used in previous *in vivo* studies (mg/kg/week).

$$Tumour\ volume = \frac{1}{6} \times \pi \times A \times B^2 \qquad \text{Equation 2.12}$$

Where $\boldsymbol{\pi} \approx 3.14$, ***A*** is the longest tumour diameter, and ***B*** is the shortest diameter.

For each animal, relative tumour volume (volume at any time-point divided by volume immediately before treatment) was plotted against time, and the area under the time–volume curves was determined by trapezoidal approximation (Sorensen *et al.*, 2012). The area under the time–volume curves was used as a measure of treatment effectiveness for the purpose of comparison between groups. For animals that were euthanized because of rapid tumour growth, before the termination of the experiment, the tumour volume curve was extrapolated at constant volume from the time of euthanasia (Sorensen *et al.*, 2012).

2.13.4 Tumour growth inhibition and delay

Tumour growth inhibition (%TGI) was determined on the last day of the study, day 20, using Equation 2.13.

$$TGI(\%) = (1 - \frac{V_{t_1}/V_{t_0}}{V_{C_1}/V_{C_0}}) * 100 \qquad \text{Equation 2.13}$$

Where V_{t1} = mean tumour volume of the treated group at time t; V_{t0} = mean tumour volume of the treated group at day 0; V_{C1} = mean tumour volume of control at time t, and V_{C0} = mean tumour volume of control at day 0.

Moreover, the mean time taken for a two-fold increase in tumour volume (T_2) or elimination from the study was calculated for each mouse. Furthermore, the growth delay is calculated as T – C; where T and C are times in days for mean tumour volume in the treated (T) and control (C) groups to reach 200% of the initial tumour volume.

2.14 Statistical analysis

Unless otherwise stated, experimental results were expressed as means and SDs of triplicate determinations from three independent experiments. A dose-response (inhibition) non-linear regression curve (with the least square models) was fitted to the experimental results, as described in GraphPad Prism's user manual (Motulsky, no date), and IC_{50s} for all cytotoxic drugs were determined. One-way or two-way analysis of variance (ANOVA) and Dunnett's or Bonferroni multiple comparison tests, where appropriate, were employed to evaluate the degree of significance in the difference between untreated cells and each dose of treated cells. For the *in vivo* study, differences in tumour

growth between experimental therapy groups were assessed by the Kruskal–Wallis test, followed by the Mann–Whitney U posthoc test. *P*-values of less than 0.05 were deemed to represent statistically significant group differences. Statistical analysis and graph presentation were carried out and generated using GraphPad Prism® (version 7.00) software for Windows®.

CHAPTER 3: Cytotoxicity evaluation of single chemotherapy on pancreatic cancer cells *in vitro*

3.1 Introduction

In order to develop effective combinations for treating pancreatic cancer, the cytotoxicity of the gold standard antimetabolite, gemcitabine, and two tyrosine kinase inhibitors, sunitinib and pazopanib, were examined as a single treatment on two pancreatic cancer cell lines (PANC-1 and MIA PaCa-2). Based on this data, novel combinations (based upon various delivery schedules) of these treatment options were designed and, then, evaluated in further studies (Chapter 4).

To assess the cytotoxicity of gemcitabine and TKIs as single treatment, both cell lines were treated for 24 hours with single drugs as a reasonable starting point. However, when IC_{50s} for single agents were found to be higher compared to the literature, doubling time for cells was assessed. In response to the doubling time results, the responses of cell lines were re-assessed following the exposure to 48-hour treatment to ensure cells to duplicate at least once in the presence of cytotoxic agents.

Cytotoxicity studies with the monotherapy were performed, in order to assess the effect of anti-cancer agents on the pancreatic cancer cell lines and to generate IC_{50} values which were used in combination therapy, using two

different methods. Firstly, the cell viability assay, in which the short-term cytotoxic effect of each drug on cell viability was evaluated with alamar blue assay (described in section 2.5), in order to explore and narrow down dose ranges of drug required to be utilised in the second method. Originally, we investigated a broader range of conncentrations of each cytotoxic agent, and then those range of concentrations were adjusted and narrowed down according to the resultant IC_{50} from the alamar blue assay. Secondly, the clonogenic assay (described in section 2.6), which is more robust than the viability test and is considered the gold standard method to determine the effectiveness of cytotoxic agents.

Based on the results of cell survival assay following 48-hour exposure to monotherapy, combination therapy schedules were designed as described in section 2.4.4.

3.2 Aims

The primary aim of this chapter was to determine the response of PANC-1 and MIA PaCa-2 pancreatic cancer cell lines to single-agent drugs in the form of gemcitabine, sunitinib, or, for the first time, pazopanib. The second aim was to design a combination therapy based on the IC_{50s} and outcome of treatment with monotherapy.

3.3 Results

3.3.1 Cell viability of PANC-1 and MIA PaCa-2 cells following 24-hour treatment with anti-cancer agents

In these experiments, alamar blue assay was conducted, as described in section 2.5, to assess the cytotoxic effect of gemcitabine, sunitinib, or pazopanib on cell viability of PANC-1 and MIA PaCa-2 cells. Alamar blue assay was utilised to enable narrowing of the dose ranges that would be utilised in the clonogenic assays which are more informative of the long-term effect of treatments on cell viability. The calculated cell viability was normalised to the untreated control group and then plotted on the Y-axis against logarithmic drug concentrations on the X-axis. IC_{50} values were calculated using non-linear regression curve fitting (the least-squares fit) of survival fraction using GraphPad Prism® software, version 7.00, as described in GraphPad Prism's user manual (Motulsky, no date).

3.3.1.1 Cell viability of PANC-1 and MIA PaCa-2 cells following 24-hour treatment with gemcitabine

Figure 3.1 (A and B) illustrates the effect of 24-hour treatment with increasing doses of gemcitabine (50, 100, 200, 400, and 800 µM) on the viability of PANC-1 and MIA PaCa-2 pancreatic cancer cell lines. There was a clear dose-dependent reduction in viability of both cell lines following 24-hour incubation with gemcitabine. PANC-1 was found to be more sensitive to gemcitabine than MIA PaCa-2 cells. The two lowest doses of gemcitabine (50 and 100 µM) failed

to decrease cell viability significantly in both cell lines compared to untreated controls ($p > 0.05$). However, all the subsequent gemcitabine concentrations reduced cell viability significantly ($p < 0.001$) in both PANC-1 and MIA PaCa-2 cell lines compared to untreated control cells. The calculated IC_{50} was 329.6 µM and 378.44 µM in PANC-1 and MIA PaCa-2, respectively (Table 3.1)

3.3.1.2 Cell viability of PANC-1 and MIA PaCa-2 cells following 24-hour treatment with sunitinib

Figure 3.1 (C and D) shows the effect of 24-hour treatment with increasing doses of sunitinib (1, 5, 10, 20, and 40 µM) on the cell viability of PANC-1 and MIA PaCa-2 pancreatic cancer cell lines. It can be observed that 24-hour treatment with sunitinib reduced the cell viability in a dose-dependent manner in both cell lines. PANC-1 was found to be more sensitive to sunitinib than MIA PaCa-2 cells. The lowest concentration of sunitinib used in the experiment (1 µM) failed to decrease cell viability significantly in both cell lines compared to untreated controls ($p > 0.05$), while 5 µM of sunitinib reduced the cell viability significantly in PANC-1 cell line only ($p < 0.01$). However, all the subsequent sunitinib concentrations resulted in a statistically significant ($p < 0.01$) viability inhibition in both PANC-1 and MIA PaCa-2 cell lines. The calculated IC_{50} was 12.05 µM and 21.53 µM in PANC-1 and MIA PaCa-2, respectively (Table 3.1).

3.3.1.3 Cell viability of PANC-1 and MIA PaCa-2 cells following 24-hour treatment with pazopanib

Figure 3.1 (E and F) demonstrates the effect of 24-hour treatment with increasing doses of pazopanib (1, 5, 10, 20, and 40 μM) on the viability of PANC-1 and MIA PaCa-2 pancreatic cancer cell lines. It has been found that incubation of cells with increasing doses of pazopanib for 24 hours failed to inhibit the cell viability of either pancreatic cancer cell line ($p > 0.05$).

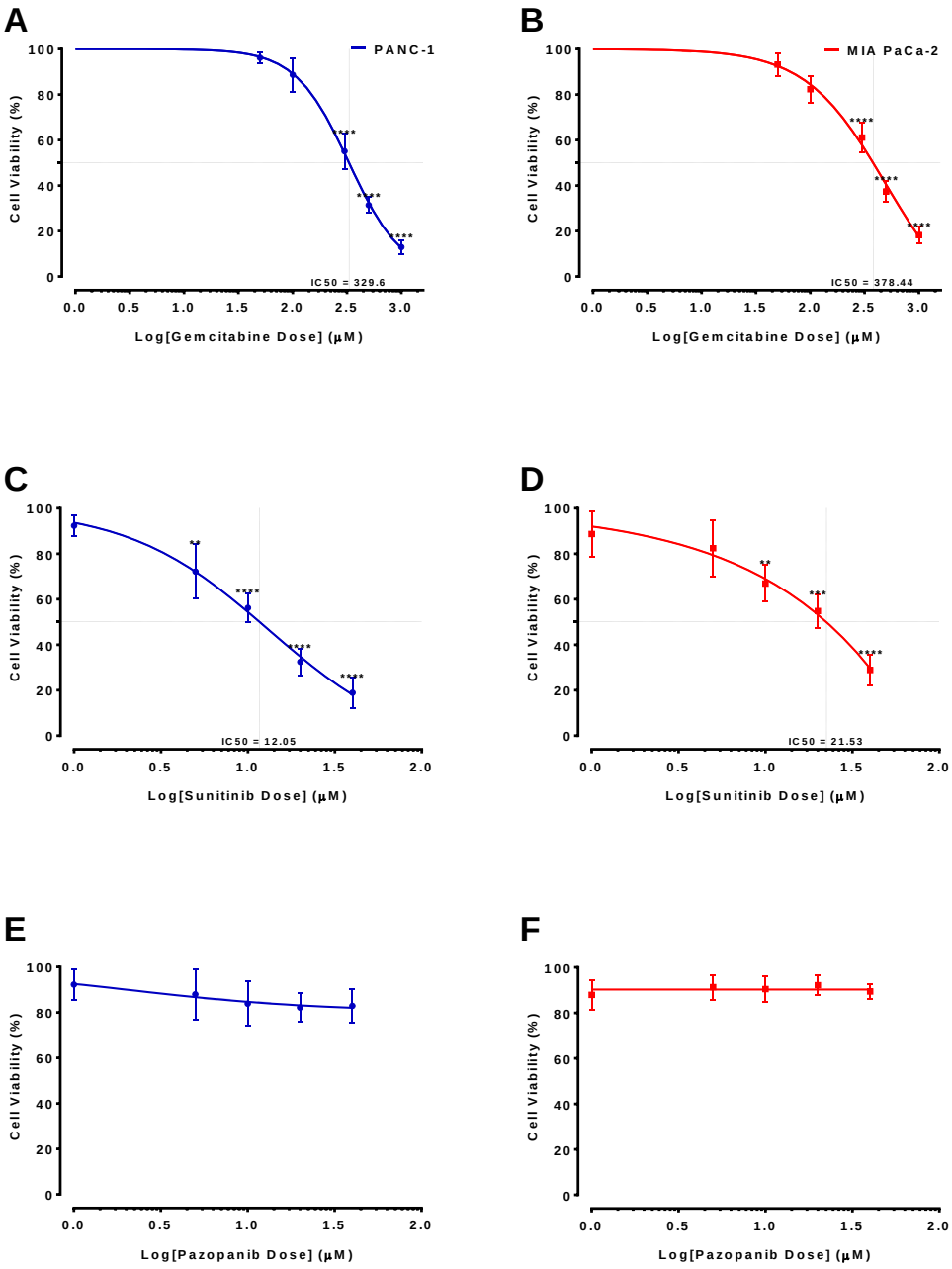

Figure 3.1 Effect of cytotoxic therapy on cell viability of PANC-1 and MIA PaCa-2 cell lines following to 24-hour treatment exposure.

Cells were treated with **A&B)** 50-800µM of gemcitabine, **C&D)** 1-40µM of sunitinib, and **E&F)** 1-40µM of pazopanib for 24 hours and then cell viability was measured by alamar blue assay. Data shown are expressed as a percentage of cell viability normalised to the control group. Statistical analysis was carried out using a one-way ANOVA with Dunnett's posthoc to compare all treatment doses to control group. Each value represents the mean ± SD of three independent experiments. *P<0.05, **P<0.01, ***P<0.001, and ****P<0.0001 compared to the untreated control group. IC_{50} values were calculated using non-linear regression curve fitting (the least-squares fit) of survival fraction using GraphPad Prism® software, version 7.0.

Table 3.1 IC_{50} of the tested anti-cancer drugs following 24 hours of exposure (in µM), determined by Alamar Blue® assay. NA=Not Achieved.

Drug	PANC-1	MIA PaCa-2
Gemcitabine	330	378
Sunitinib	12	22
Pazopanib	NA	NA

3.3.2 Clonogenic survival assay of PANC-1 and MIA PaCa-2 cells following 24 treatment with anti-cancer agents

In contrast to cell viability assay using the alamar blue dye, which was conducted to assess short term cytotoxicity, clonogenic assay was employed to assess the delayed cytotoxic effect chemotherapeutic agents (gemcitabine, sunitinib, or pazopanib) on PANC-1 and MIA PaCa-2 cells in terms of inhibition of cell division and colony formation. It is considered the gold standard and the method of choice to determine the effectiveness of ionizing radiation and other cytotoxic agents on the long-term survival of cancer cells (Franken *et al.*, 2006).

Materials and methods of the clonogenic assay were described in detail in Section 2.6. The calculated survival fraction using Equation 2.3 (explained in Section 2.6) was normalised to the control group and then plotted on the Y-axis against drug concentrations on the X-axis. IC_{50} values were calculated using non-linear regression curve fitting (the least-squares fit) of survival fraction using GraphPad Prism® software, version 7.00, as described in GraphPad Prism's user manual (Motulsky, no date).

3.3.2.1 Clonogenic survival assay of PANC-1 and MIA PaCa-2 cells following 24-hour treatment with gemcitabine

Figure 3.2 (A and B) shows the effects of 24-hour treatment with increasing doses of gemcitabine (50, 100, 200, 400, and 800 μM) on the survival fraction

of PANC-1 and MIA PaCa-2 pancreatic cell lines. It can be observed that gemcitabine reduced the survival fraction in both cell lines in a dose-dependent manner. PANC-1 cells were more sensitive to gemcitabine, especially at lower doses, than MIA PaCa-2 cells. The two lowest concentrations of gemcitabine tested in this experiment (50 and 100 μM) reduced the survival fraction significantly to 62.6 ± 5% and 53.7 ± 8%, respectively ($p < 0.0001$) in PANC-1 cell line, and to 80.1 ± 5.8% and 63 ± 10.7%, respectively ($p < 0.05$) in MIA PaCa-2 cells, compared to the untreated control cells. The calculated IC_{50} of gemcitabine was approximately 123.6 ($R^2 = 0.98$) and 162.55 ($R^2 = 0.97$) μM in PANC-1 and MIA PaCa-2 cell lines, respectively (Table 3.2).

3.3.2.2 Clonogenic survival assay of PANC-1 and MIA PaCa-2 cells following 24-hour treatment with sunitinib

Figure 3.2 (C and D) demonstrates the effects of 24-hour treatment with increasing doses of sunitinib (10, 20, 40, and 80 μM) on the survival fraction of PANC-1 and MIA PaCa-2 cells. There was a considerable reduction in the survival fraction of both cell lines in a dose-dependent manner following 24-hour sunitinib treatment compared to untreated cells. There was no statistically significant reduction in survival in both cell lines compared to the control using the lowest concentration of sunitinib tested in this experiment (10 μM). However, The second tested dose of sunitinib (20 μM) inhibited survival significantly compared to untreated cells to 72.7 ± 7.4% ($p < 0.01$) and 63.9 ± 9.4% ($p < 0.05$) in PANC-1 and MIA PaCa-2 cell lines, respectively. The highest concentration of sunitinib (80 μM) decreased the cell survival

significantly to 32.7 ± 5.6% in PANC-1 and to 33.9 ± 5% in MIA PaCa-2 cells ($p < 0.0001$) compared to untreated cells. The calculated IC_{50} of sunitinib was lower in MIA PaCa-2 cells (31.12 μM; $R^2 = 0.96$) than in PANC-1 (44.36 μM; $R^2 = 0.96$) (Table 3.2).

3.3.2.3 Clonogenic survival assay of PANC-1 and MIA PaCa-2 cells following 24-hour treatment with pazopanib

Figure 3.2 (E and F) illustrates the effects of 24-hour treatment with increasing concentrations of pazopanib (10, 20, 40, and 80 μM) on the survival fraction of PANC-1 and MIA PaCa-2 pancreatic cancer cell lines. It has been found that incubation of cells with increasing doses of pazopanib for 24 hours failed to inhibit the survival of both pancreatic cancer cell lines ($p > 0.05$). There was an exception of the highest examined dose of pazopanib (80 μM) which it decreased the survival of PANC-1 cells significantly to 65.5 ± 5% ($p < 0.05$) compared to untreated control cells. The IC_{50} for both cell lines were not achieved; demonstrating the resistance of both PANC-1 and MIA PaCa-2 pancreatic cancer cell lines to pazopanib compared to the other drugs (i.e. gemcitabine and sunitinib).

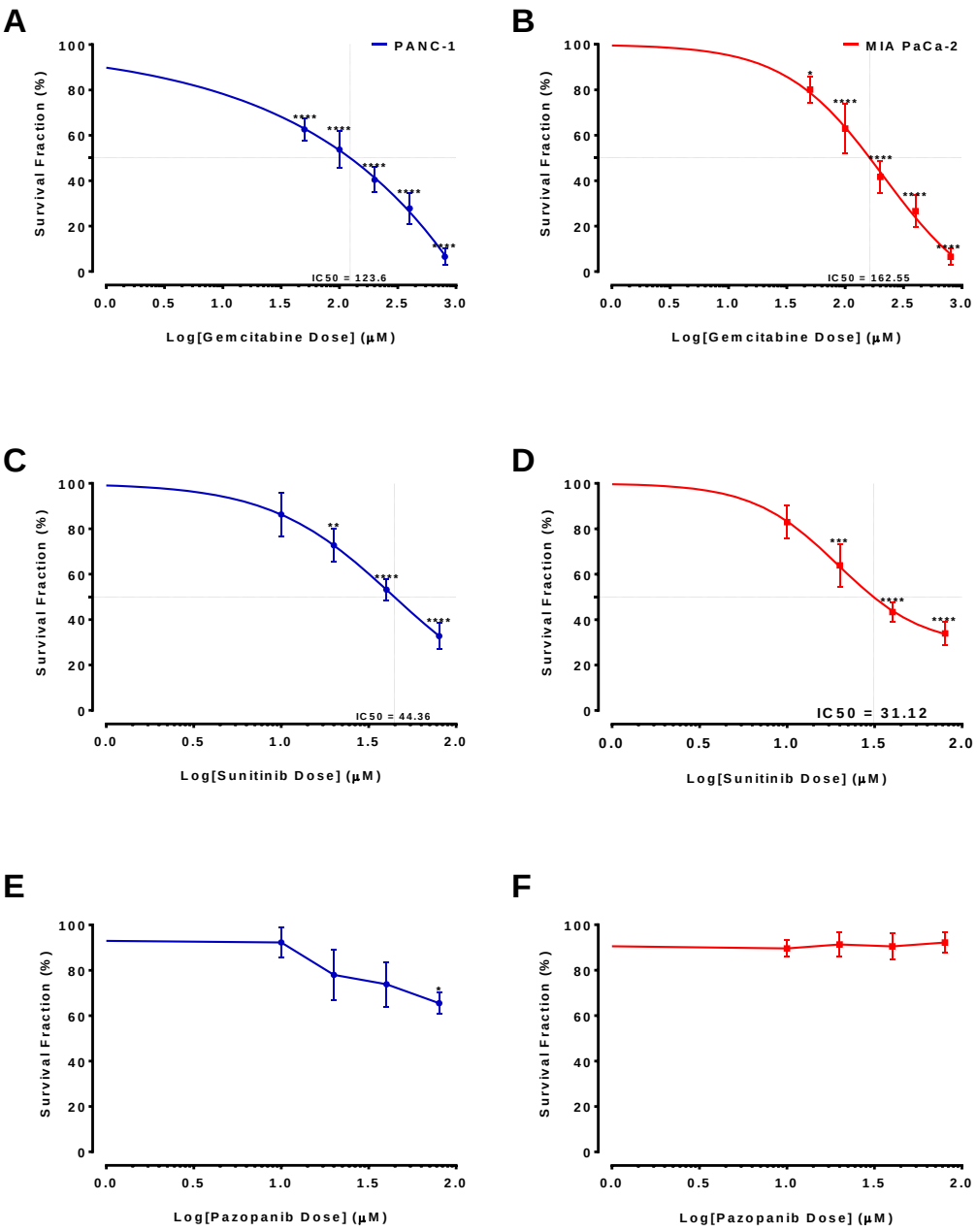

Figure 3.2 Effect of cytotoxic therapy on survival fraction of PANC-1 and MIA PaCa-2 cell lines following to 24-hour treatment exposure.

Cells were treated with **A&B)** 50-800µM of gemcitabine, **C&D)** 10-80µM of sunitinib, and **E&F)** 10-80µM of pazopanib for 24 hours and then survival fraction was measured by clonogenic assay. Data shown are expressed as a percentage of survival fraction normalised to the control group. Statistical analysis was carried out using a one-way ANOVA with Dunnett's posthoc to compare all treatment doses to control group. Each value represents the mean ± SD of three independent experiments. *P<0.05, **P<0.01, ***P<0.001, and ****P<0.0001 compared to the untreated control group. IC50 values were calculated using non-linear regression curve fitting (the least-squares fit) of survival fraction using GraphPad Prism® software, version 7.0.

Table 3.2 IC_{50} of the tested anti-cancer drugs following 24 hours of exposure (in μM), determined by clonogenic assay. NA=Not Achieved.

Drug	PANC-1	MIA PaCa-2
Gemcitabine	124	163
Sunitinib	44	31
Pazopanib	NA	NA

3.3.3 PANC-1 and MIA PaCa-2 doubling time

Doubling time is defined as the average duration of cell growth and division as reflected by the cell cycle "clock" (Bertuzzi *et al.*, 1997). This experiment aimed to determine the doubling time of pancreatic cancer cell lines (PANC-1 and MIA PaCa-2). As described in section 2.3, the doubling time was determined by plotting the growth curve for each cell line and using Equation 2.1.

The calculated doubling time for PANC-1 and MIA PaCa-2 cell lines were 30.5 ± 4.3 and 27.6 ± 2.6 hours, respectively (Figure 3.3). Therefore, both cell lines were then treated for 48 hours to allow cells to duplicate at least once in the presence of cytotoxic agents.

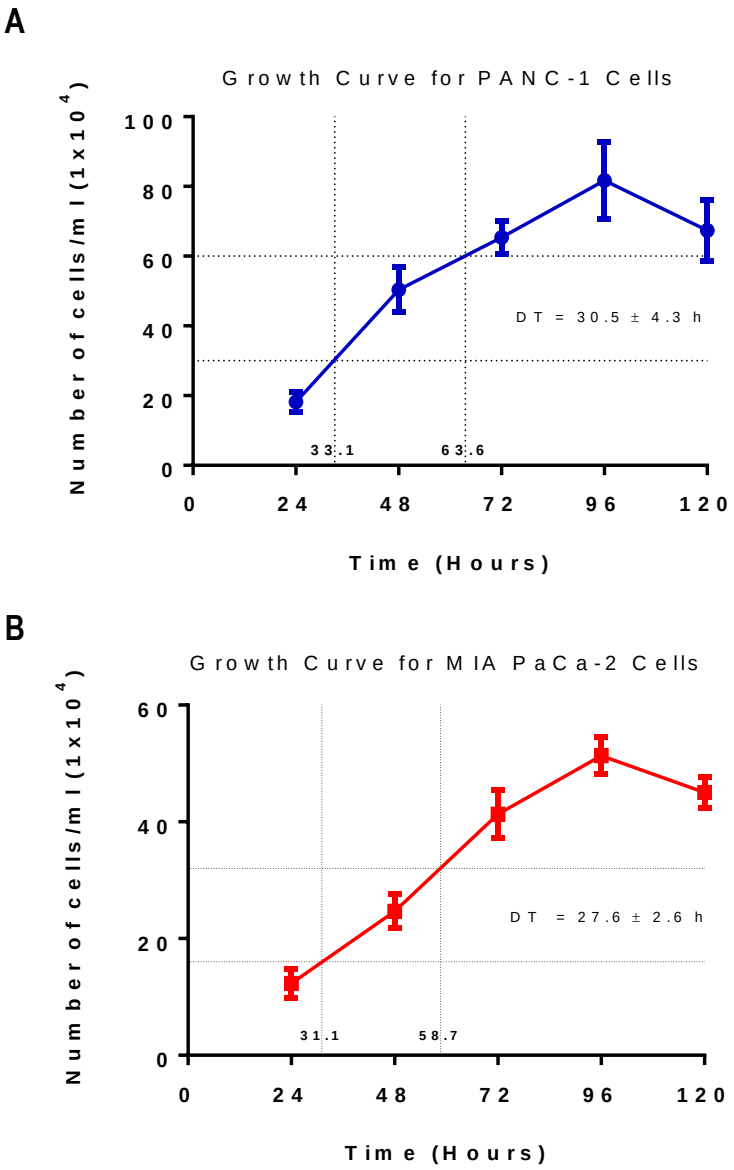

Figure 3.3 Growth curve and doubling time for pancreatic cancer cell lines.

The time taken for the cell population of **A)** PANC-1and **B)** MIA PACA-2 pancreatic cancer cells to double during the exponential growth phase was determined. The time required for the cell population to double in the exponential growth phase (DT) was calculated from the growth curve using Equation 2.1. Each value represents the mean ± SD of three independent experiments.

3.3.4 Cell viability of PANC-1 and MIA PaCa-2 cells following 48-hour treatment with anti-cancer agents

In response to the doubling time results, responses of the pancreatic cancer cell lines in terms of cell viability analysis using alamar blue assay were re-assessed following the exposure to 48-hour treatment to ensure cells to duplicate at least once in the presence of cytotoxic agents.

3.3.4.1 Cell viability of PANC-1 and MIA PaCa-2 cells following 48-hour treatment with gemcitabine

To assess the cell viability of PANC-1 and MIA PaCa-2 cells, both cell lines were treated with increasing doses of gemcitabine (10, 40, 80, 150 and 300µM) for 48 hours. Figure 3.4 (A and B) shows the effect of gemcitabine on cell viability of PANC-1 and MIA PaCa-2 cell lines, respectively. It can be observed that 48-hour treatment with gemcitabine reduced the cell viability in a dose-responsive manner in both cell lines. All administered concentrations of gemcitabine induced a significant drop in the cell viability of PANC-1 and MIA PaCa-2 cells (p <0.01). The highest administered concentration of gemcitabine in this experiment (300 µM) significantly reduced cell viability to 13.8% ± 4.4% and 18.4% ± 8.8% in PANC-1 and MIA PaCa-2 cell lines, respectively (p < 0.0001). The calculated IC_{50}, the dose which is responsible for a decrease in the cell viability of 50%, was 44.67 µM and 49.2 µM in PAN-1 and MIA PaCa-2, respectively (Table 3.3).

3.3.4.2 Cell viability of PANC-1 and MIA PaCa-2 cells following 48-hour treatment with sunitinib

Both pancreatic cancer cell lines, PANC-1 and MIA PaCa-2 were treated with increasing concentrations of sunitinib (1, 5, 10, 20, and 40 µM) for 48 hours. Figure 3.4 (C and D) shows the effect of sunitinib on cell viability of PANC-1 and MIA PaCa-2 cell lines, respectively. It can be observed that 48-hour treatment with sunitinib reduced the cell viability in a dose-responsive manner in both cell lines. However, PANC-1 was found to be more sensitive to sunitinib than MIA PaCa-2. The lowest dose of sunitinib (1 µM) failed to decrease cell viability in both cell lines compared to untreated controls ($p > 0.05$). However, the second-lowest administered dose of sunitinib (5 µM) reduced cell viability significantly to 62 ± 7% ($p < 0.0001$) and 82.8 ± 6.7% ($p < 0.01$) in PANC-1 and MIA PaCa-2, respectively. The highest sunitinib concentrations tested in this experiment (40 µM) decreased the cell viability significantly ($p < 0.0001$) to 6.6 ± 7.4% in PANC-1 cells and to 5.1 ± 4.5% in MIA PaCa-2 cells. The calculated IC_{50} was 6.49 µM and 10.4 µM in PANC-1 and MIA PaCa-2, respectively (Table 3.3).

3.3.4.3 Cell viability of PANC-1 and MIA PaCa-2 cells following 48-hour treatment with pazopanib

To assess the cell viability of PANC-1 and MIA PaCa-2 cells, both cells were treated with increasing doses of pazopanib (1, 5, 10, 20, and 40 µM) for 48 hours. Figure 3.4 (E and F) shows the effect of pazopanib on cell viability of PANC-1 and MIA PaCa-2 cell lines, respectively. It can be observed that 48-

hour treatment with pazopanib reduced the cell viability in a dose-responsive manner in both cell lines. However, PANC-1 was more sensitive to pazopanib treatment than MIA PaCa-2. The lowest two concentrations tested of pazopanib (1 and 5 μM) failed to inhibit the cell viability in both cell lines compared to the untreated control cells ($p > 0.05$). However, the highest pazopanib administered concentrations in this experiment (40 μM) decreased the cell viability significantly ($p < 0.0001$) to 25.3 ± 11.5% and 57 ± 9.9% in PANC-1 and MIA PaCa-2 cell lines, respectively. The calculated IC_{50} was 18.28 μM in PANC-1 and 55.85 μM (not achieved but extrapolated from the dose-response curve) in MIA PaCa-2 (Table 3.3).

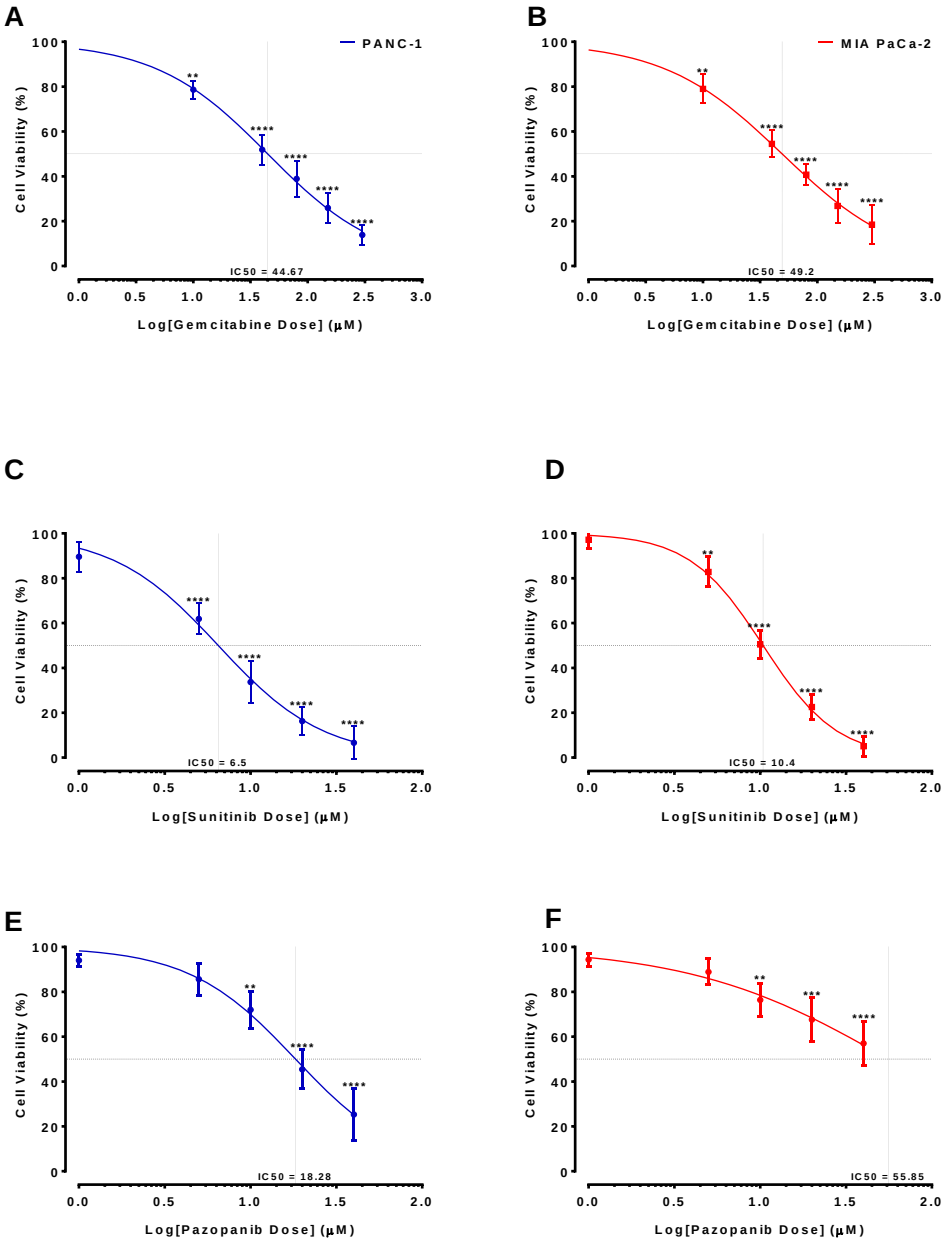

Figure 3.4 Effect of cytotoxic therapy on cell viability of PANC-1 and MIA PaCa-2 cell lines following to 48-hour treatment exposure.

Cells were treated with **A&B)** 10-300µM of gemcitabine, **C&D)** 1-40µM of sunitinib, and **E&F)** 1-40µM of pazopanib for 48 hours and then cell viability was measured by alamar blue assay. Data shown are expressed as a percentage of cell viability normalised to the control group. Statistical analysis was carried out using a one-way ANOVA with Dunnett's posthoc to compare all treatment doses to control group. Each value represents the mean ± SD of three independent experiments. **P<0.01, ***P<0.001, and ****P<0.0001 compared to the untreated control group. IC50 values were calculated using non-linear regression curve fitting (the least-squares fit) of survival fraction using GraphPad Prism® software, version 7.0

Table 3.3 IC50 of the tested anti-cancer drugs following 48 hours of exposure (in μM), determined by Alamar Blue® assay. NA=Not Achieved.

Drug	PANC-1	MIA PaCa-2
Gemcitabine	44.67	49.2
Sunitinib	6.49	10.4
Pazopanib	18.28	55.85

3.3.5 Clonogenic survival assay of PANC-1 and MIA PaCa-2 cells following 48 treatment with anti-cancer agents

In response to the doubling time results, responses of the pancreatic cancer cell lines in terms of cell survival analysis using clonogenic assay were re-assessed following the exposure to 48-hour treatment to ensure cells to duplicate at least once in the presence of cytotoxic agents.

3.3.5.1 Clonogenic survival assay of PANC-1 and MIA PaCa-2 cells following 48-hour treatment with gemcitabine

According to the IC_{50s} of gemcitabine obtained from the cell viability assay (section 0), a range of gemcitabine doses between 10 and 80 μM was examined to assess the cytotoxicity effect of gemcitabine on the survival of PANC-1 and MIA PaCa-2 cell lines. The increasing doses of gemcitabine were incubated with cells for 48 hours before the clonogenic assay was performed as described in section 2.6. This range of gemcitabine doses was found to be toxic in both cell lines and survival fraction was reduced to less than 10% with the lowest examined dose (10 μM) compared to untreated cells (data not shown; $p < 0.0001$). Therefore, lower doses of gemcitabine were examined.

Figure 3.5 (A and B) shows the effect of 48-hour treatment with increasing doses of gemcitabine (1, 2, 4, and 8 μM) on the survival fraction of PANC-1 and MIA PaCa-2 cells. It can be observed that gemcitabine reduced the survival fraction in both cell lines in a dose-dependent manner. The lowest

concentration of gemcitabine tested in this experiment (1 μM) resulted in a statistically significant reduction in the survival fraction of PANC-1 and MIA PaCa-2 to 76.3 ± 6.8% and 80.8 ± 8.6%, respectively. The PANC-1 cell line was more sensitive to the highest concentrations utilised of gemcitabine than MIA PaCa-2; hence PANC-1 survival fraction of PANC-1 decreased to 21 ± 3.4% and 8 ± 3.3% following treatment with 4 and 8 μM ($p < 0.0001$), respectively, while the same two concentrations reduced the survival of MIA PaCa-2 cells to 52.5 ± 4.6% and 67.4 ± 4% ($p < 0.0001$). The calculated IC_{50} of gemcitabine was 2.0 ± 0.9 ($R^2 = 0.99$) and 3.45 ± 1.09 ($R^2 = 0.94$) μM in PANC-1 and MIA PaCa-2 cell lines, respectively (Table 3.4).

3.3.5.2 Clonogenic survival assay of PANC-1 and MIA PaCa-2 cells following 48-hour treatment with sunitinib

Figure 3.5 (C and D) shows the effect of 48-hour treatment with increasing doses of sunitinib (1, 5, 10, and 20 μM) on the survival fraction of PANC-1 and MIA PaCa-2 cells. There was a considerable reduction in the survival fraction of both cell lines in a dose-dependent manner following 48-hour sunitinib treatment compared to untreated cells. Generally, MIA PaCa-2 cells were more sensitive to gemcitabine, especially at lower doses, than PANC-1 cells. There was no statistically significant drop in the survival fraction of PANC-1 and MIA PaCa-2 cells after treatment with the lowest concentration of sunitinib (1 μM) compared to untreated cells. However, all the subsequent higher concentrations utilised of sunitinib resulted in a statistically significant reduction of survival in both cell lines ($p < 0.001$). The highest concentration

used in this experiment reduced survival fraction to 22.4 ± 5.8% and 12.7 ± 4.7% ($p < 0.0001$), respectively. The calculated IC_{50s} of sunitinib were approximately 9.8 ± 1.01 ($R^2 = 0.94$) and 6 ± 1.0 ($R^2 = 0.98$) μM in PANC-1 and MIA PaCa-2 cell lines, respectively (Table 3.4).

3.3.5.3 Clonogenic survival assay of PANC-1 and MIA PaCa-2 cells following 48-hour treatment with pazopanib

Figure 3.5 (E and F) demonstrates the effect of 48-hour treatment with increasing doses of pazopanib (1, 5, 10, and 20 μM) on the survival fraction of PANC-1 and MIA PaCa-2 cells. It can be observed that pazopanib reduced the survival fraction in both cell lines in a dose-dependent manner. In contrast to the result of cell viability assay, MIA PaCa-2 was more sensitive to pazopanib treatment than PANC-1. The lowest concentration of pazopanib tested in this experiment (1 μM) resulted in a statistically significant reduction in the survival fraction of PANC-1 and MIA PaCa-2 to 80 ± 8.1% ($p < 0.01$) and 79.4 ± 6.4% ($p < 0.05$) compared to untreated cells, respectively. The highest concentration (20 μM) decreased the survival significantly to 45.4 ± 4.2% ($p < 0.0001$) in PANC-1 and to 22.3 ± 3.6% ($p < 0.0001$) in MIA PaCa-2. The calculated IC_{50} of pazopanib was 16.6 ± 1.2 ($R^2 = 0.95$) and 5.1 ± 1.11 ($R^2 = 0.96$) μM in PANC-1 and MIA PaCa-2 cell lines, respectively (Table 3.4).

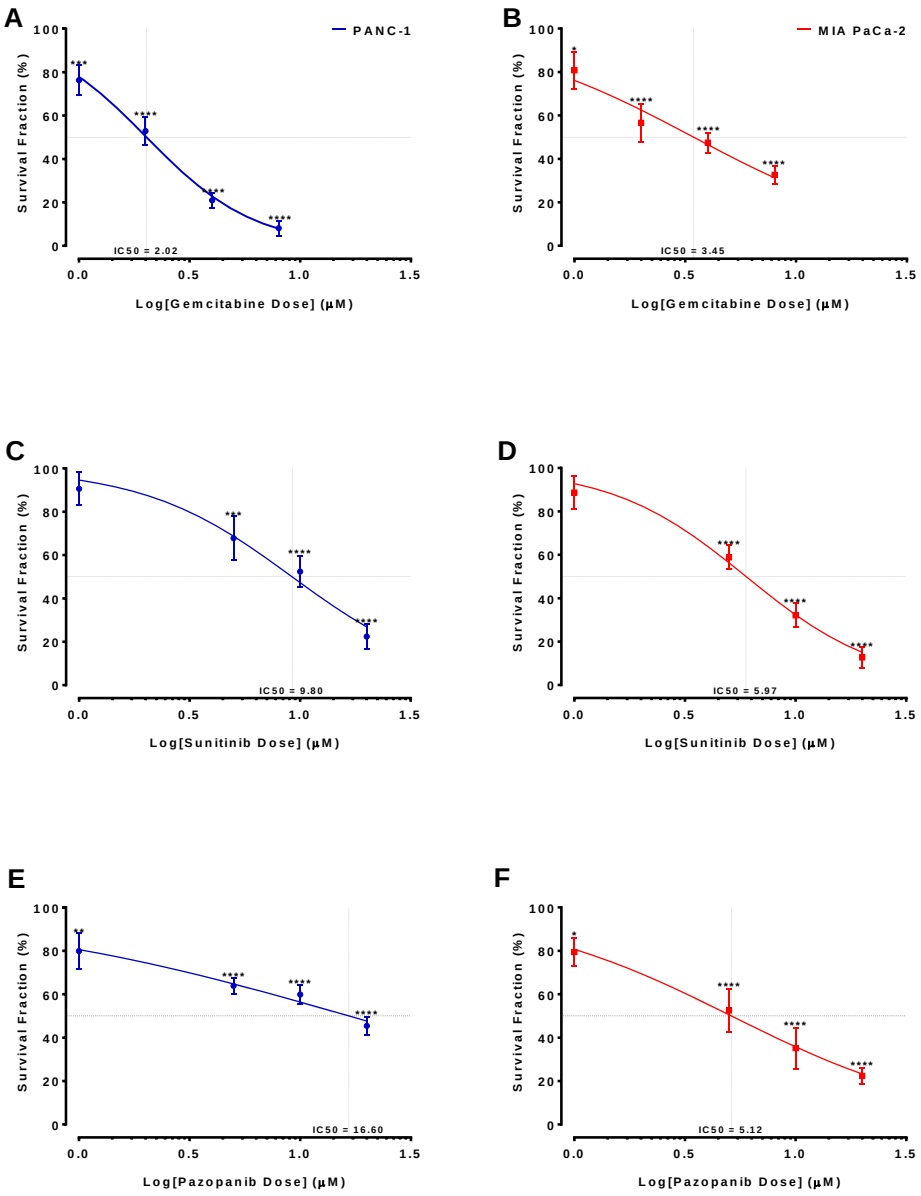

Figure 3.5 Effect of cytotoxic therapy on survival fraction of PANC-1 and MIA PaCa-2 cell lines following to 48-hour treatment exposure.

Cells were treated with **A&B)** 1-8µM of gemcitabine, **C&D)** 1-20µM of sunitinib, and **E&F)** 1-20µM of pazopanib for 48 hours and then survival fraction was measured by clonogenic assay. Data shown are expressed as a percentage of survival fraction normalised to the control group. Statistical analysis was carried out using a one-way ANOVA with Dunnett's posthoc to compare all treatment doses to control group. Each value represents the mean ± SD of three independent experiments. *P<0.05 and **P<0.01 compared to the untreated control group. IC_{50} values were calculated using non-linear regression curve fitting (the least-squares fit) of survival fraction using GraphPad Prism® software, version 7.0.

Table 3.4 IC_{50} of the tested anti-cancer drugs following 48 hours of exposure (in μM), determined by clonogenic assay. NA=Not Achieved.

Drug	PANC-1	MIA PaCa-2
Gemcitabine	2.02	3.45
Sunitinib	9.80	5.97
Pazopanib	16.6	5.12

3.3.6 Generating combination schedules based on single-agent curves

Design of combination therapy was performed as described in section 2.4.4. Briefly, combinations were evaluated using the following three treatment schedules: gemcitabine administered 48 hours before TKI (schedule 1), gemcitabine administered 48 hours after TKI (schedule 2), or gemcitabine administered simultaneously with TKI (schedule 3).

The concentrations for each drug used in combination studies were the IC_{50}, IC_{25}, and IC_{10}, which were obtained from the dose-response (inhibition) non-linear regression curve of the single-agent cytotoxicity (clonogenic assay) studies generated by GraphPad Prism® software (version 7.00), as described in GraphPad Prism's user manual (Motulsky, no date). The final concentrations of each anti-cancer drug applied in combination therapy are shown in Table 3.5.

Table 3.5 Generated doses of drugs to be used in combination therapy on PANC-1 and MIA PaCa-2 cells in μM.

	Gemcitabine		Sunitinib		Pazopanib	
	PANC-1	MIA PaCa-2	PANC-1	MIA PaCa-2	PANC-1	MIA PaCa-2
IC10	0.6	0.3	1.8	1.3	0.2	0.4
IC25	1.1	1.1	4.2	2.8	1.9	1.5
IC50	2.0	3.5	9.8	6	16.6	5.1

3.4 Discussion

The primary aim of this project was to develop novel combination strategies for the treatment of pancreatic cancer. To be able to investigate combination strategies, the cytotoxic effect of each single agent, gemcitabine, sunitinib, and pazopanib, on PANC-1 and MIA PaCa-2 human pancreatic cancer cell lines as a single therapy was assessed and the IC_{50} for those agents were determined. These mono-therapy experiments were performed to evaluate the cytotoxic effects of gemcitabine, sunitinib, and pazopanib, as single treatment, on the viability (via alamar blue assay) and on the clonogenic survival (via clonogenic assays) of pancreatic cancer, PANC-1 and MIA PaCa-2, cell lines. The cell viability assay was conducted in the first place in order to screen and narrow down the effective doses for those cytotoxic agents before assessment their long-term cytotoxicity using the clonogenic assay. The resultant IC_{50} for each drug was validated, compared between the cell lines, and compared to the literature as a primary outcome measure for the efficacy. These values were also used in designing schedules for combination therapy.

Initially as per our standard lab practice, both cell lines were treated for 24 hours with single agents. Cell lines were treated for 24 hours with single drugs. The dose-effect curves from the cell viability experiments (sections 3.3.1.1 to 3.3.1.3) and clonogenic assays (sections 3.3.2.1 to 3.3.2.3) were plotted and IC_{50s} were calculated for and compared between PANC-1 and MIA PaCa-2. However, our experimentally determined IC_{50s} values for each of the single agents were found to be higher compared to the literature. Doubling time for

the cells was assessed to allow cells to duplicate at least once in the presence of cytotoxic agents. For subsequent double and triple combinations, only 48-hour exposure was assessed in compliance with the doubling time findings.

The calculated doubling time for PANC-1 in the current experiment was 30.5 ± 4.3 hours. This is in line with findings from the literature. For example, McIntyre and Kim reported a doubling time of 28 hours (McIntyre and Kim, 1984) and the ATCC reported 32 hours in their Standard Operating Procedure (SOP) for pancreatic cancer cells (ATCC, 2012). For MIA PaCa-2 cells, the doubling time was 27.6 ± 2.6 hours in the current experiment. This again was in line with the literature: 24-30 hours (Fountzilas, Lim and Yunis, 1984) and 26 hours (McIntyre and Kim, 1984).

It can be concluded from the results of single-drug treatments discussed in sections 3.3.1.1 and 3.3.4.1 that gemcitabine had a dose-dependent cytotoxic effect on both pancreatic cancer cell lines, PANC-1 and MIA PaCa-2, after cell incubation with gemcitabine either for 24 or 48 hours. Both the short-term cytotoxicity effect, determined by the alamar blue cell viability assay, and the late cytotoxicity effect, determined by the clonogenic assay, were performed in this study. The calculated IC_{50s} for gemcitabine against pancreatic cancer cell lines were summarised in Tables 3.1 to 3.4. However, the IC_{50s} of gemcitabine from the alamar blue assay was higher, as expected, than those from the clonogenic assay. These discrepancies were because of the nature of these two assays.

Upon comparison between these two cell lines in terms of sensitivity to gemcitabine, it has been found that there was no significant difference in cell viability between the PANC-1 (IC_{50} = 44.67 µM) and the MIA PaCa-2 (IC_{50} = 49.2 µM) cell lines after incubation with gemcitabine (Figure 3.4 A & B). On the other hand, PANC-1 cells were significantly more sensitive to gemcitabine, especially at higher administered doses (4 and 8 µM), than MIA PaCa-2 ($p < 0.001$) in terms of the cell survival using clonogenic assay (Figure 3.5 A & B).

The resistance of MIA PaCa-2 cells to gemcitabine found in our experiments has also been previously reported in the literature (Taeger *et al.*, 2011). This resistance was attributed to increased expression of Aldehyde dehydrogenase 1A1 (ALDH1A1), which is one of the characteristic features of tumour-initiating cells and has an important role in both intrinsic and acquired resistance to gemcitabine (Duong *et al.*, 2014). Proto-oncogene serine/threonine-protein kinase (PIM) proteins, especially PIM1 and PIM3 (Xu *et al.*, 2014), which are overexpressed in MIA PaCa-2 cells, but not in the PANC-1 cells, could be hypothesised as another cause of resistance of MIA PaCa-2 cell line to gemcitabine compared to PANC-1 (Mallik and Karandish, 2016). However, these findings, of PANC-1 being more sensitive to gemcitabine than MIA PaCa-2, were also opposed in other studies which found that PANC-1 cells were more resistance to gemcitabine than MIA-PaCa-2 (Fryer *et al.*, 2011). Affram *et al.* (Affram, Udofot and Agyare, 2015) treated several pancreatic cancer cell lines, including PANC-1 and MIA PaCa-2, with gemcitabine for 72 hours and then assessed the cell viability using the trypan blue assay. Conversely to our results, the authors found that the most sensitive cell line for

gemcitabine was MIA PaCa-2; hence the IC_{50} in MIA PaCa-2 was 77 nM compared to 195 nM in PANC-1. The authors hypothesised that this could be due to the overexpression of the antiapoptotic p8 protein in PANC-1 three times higher than MIA PaCa-2 (Giroux *et al.*, 2006). However, the IC50 values we found in this study were in line with the majority of the literature; suggesting our data are validated.

The reported IC_{50} values for gemcitabine in PANC-1 and MIA PaCa-2 cell lines vary considerably between published studies. Several studies reported very low IC_{50}, in nanomolar (nM) concentrations (Tran Cao *et al.*, 2010; Affram *et al.*, 2015). For example, Cao *et al.* (Tran Cao *et al.*, 2010) treated PANC-1 and MIA PaCa-2 cells with gemcitabine for 72 hours and assessed cell viability using the XTT cell viability assay. Their calculated IC_{50} values were 29 nM and 14 nM in PANC-1 and MIA PaCa-2, respectively. In both studies with nanomolar IC_{50} values, cells were exposed to treatment for 72 hours, and it has been reported that longer exposure time increased the gemcitabine-induced apoptosis (Gruber *et al.*, 1996; Montano *et al.*, 2017) which was indeed found in our study treating cells for 24 and 48 hours. However, following a shorter exposure time (48 hours) cytotoxicity of gemcitabine decreased and, hence, the IC_{50} values were higher. Arora and his colleagues (Arora *et al.*, 2011) examined the cytotoxicity of gemcitabine on pancreatic cancer cells using the WST-1 cell viability assay. Their study revealed that the calculated IC_{50} values following 48-hour exposure of PANC-1 and MIA PaCa-2 were approximately 14.5 µM and 13 µM, respectively. These IC_{50} findings can be considered similar to those from our clonogenic study (Table 3.4).

In the case of sunitinib, there was a dose-dependent cytotoxic effect on both pancreatic cancer cell lines, PANC-1 and MIA PaCa-2, after cell incubation either for 24 or 48 hours with sunitinib. Both cell viability and clonogenic survival assays were performed in this study. The calculated IC_{50s} for sunitinib against pancreatic cancer cell lines were summarised in Tables 3.1 to 3.4.

Upon comparison between these two cell lines in terms of sensitivity to gemcitabine, sunitinib, or pazopanib, it has been found that there was no statistically significant difference between PANC-1 and MIA PaCa-2 in terms of cell survival following treatment with sunitinib despite the lower IC_{50s} in MIA PaCa-2 cells (Figure 3.5 C & D). On the other hand, PANC-1 cells were significantly more sensitive to sunitinib than MIA PaCa-2 ($p < 0.01$) in terms of cell viability) Figure 3.4 (C & D). This increased sensitivity of PANC-1 cells to sunitinib may be attributed to the inhibitory effect of this agent on the stem cell factor receptor (KIT) (Izzedine *et al.*, 2007; Hasinoff, Patel and O'Hara, 2008; Shukla *et al.*, 2009) which is overexpressed in PANC-1 but not in MIA PaCa-2 (Yasuda *et al.*, 2006) (Table 1.3).

For pazopanib cytotoxicity assessment, we used identical dose ranges to those used in sunitinib cytotoxicity assessment; based on the similarity of the mechanism of action and in order to compare the cytotoxic effect of these two TKI agents between PANC-1 and MIA PaCa-2 pancreatic cancer cell lines. It has been found that treatment with pazopanib for 24 hours demonstrated no statistically significant cytotoxicity on either cell line (Figure 3.1 and Figure 3.2). However, after 48-hour treatment, pazopanib inhibited both cell viability and

clonogenicity in a significant dose-dependent manner in PANC-1 and MIA PaCa-2. MIA PaCa-2 cells were significantly more sensitive to pazopanib (IC_{50} = 5.1 μM) than PANC-1 (IC_{50} = 16.6 μM). This could be due to the inhibitory effect of pazopanib on the fibroblast growth factor receptor (FGFR-3) (Keisner and Shah, 2011; Plummer *et al.*, 2013), which is overexpressed about 30 times higher in MIA PaCa-2 than PANC-1 cells (Ishiwata *et al.*, 2012).

However, these cytotoxicity effects of gemcitabine or TKI may not be reflected in the anaimal model or in human, hence in the *in vitro* survival study we incubate cancer cells with the cytotoxic agents for 24 or 48 hours, whereas in the in vivo studies or in human application these agents have very small half-lives compared to the used incubation time with medicines in the *in vitro* studies.

CHAPTER 4: Cytotoxicity evaluation of combination therapy on pancreatic cancer cells *in vitro*

4.1 Introduction

Pancreatic cancer prognosis is still poor and despite advances in cancer therapy over the last two decades, survival rates amongst patients with pancreatic cancer remain disappointing (Cunningham *et al.*, 2009; Colucci *et al.*, 2010). This poor prognosis rate can be attributed to late-stage diagnosis, early metastasis, high local recurrence risk and resistance to conventional chemotherapy (Awasthi, Schwarz and Schwarz, 2011). Gemcitabine is considered the gold standard and the historical first-line treatment for patients with pancreatic ductal adenocarcinomas (Sclafani *et al.*, 2015). However, gemcitabine mediates only a marginal clinical benefit both when administered alone (Casper *et al.*, 1994; Carmichael *et al.*, 1996; Burris *et al.*, 1997) and in combination with other conventional chemotherapy agents (Berlin *et al.*, 2002; Bramhall *et al.*, 2002; Rocha Lima *et al.*, 2004; Louvet *et al.*, 2005; Oettle *et al.*, 2005; Abou-Alfa *et al.*, 2006; Heinemann *et al.*, 2006; Poplin *et al.*, 2006; Herrmann *et al.*, 2007; Cunningham *et al.*, 2009; Colucci *et al.*, 2010) or targeted therapy agents (Van Cutsem *et al.*, 2004; Wolpin *et al.*, 2009; Philip *et al.*, 2010; Bodoky *et al.*, 2012; Infante *et al.*, 2014). Therefore, we hypothesised that combining the conventional chemotherapy (gemcitabine) with a multi-target TKI with antiangiogenic and anti-tumour activity targeted therapy (sunitinib or pazopanib) in lower therapeutic doses of each agent might

improve the outcome of pancreatic cancer treatment. We thought that combination strategies may reduce the chance of pancreatic cancer cells dose-dependent resistance to radiochemotherapy, which was reported to be the major contributor to poor prognosis (Binenbaum, Na'ara and Gil, 2015; Liu *et al.*, 2016).

4.2 Aims

The primary aim of this chapter was to evaluate the cytotoxic efficacy of novel combination strategies of gemcitabine and TKI (sunitinib and, for the first time, pazopanib) with or without exposure to XBR by investigating the clonogenic cell survival following combination treatment of PANC-1 and MIA PaCa-2 pancreatic cancer cell lines. This study also aimed to assess synergism using the combination index analysis approach and determine the most effective combination schedule of these cytotoxic agents in two-drug and three-treatment combinations. Finally, this study aimed to explore the underlying mechanisms of cytotoxic action of these potential therapeutic approaches via detection of H_2AX as a marker of DNA damage and repair, analysis of cell cycle progression, and measurement of Annexin V expression as an indicator of apoptosis.

4.3 Results

Results of this chapter were divided into three main sections to evaluate cytotoxicity and to explore the mechanism of cytotoxicity of gemcitabine, TKI (sunitinib or pazopanib), or XBR as single treatment (section 4.3.1), a two-drug

combination of gemcitabine with TKI (section 4.3.2), and a three-treatment combination of gemcitabine plus sunitinib with XBR (section 4.3.3). Each main section consists of four subsections; assessment of the efficacy of the cytotoxic agents by clonogenic survival assay, detection of DNA damage and repair by quantification of γ-H_2AX expression, analysis of cell cycle progression, and detection of apoptosis level by measurement of Annexin V expression in PANC-1 and MIA PaCa-2 pancreatic cancer cell lines.

4.3.1 Cytotoxicity and mechanistic studies of gemcitabine, TKI, or XBR as single treatment in pancreatic cancer cells *in vitro*

Before assessing the effect on pancreatic cancer cell survival of gemcitabine and TKI (sunitinib or pazopanib) in combination treatment, either without XBR (two-drug combination) or with XBR (three-treatment combination), the cytotoxic effects of each agent on pancreatic cancer cell lines were evaluated as a single agent compared to untreated control cells. These cytotoxicity evaluation studies were followed by mechanistic studies in order to understand and explore underlying mechanisms of cytotoxic action of these agents via conducting DNA damage and repair detection, cell cycle analysis, and apoptosis detection, mechanistic studies.

4.3.1.1 Cytotoxicity assessment of gemcitabine, TKI, and XBR in pancreatic cancer cells by clonogenic assay

To assess the efficacy of gemcitabine, sunitinib, and pazopanib in combination therapy, their cytotoxic effects on the survival of pancreatic cancer cell lines

(PANC-1 and MIA PaCa-2) as single treatment were evaluated first using the lower generated doses, which were planned to be utilised in the combination studies, (listed in Table 3.5) as described in section 2.4.4 and shown in Figure 4.1.

Materials and methods pertaining to the clonogenic assay were described in detail in section 2.6. The calculated survival fraction using Equation 2.3 (explained in section 2.6) was normalised to the untreated control group and then plotted on the Y-axis against drug concentrations on the X-axis. IC_{50} values were calculated using non-linear regression curve fitting (the least-squares fit) of survival fraction using GraphPad Prism® software, version 7.00, as described in GraphPad Prism's user manual (Motulsky, no date).

Cell survival of PANC-1 and MIA PaCa-2 was also assessed following exposure to increasing doses of XBR (1 to 6 Gy) by clonogenic assay as described in section 2.6. Survival fraction data were normalised to non-irradiated control cells, fitted to the linear-quadratic model (described in section 2.8), and shown in Figure 4.2. Values for R^2, α and β coefficients, and IC_{50} were calculated and shown in the table below the dose-response graph.

4.3.1.1.1 Clonogenic survival assay of PANC-1 and MIA PaCa-2 cells following treatment with gemcitabine alone

Figure 4.1 (A and B) shows the effect of 48-hour treatment with increasing doses of gemcitabine (listed in Table 3.5) on the survival fraction of PANC-1

and MIA PaCa-2 cells. It can be observed that gemcitabine reduced the survival fraction in both cell lines in a dose-dependent manner. The incubation of cells with the highest concentration of gemcitabine tested in this experiment (2 μM in PANC-1, and 3.5 μM in MIA PaCa-2) resulted in a statistically significant reduction ($p < 0.0001$) in the survival fraction of PANC-1 and MIA PaCa-2 cells to 52.8 ± 6.5% and 50.4 ± 4.1%, respectively, compared to untreated control cells.

4.3.1.1.2 Clonogenic survival assay of PANC-1 and MIA PaCa-2 cells following 48-hour treatment with sunitinib alone

Figure 4.1 (C and D) shows the effect of 48-hour treatment with increasing doses of sunitinib (listed in Table 3.5) on the survival fraction of PANC-1 and MIA PaCa-2 cells. There was a significant reduction in the survival fraction of both cell lines in a dose-dependent manner following 48-hour of treatment with sunitinib compared to untreated cells. The highest concentration of sunitinib used in this experiment (9.8 μM in PANC-1, and 6 μM in MIA PaCa-2) reduced survival fraction of PANC-1 and MIA PaCa-2 to 49.6 ± 4.5% and 53.3 ± 6.2% ($p < 0.0001$), respectively, compared to untreated control cells.

4.3.1.1.3 Clonogenic survival assay of PANC-1 and MIA PaCa-2 cells following 48-hour treatment with pazopanib alone

Figure 4.1 (E and F) demonstrates the effect of 48-hour treatment with increasing doses of pazopanib (listed in Table 3.5) on the survival fraction of

PANC-1 and MIA PaCa-2 cells. It can be observed that pazopanib reduced the survival fraction in both cell lines in a dose-dependent manner. The highest concentration of pazopanib tested in this experiment (16.6 μM in PANC-1, and 5 μM in MIA PaCa-2) resulted in a statistically significant reduction ($p < 0.0001$) in the survival fraction of PANC-1 and MIA PaCa-2 cells to 50 ± 5.4% and 52.5 ± 7.9%, respectively, compared to untreated control cells.

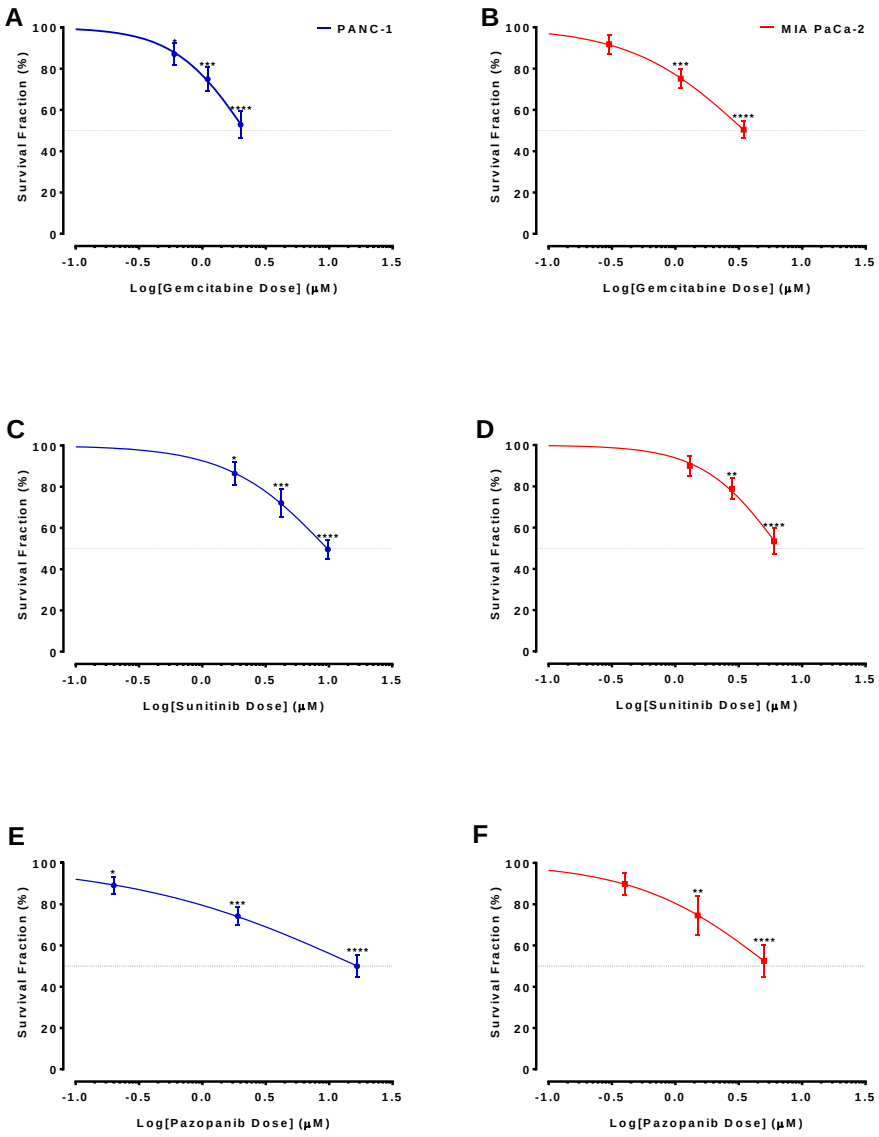

Figure 4.1 Effect of cytotoxic treatment on survival fraction of PANC-1 and MIA PaCa-2 cell lines following to 48-hour treatment exposure.

Cells were treated with the calculated concentrations for combinatorial treatments of **A&B)** gemcitabine, **C&D)** sunitinib, or **E&F)** pazopanib for 48 hours and then survival fraction was measured by clonogenic assay. Data shown are expressed as a percentage of survival fraction normalised to the control group. Statistical analysis was carried out using a one-way ANOVA with Dunnett's posthoc to compare all treatment doses to control group. Each value represents the mean ± SD of three independent experiments. *P<0.05, **P<0.01, ***P<0.001 and ****P<0.0001 compared to the untreated control group. IC_{50} values were calculated using non-linear regression curve fitting (the least-squares fit) of survival fraction using GraphPad Prism® software, version 7.0.

4.3.1.1.4 Clonogenic survival assay of PANC-1 and MIA PaCa-2 cells following exposure to XBR alone

As illustrated in Figure 4.2, exposure to increasing doses of XBR (0, 1, 2, 4, and 6 Gy) resulted in a dose-dependent reduction in clonogenic survival of PANC-1 and MIA PaCa-2 cell lines compared to non-irradiated control cells. The dose-effect relationship was best characterised using a linear-quadratic model ($R^2 > 0.99$). Statistically significant cytotoxicity, relative to non-irradiated control, was observed after exposure to XBR doses of 2, 4, and 6 Gy in both cell lines ($p < 0.01$). MIA PaCa-2 was slightly more sensitive to radiation than PANC-1, but there was no significant difference in the survival between cells. The calculated effective dose (ED_{50}) for XBR was 4.63 ± 0.91 and 3.51 ± 0.87 Gy in PANC-1 and MIA PaCa-2 cell lines, respectively.

To measure radiosensitivity of cell lines, the fraction of cells surviving a single 2 Gy dose of ionizing radiation (SF2) was utilised by several *in vitro* studies. Cell lines with high values of SF2 based on a threshold of 0.2 are considered radioresistant (i.e. cell lines with more than 20% colony survival following 2 Gy defined as radioresistant) (Hall *et al.*, 2014; Maeda *et al.*, 2016). In the present study, the calculated SF2 for PANC-1 and MIA PaCa-2 pancreatic cancer cell lines was 0.8 ± 0.06 and 0.69 ± 0.04, respectively. This confirmed the radioresistance of these cell lines, which was reported in previous studies (Zhou and Du, 2012; Wang *et al.*, 2018).

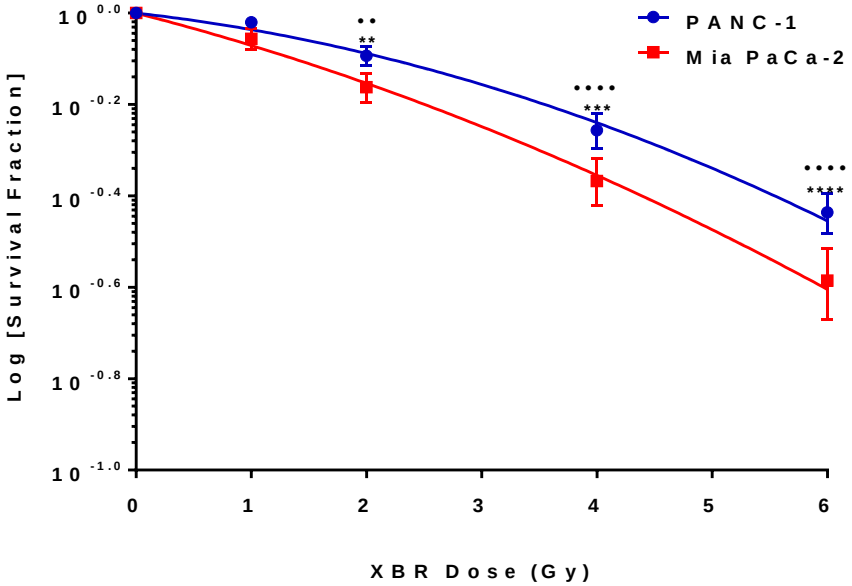

Cell line	α (Gy^{-1})	β (Gy^{-1})	R^2	ED_{50} (Gy)
PANC-1	0.0654	0.01819	0.9932	4.632
Mia PaCa-2	0.1494	0.01378	0.9966	3.507

Figure 4.2 Clonogenic survival of PANC-1 and MIA PaCa-2 cells exposed to XBR from 0-6 Gy fitted to the linear-quadratic model. Cells were exposed to 0-6 Gy of XBR and then survival fraction was measured by clonogenic assay. Data shown are expressed as a percentage of survival fraction normalised to the control group. Statistical analysis was carried out using a one-way ANOVA with Dunnett's posthoc to compare all treatment doses to control group. Each value represents the mean ± SD of three independent experiments. **P<0.01, ***P<0.001 and ****P<0.0001 (black dots for MIA PaCa-2) compared to the untreated control group. Experimental survival fractions were fitted to the linear-quadratic model using GraphPad Prism v.7.0 and the α and β coefficient, the R^2, and ED_{50} values were determined.

4.3.1.2 The effect of single cytotoxic agents on the induction and repair of DNA damage measured by γ-H_2AX in pancreatic cancer cells

As explained in section 2.12, γ-H_2AX expression was measured at three time-points (4, 24, and 48 hours after treatment) to investigate the damage caused to the DNA following exposure to the cytotoxic agents and to explore if this damage was repaired at later time-points of measurement. The higher expression of γ-H_2AX and, more important, the persistence of this DNA damage over time positively correlates with cytotoxic efficacy of the cytotoxic agent. The decreased expression of γ-H_2AX at later time-points indicates DNA damage was repaired which could support cancer cell survival.

In these experiments, the expression of γ-H_2AX, as a marker of DNA damage and repair, was assessed at 4, 24, and 48 hours after a single treatment with gemcitabine, sunitinib, or XBR in PANC-1 and MIA PaCa-2 cell lines.

4.3.1.2.1 The effect of gemcitabine, sunitinib, or XBR as single cytotoxic treatment on the induction and repair of DNA damage measured by γ-H_2AX in PANC-1 cells

The expression of γ-H_2AX in PANC-1 cells was assessed at 4, 24, and 48 hours after a single treatment with gemcitabine (0.6, 1.1, and 2 μM), sunitinib (1.8, 4.2, and 9.8 μM), or XBR (0.5, 1, and 2 Gy) as described in section 2.12. The results of this experiment were expressed as fold increase in the γ-H_2AX

expression of cells treated with increasing dose of the cytotoxic agents compared to untreated control cells and presented in Figure 4.3.

Figure 4.3 (A1) shows the fold change in γ-H_2AX expression at 4, 24, and 48 hours post-treatment of PANC-1 cells with increasing dose of gemcitabine alone compared to untreated cells. It was observed that the fold change in γ-H_2AX expression increased significantly in a dose-dependent manner at 4 hours post gemcitabine treatment ($p < 0.001$). The highest tested dose of gemcitabine (2 μM) increased γ-H_2AX expression 11.5 ± 1.3 fold compared to untreated control cells ($p < 0.0001$). However, the γ-H_2AX level decreased significantly at 24 and 48 hours compared to γ-H_2AX levels measured at 4 hours ($p < 0.05$). Figure 4.3 (A2) summarises the p-values from the two-way ANOVA and Tukey's multiple comparison tests between different time-points within each drug dose. There were no significant differences between γ-H_2AX levels between measurements at 24 and 48 hours; suggesting that the DNA damage induced by gemcitabine was being repaired within 24 hours.

Figure 4.3 (B1) shows the fold change in γ-H_2AX expression at 4, 24, and 48 hours post-treatment of PANC-1 cells with increasing dose of sunitinib alone compared to untreated cells. Apart from the highest tested dose (9.8 μM), the treatment with sunitinib failed to increase γ-H_2AX in PANC-1 cells over examined time-points. After 4 hours, there was a significant increase of γ-H_2AX level to 6.7 ± 1 fold following treatment with 9.8 μM of sunitinib compared to untreated control ($p < 0.0001$). However, the γ-H_2AX levels decreased significantly at 24 and 48 hours compared to γ-H_2AX levels measured at 4

hours to reach the basal levels. This indicates that sunitinib does not induce or interfere with DNA damage and repair, suggesting the possibility of different mechanisms of its cytotoxic action.

Figure 4.3 (C1) demonstrates the fold change in γ-H_2AX expression at 4, 24, and 48 hours post-exposure of PANC-1 cells to increasing doses of XBR alone compared to untreated cells. It has been observed that the average levels of γ-H_2AX staining increased significantly in a dose-dependent manner at 4 hours and 24 hours post XBR exposure ($p < 0.0001$). Irradiation with 2 Gy, for example, increased γ-H_2AX expression to 13.1 ± 1.5 fold compared to untreated control ($p < 0.0001$). However, the γ-H_2AX level decreased significantly at 48 hours compared to γ-H_2AX levels measured at earlier time-points. There were no significant differences in γ-H_2AX levels between measurements at 4 and 24 hours (Figure 4.3 (C2)). Thus, it can be noticed that XBR-induced DNA damaged needed a longer time to be repaired compared to the damage caused by gemcitabine or sunitinib.

A

(1)

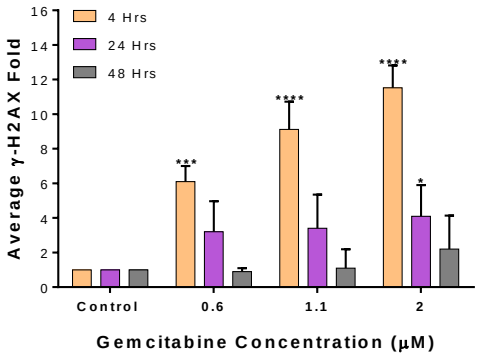

(2)

Time (Hours)	4 vs. 24	4 vs. 48	24 vs. 48
Control	ns	ns	ns
0.6	*	****	ns
1.1	****	****	ns
2	****	****	ns

B

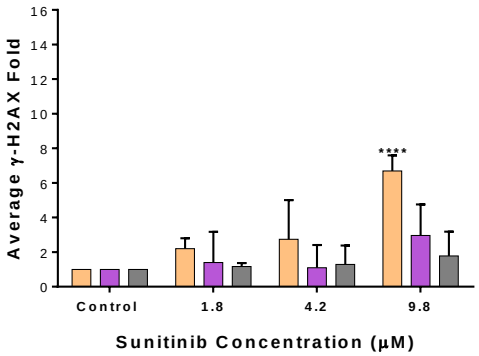

Time (Hours)	4 vs. 24	4 vs. 48	24 vs. 48
Control	ns	ns	ns
1.8	ns	ns	ns
4.2	ns	ns	ns
9.8	**	***	ns

C

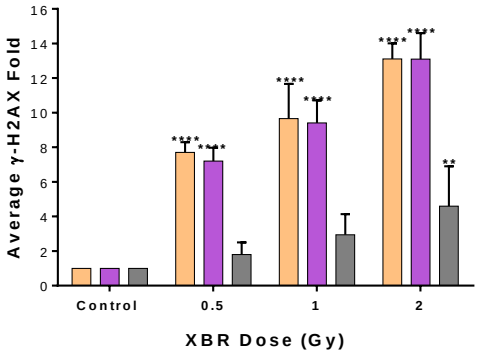

Time (Hours)	4 vs. 24	4 vs. 48	24 vs. 48
Control	ns	ns	ns
0.5	ns	****	****
1	ns	****	****
2	ns	****	****

Figure 4.3 The effect of single cytotoxic agents on the induction and repair of DNA damage measured by γ-H2AX in PANC-1 cells. The expression of γ-H2AX of PANC-1 cells was assessed at 4, 24, and 48 hours after treatment with gemcitabine (A1), sunitinib (B1), or XBR (C1) alone. Results presented are the mean ± SD fold of γ-H2AX expression compared to untreated control cells of 3 independent experiments. Statistical analysis was carried out using two-way ANOVA with (1) Dunnett's test to compare average fold of γ-H2AX resulted from all treatment doses over time-points to the untreated control group, and (2) with Tukey's test to compare γ-H2AX between different time-points after each dose of the treatment. *P<0.05, **P<0.01, ***P<0.001 and ****P<0.0001.

4.3.1.2.2 The effect of gemcitabine, sunitinib, or XBR as single cytotoxic treatment on the induction and repair of DNA damage measured by γ-H2AX in MIA PaCa-2

The expression of γ-H2AX in MIA PaCa-2 cells was assessed at 4, 24, and 48 hours after a single treatment with gemcitabine (0.3, 1.1, and 3.5 μM), sunitinib (1.3, 2.8, and 6 μM), or XBR (0.5, 1, and 2 Gy) as described in section 2.12. The results of this experiment were expressed as fold increase in the γ-H2AX expression of cells treated with increasing dose of the cytotoxic agents compared to untreated control cells and presented in Figure 4.4.

Figure 4.4 (A1) shows the average of γ-H2AX increase fold at 4, 24, and 48 hours post-treatment of MIA PaCa-2 cells with increasing dose of gemcitabine alone compared to untreated cells. It has been observed that the average of γ-H2AX increased significantly in a dose-dependent manner at 4 hours post gemcitabine treatment ($p < 0.001$). The highest tested dose of gemcitabine (3.5 μM) increased γ-H2AX expression to 10.73 ± 1.21 folds compared to control ($p < 0.0001$). However, the γ-H2AX level decreased significantly at 24 and 48 hours compared to γ-H2AX levels measured at 4 hours. Figure 4.4 (A2) summarises the p-values from the two-way ANOVA and Tukey's multiple comparison tests between different time-points within each drug dose. There were no significant differences in γ-H2AX levels between measurements at 24 and 48 hours.

Figure 4.4 (B1) shows the average of γ-H_2AX increase fold at 4, 24, and 48 hours post-treatment of MIA PaCa-2 cells with increasing dose of sunitinib alone compared to untreated cells. Apart from the highest tested dose (6 μM), the treatment with sunitinib failed to increase γ-H_2AX in MIA PaCa-2 cells over examined time-points. After 4 hours, there was a significant increase of γ-H_2AX level to 5.97 ± 1.94 folds following treatment with 6 μM of sunitinib compared to untreated control ($p < 0.0001$). However, the γ-H_2AX level decreased significantly at 24 and 48 hours compared to γ-H_2AX levels measured at 4 hours to reach the basal levels ($p < 0.05$).

Figure 4.4 (C1) demonstrates the average of γ-H_2AX increase fold at 4, 24, and 48 hours post-exposure of MIA PaCa-2 cells to increasing doses of XBR alone compared to untreated cells. It has been observed that the average of γ-H_2AX increased significantly in a dose-dependent manner at 4 hours and 24 hours post XBR exposure ($p < 0.0001$). Irradiation with 2 Gy, for example, increased γ-H_2AX expression to 15 ± 0.93 folds compared to untreated control ($p < 0.0001$). However, the γ-H_2AX level decreased significantly at 48 hours compared to γ-H_2AX levels measured at earlier time-points. There were no significant differences in γ-H_2AX levels between measurements at 4 and 24 hours (Figure 4.4 (C2)).

A

(1)

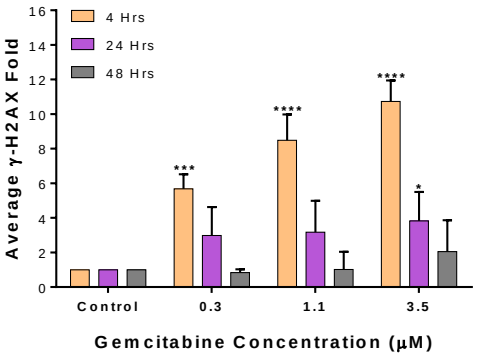

(2)

Time (Hours)	4 vs. 24	4 vs. 48	24 vs. 48
Control	ns	ns	ns
0.3	*	***	ns
1.1	****	****	ns
3.5	****	****	ns

B

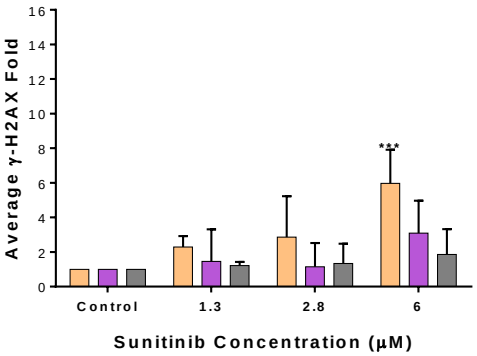

Time (Hours)	4 vs. 24	4 vs. 48	24 vs. 48
Control	ns	ns	ns
1.3	*	***	ns
2.8	****	****	ns
6.0	****	****	ns

C

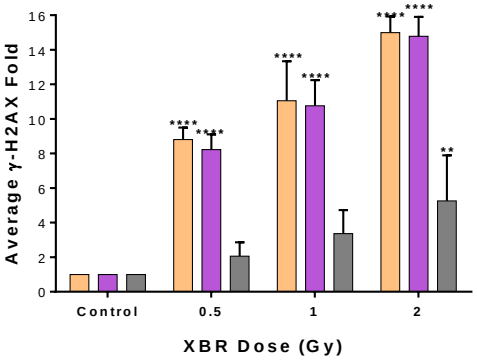

Time (Hours)	4 vs. 24	4 vs. 48	24 vs. 48
Control	ns	ns	ns
0.5	ns	****	****
1	ns	****	****
2	ns	****	****

Figure 4.4 The effect of single cytotoxic agents on the induction and repair of DNA damage measured by γ-H2AX in MIA PaCa-2 cells. The expression of γ-H2AX of MIA PaCa-2 cells was assessed at 4, 24, and 48 hours after treatment with gemcitabine (A1), sunitinib (B1), or XBR (C1) alone. Results presented are the mean ± SD fold of γ-H2AX expression compared to untreated control cells of 3 independent experiments. Statistical analysis was carried out using two-way ANOVA with (1) Dunnett's test to compare average fold of γ-H2AX resulted from all treatment doses over time-points to the untreated control group, and (2) with Tukey's test to compare γ-H2AX between different time-points after each dose of the treatment. *P<0.05, **P<0.01, ***P<0.001 and ****P<0.0001.

4.3.1.3 Analysis of the cell cycle progression of pancreatic cancer cells following exposure to single cytotoxic agents

In these experiments, the cell cycle progression of PANC-1 and MIA PaCa-2 cells was assessed at 4, 24, and 48 hours after a single treatment with gemcitabine, sunitinib, or XBR, as described in section 2.10. As a result of DNA damage reported in the previous section, we hypothesised that cell cycle arrest would be seen to allow for damage repair.

4.3.1.3.1 Analysis of the cell cycle progression of PANC-1 cells following exposure to gemcitabine, sunitinib, or XBR alone

Figure 4.5 shows the effects of gemcitabine (A), sunitinib (C), or XBR (E) on the cell cycle progression of PANC-1 cells at 4 (A1, C1, and E1), 24 (A2, C2, and E2), and 48 (A3, C3, and E3) hours post-treatment.

Incubation of PANC-1 cells with increasing doses of gemcitabine alone resulted in a statistically significant time- and dose- dependent accumulation of cells in the S phase accompanied with a decrease in the G2/M phase of the cell cycle at all measured time-points (4, 24, and 48 hours) compared to untreated control cells ($p < 0.001$). At 24-hour after treatment, cell distribution was also increased in G0/G1. Cells were released from G1 phase and increased significantly in sub G0 phase after 48 hours of treatment with gemcitabine.

The treatment of PANC-1 cells with the two highest tested doses of sunitinib (4.2 and 9.8 μM) resulted in a significant cell cycle arrest at G1 phase accompanied with a decrease in the G2/M phase of the cell cycle at 4 and 24 hours after treatment compared to untreated control cells ($p < 0.0001$). However, cells were released from the G1 phase and arrested in the G2/M phase of the cell cycle after 48 hours of treatment.

Finally, irradiation with 0.5 Gy did not affect the cell cycle distribution in PANC-1 cells at any tested time-points of measurement ($p > 0.05$). However, exposure to 1 and 2 Gy resulted in a significant cell cycle arrest at G_2/M phase ($p < 0.001$) accompanied with a decrease in the G0/1 phase ($p < 0.05$) of the cell cycle at 4 and 24 hours after radiation compared to untreated control cells. There was no significant difference in the cell cycle distribution at 48 hours post-radiation compared to untreated control cells.

A **B**

(1)

4H

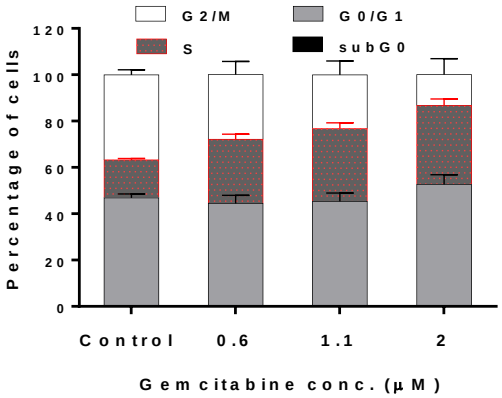

Control vs. Dose (μM)	0.6	1.1	2
subG0	ns	ns	ns
G0/G1	ns	ns	ns
S	***	****	****
G2/M	**	****	****

(2)

24H

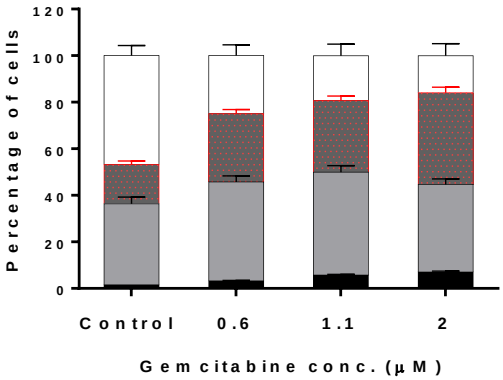

Control vs. Dose (μM)	0.6	1.1	2
subG0	ns	ns	ns
G0/G1	**	**	ns
S	****	****	****
G2/M	****	****	****

(3)

48H

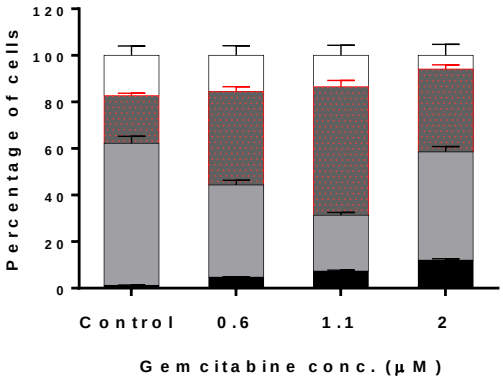

Control vs. Dose (μM)	0.6	1.1	2
subG0	ns	*	****
G0/G1	****	****	****
S	****	****	****
G2/M	ns	ns	****

Continued overleaf …

C **D**

(1)
4H

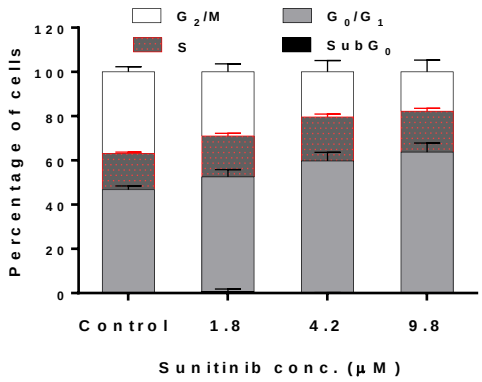

Control vs. Dose (µM)	1.8	4.2	9.8
subG0	ns	ns	ns
G0/G1	ns	****	****
S	ns	ns	ns
G2/M	**	****	****

(2)
24H

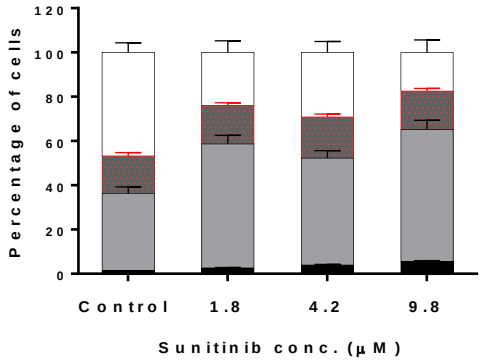

Control vs. Dose (µM)	1.8	4.2	9.8
subG0	ns	ns	ns
G0/G1	****	****	****
S	ns	ns	ns
G2/M	****	****	****

(3)
48H

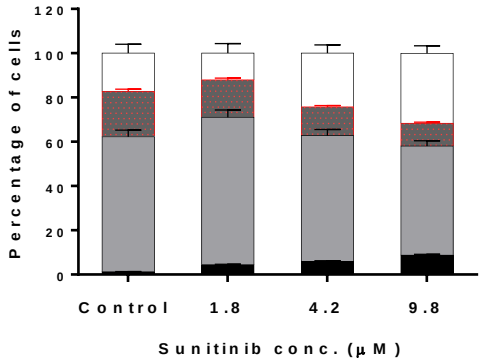

Control vs. Dose (µM)	1.8	4.2	9.8
subG0	ns	ns	**
G0/G1	*	ns	****
S	ns	**	****
G2/M	*	**	****

Continued overleaf …

E **F**

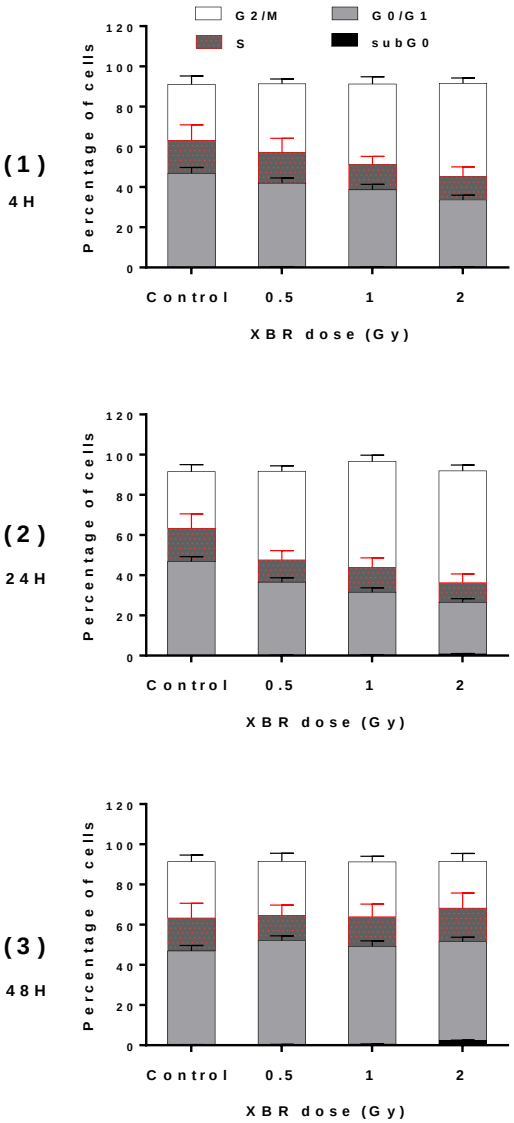

Control vs. Dose (Gy)	0.5	1	2
subG0	ns	ns	ns
G0/G1	ns	*	***
S	ns	ns	ns
G2/M	ns	***	****

Control vs. Dose (Gy)	0.5	1	2
subG0	ns	ns	ns
G0/G1	**	****	****
S	ns	ns	ns
G2/M	****	****	****

Control vs. Dose (Gy)	0.5	1	2
subG0	ns	ns	ns
G0/G1	ns	ns	ns
S	ns	ns	ns
G2/M	ns	ns	ns

Figure 4.5 Effect of gemcitabine, sunitinib, or XBR as a single treatment on the cell cycle progression of PANC-1 cells.

The effects of gemcitabine (A), sunitinib (C), or XBR (E) on the cell cycle progression were assessed in PANC-1 cells at 4 (A1, C1, and E1), 24 (A2, C2, and E2), and 48 (A3, C3, and E3) hours post-treatment. The data were analysed using FACSDiva software v6.1.3. Data are means ± SD of cells percentage in each cell cycle phase, which generated from three independent experiments. Two-way ANOVA was used to compare the means of the cell cycle phases after treatment cells to untreated control cells and shown in Tables (B, D, and F). *P<0.05, **P<0.01, ***P<0.001 and ****P<0.0001.

4.3.1.3.2 Analysis of the cell cycle progression of MIA PaCa-2 cells following exposure to gemcitabine, sunitinib, or XBR alone

Figure 4.6 shows the effects of gemcitabine (A), sunitinib (C), or XBR (E) on the cell cycle progression in MIA PaCa-2 cells at 4 (A1, C1, and E1), 24 (A2, C2, and E2), and 48 (A3, C3, and E3) hours post-treatment.

Incubation of MIA PaCa-2 cells with increasing doses of gemcitabine alone resulted in significant time- and dose- dependent accumulation of cells in the S phase accompanied with a decrease in the G2/M phase of the cell cycle at 24 and 48 hours time-points compared to untreated control cells ($p < 0.001$). At the earlier time-point (4 hours), these changes in the cell cycle were observed with only the highest tested dose of gemcitabine (3.5 μM). At 24-hour after treatment, cell distribution was also increased in G0/G1. Cells were released from G1 phase and increased significantly in sub G0 phase after 48 hours of treatment with gemcitabine.

The treatment of MIA PaCa-2 cells with the highest tested dose of sunitinib (6 μM) resulted in a significant cell cycle arrest at G1 phase accompanied with a decrease in the G2/M phase of the cell cycle at 4 and 24 hours after treatment compared to untreated control cells ($p < 0.01$). However, cells were released from the G1 phase and arrested in the G2/M phase of the cell cycle after 48 hours of treatment with sunitinib.

Finally, irradiation with 0.5 Gy resulted in a significant arrest at the G2/M phase accompanied by a decrease in G0/1 phase of the cell cycle at 4 hours post-radiation ($p < 0.001$). Exposure to 1 Gy resulted in a significant cell cycle arrest at G2/M phase ($p < 0.001$) at 4 and 24 hours accompanied with a decrease in the G0/1 phase ($p < 0.001$) and S phase ($p < 0.01$) of the cell cycle at 24 hours after radiation. Moreover, exposure to 2 Gy resulted in a significant cell cycle arrest at G2/M phase ($p < 0.0001$) accompanied with a decrease in the G0/1 phase ($p < 0.001$) of the cell cycle at 4 and 24 hours after radiation compared to untreated control cells. There was no significant difference in the cell cycle distribution at 48 hours post-radiation compared to untreated control cells.

A **B**

(1)

4H

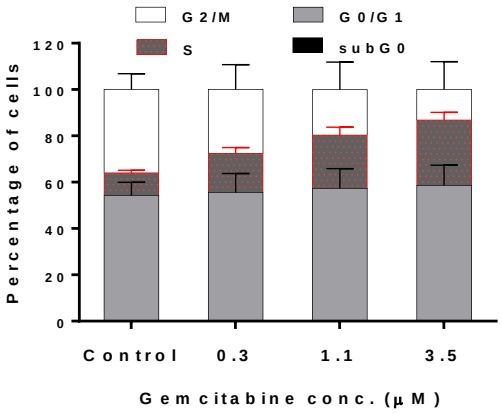

Control vs. Dose (μM)	0.3	1.1	3.5
subG0	ns	ns	ns
G0/G1	ns	ns	ns
S	ns	ns	**
G2/M	ns	*	***

(2)

24H

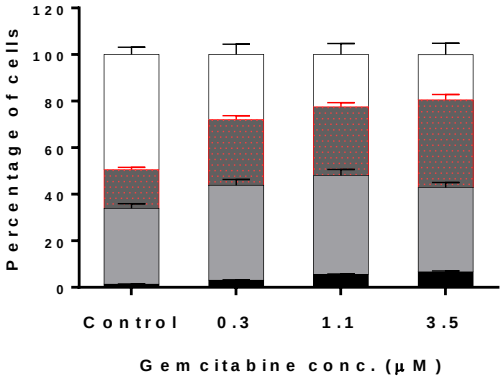

Control vs. Dose (μM)	0.3	1.1	3.5
subG0	ns	ns	*
G0/G1	**	***	ns
S	****	****	****
G2/M	****	****	****

(3)

48H

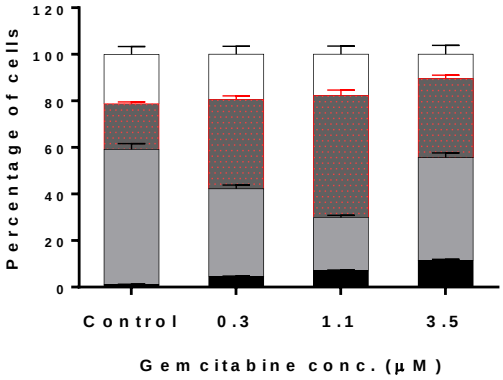

Control vs. Dose (μM)	0.3	1.1	3.5
subG0	ns	**	****
G0/G1	****	****	****
S	****	****	****
G2/M	ns	ns	****

Continued overleaf …

C **D**

(1)

4H

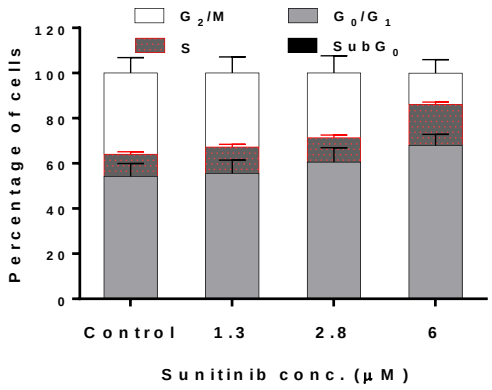

Control vs. Dose (μM)	1.3	2.8	6
subG0	ns	ns	ns
G0/G1	ns	ns	**
S	ns	ns	ns
G2/M	ns	ns	****

(2)

24H

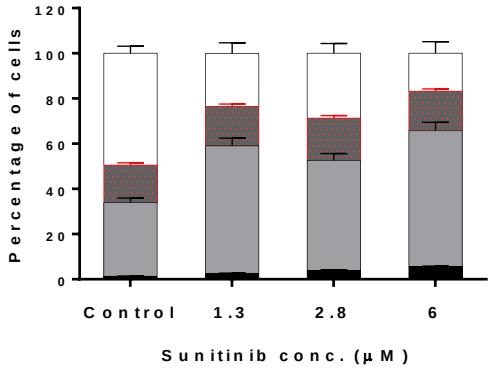

Control vs. Dose (μM)	1.3	2.8	6
subG0	ns	ns	ns
G0/G1	****	****	****
S	ns	ns	ns
G2/M	****	****	****

(3)

48H

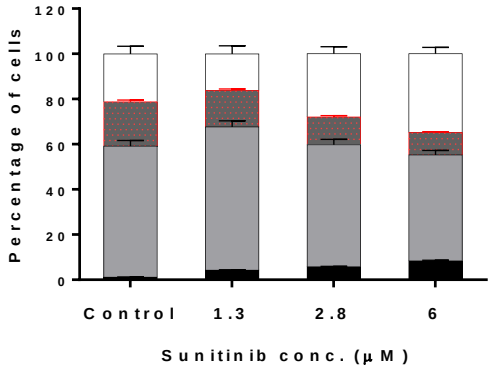

Control vs. Dose (μM)	1.3	2.8	6
subG0	ns	*	***
G0/G1	**	ns	****
S	ns	***	****
G2/M	*	**	****

Continued overleaf …

E **F**

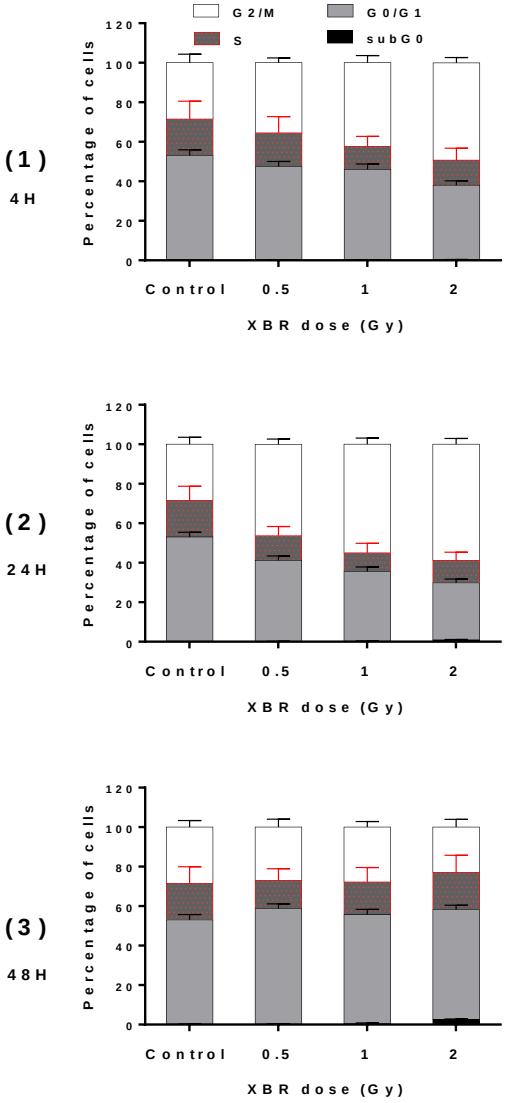

Control vs. Dose (Gy)	0.5	1	2
subG0	ns	ns	ns
G0/G1	ns	ns	***
S	ns	ns	ns
G2/M	ns	***	****

Control vs. Dose (Gy)	0.5	1	2
subG0	ns	ns	ns
G0/G1	***	****	****
S	ns	**	*
G2/M	****	****	****

Control vs. Dose (Gy)	0.5	1	2
subG0	ns	ns	ns
G0/G1	ns	ns	ns
S	ns	ns	ns
G2/M	ns	ns	ns

Figure 4.6 Effect of gemcitabine, sunitinib, or XBR as a single treatment on the cell cycle progression of MIA PaCa-2 cells.

The effects of gemcitabine (A), sunitinib (C), or XBR (E) on the cell cycle progression were assessed in MIA PaCa-2 cells at 4 (A1, C1, and E1), 24 (A2, C2, and E2), and 48 (A3, C3, and E3) hours post-treatment. The data were analysed using FACSDiva software v6.1.3. Data are means ± SD of cells percentage in each cell cycle phase, which generated from three independent experiments. Two-way ANOVA was used to compare the means of the cell cycle phases after treatment cells to untreated control cells and shown in Tables (B, D, and F). *P<0.05, **P<0.01, ***P<0.001 and ****P<0.0001.

4.3.1.4 The effect of single cytotoxic agents on the induction of apoptosis measured by Annexin V assay in pancreatic cancer cells

In these experiments, the expression of Annexin V, as an indicator of apoptosis, was assessed at 4, 24, and 48 hours after a single treatment with gemcitabine, sunitinib, or XBR in PANC-1 and MIA PaCa-2 cell lines as described in section 2.11. An increase in cell death, DNA damage and cell cycle arrest had previously been reported in our mechanistic studies, therefore we hypothesised that an increase in the size of the apoptotic population would be seen following the treatment with those agents.

4.3.1.4.1 The effect of gemcitabine, sunitinib, or XBR as single cytotoxic treatment on the induction of apoptosis measured by Annexin V assay in PANC-1 cells

The induction of apoptosis of PANC-1 cells was assessed at 4, 24, and 48 hours after a single treatment with gemcitabine (0.6, 1.1, and 2 μM), sunitinib (1.8, 4.2, and 9.8 μM), or XBR (0.5, 1, and 2 Gy) as described in section 2.11. The results of this experiment were calculated by addition of the percentage of cells in early and late apoptosis and presented in Figure 4.7. Generally, gemcitabine induced higher and earlier apoptosis in PANC-1 cells than sunitinib or XBR.

Figure 4.7 (A1) shows the apoptosis rate at 4, 24, and 48 hours post-treatment of PANC-1 cells with increasing dose of gemcitabine. In our study, it has been observed that the apoptosis rate increased in a dose and time-dependent manner after treatment with gemcitabine alone compared to untreated control cells. The apoptosis rate of PANC-1 cells increased significantly from 3.6 ± 1.2% in untreated control cells to 13.5 ± 3.1, 19.3 ± 3.8, and 29.4 ± 3.7 at 4, 24, and 48 hours, respectively, after treatment with 2 μM of gemcitabine ($p < 0.001$). Figure 4.7 (A2) summarises the effect of time on the induction of the apoptosis process in PANC-1 after treatment with gemcitabine alone. It can be seen that apoptosis increased significantly after 48 hours of treatment with all tested doses of gemcitabine compared to the earlier time-points ($p < 0.01$) in a dose-dependent manner. These results were expected and consistent with our results from clonogenic assay (4.3.1.1.1), DNA damage and repair process which was detected by the expression of γ-H_2AX (section 4.3.1.2.1), and cell cycle analysis (section 4.3.1.4.1).

Figure 4.7 (B1) shows the apoptosis level at 4, 24, and 48 hours post-treatment of PANC-1 cells with increasing dose of sunitinib. We observed that the apoptosis level increased in a dose- and time- dependent manner after treatment with sunitinib alone compared to untreated control cells. In contrast to gemcitabine, there was no observed increase in apoptosis in PANC-1 cells at 4 hours after treatment with sunitinib alone. However, the apoptosis rate of PANC-1 cells increased significantly from 3.6 ± 1.2% in untreated control cells to 13.3 ± 3.4, and 23.4 ± 2.9 at 24 and 48 hours, respectively, after treatment with 9.8 μM of sunitinib ($p < 0.0001$). Two-way ANOVA to assess the effect of

time on the induction of the apoptosis process in PANC-1 after treatment with sunitinib alone was summarised in Figure 4.7 (B2). Apoptosis increased significantly after 48 hours of treatment with all tested doses of sunitinib compared to the earlier time-points ($p < 0.01$).

Figure 4.7 (C1) demonstrates the apoptosis level in PANC-1 cells at 4, 24, and 48 hours post-irradiation. It can be observed that there was no significant increase in the level of apoptosis at 4 and 24 hours post-irradiation compared to non-irradiated control. However, apoptosis increased significantly from 3.6 ± 1.2% in non-irradiated control cells to 12.4 ± 2.7 ($p < 0.01$), and 16.7 ± 3.9 ($p < 0.0001$) at 48 hours after exposure to 1 Gy and 2 Gy, respectively.

A

(1)

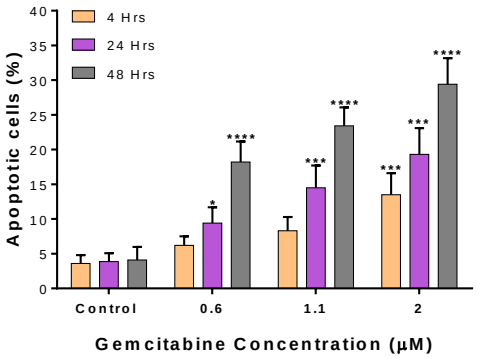

(2)

Time (Hours)	4 vs. 24	4 vs. 48	24 vs. 48
Control	ns	ns	ns
0.6	ns	****	**
1.1	ns	****	***
2	*	****	***

B

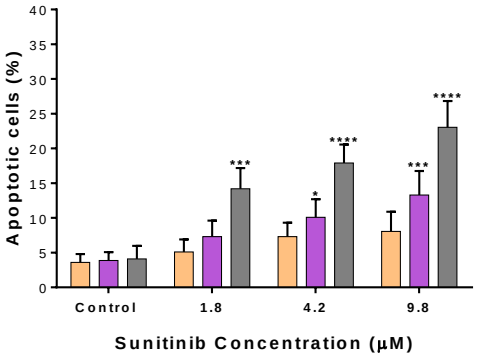

Time (Hours)	4 vs. 24	4 vs. 48	24 vs. 48
Control	ns	ns	ns
1.8	ns	***	**
4.2	ns	****	**
9.8	ns	****	***

C

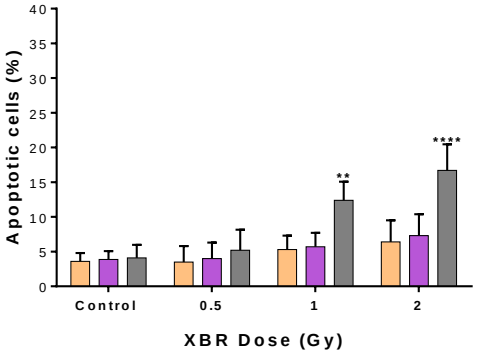

Time (Hours)	4 vs. 24	4 vs. 48	24 vs. 48
Control	ns	ns	ns
0.5	ns	ns	ns
1	ns	**	**
2	ns	***	***

Figure 4.7 The effect of single cytotoxic agents on apoptosis induction of PANC-1 cells.

The induction of apoptosis in PANC-1 cells was assessed at 4, 24, and 48 hours after treatment with gemcitabine (A1), sunitinib (B1), or XBR (C1) alone. Results presented are the mean ± SD percentage of apoptotic cells of 3 independent experiments. Statistical analysis was carried out using two-way ANOVA with (1) Dunnett's test to compare apoptosis rate resulted from all treatment doses over time-points to the untreated control group, and (2) with Tukey's test to compare apoptosis between different time-points after each dose of the treatment. *P<0.05, **P<0.01, ***P<0.001 and ****P<0.0001.

4.3.1.4.2 The effect of gemcitabine, sunitinib, or XBR as single cytotoxic treatment on the induction of apoptosis measured by Annexin V assay in MIA PaCa-2 cells

The induction of apoptosis of MIA PaCa-2 cells was assessed at 4, 24, and 48 hours after a single treatment with gemcitabine (0.3, 1.1, and 3.5 μM), sunitinib (1.3, 2.8, and 6 μM), or XBR (0.5, 1, and 2 Gy) as described in section 2.11. The results of this experiment were calculated by addition of the percentage of cells in early and late apoptosis and presented in Figure 4.8. Generally, gemcitabine caused higher and earlier apoptosis in PANC-1 cells than sunitinib or XBR.

Figure 4.8 (A1) shows the apoptosis rate at 4, 24, and 48 hours post-treatment of MIA PaCa-2 cells with increasing dose of gemcitabine. It has been observed that the apoptosis rate increased in a dose- and time- dependent manner after treatment with gemcitabine alone compared to untreated control cells. The apoptosis rate of MIA PaCa-2 cells increased significantly from 3.8 ± 1.3% in untreated control cells to 12.6 ± 2.9, 18 ± 3.4, and 27.4 ± 3.5 at 4, 24, and 48 hours, respectively, after treatment with 3.5 μM of gemcitabine ($p < 0.001$). Figure 4.8 (A2) summarised the effect of time on the induction of the apoptosis process in MIA PaCa-2 after treatment with gemcitabine alone. It can be seen that apoptosis increased significantly after 48 hours of treatment with all tested doses of gemcitabine compared to the earlier time-points ($p < 0.01$).

Figure 4.8 (B1) shows the apoptosis rate at 4, 24, and 48 hours post-treatment of MIA PaCa-2 cells with increasing dose of sunitinib. It has been observed that the apoptosis rate increased in a dose- and time- dependent manner after treatment with sunitinib alone compared to untreated control cells. In contrast to gemcitabine, there was no observed increase in apoptosis in MIA PaCa-2 cells at 4 hours after treatment with sunitinib alone. However, the apoptosis rate of MIA PaCa-2 cells increased significantly from 3.8 ± 1.3% in untreated control cells to 15.2 ± 3.9, and 26.3 ± 4.3 at 24 and 48 hours, respectively, after treatment with 6 μM of sunitinib ($p < 0.0001$). Two-way ANOVA to assess the effect of time on the induction of the apoptosis process in MIA PaCa-2 after treatment with sunitinib alone was summarised in Figure 4.8 (B2). It can be seen that apoptosis increased significantly after 48 hours of treatment with all tested doses of sunitinib compared to the earlier time-points ($p < 0.01$).

Figure 4.8 (C1) demonstrates the apoptosis rate in MIA PaCa-2 cells at 4, 24, and 48 hours post-irradiation with 0.5, 1, and 2 Gy. It can be observed that there was no significant increase in apoptosis rate at 4 and 24 hours post-irradiation compared to non-irradiated control. However, apoptosis increased significantly from 3.8 ± 1.3% in non-irradiated control cells to 8.3 ± 3.5 ($p < 0.01$), and 19.1 ± 4.1 ($p < 0.0001$) at 48 hours after exposure to 1 Gy and 2 Gy, respectively.

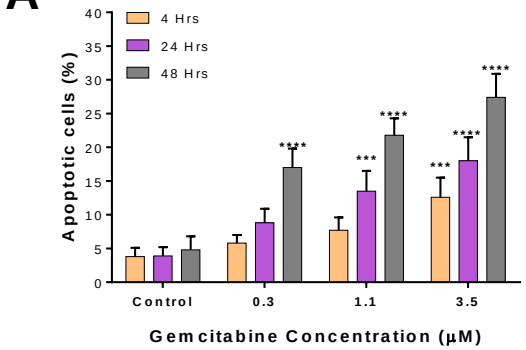

Time (Hours)	4 vs. 24	4 vs. 48	24 vs. 48
Control	ns	ns	ns
0.3	ns	****	**
1.1	*	****	**
3.5	*	****	***

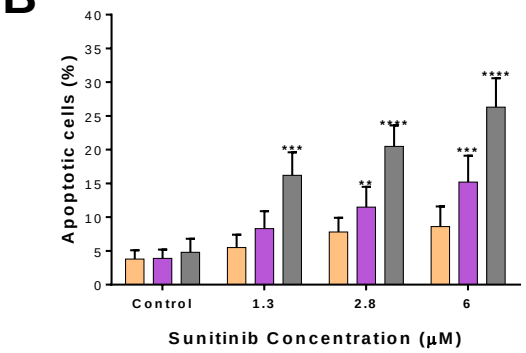

Time (Hours)	4 vs. 24	4 vs. 48	24 vs. 48
Control	ns	ns	ns
1.3	ns	***	**
2.8	ns	****	**
6	*	****	***

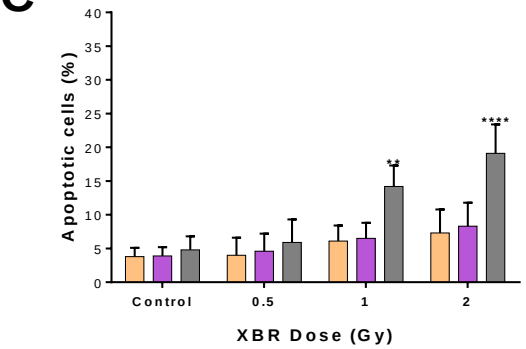

Time (Hours)	4 vs. 24	4 vs. 48	24 vs. 48
Control	ns	ns	ns
0.5	ns	ns	ns
1	ns	**	**
2	ns	****	***

Figure 4.8 The effect of single cytotoxic agents on apoptosis induction of MIA PaCa-2 cells.

The induction of apoptosis in MIA PaCa-2 cells was assessed at 4, 24, and 48 hours after treatment with gemcitabine (A1), sunitinib (B1), or XBR (C1) alone. Results presented are the mean ± SD percentage of apoptotic cells of 3 independent experiments. Statistical analysis was carried out using two-way ANOVA with (1) Dunnett's test to compare apoptosis rate resulted from all treatment doses over time-points to the untreated control group, and (2) with Tukey's test to compare apoptosis between different time-points after each dose of the treatment. *P<0.05, **P<0.01, ***P<0.001 and ****P<0.0001.

4.3.2 Cytotoxicity and mechanistic studies of gemcitabine and TKI as two-drug combination treatment in pancreatic cancer cells *in vitro*

The cytotoxicity effects of two-drug combination treatment of gemcitabine and TKI agents (sunitinib or pazopanib) on PANC-1 and MIA PaCa-2 cell lines were evaluated by clonogenic assays, DEF and combination index analysis. Gemcitabine was administered 48 hours before (schedule 1), after (schedule 2), or simultaneously with (schedule 3) TKI. These cytotoxicity studies were followed by the mechanistic studies of the two-drug combination treatment of gemcitabine and sunitinib (H_2AX detection, cell cycle analysis, and apoptosis) measured at three different time-points (4, 24, and 48 hours).

In response to the results of cytotoxic efficacy experiments (clonogenic assay, DEF, and CI analysis) presented in section 4.3.2.1.2, pazopanib in combination with gemcitabine, either without XBR (two-drug combination) or with XBR (three-treatment combination) was excluded from the mechanistic studies because it shows, unexpectedely, negligible cytotoxic effect in PANC-1 and MIA PaCa-2 pancreatic cancer cell lines compared to the another examined targeted therapy, sunitinib.

4.3.2.1 Assessment of cytotoxic effects of gemcitabine in combination with TKI on PANC-1 and MIA PaCa-2 cells by clonogenic assay, combination index analysis, and DEF.

We undertook combination index analysis using clonogenic survival assay data as described in section 2.7. In order to interrogate the data in an alternative way we also examined our clonogenic survival data from combination treatment with respect to the calculation of dose enhancement factors (DEF) as described in section 2.9.

Cell survival data which resulted from the two-drug combination treatment of gemcitabine and TKI were compared to those which resulted from the treatment with gemcitabine alone. The aim of these experiments was to evaluate the ability of TKI agents to sensitise pancreatic cancer cells to gemcitabine or vice versa.

4.3.2.1.1 Clonogenic survival assay of PANC-1 and MIA PaCa-2 cells following treatment with gemcitabine in combination with sunitinib

Figure 4.9 (A & B) demonstrates the cytotoxic effect of treatment with increasing doses of gemcitabine and sunitinib either as single treatment or in combination on the survival of PANC-1 (A) and MIA PaCa-2 (B) cells. For combination therapy, gemcitabine was administered 48 hours before (schedule 1), after (schedule 2), or simultaneously with (schedule 3) sunitinib.

The administered doses of gemcitabine and sunitinib were used in the combination therapy are presented in Table 3.5 and described in section 2.4.4. Generally, all combination doses of gemcitabine and sunitinib induced significant dose-dependent cytotoxicity in both cell lines regardless of the treatment schedule compared to untreated cells. The concurrent administration of gemcitabine and sunitinib (schedule 3) was the most effective combination schedule in both cell lines.

In PANC-1 cells (Figure 4.9 A), treatment with gemcitabine after sunitinib (schedule 2) was the least effective schedule compared to other schedules; hence all combined doses resulted in a significantly lower cytotoxicity effect following treatment with schedule 2 compared to concurrent treatment (schedule 3). Furthermore, there was no significant reduction in survival following schedule 2 combination of gemcitabine and sunitinib compared to gemcitabine alone ($p > 0.05$). In contrast, the simultaneous administration of gemcitabine and sunitinib (schedule 3) inhibited the survival of PANC-1 cells significantly with all tested doses compared to gemcitabine alone ($p < 0.01$). However, the effect of administration of gemcitabine before sunitinib (schedule 1) was similar to the effect of the concurrent therapy of both drugs (schedule 3) ($p > 0.05$) except at the highest examined doses of both drugs; hence the reduction in the survival of cells was approximately 77% and 91% following treatment with schedule 1 and 3, respectively ($p < 0.05$).

Similarly, treatment of MIA PaCa-2 cells (Figure 4.9 B) with schedule 2 resulted in the lowest toxicity compared to schedules 1 and 3. The reduction in cell

survival following the exposure to the three increasing doses of schedule 2 combination therapy was approximately 16%, 42%, and 51%, respectively. The concurrent treatment with gemcitabine and sunitinib (schedule 3) revealed significantly higher cytotoxicity than schedule 1 with the middle ($p < 0.01$) and the highest ($p < 0.05$) doses.

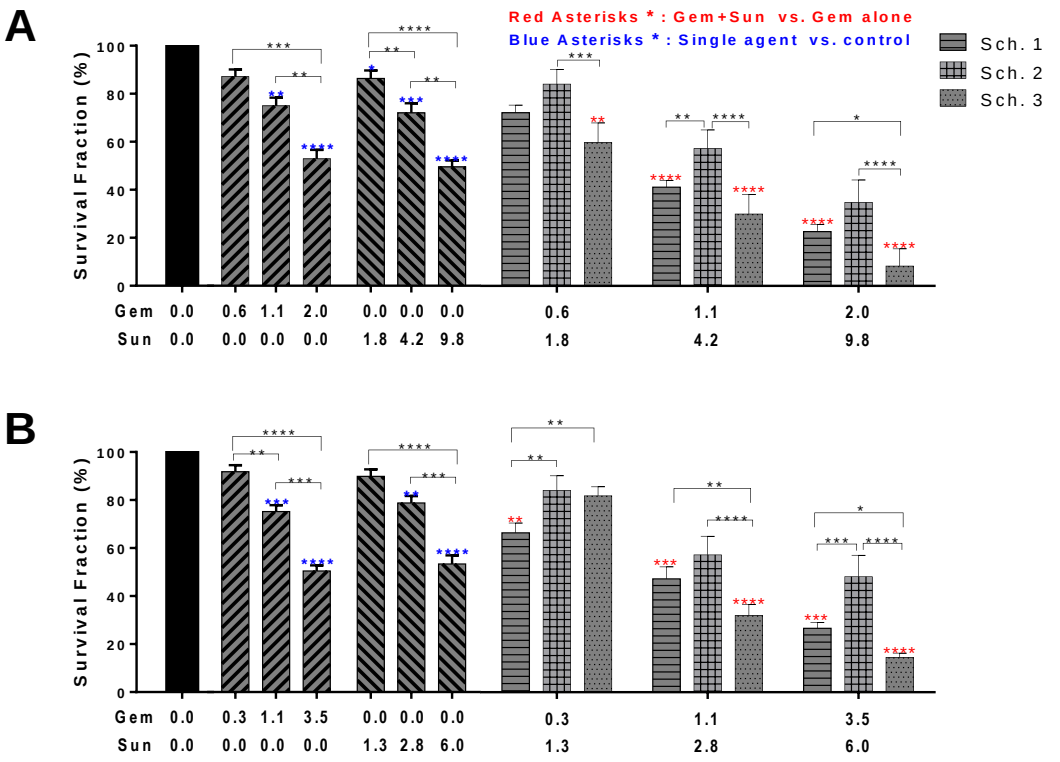

Figure 4.9 Effect of gemcitabine and sunitinib as single or combination chemotherapy on survival of PANC-1 and MIA PaCa-2 cell lines.

PANC-1 **(A)** or MIA PaCa-2 **(B)** cells were treated with monotherapy of gemcitabine or sunitinib, or in combination with gemcitabine before (Sch. 1), after (Sch. 2), or simultaneously with (Sch. 3), sunitinib for 48 hours and then survival fraction was measured by clonogenic assay. Data shown are expressed as a percentage of survival fraction normalised to the untreated control group. Statistical analysis was carried out using a two-way ANOVA followed by Tukey's test to compare all treatment doses in monotherapy or alternative combination schedules. Each value represents the mean ± SD of three independent experiments. *P<0.05, **P<0.01, ***P<0.001 and ****P<0.0001 compared to the survival fraction between different treatment groups.

Synergy analysis of the scheduled combinations was examined according to the method of Chou and Talalay (Chou and Talalay, 1984), which is based on the median-effect principle, as described in detail in section 2.7. Median-effect curves and combination-index analysis of the three combination schedules of gemcitabine and sunitinib treatment in PANC-1 and MIA PaCa-2 cells are shown in Figure 4.10. In both cell lines, schedule 2 (gemcitabine 48 hrs after sunitinib) was the least effective treatment and induced antagonistic responses with all examined doses. In contrast, the lowest combination doses of gemcitabine and sunitinib induced additive responses, and the higher two doses induced synergistic responses following schedule 1 and schedule 3 treatments in both cell lines. However, dose-dependent synergism was observed in PANC-1 but not in MIA PaCa-2 cells.

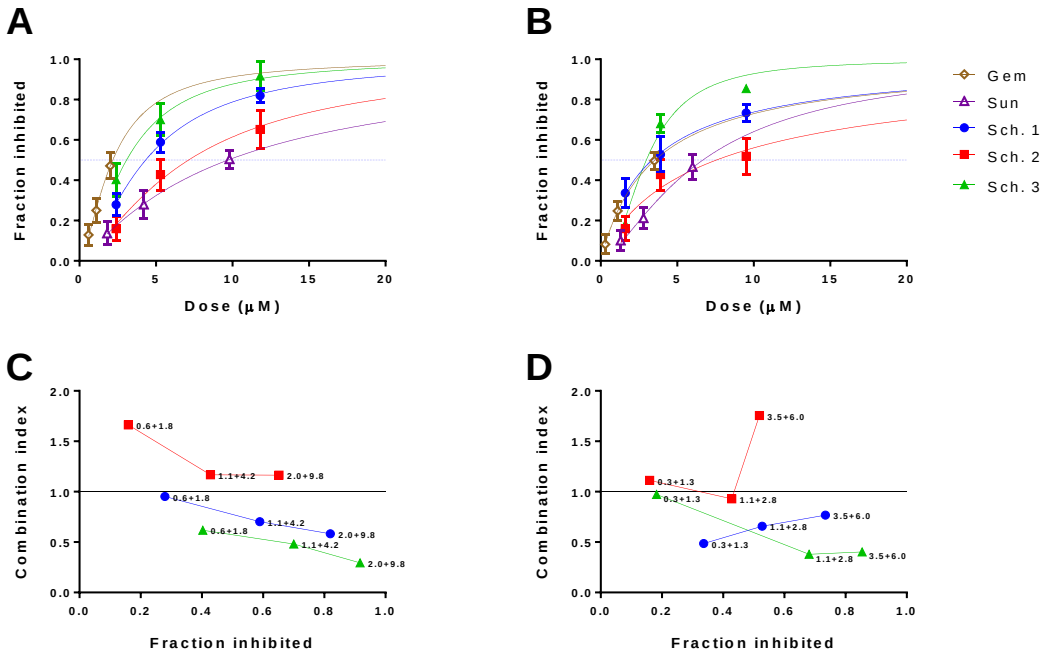

Figure 4.10 Combination index (CI) analysis of the combined effect of gemcitabine and sunitinib on clonogenic survival of PANC-1 and MIA PaCa-2 cells.

Median-effect curves for PANC-1 (A) and MIA PaCa-2 were plotted for single cytotoxic agents and combination schedules. Combination index (CI) with the corresponding fraction inhibited following the combination schedules were plotted for PANC-1 (C) and MIA PaCa-2 (D). CI > 1.1, CI between 0.9 and 1.1, and CI < 0.9 indicate antagonism, additivity, and synergism, respectively. Each value represents the median CI of three separate experiments.

Optimised ratio of each drug combination

Figure 4.11 (A & C) demonstrates that the survival fraction of PANC-1 cells was decreased significantly following the treatment with 4.2 and 9.8 μM of sunitinib in combination with gemcitabine compared to treatment with gemcitabine alone ($p < 0.05$). Figure 4.11 (E) shows the R^2 for the response curve fit, IC_{50}, and the dose enhancement factor (described in section 2.9) at the 50% cytotoxicity level (DEF_{50}) following treatment PANC-1 cells with sunitinib in combination with gemcitabine compared to gemcitabine alone. It can be seen that sunitinib sensitized the cells to gemcitabine treatment and the DEF50 achieved was 1.45, 1,67, and 1.85 following the administration of 1.8, 4.2, and 9.8 μM of sunitinib, respectively.

Figure 4.11 (B & D) demonstrates that the survival fraction of MIA PaCa-2 cells was decreased significantly following the treatment with all tested doses of sunitinib in combination with gemcitabine compared to treatment with gemcitabine alone ($p < 0.05$). Sunitinib sensitised MIA PaCa-2 cells to gemcitabine. MIA PaCa-2 was more sensitive to sunitinib than PANC-1; the DEF_{50} achieved was 1.94, 3.7, and 3.02 following the administration of 1.3, 2.8, and 6 μM of sunitinib, respectively (Figure 4.11 - F).

The other way of sensitisation was also investigated to assess whether gemcitabine can sensitise pancreatic cancer cell to sunitinib. We found that gemcitabine sensitised both PANC-1 and MIA PaCa-2 cells to sunitinib; and the calculated DEF_{50} was reported in Figure 4.12. The sensitivity of pancreatic cancer cells to sunitinib treatment was enhanced and the calculated DEF_{50} were 2.54 and

2.87 when sunitinib combined with 2 μM and 3.5 μM gemcitabine in PANC-1 and MIA PaCa-2 cells, compared to sunitinib alone, respectively.

A

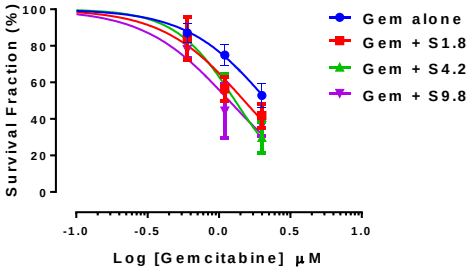

B

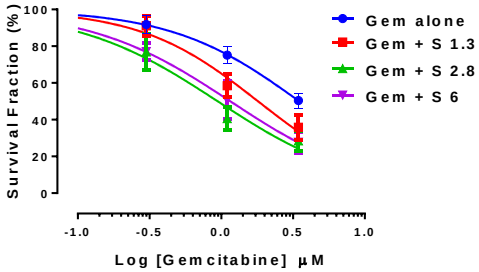

C

P-values summary from Bonferroni's test

Gem (µM)	Gem+S1.8	Gem+S4.2	Gem+S9.8
0.6	> .05	> .05	.42
1.1	.014	.019	<.0001
2.0	.23	.002	.031

D

P-values summary from Bonferroni's test

Gem (µM)	Gem+S1.3	Gem+S2.8	Gem+S6.0
0.3	> .05	.0084	.0095
1.1	.003	< .0001	<.0001
3.5	.014	.001	<.0001

E

Sunitinib Dose	0 µM	1.8 µM	4.2 µM	9.8 µM
R^2	0.94	0.91	0.94	0.89
IC_{50}	2.17	1.50	1.30	1.18
DEF_{50}	1.00	1.45	1.67	1.85

F

Sunitinib Dose	0 µM	1.3 µM	2.8 µM	6.0 µM
R^2	0.97	0.96	0.95	0.96
IC_{50}	3.50	1.80	0.94	1.16
DEF_{50}	1.00	1.94	3.70	3.02

Figure 4.11 Sunitinib sensitises pancreatic cancer cells to gemcitabine.

PANC-1 **(A)** or MIA PaCa-2 **(B)** cells were treated with increasing doses of gemcitabine (Gem) alone or in simultaneous combination (schedule 3) with sunitinib (S) for 48 hours and then survival fraction was measured by clonogenic assay. Data shown are expressed as a percentage of survival fraction normalised to the gemcitabine alone group. Statistical analysis was carried out using a two-way ANOVA followed by Bonferroni's test to compare gemcitabine doses alone with those in combination with sunitinib in PANC-1 **(C)** and MIA PaCa-2 **(D)**. R^2, $IC_{50,}$ and dose-enhancement factor (DEF_{50}) are calculated for PANC-1 **(E)** and MIA PaCa-2 **(F)**. $DEF_{50} > 1$ indicates the sensitization effect of sunitinib for cells to gemcitabine treatment.

A

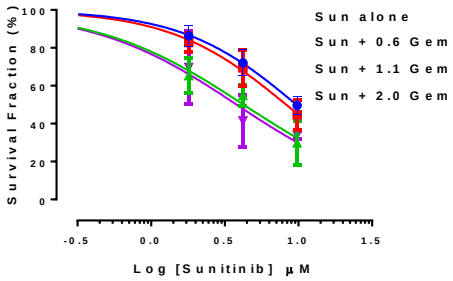

B

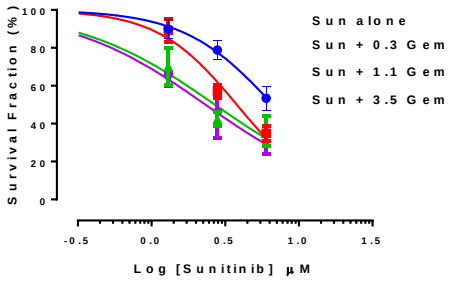

C

P-values summary from Bonferroni's test

Sun (µM)	Sun+G0.6	Sun+G1.1	Sun+G2.0
1.8	> .99	0.01	0.056
4.2	> .99	.047	.0002
9.8	> .99	.019	.0808

D

P-values summary from Bonferroni's test

Sun (µM)	Sun+G0.3	Sun+G1.1	Sun+G3.5
1.3	> .999	.0007	<.0001
2.8	.0002	< .0001	<.0001
6.0	.0015	.0027	<.0001

E

Gemcitabine Dose	0 µM	0.6 µM	1.1 µM	2.0 µM
R^2	0.95	0.93	0.93	0.86
IC_{50}	9.70	8.27	4.25	3.81
DEF_{50}	1.00	1.17	2.29	2.54

F

Gemcitabine Dose	0 µM	0.3 µM	1.1 µM	3.5 µM
R^2	0.95	0.97	0.93	0.95
IC_{50}	6.67	3.80	2.69	2.33
DEF_{50}	1.00	1.76	2.48	2.87

Figure 4.12 Gemcitabine sensitises pancreatic cancer cells to sunitinib.

PANC-1 **(A)** or MIA PaCa-2 **(B)** cells were treated with increasing doses of sunitinib (Sun) alone or in simultaneous combination (schedule 3) with gemcitabine (Gem) for 48 hours and then survival fraction was measured by clonogenic assay. Data shown are expressed as a percentage of survival fraction normalised to the sunitinib alone group. Statistical analysis was carried out using a two-way ANOVA followed by Bonferroni's test to compare sunitinib doses alone with those in combination with gemcitabine in PANC-1 **(C)** and MIA PaCa-2 **(D)**. R^2, $IC_{50,}$ and dose-enhancement factor (DEF_{50}) are calculated for PANC-1 **(E)** and MIA PaCa-2 **(F)**. DEF_{50} > 1 indicates the sensitization effect of gemcitabine for cells to sunitinib treatment.

4.3.2.1.2 Clonogenic survival assay of PANC-1 and MIA PaCa-2 cells following treatment with gemcitabine in combination with pazopanib

Figure 4.13 demonstrates the effect of treatment with increasing doses of gemcitabine administered in combination with increasing doses of pazopanib on the survival of PANC-1 and MIA PaCa-2 cells. Gemcitabine was administered 48 hours before (schedule 1), after (schedule 2), or simultaneously with (schedule 3) pazopanib. The administered doses of gemcitabine and pazopanib which were used in the combination treatment are shown in the figure. Generally, apart from the smallest combination dose in schedule 2 treatment, all three schedules of gemcitabine and pazopanib induced significant dose-dependent cytotoxicity with all three examined doses in PANC-1 and MIA PaCa-2 cells, compared to the untreated cells. However, there was no significant increase in the cytotoxicity following the combination treatment of gemcitabine and pazopanib compared to treatment with gemcitabine alone in both cell lines regardless of the treatment scheduling ($p < 0.05$). Therefore, this combination treatment was excluded from the mechanistic studies of both two-drug and three-treatment combination strategies.

In PANC-1 cells [Figure 4.13 A], with an exception of the treatment at the highest applied dose of gemcitabine and pazopanib, which induced a significantly higher cytotoxicity following the concurrent combination therapy

(schedule 3) than schedule 2 treatment ($p < 0.05$), there was no significant difference in the efficacy between the three schedules.

Conversely, the treatment of MIA PaCa-2 cells [Figure 4.13 B] with simultaneous administration of 3.5 μM of gemcitabine and 5.1 μM of pazopanib (schedule 3) reduced clonogenic survival to approximately 28% ± 4.8% compared to inhibition to 41% ± 4.5% with schedule 1 ($p < 0.01$) or to 43% ± 3.2% with schedule 2 ($p < 0.001$). A higher efficacy was also observed at the middle dose in the concurrent combination compared to schedule 2. The smallest dose failed to show any significant difference in the cytotoxicity between the three combination schedules.

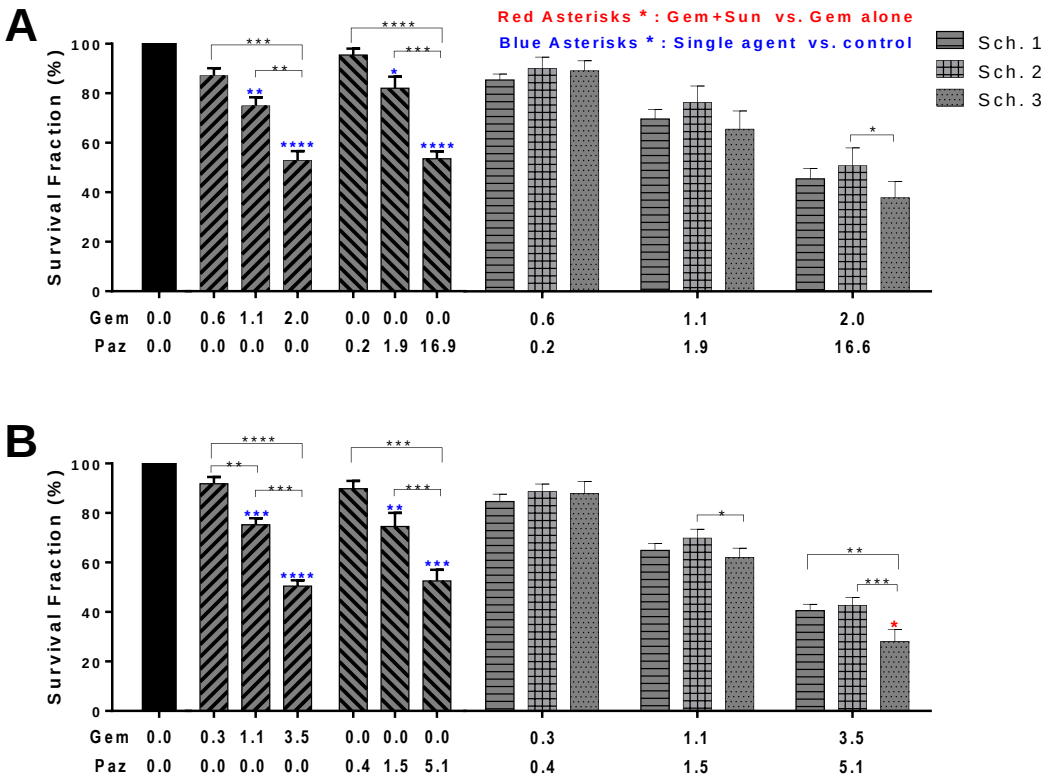

Figure 4.13 Effect of gemcitabine and pazopanib as single or combination chemotherapy on survival of PANC-1 and MIA PaCa-2 cell lines.

PANC-1 **(A)** or MIA PaCa-2 **(B)** cells were treated with monotherapy of gemcitabine or pazopanib, or in combination gemcitabine before (Sch. 1), after (Sch. 2), or simultaneously with (Sch. 3), pazopanib for 48 hours and then survival fraction was measured by clonogenic assay. Data shown are expressed as a percentage of survival fraction normalised to the untreated control group. Statistical analysis was carried out using a two-way ANOVA followed by Tukey's test to compare all treatment doses in monotherapy or alternative combination schedules. Each value represents the mean ± SD of three independent experiments. *P<0.05, **P<0.01 and ***P<0.001 compared to the survival fraction between different treatment groups.

Combination-index analysis of gemcitabine and pazopanib treatments in PANC-1 and MIA PaCa-2 cells are shown in Figure 4.13 (C & D). In both cell lines, schedule 2 (gemcitabine after pazopanib) was the least effective treatment and induced antagonistic responses with all examined doses. In PANC-1 cells, all three schedules induced antagonistic responses (CI > 1). In schedules 1 and 2, the antagonism effect was dose-dependent, i.e. the higher doses of drugs the higher antagonism observed. In MIA PaCa-2 cells, schedule 1 induced dose-dependent antagonism response whereas the simultaneous treatment (schedule 3) induced antagonism, additivity, and synergism with the lowest, the middle, and the highest doses, respectively.

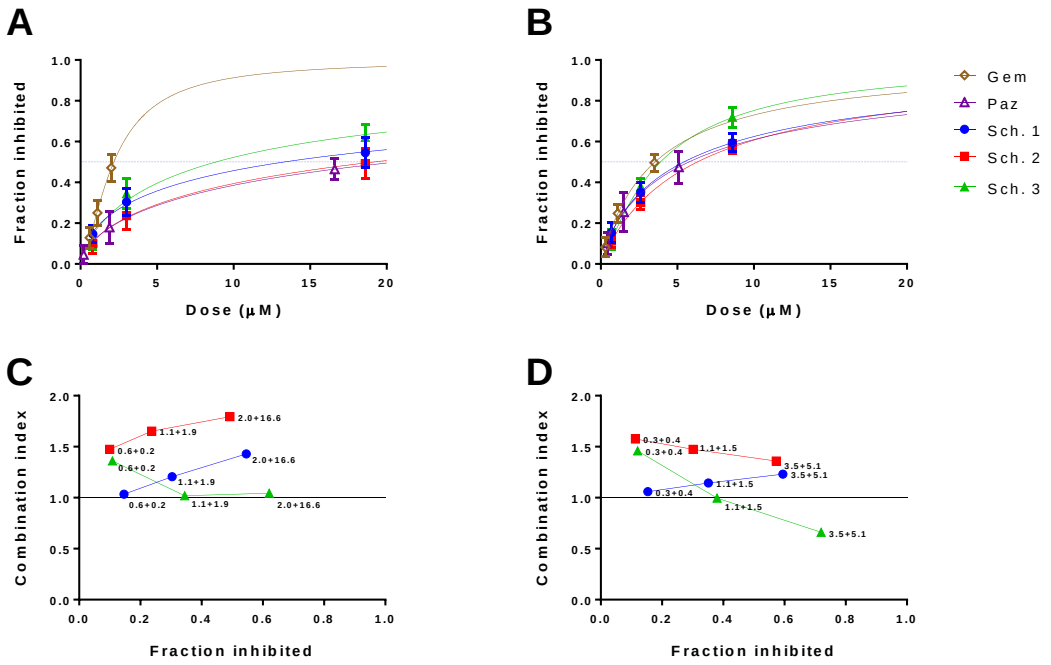

Figure 4.14 Combination index (CI) analysis of the combined effect of gemcitabine and pazopanib on clonogenic survival of PANC-1 and MIA PaCa-2 cells.

Median-effect curves for PANC-1 (A) and MIA PaCa-2 were plotted for single cytotoxic agents and combination schedules. Combination index (CI) with the corresponding fraction inhibited following the combination schedules were plotted for PANC-1 (C) and MIA PaCa-2 (D). CI > 1.1, CI between 0.9 and 1.1, and CI < 0.9 indicate antagonism, additivity, and synergism, respectively. Each value represents the CI median of three separate experiments.

Figure 4.14 (A - D) reveals that the treatment with pazopanib has no additional cytotoxic effect when combined with gemcitabine in terms of cell survival compared to the treatment with gemcitabine alone in both cell lines ($p > 0.05$). The IC_{50} and DEF_{50} of the combination treatment with gemcitabine and pazopanib suggested that pazopanib decreased the sensitivity of PANC-1 and MIA PaCa-2 cells to gemcitabine.

A

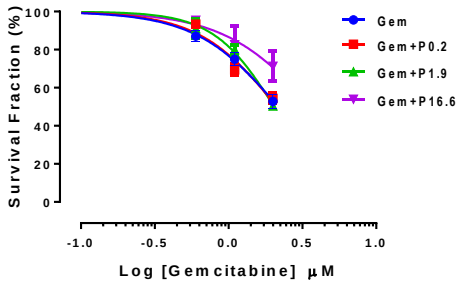

B

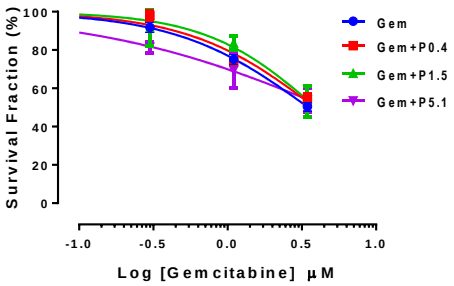

C

P-values summary from Bonferroni's test

Gem (µM)	Gem+P0.2	Gem+P1.9	Gem+P16.6
0.6	> .05	> .05	> .05
1.1	> .05	> .05	> .05
2.0	> .05	> .05	.0083

D

P-values summary from Bonferroni's test

Gem (µM)	Gem+P0.4	Gem+P1.5	Gem+P5.1
0.3	> .05	> .05	> .05
1.1	> .05	> .05	> .05
3.5	> .05	> .05	> .05

E

Pazopanib Dose	0 µM	0.2 µM	1.9 µM	16.6 µM
R^2	0.94	0.93	0.95	0.59
IC_{50}	2.17	2.12	2.04	3.69
DEF_{50}	1.00	1.03	1.07	0.59

F

Pazopanib Dose	0 µM	0.4 µM	1.5 µM	5.1 µM
R^2	0.97	0.95	0.78	0.82
IC_{50}	3.50	3.90	3.95	4.69
DEF_{50}	1.00	0.90	0.89	0.75

Figure 4.15 Pazopanib decreases the sensitivity of pancreatic cancer cells to gemcitabine.

PANC-1 **(A)** or MIA PaCa-2 **(B)** cells were treated with increasing doses of gemcitabine (Gem) alone or in simultaneous combination with pazopanib (P) for 48 hours and then survival fraction was measured by clonogenic assay. Data shown are expressed as a percentage of survival fraction normalised to the gemcitabine alone group. Statistical analysis was carried out using a two-way ANOVA followed by Bonferroni's test to compare gemcitabine doses alone with those in combination with pazopanib in PANC-1 **(C)** and MIA PaCa-2 **(D)**. R^2, IC_{50}, and dose-enhancement factor (DEF_{50}) are calculated for PANC-1 **(E)** and MIA PaCa-2 **(F)**. DEF_{50} > 1 indicates the sensitization effect of pazopanib for cells to gemcitabine treatment.

4.3.2.2 The effect of two-drug combination treatments on the induction and repair of DNA damage measured by γ-H_2AX in pancreatic cancer cells

In these experiments, the expression of γ-H_2AX, as a marker of DNA damage and repair, was assessed at 4, 24, and 48 hours after treatment with gemcitabine and sunitinib, in three different combination schedules, in PANC-1 and MIA PaCa-2 cell lines as described in section 2.12.

4.3.2.2.1 The effect of gemcitabine and sunitinib as two-drug combination treatments on the induction and repair of DNA damage measured by γ-H2AX in PANC-1 cells

Figure 4.16 (A) shows the average fold increase in γ-H_2AX expression at 4, 24, and 48 hours post-treatment of PANC-1 cells with increasing doses of gemcitabine administered before (A1), after (A2), or simultaneously with (A3) increasing doses of sunitinib compared to γ-H_2AX levels after gemcitabine alone (presented in Figure 4.3A).

Although the combination treatment with sunitinib and gemcitabine significantly increased the γ-H_2AX expression compared to untreated control cells ($p < 0.0001$), there was no significant additional effect on γ-H_2AX levels for this combination compared to treatment with gemcitabine alone at all time-points and all combination schedules. The γ-H_2AX levels decreased

significantly after 24 and 48 hours of treatment with all combination schedules compared to its levels at 4 hours ($p < 0.01$; Figure 4.16 B).

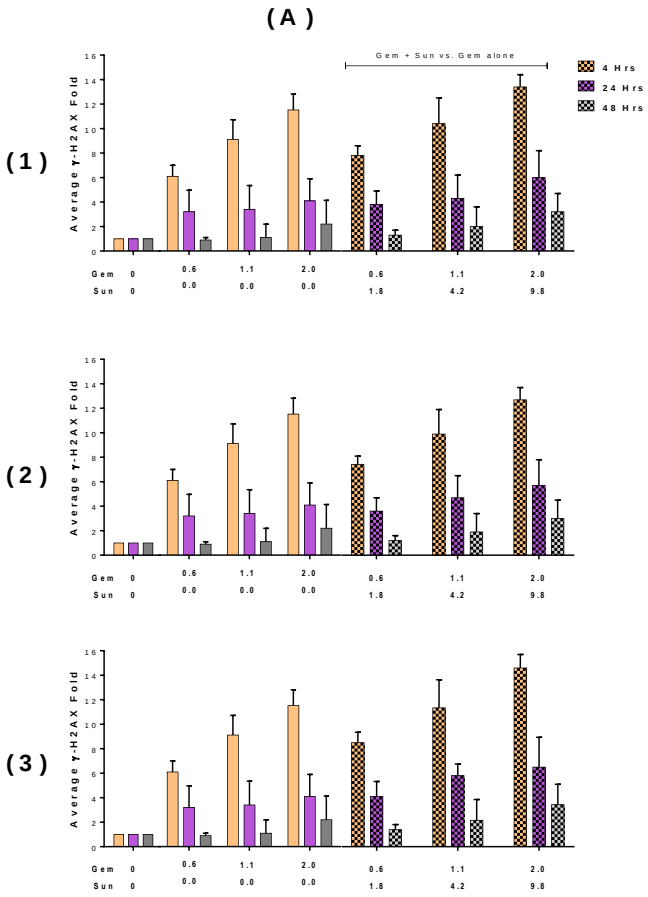

Time (Hours)	4 vs. 24	4 vs. 48	24 vs. 48
Control	ns	ns	ns
T1	*	***	ns
T2	***	****	ns
T3	****	****	ns

Time (Hours)	4 vs. 24	4 vs. 48	24 vs. 48
Control	ns	ns	ns
T1	*	***	ns
T2	***	****	ns
T3	****	****	ns

Time (Hours)	4 vs. 24	4 vs. 48	24 vs. 48
Control	ns	ns	ns
T1	**	****	ns
T2	****	****	**
T3	****	****	*

Figure 4.16 The effect of gemcitabine and sunitinib as two-drug combination treatments on the induction and repair of DNA damage measured by γ-H2AX in PANC-1 cells.

The expression of γ-H2AX of PANC-1 cells was assessed at 4, 24, and 48 hours after treatment with gemcitabine administered before (A1), after (A2), or simultaneously with (A3) sunitinib. Results presented are the mean ± SD fold of γ-H2AX expression compared to untreated control cells of 3 independent experiments. Statistical analysis was carried out using two-way ANOVA with Dunnett's test to compare average fold of γ-H2AX resulted from all treatment doses over time-points to gemcitabine alone (A1, A2, and A3), and with Tukey's test to compare γ-H2AX between different time-points after each dose of the treatment (B1, B2, and B3). Effect of gemcitabine alone on γ-H2AX is illustrated in Figure 4.3. **P<0.01, ***P<0.001 and ****P<0.0001. Gem = gemcitabine; Sun = sunitinib; T1 = 0.6 μM gem + 1.8 μM Sun; T2 = 1.1 μM gem + 4.2 μM sun; T3 = 2 μM gem + 9.8 μM sun; ns = Not significant.

4.3.2.2.2 The effect of gemcitabine and sunitinib as two-drug combination treatments on the induction and repair of DNA damage measured by γ-H2AX in MIA PaCa-2 cells

Figure 4.17 (A) shows the average of fold increase in γ-H_2AX at 4, 24, and 48 hours post-treatment of MIA PaCa-2 cells with increasing doses of gemcitabine administered before (A1), after (A2), or simultaneously with (A3) increasing doses of sunitinib compared to γ-H_2AX levels after gemcitabine alone (presented in Figure 4.4A).

Although the combination treatment with sunitinib and gemcitabine significantly increased the γ-H_2AX expression compared to untreated control cells ($p < 0.0001$), there was no significant additional effect on γ-H_2AX levels for this combination compared to treatment with gemcitabine alone at all time-points and all combination schedules. The γ-H_2AX levels decreased significantly after 24 and 48 hours of treatment compared to its levels at 4 hours ($p < 0.01$; Figure 4.17 B).

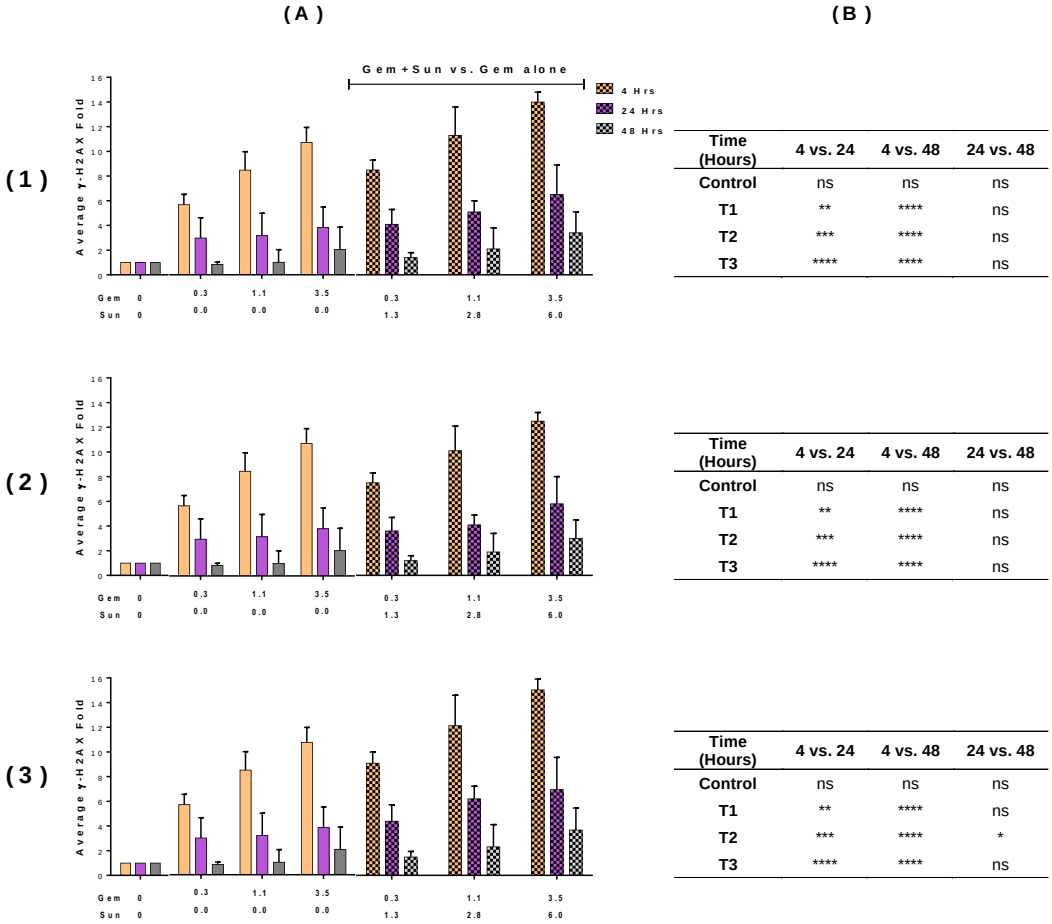

Time (Hours)	4 vs. 24	4 vs. 48	24 vs. 48
Control	ns	ns	ns
T1	**	****	ns
T2	***	****	ns
T3	****	****	ns

Time (Hours)	4 vs. 24	4 vs. 48	24 vs. 48
Control	ns	ns	ns
T1	**	****	ns
T2	***	****	ns
T3	****	****	ns

Time (Hours)	4 vs. 24	4 vs. 48	24 vs. 48
Control	ns	ns	ns
T1	**	****	ns
T2	***	****	*
T3	****	****	ns

Figure 4.17 The effect of two-drug combination treatments on the induction and repair of DNA damage measured by γ-H2AX in MIA PaCa-2 cells.

The expression of γ-H2AX of MIA PaCa-2 cells was assessed at 4, 24, and 48 hours after treatment with gemcitabine administered before (A1), after (A2), or simultaneously with (A3) sunitinib. Results presented are the mean ± SD fold of γ-H2AX expression compared to untreated control cells of 3 independent experiments. Statistical analysis was carried out using two-way ANOVA with Dunnett's test to compare average fold of γ-H2AX resulted from all treatment doses over time-points to gemcitabine alone (A1, A2, and A3), and with Tukey's test to compare γ-H2AX between different time-points after each dose of the treatment (B1, B2, and B3). Effect of gemcitabine alone on γ-H2AX is illustrated in Figure 4.4 **P<0.01, ***P<0.001 and ****P<0.0001. Gem = gemcitabine; Sun = sunitinib; T1 = 0.3 μM gem + 1.3 μM Sun; T2 = 1.1 μM gem + 2.8 μM sun; T3 = 3.5 μM gem + 6 μM sun; ns = Not significant.

4.3.2.3 Analysis of the cell cycle progression of pancreatic cancer cells following two-drug combination treatment

In these experiments, the cell cycle progression of PANC-1 and MIA PaCa-2 cells was assessed at 4, 24, and 48 hours after treatment with gemcitabine and sunitinib, in three different combination schedules, as described in section 2.10.

4.3.2.3.1 Analysis of the cell cycle progression of PANC-1 cells following treatment with gemcitabine in combination with sunitinib

Figure 4.18 shows the effect of increasing doses of gemcitabine and sunitinib as a double combination treatment on the cell cycle progression of PANC-1 cells. The cells were treated with gemcitabine administered before (schedule 1; A), after (schedule 2; C) and simultaneously with (schedule 3; E) sunitinib and the cell cycle analysis was carried out at 4 (A1, C1 & E1), 24 (A2, C2 & E2), and 48 (A3, C3 & E3) hours post-treatment.

Schedule 1 combination treatment of PANC-1 cells resulted in a significant accumulation of cells in the S phase accompanied by a decrease in the G2/M phase of the cell cycle ($p < 0.001$) compared to untreated control cells. With the highest dose of combination, in addition to the accumulation in the S phase, cells were also increased significantly in the G0/1 phase from 46.7 ± 1.7% to 58.8 ± 6% ($p < 0.01$) at 4 hours post-treatment. At 24 hours following treatment, cell distribution increased significantly in G0/1 ($p < 0.0001$) compared to

untreated control cells. At 48 hours, the two highest doses of gemcitabine and sunitinib resulted in a significant increase of cells in the subG0 phase to reach 32 ± 1.6% accompanied with a decrease in the G0/1, S, and G2/M phases compared to untreated control cells ($p < 0.0001$).

Following the treatment PANC-1 cells with the schedule 2 combination strategy, there was a significant accumulation of cells in the G0/1 phase accompanied with a decrease in the G2/M phase of the cell cycle only with the highest dose of combination ($p < 0.05$) compared to untreated control cells at all time-points of measurement. However, cell distribution in the S phase was decreased with further accumulation in G0/1 phase in the highest dose treatment group compared to the untreated cell group ($p < 0.0001$).

Treatment PANC-1 cells with gemcitabine simultaneously administered with sunitinib (schedule 3) resulted in a significant accumulation of cells in the G0/1 phase accompanied with a decrease in the G2/M phase of the cell cycle only with the two highest doses of combination ($p < 0.001$) at all time-points of measurement. At 48 hours, however, cell distribution in the S phase was decreased accompanied with cell arrest in the G2/M and subG0 phases in the highest dose treatment group compared to an untreated cell group ($p < 0.001$).

A **B**

1

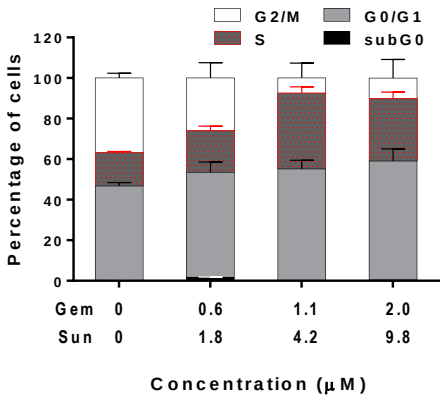

Control vs. Dose (μM)	T1	T2	T3
subG0	ns	ns	ns
G0/G1	ns	ns	**
S	ns	****	***
G2/M	*	****	****

2

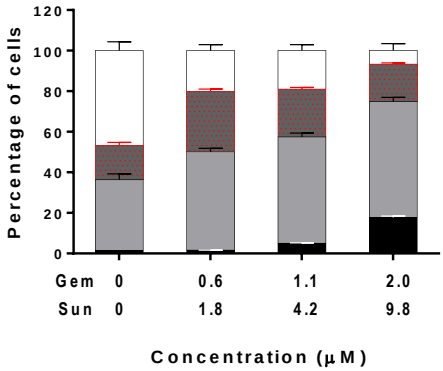

Control vs. Dose (μM)	T1	T2	T3
subG0	ns	ns	****
G0/G1	****	****	****
S	****	**	ns
G2/M	****	****	****

3

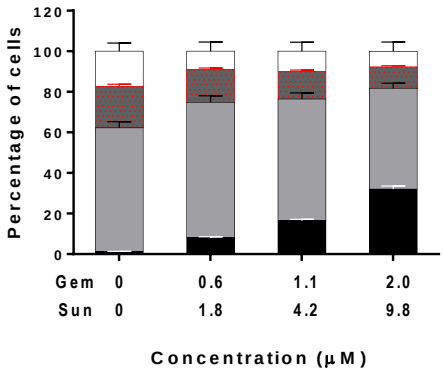

Control vs. Dose (μM)	T1	T2	T3
subG0	*	****	****
G0/G1	*	ns	****
S	ns	*	***
G2/M	**	**	***

Continued overleaf …

C

D

1

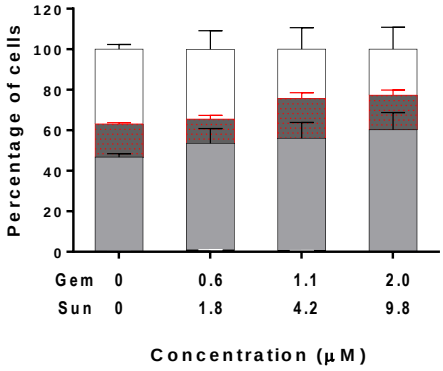

Control vs. Dose (μM)	T1	T2	T3
subG0	ns	ns	ns
G0/G1	ns	ns	*
S	ns	ns	ns
G2/M	ns	*	*

2

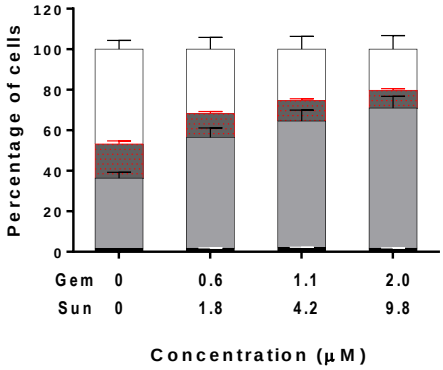

Control vs. Dose (μM)	T1	T2	T3
subG0	ns	ns	ns
G0/G1	****	****	****
S	ns	ns	*
G2/M	***	****	****

3

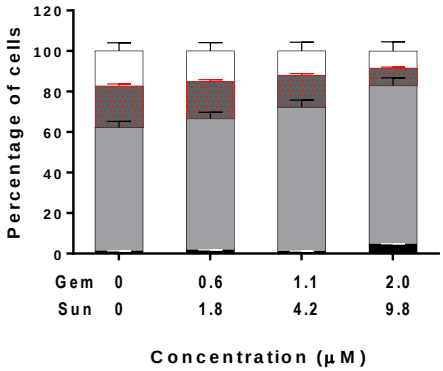

Control vs. Dose (μM)	T1	T2	T3
subG0	ns	ns	ns
G0/G1	ns	***	****
S	ns	ns	****
G2/M	ns	ns	**

Continued overleaf …

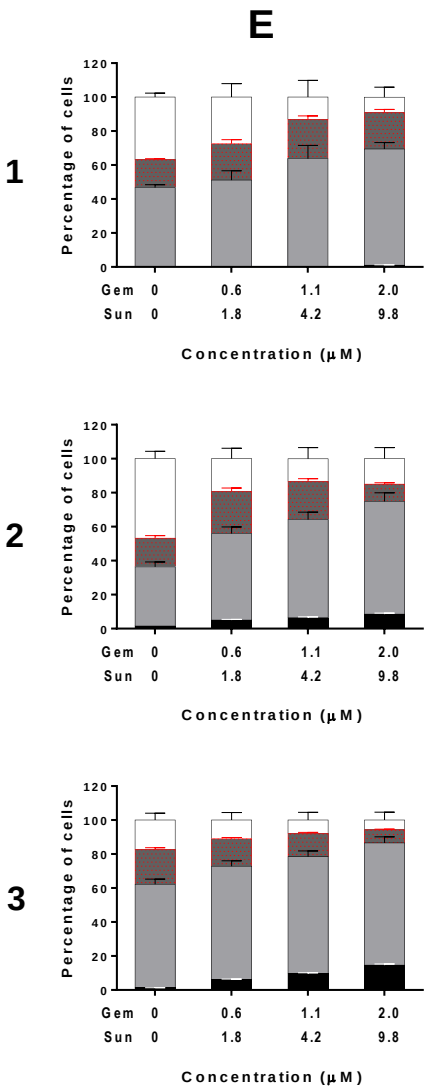

F

Control vs. Dose (µM)	T1	T2	T3
subG0	ns	ns	ns
G0/G1	ns	***	****
S	ns	ns	ns
G2/M	*	****	****

Control vs. Dose (µM)	T1	T2	T3
subG0	ns	ns	ns
G0/G1	****	****	****
S	*	ns	ns
G2/M	****	****	****

Control vs. Dose (µM)	T1	T2	T3
subG0	ns	**	****
G0/G1	*	**	***
S	ns	*	****
G2/M	*	***	****

Figure 4.18 Effect of gemcitabine and sunitinib as a double combination treatment on the cell cycle progression of PANC-1 cells.

The effects of gemcitabine administered before (A), after (C) and simultaneously with (E) sunitinib on cell cycle progression, were assessed in PANC-1 cells at 4 (A1, C1 & E1), 24 (A2, C2 & E2), and 48 (A3, C3 & E3) hours post-treatment. The data were analysed using FACSDiva software v6.1.3. Data are means ± SD of cells percentage in each cell cycle phase, which generated from three independent experiments. Two-way ANOVA was used to compare the means of the cell cycle phases after cells were treated with gemcitabine plus sunitinib to cells untreated control cells. *P<0.05, **P<0.01, ***P<0.001 and ****P<0.0001. Gem = gemcitabine; Sun = sunitinib; T1 = 0.3 µM gem + 1.3 µM Sun; T2 = 1.1 µM gem + 2.8 µM sun; T3 = 3.5 µM gem + 6 µM sun; ns = Not significant.

4.3.2.3.2 Analysis of the cell cycle progression of MIA PaCa-2 cells following treatment with gemcitabine in combination with sunitinib

Figure 4.19 demonstrates the effect of increasing doses of gemcitabine and sunitinib as a double combination treatment on the cell cycle progression of MIA PaCa-2 cells. The cells were treated with gemcitabine administered before (schedule 1; A), after (schedule 2; C) and simultaneously with (schedule 3; E) sunitinib and the cell cycle analysis was carried out at 4 (A1, C1 & E1), 24 (A2, C2 & E2), and 48 (A3, C3 & E3) hours post-treatment.

Schedule 1 combination treatment of MIA PaCa-2 cells resulted in a significant accumulation of cells in the S phase accompanied by a decrease in the G2/M phase of the cell cycle ($p < 0.001$). With the highest dose of combination, in addition to the accumulation in the S phase, cells were also increased slightly but significantly in the G0/1 phase from 54 ± 5.6% to 68.6 ± 4.5% ($p < 0.01$) at 4 hours post-treatment. At 24 hours following treatment, cell distribution increased significantly in G0/1 ($p < 0.0001$) compared to untreated control cells. At 48 hours, the two highest doses of gemcitabine and sunitinib resulted in a significant increase of cells in the subG0 phase to reach 30.5 ± 1.3% accompanied with a decrease in the G0/1, S, and G2/M phases compared to untreated control cells ($p < 0.0001$).

Following the treatment MIA PaCa-2 cells with the schedule 2 combination strategy, there was a significant accumulation of cells in the G0/1 phase

accompanied with a decrease in the G2/M phase of the cell cycle only with the highest dose of combination ($p < 0.05$) at all time-points of measurement. However, cell distribution in the S phase was decreased with further accumulation in G0/1 phase in the highest dose treatment group at 4 and 24 hours post-treatment compared to the untreated cell group ($p < 0.01$) and increased at 48 hours ($p < 0.0001$).

Treatment MIA PaCa-2 cells with gemcitabine simultaneously administered with sunitinib (schedule 3) resulted in a significant accumulation of cells in the G0/1 and S phases accompanied with a decrease in the G2/M phase of the cell cycle only with the two highest doses of combination ($p < 0.01$) at 4 hours post-treatment. At 24 hours, the cell distribution increased significantly in subG0 to 9.8 ± 0.6% ($p < 0.0001$) with the highest dose of the combination. At 48 hours following the treatment with two lowest doses of gemcitabine and sunitinib, cell distribution in all cell cycle phases was similar to untreated control cells ($p > 0.05$). However, the highest dose induced increase in the subG0 phase accompanied by a decrease in the S compared to the untreated cell group ($p < 0.05$).

A **B**

1

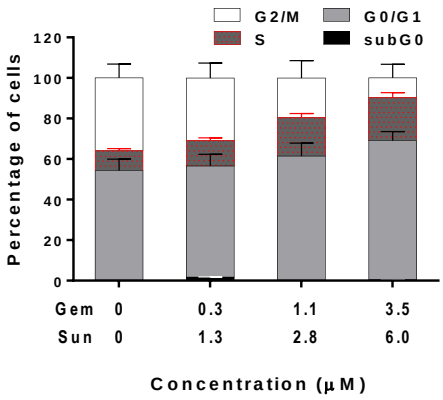

Control vs. Dose (μM)	T1	T2	T3
subG0	ns	ns	ns
G0/G1	ns	ns	**
S	ns	ns	*
G2/M	ns	***	****

2

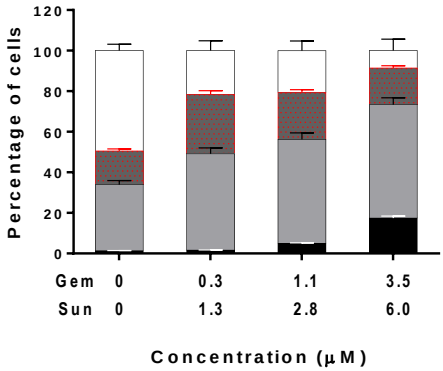

Control vs. Dose (μM)	T1	T2	T3
subG0	ns	ns	****
G0/G1	****	****	****
S	****	*	ns
G2/M	****	****	****

3

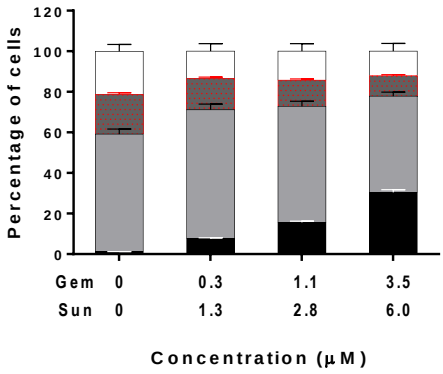

Control vs. Dose (μM)	T1	T2	T3
subG0	**	****	****
G0/G1	*	ns	****
S	ns	**	****
G2/M	***	**	****

Continued overleaf …

C

D

1

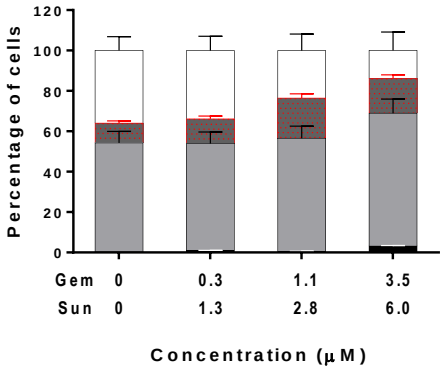

Control vs. Dose (μM)	T1	T2	T3
subG0	ns	ns	ns
G0/G1	ns	ns	*
S	ns	ns	ns
G2/M	ns	*	****

2

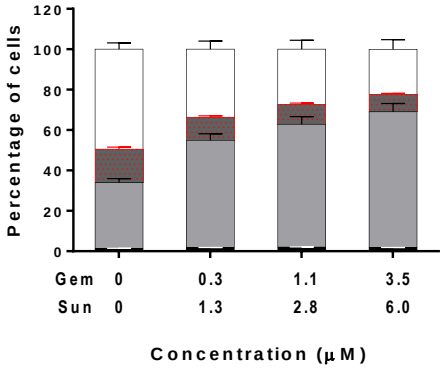

Control vs. Dose (μM)	T1	T2	T3
subG0	ns	ns	ns
G0/G1	****	****	****
S	ns	*	**
G2/M	****	****	****

3

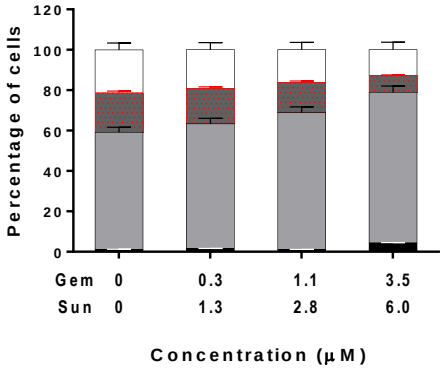

Control vs. Dose (μM)	T1	T2	T3
subG0	ns	ns	ns
G0/G1	ns	****	****
S	ns	ns	****
G2/M	ns	*	***

Continued overleaf …

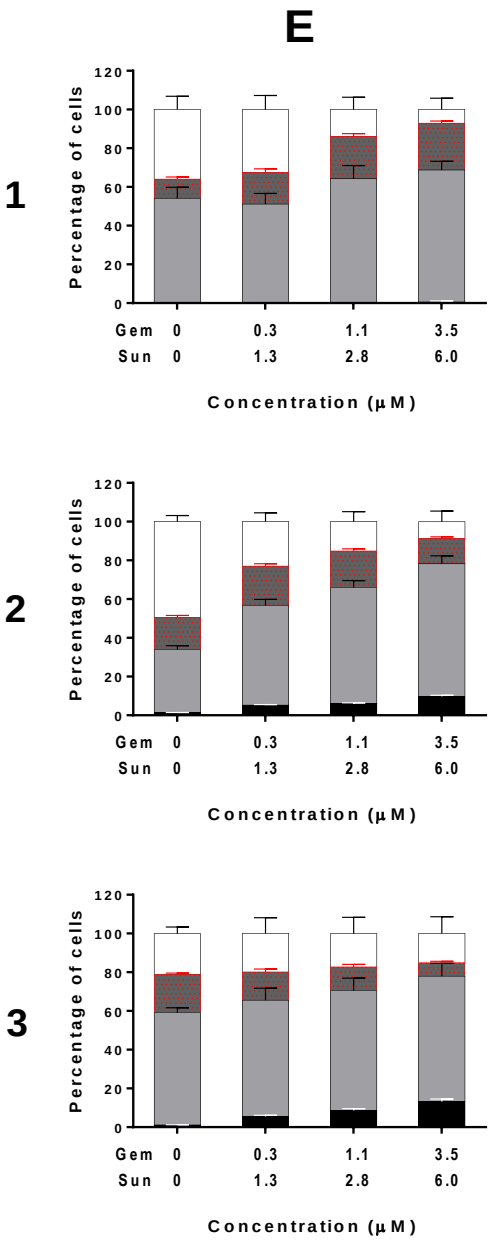

F

Control vs. Dose (µM)	T1	T2	T3
subG0	ns	ns	ns
G0/G1	ns	*	**
S	ns	**	**
G2/M	ns	****	****

Control vs. Dose (µM)	T1	T2	T3
subG0	ns	ns	**
G0/G1	****	****	****
S	ns	ns	ns
G2/M	****	****	****

Control vs. Dose (µM)	T1	T2	T3
subG0	SSS	ns	*
G0/G1	ns	ns	ns
S	ns	ns	**
G2/M	ns	ns	ns

Figure 4.19 Effect of cytotoxic agents as double combination treatment on cell cycle progression of MIA PaCa-2 cells.

The effects of gemcitabine administered before (A), after (C), and simultaneously with (E) sunitinib on cell cycle progression were assessed in MIA PaCa-2 cells at 4 (A1, C1 & E1), 24 (A2, C2 & E2), and 48 (A3, C3 & E3) hours post-treatment. The data were analysed using FACSDiva software v6.1.3. Data are means ± SD of cells percentage in each cell cycle phase, which generated from three independent experiments. Two-way ANOVA was used to compare the means of the cell cycle phases after cells treatment with gemcitabine plus sunitinib to cells untreated control cells. *P<0.05, **P<0.01, ***P<0.001 and ****P<0.0001. Gem = gemcitabine; Sun = sunitinib; T1 = 0.3 µM gem + 1.3 µM Sun; T2 = 1.1 µM gem + 2.8 µM sun; T3 = 3.5 µM gem + 6 µM sun; ns = Not significant.

4.3.2.4 The effect of two-drug combination treatments on the induction of apoptosis measured by Annexin V assay in pancreatic cancer cells

In these experiments, the expression of Annexin V, as an indicator of apoptosis, was assessed at 4, 24, and 48 hours after treatment with gemcitabine and sunitinib, in three different combination schedules, in PANC-1 and MIA PaCa-2 cell lines as described in section 2.11.

4.3.2.4.1 The effect of gemcitabine in combination with sunitinib on the induction of apoptosis measured by Annexin V assay in PANC-1 cells

Figure 4.20 (A) shows the apoptosis rate at 4, 24, and 48 hours post-treatment of PANC-1 cells with increasing doses of gemcitabine administered before (A1), after (A2), or simultaneously with (A3) increasing doses of sunitinib compared to apoptosis induced after treatment with gemcitabine alone (presented in Figure 4.7 A-1). There was a dose- and time- dependent increase in apoptosis in PANC-1 cells. The most effective combination schedule of gemcitabine and sunitinib compared to gemcitabine alone in the induction of apoptosis was the simultaneous administration of gemcitabine and sunitinib (i.e. schedule 3). Figure 4.20 (B) shows the p-values of comparison between the means of apoptosis levels rate within each combination treatment doses over different time-points of measurement.

Incubation of cells with the highest tested dose of gemcitabine (2 μM) for 48 hours prior the treatment with the corresponding dose of sunitinib (9.8 μM) (i.e. schedule 1) induced a significant time-dependent increase in apoptosis of PANC-1 cells ($p < 0.01$) (Figure 4.20 A1 & B1). The lowest combination dose of this schedule (0.6 μM gemcitabine before 1.8 μM sunitinib) elevated apoptosis significantly at 48 hours post-treatment to 24 ± 3.7% compared to untreated control cells (4.1 ± 1.8%; $p < 0.0001$) but without any meaningful increase compared to gemcitabine alone (18.2 ± 2.8; $p > 0.05$).

Figure 4.20 (A2) reveals that the administration of sunitinib before gemcitabine (schedule 2) was the least effective combination strategy in terms of the induction of apoptosis in PANC-1 cells. The lowest two doses of the combination in this schedule had no additional effect on the induction of apoptosis compared to the corresponding doses of gemcitabine alone at 4 and 24 hours time-points. However, the highest dose of combination treatment with 9.8 μM of sunitinib followed by 2 μM of gemcitabine induced apoptosis significantly at 4 hours ($p < 0.05$) and 24 hours ($p < 0.001$) time-points compared to treatment with 2 μM of gemcitabine alone.

Finally, the simultaneous administration of gemcitabine and sunitinib (i.e. schedule 3) was the most effective combination scheduling in terms of apoptosis induction in PANC-1 cells. The treatment of cells with concurrent administration of 2 μM of gemcitabine and 9.8 μM of sunitinib caused a significant time-dependent increase in apoptosis rate compared to gemcitabine alone ($p < 0.001$) (Figure 4.20 A-3 & B-3).

(A) (B)

(1)

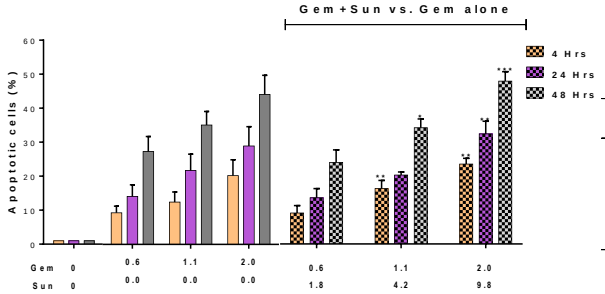

Time (Hours)	4 vs. 24	4 vs. 48	24 vs. 48
Control	ns	ns	ns
T1	ns	****	***
T2	ns	****	****
T3	**	****	****

(2)

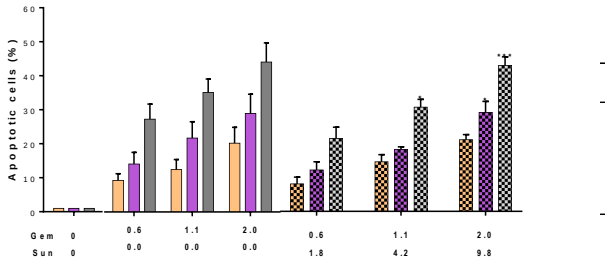

Time (Hours)	4 vs. 24	4 vs. 48	24 vs. 48
Control	ns	ns	ns
T1	ns	****	***
T2	ns	****	****
T3	**	****	****

(3)

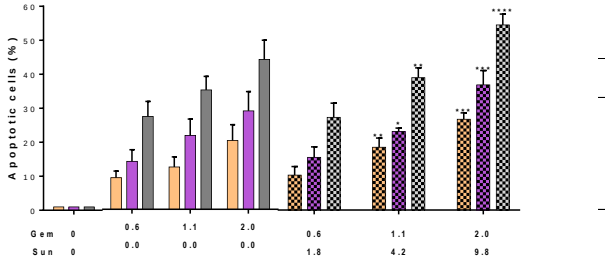

Time (Hours)	4 vs. 24	4 vs. 48	24 vs. 48
Control	ns	ns	ns
T1	ns	****	***
T2	ns	****	****
T3	**	****	****

Figure 4.20 The effect of two-drug combination treatments on apoptosis induction of PANC-1 cells.

The induction of apoptosis in PANC-1 cells was assessed at 4, 24, and 48 hours after treatment with gemcitabine administered before (A1), after (A2), or simultaneously with (A3) sunitinib. Results presented are the mean ± SD percentage of apoptotic cells of 3 independent experiments. Statistical analysis was carried out using two-way ANOVA with Dunnett's test to compare apoptosis rate resulted from all treatment doses over time-points to gemcitabine alone (A1, A2, and A3), and with Tukey's test to compare apoptosis between different time-points after each dose of the treatment. The effect of gemcitabine alone on the induction of apoptosis is illustrated in Figure 4.7.*P<0.05, **P<0.01, ***P<0.001 and ****P<0.0001. Gem = gemcitabine; Sun = sunitinib; T1 = 0.6 µM gem + 1.8 µM Sun; T2 = 1.1 µM gem + 4.2 µM sun; T3 = 2 µM gem + 9.8 µM sun; ns = Not significant.

4.3.2.4.2 The effect of gemcitabine in combination with sunitinib on the induction of apoptosis measured by Annexin V assay in MIA PaCa-2 cells

Figure 4.21 (A) shows the apoptosis rate at 4, 24, and 48 hours post-treatment of MIA PACA-2 cells with increasing doses of gemcitabine administered before (A1), after (A2), or simultaneously with (A3) increasing doses of sunitinib compared to apoptosis induced after treatment with gemcitabine alone (presented in Figure 4.8 A-1). There was a dose- and time- dependent increase in apoptosis in MIA PACA-2 cells. The most effective combination schedule in the induction of apoptosis was the simultaneous administration of gemcitabine and sunitinib (i.e. schedule 3). Figure 4.21 (B) shows the p-values of comparison between the means of apoptosis rate within each combination treatment doses over different time-points of measurement.

Incubation of cells with the two highest tested doses of gemcitabine (1.1 and 3.5 μM) for 48 hours prior the treatment with the corresponding doses of sunitinib (2.8 and 6 μM) (i.e. schedule 1) induced a significant time-dependent increase in apoptosis of MIA PACA-2 cells compared to gemcitabine alone ($p < 0.001$) (Figure 4.21 A1 & B1). The lowest combination dose of this schedule (0.3 μM gemcitabine before 1.3 μM sunitinib) elevated apoptosis significantly at 48 hours post-treatment to 27.1 ± 4.2% compared to untreated control cells (4.8 ± 2%; $p < 0.0001$) and also compared to gemcitabine alone (17 ± 2.8; $p < 0.05$). However, this dose induced no significant increase in apoptosis rate at

the earlier time-point (4 and 24 hours) compared to apoptosis induced after the lowest dose of gemcitabine alone.

Figure 4.21 (A2) reveals that the administration of sunitinib before gemcitabine (schedule 2) was the least effective combination strategy in terms of the induction of apoptosis in MIA PACA-2 cells. The lowest dose of the combination in this schedule had no additional effect on the induction of apoptosis compared to the corresponding doses of gemcitabine alone at all examined time-points. However, the highest dose of combination treatment with 6 μM of sunitinib followed by 3.5 μM of gemcitabine induced apoptosis significantly at 4 hours ($p < 0.001$), 24 hours ($p < 0.01$), and 48 hours ($p < 0.01$) time-points compared to treatment with 3.5 μM of gemcitabine alone.

Finally, the simultaneous administration of gemcitabine and sunitinib (i.e. schedule 3) was the most effective combination scheduling in terms of apoptosis induction in MIA PACA-2 cells. The treatment of cells with concurrent administration of 3.5 μM of gemcitabine and 6 μM of sunitinib caused a significant time-dependent increase in apoptosis rate compared to gemcitabine alone ($p < 0.0001$) at all examined time-points (Figure 4.21 A-3 & B-3).

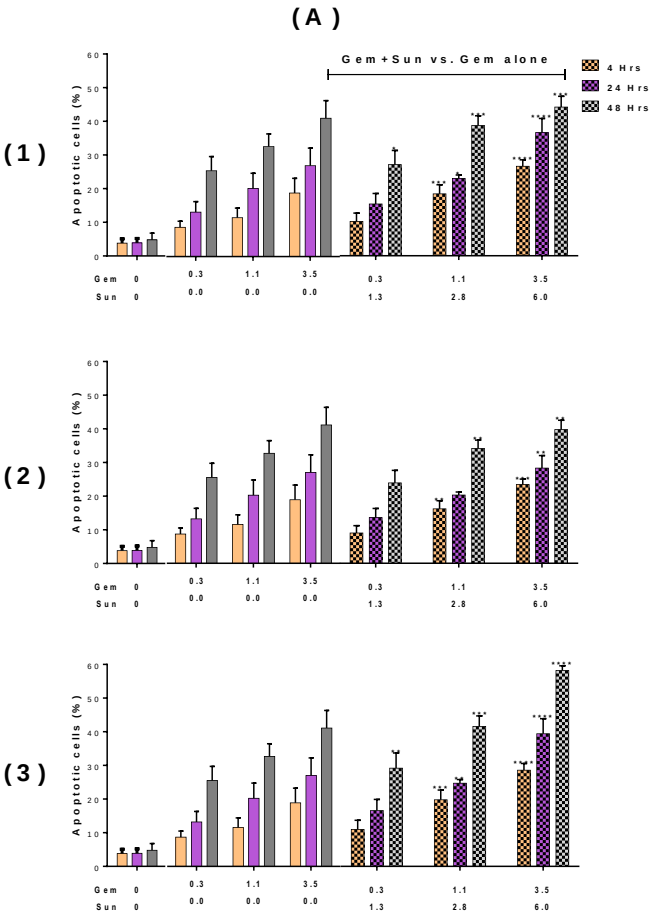

Time (Hours)	4 vs. 24	4 vs. 48	24 vs. 48
Control	ns	ns	ns
T1	ns	****	***
T2	ns	****	****
T3	**	****	****

Time (Hours)	4 vs. 24	4 vs. 48	24 vs. 48
Control	ns	ns	ns
T1	ns	****	***
T2	ns	****	****
T3	ns	****	***

Time (Hours)	4 vs. 24	4 vs. 48	24 vs. 48
Control	ns	ns	ns
T1	ns	****	***
T2	ns	****	****
T3	**	****	****

Figure 4.21 The effect of two-drug combination treatments on apoptosis induction of MIA PaCa-2 cells.

The induction of apoptosis in MIA PaCa-2 cells was assessed at 4, 24, and 48 hours after treatment with gemcitabine administered before (A1), after (A2), or simultaneously with (A3) sunitinib. Results presented are the mean ± SD percentage of apoptotic cells of 3 independent experiments. Statistical analysis was carried out using two-way ANOVA with Dunnett's test to compare apoptosis rate resulted from all treatment doses over time-points to gemcitabine alone (A1, A2, and A3), and with Tukey's test to compare apoptosis between different time-points after each dose of the treatment. The effect of gemcitabine alone on the induction of apoptosis is illustrated in Figure 4.8 *P<0.05, **P<0.01, ***P<0.001 and ****P<0.0001. Gem = gemcitabine; Sun = sunitinib; T1 = 0.3 μM gem + 1.3 μM Sun; T2 = 1.1 μM gem + 2.8 μM sun; T3 = 3.5 μM gem + 6 μM sun; ns = Not significant.

4.3.3 Cytotoxicity and mechanistic studies of gemcitabine, sunitinib, and XBR as three-treatment combination in pancreatic cancer cells *in vitro*

The cytotoxicity effects of three-treatment combination of gemcitabine plus sunitinib and XBR on PANC-1 and MIA PaCa-2 cell lines were evaluated by clonogenic assays and combination index analysis. Gemcitabine plus sunitinib was administered 48 hours before (schedule 1), after (schedule 2), or simultaneously with (schedule 3) 1 Gy or 2 Gy of XBR. These cytotoxicity studies were followed by the mechanistic studies (H_2AX detection, cell cycle analysis, and apoptosis) measured at three different time-points (4, 24, and 48 hours).

4.3.3.1 Assessment of cytotoxic effects of gemcitabine plus sunitinib in combination with XBR on PANC-1 and MIA PaCa-2 cells by clonogenic assay and combination index analysis

Clonogenic survival assays and combination index analysis experiments were conducted to evaluate the efficacy of gemcitabine plus sunitinib (administered simultaneously) in combination with XBR on pancreatic cancer cell lines as described in sections 2.6 and 2.7, respectively. Cell survival data which resulted from the three-treatment combination of gemcitabine plus sunitinib and XBR were compared to those resulted from the treatment with two-drug concurrent administration of gemcitabine and sunitinib. These experiments

aimed to evaluate the ability of XBR to sensitise pancreatic cancer cells to gemcitabine/sunitinib treatment.

Figure 4.22 (A & B) demonstrates the cytotoxic effect of treatment with concurrent administration of gemcitabine plus sunitinib alone, or in combination with XBR (1 Gy and 2 Gy) before (schedule 1), after (schedule 2), or simultaneously with (schedule 3), gemcitabine plus sunitinib for 48 hours on the survival of PANC-1 (A) and MIA PaCa-2 (B) cells. Exposure to XBR before treatment with gemcitabine plus sunitinib (schedule 2) was the most effective three-treatment combination schedule in both cell lines.

In PANC-1 cells (Figure 4.22 A), exposure to 1 Gy failed to enhance the cytotoxicity effect of gemcitabine plus sunitinib with all combination schedules. However, irradiation PANC-1 cells with 2 Gy in combination with gemcitabine plus sunitinib increased the cytotoxicity and inhibited the survival significantly compared to treatment with gemcitabine plus sunitinib alone in schedules 2 and 3 ($p < 0.05$). Schedule 1 was the least effective triple combination schedule compared to other schedules; hence all doses tested of gemcitabine plus sunitinib prior to irradiation cells with 1 and 2 Gy XBR failed to increase the cytotoxicity of PANC-1 cells compared to the two-drug combination alone ($p > 0.05$).

Similarly, incubation of MIA PaCa-2 cells with gemcitabine plus sunitinib prior exposure to XBR (i.e. schedule 1) resulted in the lowest cytotoxicity compared to schedules 2 and 3 (Figure 4.22 B). This combination schedule failed to

reduce the cell survival compared to gemcitabine plus sunitinib alone except at the lowest combination dose (0.3 μM of gemcitabine plus 1.3 μM of sunitinib) when cells were irradiated with 2 Gy. However, incubation cells with 0.3 μM gemcitabine plus 1.3 μM sunitinib post-exposure to 2 Gy irradiation deceased MIA PaCa-2 survival significantly to 42.8 ± 7.8% compared to survival fraction following two-drug treatment alone (72.11 ± 5.6%; $p < 0.0001$).

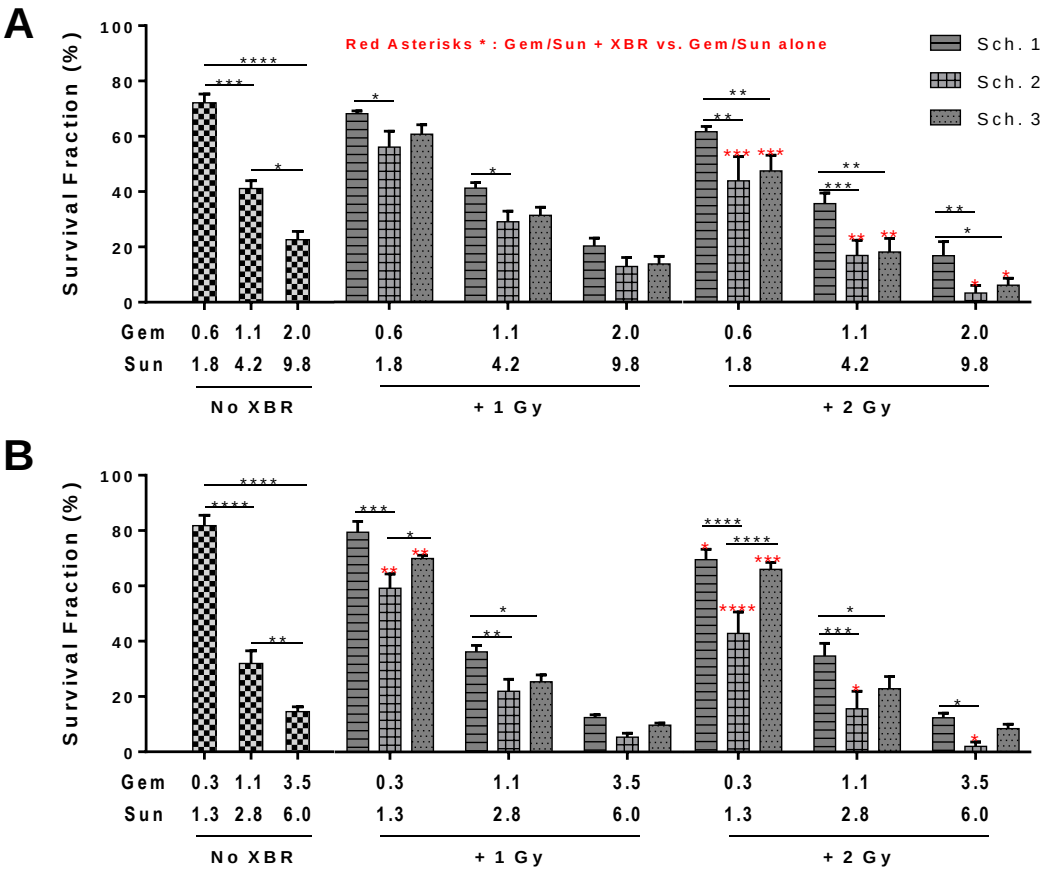

Figure 4.22 Effect of gemcitabine plus sunitinib as two-drug concurrent combination alone or in combination with XBR on the survival of PANC-1 and MIA PaCa-2 cell lines.

PANC-1 **(A)** or MIA PaCa-2 **(B)** cells were treated with a concurrent combination of gemcitabine plus sunitinib alone, or in combination with XBR (1 Gy and 2 Gy) before (Sch. 1), after (Sch. 2), or simultaneously with (Sch. 3), gemcitabine plus sunitinib for 48 hours and then survival fraction was measured by clonogenic assay. Data shown are expressed as a percentage of survival fraction normalised to the untreated control group. Statistical analysis was carried out using a two-way ANOVA followed by Tukey's test to compare all treatment doses in gemcitabine plus sunitinib combination and alternative combination schedules with XBR. Each value represents the mean ± SD of three independent experiments. *P<0.05, **P<0.01, ***P<0.001 and ****P<0.0001 compared to the survival fraction between different treatment groups.

Synergy analysis of the scheduled combinations was examined according to the method of Chou and Talalay (Chou and Talalay, 1984), which is based on the median-effect principle, as described in detail in section 2.7. Figure 4.23 shows the combination-index (CI) analysis of the three combination schedules of gemcitabine plus sunitinib and 1 Gy or 2 Gy XBR in PANC-1 (A) and MIA PaCa-2 (B) cells.

In both cell lines, schedule 1 (gemcitabine + sunitinib before XBR) was the least effective schedule and induced antagonistic responses with all examined doses of treatment and XBR. In contrast, exposure to 1 Gy or 2 Gy before the treatment with gemcitabine plus sunitinib (i.e. schedule 2) induced dose-dependent synergistic responses in both cell lines at all tested doses of combination.

Simultaneous administration of gemcitabine plus sunitinib and XBR (i.e. schedule 3) induced synergism with the two highest doses tested of combinations in PANC-1 and MIA PaCa-2. In PANC-1, however, the lowest tested dose of gemcitabine plus sunitinib induced an additive and synergism responses when cells were irradiated simultaneously with 1 Gy in PANC-1 and antagonism response in MIA PaCa-2 when cells were irradiated simultaneously with 1 Gy and 2 Gy, respectively. In MIA PaCa-2, the interaction of the lowest dose of gemcitabine plus sunitinib with both 1GY or 2GY radiation doses was antagonistic with respect to cell kill, i.e. the combination resulting in less cell kill than the sum of the cell kill of the drugs individually.

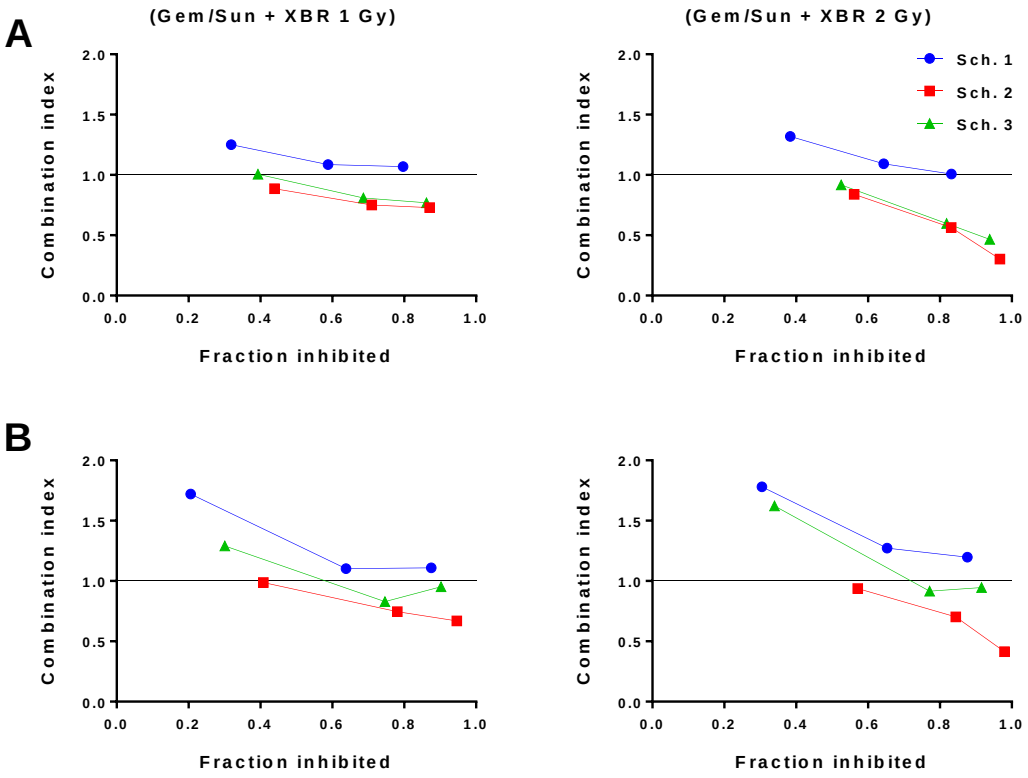

Figure 4.23 Combination index (CI) analysis of the combined effect of gemcitabine plus sunitinib as a single drug with XBR on clonogenic survival of PANC-1 and MIA PaCa-2 cells.

Combination index (CI) with the corresponding fraction inhibited following the combination schedules of gemcitabine plus sunitinib as a single drug with 1 Gy and 2 Gy were plotted for PANC-1 (A) and MIA PaCa-2 (B). CI > 1.1, CI between 0.9 and 1.1, and CI < 0.9 indicate antagonism, additivity, and synergism, respectively. Each value represents the median CI of three separate experiments.

4.3.3.2 The effect of three-treatment combination on the induction and repair of DNA damage measured by γ-H_2AX in pancreatic cancer cells

In these experiments, the expression of γ-H_2AX, as a marker of DNA damage and repair, was assessed at 4, 24, and 48 hours after treatment with gemcitabine plus sunitinib with XBR, in three different combination schedules, in PANC-1 and MIA PaCa-2 cell lines as described in section 2.12.

4.3.3.2.1 The effect of gemcitabine plus sunitinib in combination with XBR on the induction and repair of DNA damage measured by γ-H2AX in PANC-1 cells

Figure 4.24 (A) shows the average of fold increase in γ-H_2AX at 4, 24, and 48 hours post-treatment of PANC-1 cells with increasing doses of gemcitabine plus sunitinib administered before (A1), after (A2), or simultaneously with (A3) XBR (1 Gy and 2 Gy) compared to γ-H_2AX levels after treatment with gemcitabine plus sunitinib (presented in Figure 4.16 A-3). Generally, γ-H_2AX increased at 4 hours post-exposure to the triple therapy of gemcitabine plus sunitinib and XBR; then it decreased at 24- and 48-hour time-points. The exposure to XBR before incubation cells with gemcitabine/sunitinib, i.e. schedule 2, was the most effective combination strategy in terms of γ-H_2AX expression as a marker for the double-strand DNA (dsDNA) damage. Figure 4.24 (B) shows the p-values of comparison between the means of γ-H_2AX fold

increased within each combination treatment doses over different time-points of measurement.

Incubation of cells with gemcitabine and sunitinib for 48 hours prior exposure to radiation (i.e. schedule 1) was the least effective combination strategy in terms of the DNA damage and γ-H_2AX expression in PANC-1 cells over all tested time-points. Irradiation with 1 Gy after gemcitabine/sunitinib induced no significant difference in the γ-H_2AX expression compared to gemcitabine/sunitinib alone at the 4 and 24 hour time-point measurements. Later, at 48 hours, the γ-H_2AX expression was higher with triple combination treatment compared to gemcitabine plus sunitinib ($p < 0.05$) (Figure 4.24 A-1). However, the exposure to higher XBR dose (2 Gy) after gemcitabine/sunitinib treatment caused a dose-dependent increase in γ-H_2AX expression at 24 and 48 hours compared to the double combination. There was no significant difference in γ-H_2AX levels between the double and the triple combination strategies.

In contrast, for schedule 2, in which the cells were exposed to XBR before the incubation with gemcitabine plus sunitinib, caused a dose-dependent statistically significant increase in the γ-H_2AX levels with both XBR doses (1 Gy and 2 Gy) at all examined time-points. For example, γ-H_2AX expression increased to 14.6 ± 1.1 fold at 48 hours post-incubation cells with 2 μM of gemcitabine plus 9.8 μM of sunitinib without radiation, and to 25.9 ± 1.9 fold with same doses of gemcitabine/sunitinib post-exposure to 2 Gy ($p < 0.0001$) (Figure 4.24 A-2).

Finally, the concurrent administration of gemcitabine/sunitinib with exposure to XBR (schedule 3) caused a significant XBR dose-dependent increase in the γ-H_2AX expression compared to gemcitabine/sunitinib alone (Figure 4.24 A-3).

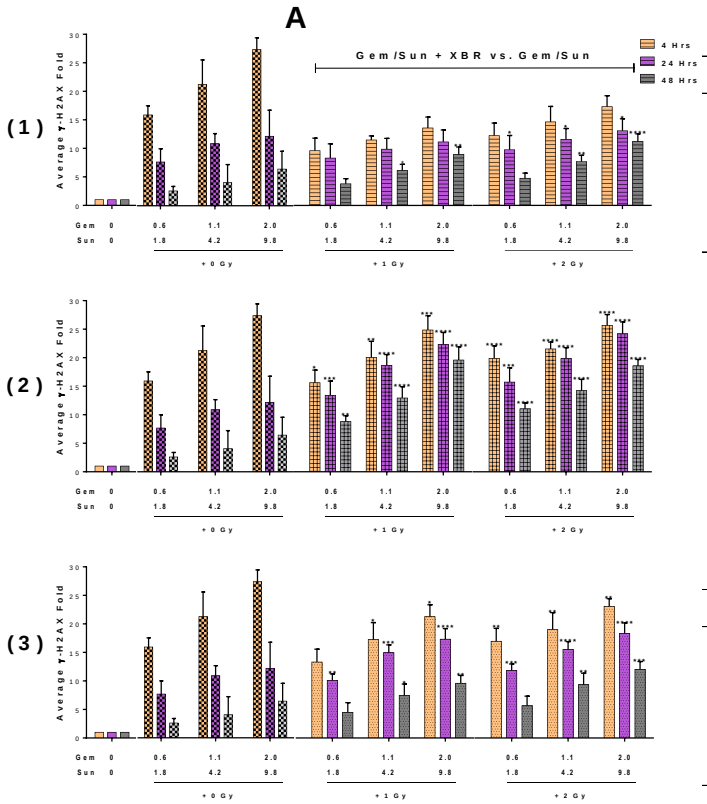

Time (Hours)	4 vs. 24	4 vs. 48	24 vs. 48
T1 + 1Gy	ns	**	*
T2 + 1Gy	ns	**	*
T3 + 1Gy	ns	*	ns
T1 + 2Gy	ns	***	*
T2 + 2Gy	ns	***	ns
T3 + 2Gy	*	**	ns

Time (Hours)	4 vs. 24	4 vs. 48	24 vs. 48
T1 + 1Gy	ns	**	*
T2 + 1Gy	ns	**	*
T3 + 1Gy	ns	*	ns
T1 + 2Gy	*	****	*
T2 + 2Gy	ns	***	**
T3 + 2Gy	ns	***	**

Time (Hours)	4 vs. 24	4 vs. 48	24 vs. 48
T1 + 1Gy	ns	****	**
T2 + 1Gy	ns	****	***
T3 + 1Gy	ns	****	***
T1 + 2Gy	**	****	**
T2 + 2Gy	ns	****	**
T3 + 2Gy	*	****	**

Figure 4.24 The effect of three-treatment combination on the induction and repair of DNA damage measured by γ-H2AX in PANC-1 cells.

The expression of γ-H2AX of PANC-1 cells was assessed at 4, 24, and 48 hours after treatment with gemcitabine plus sunitinib administered before (A1), after (A2), or simultaneously with (A3) 1 Gy and 2 Gy XBR. Results presented are the mean ± SD fold of γ-H2AX expression compared to untreated control cells of 3 independent experiments. Statistical analysis was carried out using two-way ANOVA with Dunnett's test to compare average fold of γ-H2AX resulted from all treatment doses over time-points to gemcitabine plus sunitinib (A1, A2, and A3), and with Tukey's test to compare γ-H2AX between different time-points after each dose of the treatment (B1, B2, and B3). *P<0.05, **P<0.01, ***P<0.001 and ****P<0.0001. Gem = gemcitabine; Sun = sunitinib; T1 = 0.6 μM gem + 1.8 μM Sun; T2 = 1.1 μM gem + 4.2 μM sun; T3 = 2 μM gem + 9.8 μM sun; ns = Not significant.

4.3.3.2.2 The effect of gemcitabine plus sunitinib in combination with XBR on the induction and repair of DNA damage measured by γ-H2AX in MIA PaCa-2 cells

Figure 4.25 (A) shows the average of fold increase in γ-H_2AX at 4, 24, and 48 hours post-treatment of MIA PaCa-2 cells with increasing doses of gemcitabine plus sunitinib administered before (A1), after (A2), or simultaneously with (A3) XBR (1 Gy and 2 Gy) compared to γ-H_2AX levels after treatment with gemcitabine plus sunitinib alone (presented in Figure 4.17 A-3). Generally, γ-H_2AX increased at 4 hours post-exposure to the triple therapy of gemcitabine plus sunitinib and XBR; then it decreased at 24- and 48-hour time-points. The exposure to XBR before incubation cells with gemcitabine/sunitinib, i.e. schedule 2, was the most effective combination strategy in terms of γ-H_2AX expression as a marker for the double-strand DNA (dsDNA) damage. Figure 4.25 (B) shows the p-values of comparison between the means of γ-H_2AX fold increased within each combination treatment doses over different time-points of measurement.

Incubation of cells with gemcitabine and sunitinib for 48 hours prior exposure to radiation (i.e. schedule 1) was the least effective combination strategy in terms of the DNA damage and γ-H_2AX expression in MIA PaCa-2 cells over all tested time-points. Irradiation with 1 Gy after gemcitabine/sunitinib induced no significant difference in the γ-H_2AX expression compared to gemcitabine/sunitinib alone at the 4 and 24 hour time-point measurements. Later, at 48 hours, the γ-H_2AX expression was significantly higher with triple

combination treatment compared to gemcitabine plus sunitinib ($p < 0.05$) (Figure 4.25 A-1). However, the exposure to higher XBR dose (2 Gy) after gemcitabine/sunitinib treatment caused a dose-dependent increase in γ-H_2AX expression at 24 and 48 hours compared to the double combination. However, there was no significant difference in γ-H_2AX levels between the double and the triple combination strategies.

In contrast, for schedule 2 treatment administration, in which cells were exposed to XBR before the incubation with gemcitabine plus sunitinib, there was a dose-dependent significant increase in the γ-H_2AX levels with both XBR doses (1 Gy and 2 Gy) at all examined time-points ($p < 0.5$). For example, γ-H_2AX expression increased to 15.0 ± 0.9 fold at 48 hours post-incubation cells with 3.5 μM of gemcitabine plus 6 μM of sunitinib without radiation, and to 27.9 ± 2.1 fold with same doses of gemcitabine/sunitinib post-exposure to 2 Gy ($p < 0.0001$) (Figure 4.25 A-2).

Finally, the concurrent administration of gemcitabine/sunitinib with exposure to XBR (schedule 3) caused a significant XBR dose-dependent increase in the γ-H_2AX expression compared to gemcitabine/sunitinib alone at all time-points of measurement (Figure 4.25 A-3).

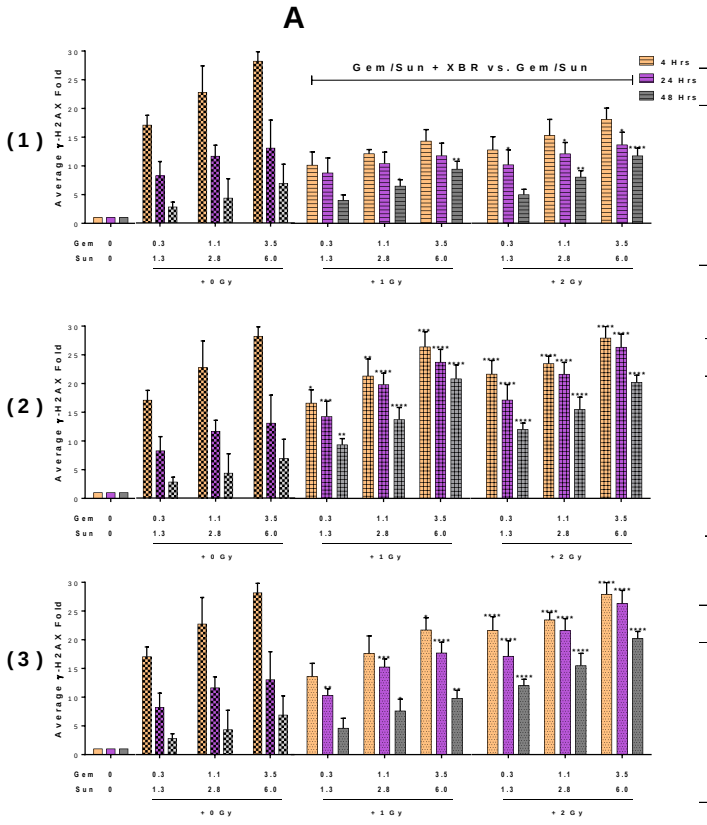

Time (Hours)	4 vs. 24	4 vs. 48	24 vs. 48
T1 + 1Gy	ns	**	*
T2 + 1Gy	ns	**	*
T3 + 1Gy	ns	*	ns
T1 + 2Gy	ns	***	*
T2 + 2Gy	ns	***	ns
T3 + 2Gy	*	**	ns

Time (Hours)	4 vs. 24	4 vs. 48	24 vs. 48
T1 + 1Gy	ns	**	*
T2 + 1Gy	ns	**	*
T3 + 1Gy	ns	*	ns
T1 + 2Gy	*	****	*
T2 + 2Gy	ns	***	**
T3 + 2Gy	ns	***	**

Time (Hours)	4 vs. 24	4 vs. 48	24 vs. 48
T1 + 1Gy	ns	****	**
T2 + 1Gy	ns	****	***
T3 + 1Gy	ns	****	***
T1 + 2Gy	*	****	*
T2 + 2Gy	ns	***	**
T3 + 2Gy	ns	***	**

Figure 4.25 The effect of three-treatment combination on the induction and repair of DNA damage measured by γ-H2AX in MIA PaCa-2 cells.

The expression of γ-H2AX of MIA PaCa-2 cells was assessed at 4, 24, and 48 hours after treatment with gemcitabine plus sunitinib administered before (A1), after (A2), or simultaneously with (A3) 1 Gy and 2 Gy XBR. Results presented are the mean ± SD fold of γ-H2AX expression compared to untreated control cells of 3 independent experiments. Statistical analysis was carried out using two-way ANOVA with Dunnett's test to compare average fold of γ-H2AX resulted from all treatment doses over time-points to gemcitabine plus sunitinib (A1, A2, and A3), and with Tukey's test to compare γ-H2AX between different time-points after each dose of the treatment (B1, B2, and B3). *P<0.05, **P<0.01, ***P<0.001 and ****P<0.0001. Gem = gemcitabine; Sun = sunitinib; T1 = 0.3 μM gem + 1.3 μM Sun; T2 = 1.1 μM gem + 2.8 μM sun; T3 = 3.5 μM gem + 6 μM sun; ns = Not significant.

4.3.3.3 Analysis of the cell cycle progression of pancreatic cancer cells following three-treatment combination

In these experiments, the cell cycle progression of PANC-1 and MIA PaCa-2 cells was assessed at 4, 24, and 48 hours after treatment with gemcitabine plus sunitinib with XBR, in three different combination schedules, as described in section 2.10.

4.3.3.3.1 Analysis of the cell cycle progression of PANC-1 cells following treatment with gemcitabine plus sunitinib in combination with XBR

Figure 4.26 shows the effect of increasing doses of gemcitabine plus sunitinib and XBR as triple combination treatment on the cell cycle progression of PANC-1 cells. The cells were treated with gemcitabine plus sunitinib (given simultaneously) administered before (schedule 1; A), after (schedule 2; C) and simultaneously with (schedule 3; E) 1Gy and 2Gy XBR and the cell cycle analysis was carried out at 4 (A1, C1 & E1), 24 (A2, C2 & E2), and 48 (A3, C3 & E3) hours post-treatment.

Incubation of PANC-1 cells with the two highest doses of gemcitabine plus sunitinib before irradiation with 1 or 2 Gy (schedule 1) resulted in a statistically significant accumulation of cells in the S phase accompanied with a decrease in the G2/M phase of the cell cycle at 4 hours post-treatment ($p < 0.001$). With the highest dose of gemcitabine plus sunitinib combination administered

before irradiation with 2 Gy, cells were also increased slightly but significantly in the G0/1 phase ($p < 0.01$) at 4 hours post-treatment in addition to the accumulation in the S phase. At 24 hours following treatment, cell distribution increased significantly in G0/1 and decreased in G2/M in a dose-dependent manner ($p < 0.0001$) compared to untreated control cells with both doses utilised of XBR. At 48 hours, all tested doses of gemcitabine plus sunitinib induced a significant increase of cells in the subG0 phase accompanied with a decrease in the G0/1 and G2/M phases compared to untreated control cells ($p < 0.05$).

Schedule 2 combination strategy, in which XBR was given before administration of gemcitabine plus sunitinib treatment, resulted in a significant cell cycle arrest of the PANC-1 cells in the G2/M phase with irradiation with 2 Gy at 4, 24, and 48 hours post-treatment ($p < 0.01$). This arrest was accompanied by a significant decrease in cell distribution in G0/1 and S phases at 4 hours after triple combination treatment ($p < 0.05$).

Treatment PANC-1 cells with gemcitabine plus sunitinib simultaneously administered with XBR (schedule 3) resulted in a significant decrease of cells in the G2/M phase of cell cycle accompanied with accumulation cells in G0/1 with the triple combination regardless of the dose of XBR at all tested time-points of measurement ($p < 0.05$). At 48 hours, however, cell distribution in the S phase was decreased accompanied with cell arrest in the G2/M and subG0 phases in the two highest doses of treatment with XBR compared to the untreated cell group ($p < 0.01$).

A **B**

1

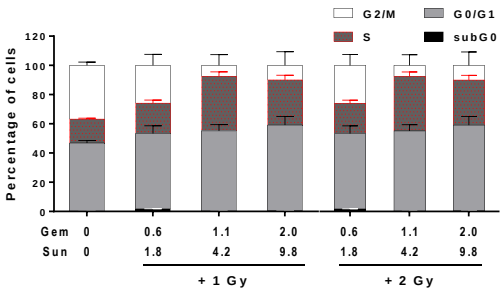

Control vs. Dose (μM)	subG0	G0/G1	S	G2/M
T1 + 1 Gy	ns	ns	ns	*
T2 + 1 Gy	ns	ns	****	****
T3 + 1 Gy	ns	**	***	****
T1 + 2 Gy	ns	ns	ns	*
T2 + 2 Gy	ns	ns	****	****
T3 + 2 Gy	ns	**	***	****

2

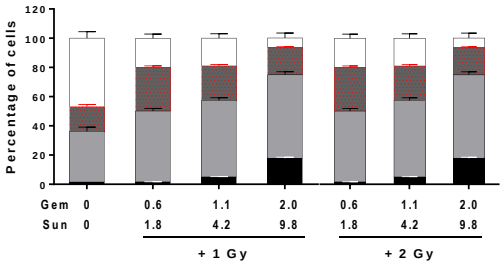

Control vs. Dose (μM)	subG0	G0/G1	S	G2/M
T1 + 1 Gy	ns	****	****	****
T2 + 1 Gy	ns	****	**	****
T3 + 1 Gy	****	****	ns	****
T1 + 2 Gy	ns	****	****	****
T2 + 2 Gy	ns	****	**	****
T3 + 2 Gy	****	****	ns	****

3

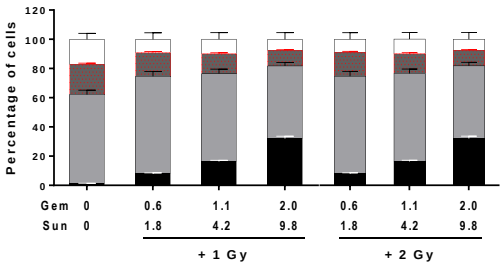

Control vs. Dose (μM)	subG0	G0/G1	S	G2/M
T1 + 1 Gy	*	*	ns	**
T2 + 1 Gy	****	ns	*	**
T3 + 1 Gy	****	****	***	***
T1 + 2 Gy	*	*	ns	**
T2 + 2 Gy	****	ns	*	**
T3 + 2 Gy	****	****	***	***

Continued overleaf …

C

D

1

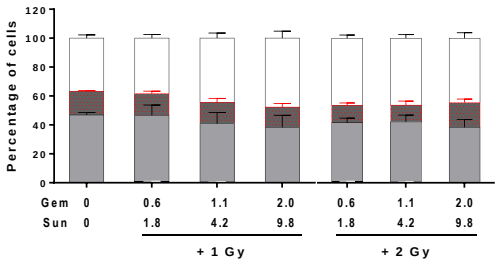

Control vs. Dose (μM)	subG0	G0/G1	S	G2/M
T1 + 1 Gy	ns	ns	ns	ns
T2 + 1 Gy	ns	ns	ns	ns
T3 + 1 Gy	ns	*	ns	**
T1 + 2 Gy	ns	****	****	****
T2 + 2 Gy	ns	****	****	****
T3 + 2 Gy	ns	****	****	****

2

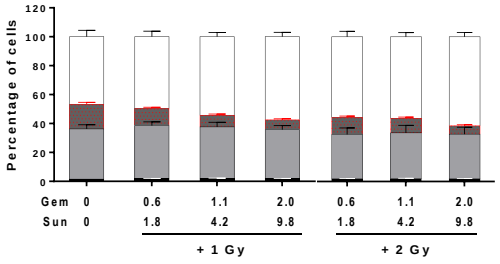

Control vs. Dose (μM)	subG0	G0/G1	S	G2/M
T1 + 1 Gy	ns	ns	*	ns
T2 + 1 Gy	ns	ns	***	**
T3 + 1 Gy	ns	ns	****	****
T1 + 2 Gy	ns	ns	ns	**
T2 + 2 Gy	ns	ns	*	**
T3 + 2 Gy	ns	ns	***	****

3

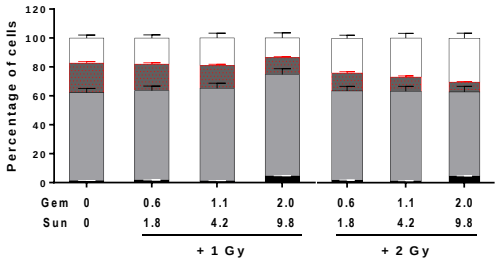

Control vs. Dose (μM)	subG0	G0/G1	S	G2/M
T1 + 1 Gy	ss	ns	ns	ns
T2 + 1 Gy	ns	ns	*	ns
T3 + 1 Gy	ns	****	***	ns
T1 + 2 Gy	ns	ns	***	**
T2 + 2 Gy	ns	ns	****	****
T3 + 2 Gy	ns	ns	****	**

Continued overleaf …

E **F**

1

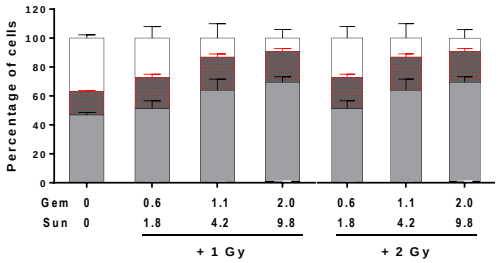

Control vs. Dose (μM)	subG0	G0/G1	S	G2/M
T1 + 1 Gy	ns	ns	ns	*
T2 + 1 Gy	ns	***	ns	****
T3 + 1 Gy	ns	****	ns	****
T1 + 2 Gy	ns	ns	ns	*
T2 + 2 Gy	ns	***	ns	****
T3 + 2 Gy	ns	****	ns	****

2

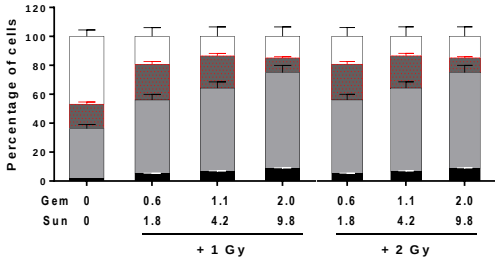

Control vs. Dose (μM)	subG0	G0/G1	S	G2/M
T1 + 1 Gy	ns	****	*	****
T2 + 1 Gy	ns	****	ns	****
T3 + 1 Gy	ns	****	ns	****
T1 + 2 Gy	ns	****	*	****
T2 + 2 Gy	ns	****	ns	****
T3 + 2 Gy	ns	****	ns	****

3

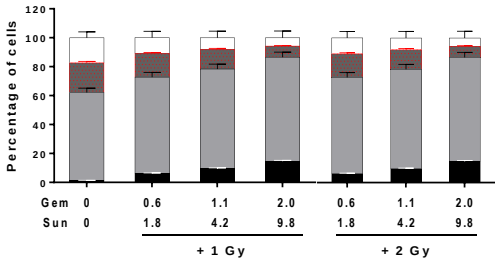

Control vs. Dose (μM)	subG0	G0/G1	S	G2/M
T1 + 1 Gy	ns	*	ns	*
T2 + 1 Gy	**	**	*	***
T3 + 1 Gy	****	***	****	****
T1 + 2 Gy	ns	*	ns	*
T2 + 2 Gy	**	**	*	***
T3 + 2 Gy	****	***	****	****

Figure 4.26 Effect of cytotoxic agents as three-treatment combination on cell cycle progression of PANC-1 cells.

The effects of gemcitabine plus sunitinib administered before (A), after (C), and simultaneously with (E) 1Gy and 2Gy XBR on the cell cycle progression were assessed in PANC-1 cells at 4 (A1, C1 & E1), 24 (A2, C2 & E2), and 48 (A3, C3 & E3) hours post-treatment. The data were analysed using FACSDiva software v6.1.3. Data are means ± SD of cells percentage in each cell cycle phase, which generated from three independent experiments. Two-way ANOVA was used to compare the means of the cell cycle phases after cells treatment with triple combination strategies to untreated control cells (B, D, and F). *P<0.05, **P<0.01, ***P<0.001 and ****P<0.0001. Gem = gemcitabine; Sun = sunitinib; T1 = 0.6 μM gem + 1.8 μM Sun; T2 = 1.1 μM gem + 4.2 μM sun; T3 = 2 μM gem + 9.8 μM sun; ns = Not significant.

4.3.3.3.2 Analysis of the cell cycle progression of MIA PaCa-2 cells following treatment with gemcitabine plus sunitinib in combination with XBR

Figure 4.27 shows the effect of increasing doses of gemcitabine plus sunitinib and XBR as triple combination treatment on the cell cycle progression of MIA PaCa-2 cells. The cells were treated with gemcitabine plus sunitinib (given simultaneously) administered before (schedule 1; A), after (schedule 2; C) and simultaneously with (schedule 3; E) 1Gy and 2Gy XBR and the cell cycle analysis was carried out at 4 (A1, C1 & E1), 24 (A2, C2 & E2), and 48 (A3, C3 & E3) hours post-treatment.

Incubation of MIA PaCa-2 cells with gemcitabine plus sunitinib before irradiation with 1 or 2 Gy (schedule 1) resulted in a significant decrease of cells in the G2/M phase at all time-points of measurements ($p < 0.01$). This decrease of cells in the G2/M was accompanied with a significant accumulation of cells in the S phase at 4 and 48 hours after treatment with the two highest doses of gemcitabine plus sunitinib ($p < 0.01$), and in the G0/1 and subG0 at all time-points with the highest dose of treatment ($0 < 0.001$).

Schedule 2 combination strategy, in which XBR was given prior to administration of gemcitabine plus sunitinib treatment, resulted in a significant cell cycle arrest in the G2/M phase with irradiation with 2 Gy at 4, 24, and 48 hours post-treatment ($p < 0.01$). This arrest was accompanied by a significant

decrease in cell distribution in G0/1 and S phases at 4 hours after triple combination treatment ($p < 0.05$).

Treatment of MIA PaCa-2 cells with gemcitabine plus sunitinib simultaneously administered with XBR (schedule 3) resulted in a significant decrease of cells in the G2/M phase of cell cycle accompanied with accumulation cells in G0/1 with the triple combination regardless of the dose of XBR at all tested time-points of measurement ($p < 0.05$). At 48 hours, however, cell distribution in the S phase was decreased accompanied with cell arrest in the G2/M and subG0 phases in the two highest doses of treatment with XBR compared to the untreated cell group ($p < 0.01$).

A **B**

1

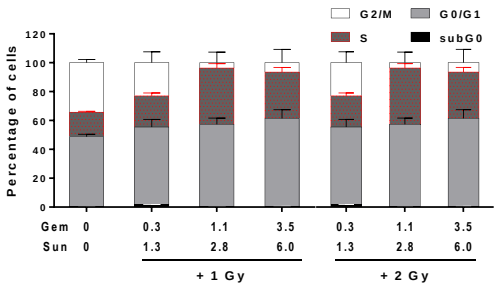

Control vs. Dose (μM)	subG0	G0/G1	S	G2/M
T1 + 1 Gy	ns	ns	ns	**
T2 + 1 Gy	ns	ns	****	****
T3 + 1 Gy	ns	**	***	****
T1 + 2 Gy	ns	ns	ns	**
T2 + 2 Gy	ns	ns	****	****
T3 + 2 Gy	ns	**	***	****

2

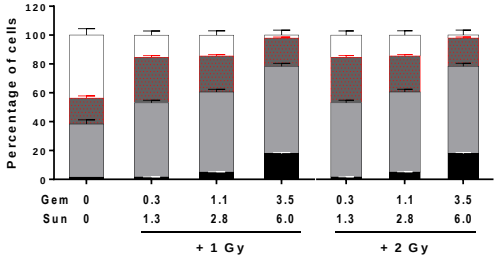

Control vs. Dose (μM)	subG0	G0/G1	S	G2/M
T1 + 1 Gy	ns	****	****	****
T2 + 1 Gy	ns	****	***	****
T3 + 1 Gy	****	****	ns	****
T1 + 2 Gy	ns	****	****	****
T2 + 2 Gy	ns	****	***	****
T3 + 2 Gy	****	****	ns	****

3

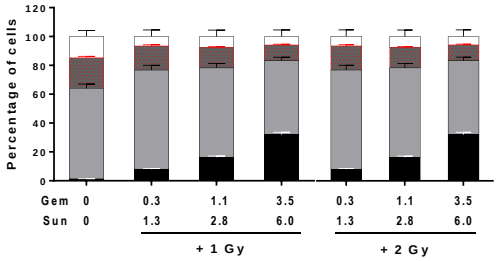

Control vs. Dose (μM)	subG0	G0/G1	S	G2/M
T1 + 1 Gy	*	*	ns	**
T2 + 1 Gy	****	ns	**	**
T3 + 1 Gy	****	****	***	***
T1 + 2 Gy	*	*	ns	**
T2 + 2 Gy	****	ns	**	**
T3 + 2 Gy	****	****	***	***

Continued overleaf …

C

D

1

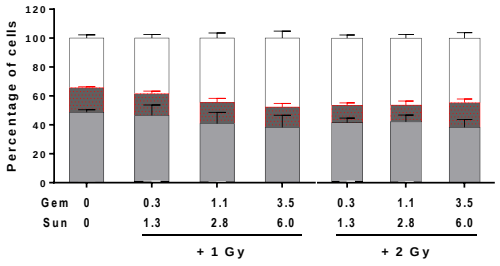

Control vs. Dose (μM)	subG0	G0/G1	S	G2/M
T1 + 1 Gy	ns	ns	ns	ns
T2 + 1 Gy	ns	*	ns	*
T3 + 1 Gy	ns	**	ns	***
T1 + 2 Gy	ns	**	ns	****
T2 + 2 Gy	ns	**	ns	****
T3 + 2 Gy	ns	***	ns	***

2

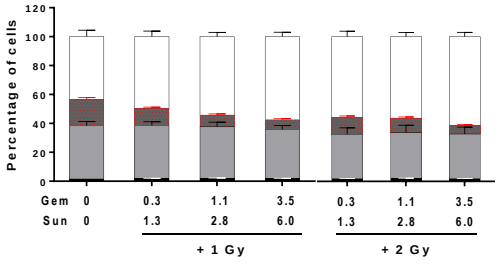

Control vs. Dose (μM)	subG0	G0/G1	S	G2/M
T1 + 1 Gy	ns	ns	**	**
T2 + 1 Gy	ns	ns	****	****
T3 + 1 Gy	ns	ns	****	****
T1 + 2 Gy	ns	*	*	****
T2 + 2 Gy	ns	ns	**	****
T3 + 2 Gy	ns	ns	****	****

3

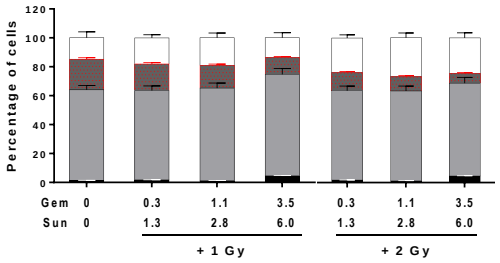

Control vs. Dose (μM)	subG0	G0/G1	S	G2/M
T1 + 1 Gy	ns	ns	ns	ns
T2 + 1 Gy	ns	ns	*	ns
T3 + 1 Gy	ns	**	***	ns
T1 + 2 Gy	ns	ns	***	***
T2 + 2 Gy	ns	ns	****	****
T3 + 2 Gy	ns	ns	****	****

Continued overleaf …

E **F**

1

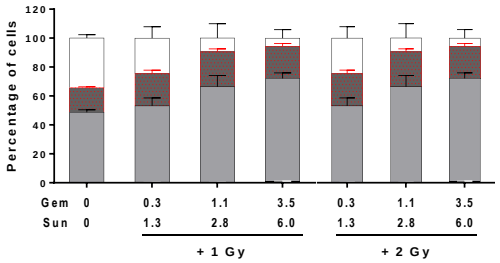

Control vs. Dose (μM)	subG0	G0/G1	S	G2/M
T1 + 1 Gy	ns	ns	ns	*
T2 + 1 Gy	ns	***	ns	****
T3 + 1 Gy	ns	****	ns	****
T1 + 2 Gy	ns	ns	ns	*
T2 + 2 Gy	ns	***	ns	****
T3 + 2 Gy	ns	****	ns	****

2

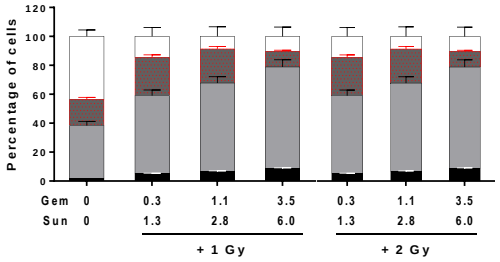

Control vs. Dose (μM)	subG0	G0/G1	S	G2/M
T1 + 1 Gy	ns	****	*	****
T2 + 1 Gy	ns	****	ns	****
T3 + 1 Gy	ns	****	ns	****
T1 + 2 Gy	ns	****	*	****
T2 + 2 Gy	ns	****	ns	****
T3 + 2 Gy	ns	****	ns	****

3

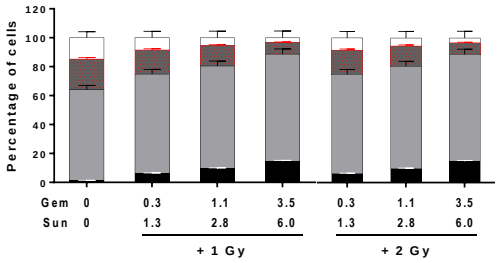

Control vs. Dose (μM)	subG0	G0/G1	S	G2/M
T1 + 1 Gy	ns	*	ns	*
T2 + 1 Gy	**	**	*	***
T3 + 1 Gy	****	****	****	****
T1 + 2 Gy	ns	*	ns	*
T2 + 2 Gy	**	**	*	***
T3 + 2 Gy	****	****	****	****

Figure 4.27 Effect of cytotoxic agents as three-treatment combination on cell cycle progression of MIA PaCa-2 cells.

The effects of gemcitabine plus sunitinib administered before (A), after (C), and simultaneously with (E) 1Gy and 2Gy XBR on the cell cycle progression were assessed in PANC-1 cells at 4 (A1, C1 & E1), 24 (A2, C2 & E2), and 48 (A3, C3 & E3) hours post-treatment. The data were analysed using FACSDiva software v6.1.3. Data are means ± SD of cells percentage in each cell cycle phase, which generated from three independent experiments. Two-way ANOVA was used to compare the means of the cell cycle phases after cells treatment with triple combination strategies to untreated control cells (B, D, and F). *P<0.05, **P<0.01, ***P<0.001 and ****P<0.0001. Gem = gemcitabine; Sun = sunitinib; T1 = 0.3 μM gem + 1.3 μM Sun; T2 = 1.1 μM gem + 2.8 μM sun; T3 = 3.5 μM gem + 6 μM sun; ns = Not significant.

4.3.3.4 The effect of three-treatment combination on the induction of apoptosis measured by Annexin V assay in pancreatic cancer cells

In these experiments, the expression of Annexin V, as an indicator of apoptosis, was assessed at 4, 24, and 48 hours after treatment with gemcitabine plus sunitinib with XBR, in three different combination schedules, in PANC-1 and MIA PaCa-2 cell lines as described in section 2.11.

4.3.3.4.1 The effect of gemcitabine plus sunitinib in combination with XBR on the induction of apoptosis measured by Annexin V assay in PANC-1 cells

Figure 4.28 (A) demonstrates the apoptosis levels at 4, 24, and 48 hours post-treatment of PANC-1 cells with increasing doses of gemcitabine plus sunitinib administered before (A1), after (A2), or simultaneously with (A3) XBR (1 Gy and 2 Gy) compared to apoptosis induced after treatment with gemcitabine plus sunitinib. Overall, there was a dose- and time- dependent increase in apoptosis in PANC-1 cells following treatment with gemcitabine plus sunitinib and XBR in all combination schedules compared to gemcitabine plus sunitinib combination. However, the exposure to XBR before incubation cells with gemcitabine/sunitinib, i.e. schedule 2, was the most effective combination strategy in terms of induction of apoptosis in PANC-1 cells. Figure 4.28 (B) shows the p-values of comparison between the means of apoptosis rate within each combination treatment doses over different time-points of measurement.

Figure 4.28 A-1 shows the apoptosis rate following the incubation of PANC-1 cells with gemcitabine plus sunitinib for 48 hours prior exposure to XBR (i.e. schedule 1). This schedule was the least effective combination strategy in terms of the induction of apoptosis in PANC-1 cells over all tested time-points compared to gemcitabine plus sunitinib alone. Although the combination treatment with gemcitabine plus sunitinib prior exposure to XBR significantly increased the apoptosis of PANC-1 cells compared to untreated control cells ($p < 0.0001$), there was no significant increase in apoptosis after this combination strategy compared to gemcitabine plus sunitinib alone regardless of dose and time of measurement ($p > 0.05$). Tukey's test multiple comparisons between the effect of time of measurement (Figure 4.28 B-1) reveals that apoptosis was significantly higher at 48 hours compared to the measurement at either 4 or 24 hours ($p < 0.0001$). There was no significant difference between apoptosis measured at 4 and 24 hours. Thus, cell irradiation post gemcitabine/sunitinib treatment had no statistically significant effect on the apoptosis levels or time of cell death compared to treatment with the two-drug treatment only.

In contrast, schedule 2, in which cells were exposed to XBR before the incubation with gemcitabine plus sunitinib, caused a dose- and time-dependent significant increase in apoptosis rate with both XBR doses (1 Gy and 2 Gy) at all examined time-points (Figure 4.28 A-2 & B-2). For example, apoptosis increased to 43 ± 2.5% at 48 hours post-incubation cells with 2 μM of gemcitabine plus 9.8 μM of sunitinib without radiation, and to 76.8.9 ± 2.7% with same doses of gemcitabine/sunitinib post-irradiation with 2 Gy ($p <$

0.0001). Thus, cell irradiation with 1 Gy or 2 Gy had increased and accelerated the apoptosis induction in PANC-1 cells compared to gemcitabine/sunitinib combination.

Finally, the concurrent administration of gemcitabine plus sunitinib with exposure to 2 Gy XBR (i.e. schedule 3) caused a significant dose- and time-dependent increase in apoptosis compared to gemcitabine plus sunitinib alone (Figure 4.28 A-3 & B-3). There was no significant increase in apoptosis with 1 Gy XBR when administered concurrently with gemcitabine plus sunitinib compared to gemcitabine plus sunitinib alone ($p < 0.05$).

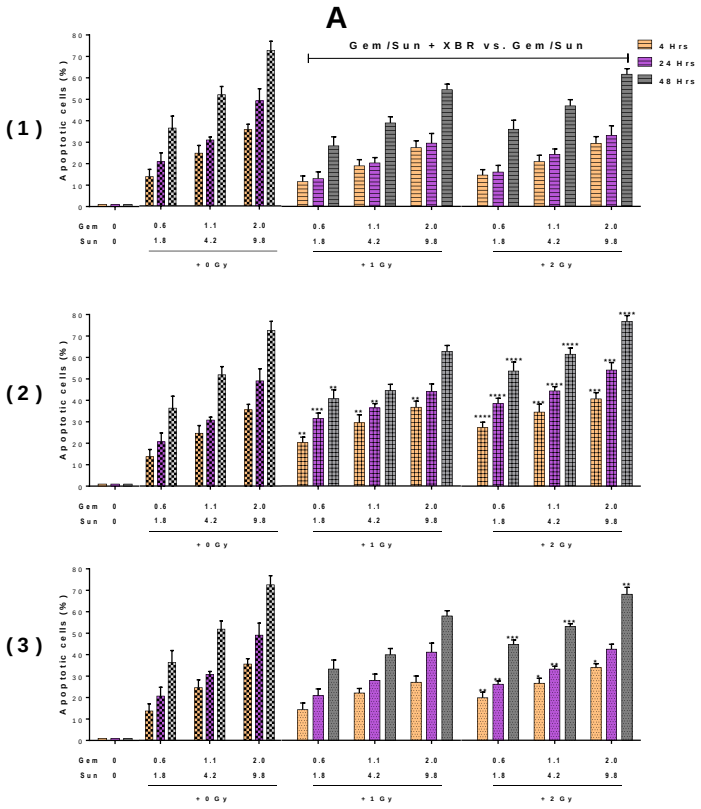

B

Time (Hours)	4 vs. 24	4 vs. 48	24 vs. 48
T1 + 1Gy	ns	****	****
T2 + 1Gy	ns	****	****
T3 + 1Gy	ns	****	****
T1 + 2Gy	ns	****	****
T2 + 2Gy	ns	****	****
T3 + 2Gy	ns	****	****

Time (Hours)	4 vs. 24	4 vs. 48	24 vs. 48
T1 + 1Gy	***	****	**
T2 + 1Gy	*	****	*
T3 + 1Gy	*	****	****
T1 + 2Gy	***	****	****
T2 + 2Gy	**	****	****
T3 + 2Gy	***	****	****

Time (Hours)	4 vs. 24	4 vs. 48	24 vs. 48
T1 + 1Gy	*	****	***
T2 + 1Gy	ns	****	***
T3 + 1Gy	***	****	****
T1 + 2Gy	**	****	****
T2 + 2Gy	**	****	****
T3 + 2Gy	***	****	****

Figure 4.28 The effect of three-treatment combination on apoptosis induction of PANC-1 cells.

The induction of apoptosis in PANC-1 cells was assessed at 4, 24, and 48 hours after treatment with gemcitabine plus sunitinib administered before (A1), after (A2), or simultaneously with (A3) 1 Gy and 2 Gy XBR. Results presented are the mean ± SD percentage of apoptotic cells of 3 independent experiments. Statistical analysis was carried out using two-way ANOVA with Dunnett's test to compare apoptosis rate resulted from all treatment doses over time-points to gemcitabine plus sunitinib (A1, A2, and A3), and with Tukey's test to compare apoptosis between different time-points after each dose of the treatment. *P<0.05, **P<0.01, ***P<0.001 and ****P<0.0001. Gem = gemcitabine; Sun = sunitinib; T1 = 0.6 μM gem + 1.8 μM Sun; T2 = 1.1 μM gem + 4.2 μM sun; T3 = 2 μM gem + 9.8 μM sun; ns = Not significant.

4.3.3.4.2 The effect of gemcitabine plus sunitinib in combination with XBR on the induction of apoptosis measured by Annexin V assay in MIA PaCa-2 cells

Figure 4.29 (A) demonstrates the apoptosis rate at 4, 24, and 48 hours post-treatment of MIA PaCa-2 cells with increasing doses of gemcitabine plus sunitinib administered before (A1), after (A2), or simultaneously with (A3) XBR (1 Gy and 2 Gy) compared to apoptosis induced after treatment with gemcitabine plus sunitinib (presented in Figure 4.21 A-3). Overall, there was a dose- and time- dependent increase in apoptosis in MIA PaCa-2 cells following treatment with gemcitabine plus sunitinib and XBR in all combination schedules. However, the exposure to XBR before incubation cells with gemcitabine/sunitinib, i.e. schedule 2, was the most effective combination strategy in terms of induction of apoptosis in MIA PaCa-2 cells. Figure 4.29 (B) shows the p-values of comparison between the means of apoptosis rate within each combination treatment doses over different time-points of measurement.

Figure 4.29 A-1 shows the apoptosis rate following the incubation of MIA PaCa-2 cells with gemcitabine plus sunitinib for 48 hours prior exposure to XBR (i.e. schedule 1). This schedule was the least effective combination strategy in terms of the induction of apoptosis in MIA PaCa-2 cells over all tested time-points compared to gemcitabine plus sunitinib alone. Although the combination treatment with gemcitabine plus sunitinib prior exposure to XBR significantly increased the apoptosis of MIA PaCa-2 cells compared to untreated control cells ($p < 0.0001$), there was no significant increase in

apoptosis after this combination strategy compared to gemcitabine plus sunitinib alone regardless of dose and time of measurement ($p > 0.05$). Tukey's test multiple comparisons between the effect of time of measurement (Figure 4.29 B-1) reveals that apoptosis was significantly higher at 48 hours compared to the measurement at either 4 or 24 hours ($p < 0.0001$). There was no significant difference between apoptosis measured at 4 and 24 hours.

In contrast, schedule 2, in which cells were exposed to XBR before the incubation with gemcitabine plus sunitinib, caused a dose- and time-dependent significant increase in apoptosis rate with both XBR doses (1 Gy and 2 Gy) at all examined time-points (Figure 4.29 A-2 & B-2). For example, apoptosis increased to 58.2 ± 1.4% at 48 hours post-incubation cells with 3.5 μM of gemcitabine plus 6 μM of sunitinib without radiation, and to 75.5 ± 3% with same doses of gemcitabine/sunitinib post-irradiation with 2 Gy ($p < 0.0001$).

Finally, the concurrent administration of gemcitabine plus sunitinib with exposure to 2 Gy XBR (i.e. schedule 3) caused a significant dose- and time-dependent increase in apoptosis compared to gemcitabine plus sunitinib alone (Figure 4.29 A-3 & B-3). There was no significant increase in apoptosis with 1 Gy XBR when administered concurrently with gemcitabine plus sunitinib compared to gemcitabine plus sunitinib alone ($p < 0.05$).

A

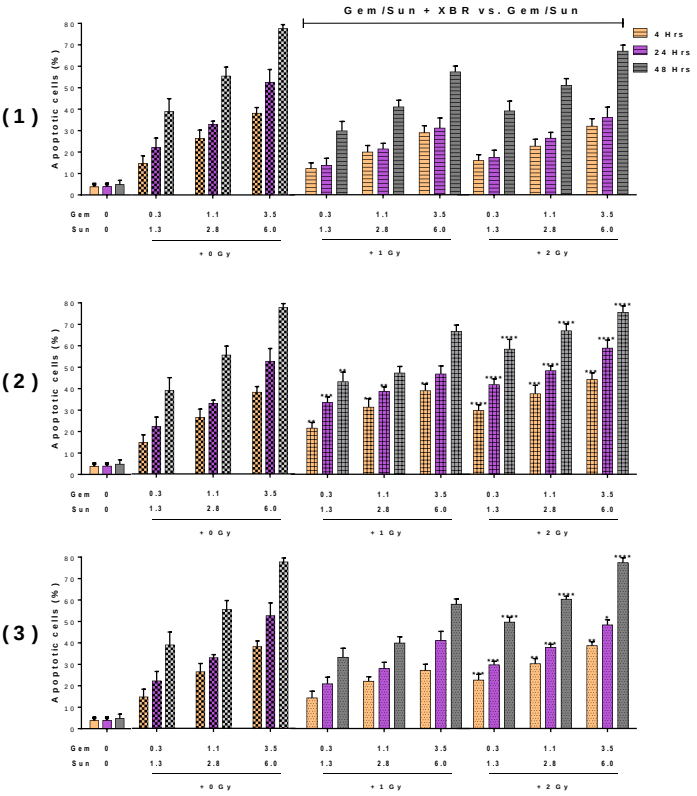

B

(1)

Time (Hours)	4 vs. 24	4 vs. 48	24 vs. 48
T1 + 1Gy	ns	****	****
T2 + 1Gy	ns	****	****
T3 + 1Gy	ns	****	****
T1 + 2Gy	ns	****	****
T2 + 2Gy	ns	****	****
T3 + 2Gy	ns	****	****

(2)

Time (Hours)	4 vs. 24	4 vs. 48	24 vs. 48
T1 + 1Gy	***	****	**
T2 + 1Gy	*	****	*
T3 + 1Gy	*	****	****
T1 + 2Gy	***	****	****
T2 + 2Gy	**	****	****
T3 + 2Gy	***	****	****

(3)

Time (Hours)	4 vs. 24	4 vs. 48	24 vs. 48
T1 + 1Gy	*	****	***
T2 + 1Gy	ns	****	***
T3 + 1Gy	***	****	****
T1 + 2Gy	**	****	****
T2 + 2Gy	**	****	****
T3 + 2Gy	***	****	****

Figure 4.29 The effect of three-treatment combination on apoptosis induction of MIA PaCa-2 cells.

The induction of apoptosis in MIA PaCa-2 cells was assessed at 4, 24, and 48 hours after treatment with gemcitabine plus sunitinib administered before (A1), after (A2), or simultaneously with (A3) 1 Gy and 2 Gy XBR. Results presented are the mean ± SD percentage of apoptotic cells of 3 independent experiments. Statistical analysis was carried out using two-way ANOVA with Dunnett's test to compare apoptosis rate resulted from all treatment doses over time-points to gemcitabine plus sunitinib (A1, A2, and A3), and with Tukey's test to compare apoptosis between different time-points after each dose of the treatment. *P<0.05, **P<0.01, ***P<0.001 and ****P<0.0001. Gem = gemcitabine; Sun = sunitinib; T1 = 0.3 μM gem + 1.3 μM Sun; T2 = 1.1 μM gem + 2.8 μM sun; T3 = 3.5 μM gem + 6 μM sun; ns = Not significant.

4.4 Discussion

This chapter aimed to determine the cytotoxicity of novel combination treatment of gemcitabine and the TKIs sunitinib and, for the first time, pazopanib with or without exposure to XBR by investigating the clonogenic cell survival of PANC-1 and MIA PaCa-2 pancreatic cancer cell lines following treatment administration. Additionally, the synergistic or antagonistic interaction between those agents and the underlying mechanisms of cytotoxicity were also assessed in cells treated with two-drug and three-treatment combinations. Three combination schedules were examined for the first time in PANC-1 and MIA PaCa-2 cells. In this chapter, it was hypothesised that the treatment with gemcitabine in combination with TKI (two-treatment) or with TKI plus XBR (three-treatment) combination schedules would result in a synergistic and superior cytotoxic effect in pancreatic cancer cells compared to gemcitabine alone.

In the previous chapter, we examined the cytotoxicity of gemcitabine and TKIs sunitinib and pazopanib on PANC-1 and MIA PaCa-2 cells as single treatments by clonogenic assay and, consequently, lower doses of each agent were determined to be used in combination studies (Table 3.5) in order to assess the effect of anti-cancer agents on the pancreatic cancer cell lines and to generate IC_{50} values which were used in combination therapy. In the present chapter, the cytotoxicity of those agents in lower doses with XBR was examined as a single-agent treatment before assessing their cytotoxicity in two- and three-treatment combination regimens.

There was a statistically significant dose-dependent reduction in the clonogenic survival fraction of both cell lines following 48-hour treatment with increasing doses of gemcitabine, sunitinib, pazopanib, or XBR as single treatment compared to untreated control cells. The results of previous studies which were performed to evaluate the cytotoxicity of gemcitabine (Thoennissen *et al.*, 2009; Cieslak *et al.*, 2015; Kausar *et al.*, 2015; Li *et al.*, 2017), sunitinib (Cuneo *et al.*, 2008), and XBR (Cuneo *et al.*, 2008; Li *et al.*, 2017) alone using clonogenic survival assay in PANC-1 and MIA PaCa-2 pancreatic cancer cell lines have demonstrated similar effects to results described in this chapter.

Pazopanib was not tested, to the best of our knowledge, in terms of its effect on clonogenic capacity in pancreatic cancer cells before our study. Thus, we have shown for the first time that the TKI pazopanib kills the pancreatic cancer cells and we established a novel proof-of-concept on the effect of pazopanib on PANC-1 and MIA PaCa-2 pancreatic cancer cell lines. However, pazopanib inhibited colony formation profoundly at the concentration of 15 µM in MEB-Med-8A and DAOY medulloblastoma cells (Craveiro *et al.*, 2014).

On the other hand, the effect of sunitinib on clonogenic survival was assessed in several types of cancer cells. For example, sunitinib inhibited colony formation significantly in a dose-dependent manner in prostate cancer cells (DU145 and PC3) (Brooks *et al.*, 2012), five human bladder cancer cells (HTB5, HTB9, UMU14, J82, and SW1710) (Yoon *et al.*, 2011), oesophageal squamous cell carcinoma cells (TE13 and Eaca109) (Ding *et al.*, 2016), human

umbilical vein endothelial cells (HUVECs) (Zhang *et al.*, 2010; El Kaffas *et al.*, 2014), Lewis lung carcinoma (LLC) cells (Zhang *et al.*, 2010), breast cancer cells (MDA-MB-231) (El Kaffas *et al.*, 2014), renal cancer cells (786-O, A498, Caki-1, Caki-2, and ACHN) (Mahalingam *et al.*, 2011), pancreatic neuroendocrine tumours cells (BON1) (Wiedmer *et al.*, 2017), and pancreatic cancer cells (PANC-1 and MIA PaCa-2) (Cuneo *et al.*, 2008).

4.4.1 Gemcitabine

In the current study, the effect of gemcitabine alone on the cell cycle progression, γ-H_2AX expression, as a marker of DNA damage and repair, Annexin V expression, as an indicator of apoptosis, in PANC-1 and MIA PaCa-2 pancreatic cancer cells were assessed at 4, 24, and 48 hours post-treatment.

When the level of DNA damage was measured by detection of γ-H2AX, a statistically significant dose-dependent increase in DNA damage was observed in both PANC-1 and MIA PaCa-2 pancreatic cancer cell lines after 4 hours of treatment with gemcitabine alone ($p < 0.001$) compared untreated control cells (Figure 4.3A & Figure 4.4A). However, the γ-H_2AX levels decreased significantly at 24 and 48 hours compared to γ-H_2AX levels measured at 4 hours. Similar to our results, researchers found that gemcitabine increased the expression of γ-H2AX In AsPC-1 pancreatic cancer cell line within 24 hours after treatment and then dropped significantly to its baseline levels at 42 hours post-treatment (Montano *et al.*, 2017). This may indicate a rapid DNA repair following the treatment with gemcitabine alone in

pancreatic cancer cells. Another previous study showed that treatment with gemcitabine in PANC-1 and MIA PaCa-2 cells induced significant DNA damage, which was evidenced by an increase of γ-H2AX staining when administered in combination with ku70 inhibitors (Ma *et al.*, 2017). However, Ma ***et al's*** study did not quantify γ-H2AX expression when gemcitabine administered alone and did not consider changes of γ-H2AX levels over the time as we did in our study. Thus, it is difficult to determine whether the elevation in γ-H2AX expression was attributed, entirely or partially, to gemcitabine. We could not detect from our study the mechanism behind this elevation in γ-H2AX. Nevertheless, other studies (Qiao *et al.*, 2013; Montano *et al.*, 2017) found that gemcitabine treatment resulted in induction of CHK1 (checkpoint kinase 1) which is a critical protein in cell cycle checkpoint pathways and DNA DSB repair (Dai and Grant, 2010). Thus, it can be suggested that the rapid decrease in γ-H2AX within 24 hours of gemcitabine alone treatment was likely related to the release of pancreatic cancer cells from the cell cycle arrest resulted from CHK1 induction. We, however, also investigated the effect of gemcitabine of the cell cycle progression.

In response to DNA damage, cells activate both cell cycle checkpoint and DNA repair pathways which function cooperatively to prevent the propagation of cells with damaged DNA (Sancar *et al.*, 2004; Montano *et al.*, 2013; Liubavičiute *et al.*, 2015; Morgan and Lawrence, 2015). Previous studies demonstrated that this level of DNA damage following treatment with gemcitabine activated cell cycle checkpoints and induced early S phase cell cycle arrest (Kufe *et al.*, 1980; Huang *et al.*, 1991; Xie and Plunkett, 1995;

Pauwels *et al.*, 2002, 2003). The results from the current study were in agreement with previous studies; hence the incubation of cells with increasing doses of gemcitabine alone resulted in a significant time- and dose- dependent accumulation of cells in the S phase accompanied with a decrease in the G2/M phase of the cell cycle at all measured time-points (4, 24, and 48 hours) in PANC-1 cells and at 24 and 48 hours time-points in MIA PaCa-2 cells compared to untreated control cells ($p < 0.001$). At 24-hour after treatment with gemcitabine alone, cell distribution was also increased in G0/G1 in both cell lines. Cells were released from G1 phase and increased significantly in sub G0 phase after 48 hours of treatment with gemcitabine alone in PANC-1 and MIA PaCa-2 cells. Therefore, this release from cell cycle arrest which accompanied with decreased γ-H_2AX levels after 48 hours of gemcitabine cessation may indicate that most of the cells' DNA damage was repaired at that time-point. A small portion of cells went through apoptosis or died by other mechanisms. These findings from our study were also in agreement with another study which was conducted to study the cell cycle perturbation induced by gemcitabine alone or in combination with a CHK1 inhibitor in cell culture (bladder and pancreatic cancer cells), xenografts, and bladder cancer patients (Montano *et al.*, 2017). Montano and his colleagues demonstrated that gemcitabine induced cell cycle arrest of MDA-MB-231 and AsPC-1 cells in mid-S phase (at low concentrations) and early-S phase (at higher concentrations) at 24 hours, and the cells appeared to have fully recovered by 48 hours (Montano *et al.*, 2017). Thus, our findings of a rapid decrease in γ-H2AX expression was in alignment with our findings of cell release from S-phase

arrest at 48 hours. After the assessment of the γ-H2AX expression and the cell cycle progression, we investigated whether the DNA damage and cell arrest would induce apoptosis in pancreatic cancer cell following the treatment with gemcitabine alone.

Irreparable DNA damage can result in permanent cell cycle arrest, induction of apoptosis, or mitotic cell death caused by loss of genomic material (Liubavičiute *et al.*, 2015). In the present study of the apoptotic effect of gemcitabine alone on pancreatic cancer cell lines, it has been observed that the apoptosis rate increased in a dose- and time- dependent manner after treatment with gemcitabine alone compared to untreated control cells. Apoptosis increased significantly after 48 hours of treatment with all tested doses of gemcitabine compared to the earlier time-points in both cell lines ($p < 0.01$). Gemcitabine-induced cell cycle arrest at S phase in pancreatic cancer cells has been described in previous studies in which gemcitabine cytotoxicity was enhanced by increased S phase arrest with checkpoint kinase inhibitors (Matthews *et al.*, 2007; Ono, Basson and Ito, 2015). These results confirmed the findings of γ-H_2AX assay and cell cycle analysis following the treatment of PANC-1 and MIA PaCa-2 cells with gemcitabine alone; hence γ-H_2AX levels decreased to its basal levels and the majority of cells were released from S phase arrest during 48 hours of gemcitabine cessation. These results may suggest also that cells can tolerate arrest in S phase for several days, but the prolonged arrest is lethal (Montano *et al.*, 2017).

4.4.2 Sunitinib

In the current study, the effect of sunitinib alone on the cell cycle progression, γ-H_2AX expression, as a marker of DNA damage and repair, and Annexin V expression, as an indicator of apoptosis, in PANC-1 and MIA PaCa-2 pancreatic cancer cells were assessed at 4, 24, and 48 hours post-treatment.

When the level of DNA damage was measured by detection of γ-H2AX, it was observed that apart from the highest tested dose (9.8 μM in PANC-1 and 6 μM in MIA PaCa-2), the treatment with sunitinib failed to increase γ-H_2AX in both cell lines over the examined time-points. After 4 hours, there was a significant increase in γ-H_2AX expression following treatment with the highest tested dose of sunitinib compared to untreated control ($p < 0.0001$). However, the γ-H_2AX level decreased significantly at 24 and 48 hours compared to γ-H_2AX levels measured at 4 hours to reach the basal levels in both cell lines. Thus, these results suggest that sunitinib may impose a minor effect on the DNA damage and repair pathways and more likely to kill the pancreatic cancer cells with other mechanisms of actions. These findings are in alignment with a previous study in which sunitinib was evaluated as a radiosensitiser in prostate cancer cell lines (DU145, PC3 and LNCaP) (Brooks *et al.*, 2012). Brooks and his colleagues observed a minor radiosensitisation effect of sunitinib on DU145 and PC3 cells whereas LNCaP cells were not radiosensitised by sunitinib. Furthermore, the authors were unable to detect any prolongation of the presence of γH2AX foci by sunitinib suggesting that sunitinib did not interfere with the repair of radiation-induced DSBs (Brooks *et al.*, 2012). In contrast to

our result, the levels of γ-H_2AX at 30 minutes, 2 hours, and 24 hours after 4 Gy irradiation were determined by immunofluorescence to investigate the impact of sunitinib on XBR-induced DSB repair kinetics in oesophageal squamous cell carcinoma cells (Ding *et al.*, 2016). The authors found that the formation of γ-H_2AX foci at 30 minutes post combination treatment with sunitinib and XBR increased significantly compared to irradiation alone and the number of foci subsided to near basal level at 24 hours. These results from Ding's study contradicted our results of the γ-H2AX analysis as they indicated that sunitinib markedly increased the induction and persistence of irradiation-induced γ-H2AX foci (Ding *et al.*, 2016). However, our findings of the DNA damage and repair analysis and γ-H2AX expression were in harmony with and supported by the cell cycle progression and apoptosis detection assays from our mechanistic studies.

In the current study, the cell cycle distribution of PANC-1 and MIA PaCa-2 pancreatic cancer cells was examined in order to investigate the mechanism responsible for the sunitinib-mediated antiproliferative effect. The treatment of cells with the two highest tested doses of sunitinib (4.2 and 9.8 μM in PANC-1 cells) and the highest tested dose (6 μM in MIA PaCa-2 cells) resulted in a significant cell cycle arrest at G1 phase accompanied with a decrease in the G2/M phase of the cell cycle at 4 and 24 hours after treatment compared to untreated control cells ($p < 0.0001$). However, cells were released from the G1 phase and arrested in the G2/M phase of the cell cycle after 48 hours of treatment with sunitinib. These findings are in accordance with a previous study conducted to investigate the precise mechanism of sunitinib action

against acute myeloid leukaemia (AML) cells (Teng *et al.*, 2013). The authors found that the exposure of HL60 and KG-1 AML cells to sunitinib for 24 hours led to an accumulation of cells in the G0/G1 phase compared with control cells, coupled with a concomitant decrease in the proportion of cells in the S and G2/M phases. Sunitinib induced G1 phase arrest associated with decreased cyclin D1, cyclin D3, and cyclin-dependent kinase (Cdk)2 and increased p27, retinoblastoma protein (pRb1), and p130/Rb2 expression and phosphorylated activation of protein kinase C alpha and beta (PKCα/β) (Teng *et al.*, 2013). These findings were also supported by another study which investigated the effect of sunitinib on papillary thyroid cancer cells (Fenton MS, Marion KM, Salem AK, Hogen R, Naeim F, 2010). The study demonstrated that sunitinib caused cell cycle arrest in the G0/G1 phase and dephosphorylation of pRb1 in the papillary thyroid cancer cell. However, subG0 population, which is indicative of degraded DNA and a hallmark of apoptosis, was observed following 24 hours of sunitinib treatment and increased continuously after 48 hours incubation in AML cell lines (Teng *et al.*, 2013), whereas pancreatic cells (PANC-1 and MIA PaCa-2) released from G0/G1 arrest and accumulated in G2/M after 48 hours of treatment with sunitinib in our study. Thus, accumulation of cells in G2/M and released from G0/G1 phase confirm the findings from our γ-H2AX analysis, which indicated a minor effect of sunitinib alone on DNA degradation.

In the present study, sunitinib increased the apoptosis rate significantly in a dose- and time- dependent manner compared to untreated control pancreatic cancer cells. In contrast to gemcitabine, there was no observed increase in

apoptosis in PANC-1 and MIA PaCa-2 cells at 4 hours after treatment with sunitinib alone. Apoptosis increased significantly after 48 hours of treatment with all tested doses of sunitinib compared to the earlier time-points ($p < 0.01$). Therefore, the increased apoptosis at 48 hours indicated a late effect of sunitinib alone on the pancreatic cancer cells and mirror the results from the cell cycle analysis in which cells were released from G0/G1 arrest and accumulated in the G2/M phase by 48 hours of treatment. Similar to these findings, it has been demonstrated that sunitinib, either alone or in combination with gemcitabine, caused a significant increase in the expression of cleaved caspase-3 and cleaved PARP-1 protein, thereby indicating the induction of caspase-dependent apoptosis in AsPC-1 pancreatic cancer cell line, WI-38 human fibroblast cell line, and HUVECs primary human umbilical vein endothelial cells (Awasthi, Schwarz and Schwarz, 2011). In another study, Yang and his colleagues reported that sunitinib induced apoptosis and inhibited cell proliferation of both a short-term primary culture (VC312) and an established cell line (DAOY) of human medulloblastomas and resulted in the activation of caspase-3 and cleavage of poly(ADP-ribose) polymerase and upregulation of proapoptotic genes, *Bak* and *Bim*, and inhibited the expression of survivin, an antiapoptotic protein (Yang *et al.*, 2010). Thus, previous studies supported our findings that sunitinib can induce apoptosis in pancreatic cancer cells. We, however, had not investigated the apoptosis pathway in this study due to the time constraints and we recommend exploring these pathways in future studies.

4.4.3 Pazopanib

Pazopanib was originally approved for the treatment of renal cell carcinoma (Motzer *et al.*, 2014). It was also repurposed and approved for the treatment of sarcoma (Sorokin *et al.*, 2018). Several preclinical and clinical studies investigated pazopanib in pancreatic neuroendocrine tumours (Ahn *et al.*, 2013; Grande *et al.*, 2014; Kalyan *et al.*, 2015; Kwekkeboom, 2015). However, based on its biological rationale and previous strong positive efficacy in pancreatic neuroendocrine tumours (Ahn *et al.*, 2013; Kalyan *et al.*, 2015) and other cancers (Sternberg *et al.*, 2013; Kim *et al.*, 2014), we investigated the cytotoxic efficacy of pazopanib, for the first time, to the best of our knowledge, in pancreatic ductal adenocarcinoma cell lines *in vitro*.

Pazopanib, when administered alone reduced the survival fraction significantly in both PANC-1 and MIA PaCa-2 cell lines in a dose-dependent manner compared to untreated control cells. However, this TKI agent failed to decrease cell survival when combined with gemcitabine in both cell lines regardless of the treatment schedule compared to gemcitabine alone. In response to the results of cytotoxic efficacy experiments (clonogenic assay, DEF, and CI analysis) presented in section 4.3.2.1.2, pazopanib in combination with gemcitabine, either without XBR (two-drug combination) or with XBR (three-treatment combination) was excluded from the mechanistic studies, *in vitro* three-treatment combination cytotoxicity studies, and *in vivo* study. Interestingly, this modest efficacy of pazopanib and such large differences between pazopanib and sunitinib activities on the pancreatic

cancer cells, even though they have a similar pharmacological profile, were unxpected. It has been reported that pazopanib targets the fibroblast growth factor receptor (FGFR) subtypes 1 and 3 (Keisner and Shah, 2011; Plummer *et al.*, 2013) and FGFR-2 (Ranieri *et al.*, 2014), which were revealed to be overexpressed in both PANC-1 and MIA PaCa-2 pancreatic cancer cell lines (Ishiwata *et al.*, 2012). Because the fact that sunitinib does not target FGFR (*see* Figure 1.3), we expected that pazopanib could be impse more potent inhibitory effect against the pancreatic cancer cells for this reason. However, this was not the case and we suspected that may be reflecting a solubility or stability issue for pazopanib. Thus, we recommend interrogation of these issues in future studies.

4.4.4 Gemcitabine plus sunitinib

In the current study, clonogenic survival assay, combination index analysis, and DEF experiments were conducted to evaluate the efficacy of gemcitabine in combination with sunitinib on pancreatic cancer cell lines as described in sections 2.6, 2.7, and 2.9, respectively. We, for the first time, to the best of our knowledge, investigated three combination schedules. Gemcitabine was administered 48 hours before (schedule 1), after (schedule 2), or simultaneously with (schedule 3) sunitinib. The results were presented in section 4.3.2. This study aimed to assess synergism using the combination index analysis approach and determine the most effective combination schedule of gemcitabine and sunitinib combinations. Also, DEF was employed

to explore whether sunitinib can sensitise pancreatic cancer cells to gemcitabine and vice versa.

Therefore, we hypothesised that combining the conventional chemotherapy (gemcitabine) with a multi-target TKI with antiangiogenic and anti-tumour activity targeted therapy (sunitinib) in lower therapeutic doses of each agent might result in a synergistic interaction between them and improve the outcome of pancreatic cancer treatment. We thought that combination strategies may reduce the chance of pancreatic cancer cells dose-dependent resistance to chemotherapy, which was reported to be the major contributor to poor prognosis.

This hypothesis was validated in this two-drug combination study, hence the lowest combination doses of gemcitabine and sunitinib induced additive responses, and the higher two doses induced synergistic responses following schedule 1 and schedule 3 treatments in both cell lines compared to gemcitabine alone. The concurrent administration of gemcitabine and sunitinib (schedule 3) was the most effective combination schedule and the two highest tested doses of combination inhibited the clonogenic survival compared to gemcitabine alone ($p < 0.01$). In contrast, there was no significant reduction in survival following schedule 2 combination of gemcitabine and sunitinib compared to gemcitabine alone in both cell lines ($p > 0.05$). Moreover, in combination index analysis, schedule 2 also induced antagonistic responses with all examined doses in both cell lines. This antagonism interaction of schedule 2 combination of gemcitabine and sunitinib in pancreatic cancer was

expected and supported with a previous study (Humbert *et al.*, 2010). The study found that antagonistic effect was also observed when MIA PaCa-2 cells were pre-incubated with 10 μM of TKIs (imatinib or dasatinib), before the treatment with gemcitabine (Humbert *et al.*, 2010).

Similarly, a previous study demonstrated that the simultaneous combination of gemcitabine and sunitinib showed significantly greater growth inhibition *in vitro* pancreatic ductal adenocarcinoma cell lines (PANC-1 and MIA PaCa-2) as compared to either agent alone (Tran Cao *et al.*, 2010). Furthermore, on synergy analysis, this combination treatment exerted a synergistic inhibitory effect on MIA PaCa-2 cells at low doses, and the antagonistic effect was observed at higher doses of combination (Tran Cao *et al.*, 2010). This synergistic enhancement in anti-tumour effect between sunitinib and gemcitabine was also observed in bladder cancer cells (Yoon *et al.*, 2011). Therefore, in response to our CI analysis results, we used the concurrent administration (schedule 3) of gemcitabine and sunitinib in the three-treatment combination *in vitro* study and later in our *in vivo* study.

Figure 4.11 demonstrates that the survival fraction of PANC-1 and MIA PaCa-2 cells was decreased significantly following the treatment with sunitinib in combination with gemcitabine compared to treatment with gemcitabine alone ($p < 0.05$). This combination has been also evaluated in genitourinary malignancies. For instance, in a bladder cancer cell line, HTB5, sunitinib was synergistic with gemcitabine by both the isobolic method and clonogenic assay (Yoon *et al.*, 2011). In our study, sunitinib sensitized PANC-1 cells to

gemcitabine treatment and the DEF50 achieved was 1.45, 1,67, and 1.85 following the administration of 1.8, 4.2, and 9.8 μM of sunitinib, respectively. MIA PaCa-2 was more sensitive to sunitinib than PANC-1; the DEF_{50} achieved was 1.94, 3.7, and 3.02 following the administration of 1.3, 2.8, and 6 μM of sunitinib, respectively (Figure 4.11 - F). From another angle of analysis and for completion, we also evaluated whether gemcitabine could sensitise cells to sunitinib. The results of this analysis were presented in Figure 4.12. No previous studies, to the best of our knowledge, found to evaluate the dose enhancement between gemcitabine and sunitinib either in pancreatic cancer cells or in other solid tumours. However, two studies demonstrated an additive anti-tumour effect between gemcitabine and sunitinib in AsPC-1 pancreatic cancer cells only at low concentrations (100 nM) (Awasthi, Schwarz and Schwarz, 2011), and a synergistic effect in bladder cancer cells (Yoon *et al.*, 2011). Thus, our hypothesis was validated as we found, from the CI analysis, a synergistic interaction between gemcitabine and sunitinib. Furthermore, we revealed for the first time that sunitinib sensitised PANC-1 and MIA PaCa-2 pancreatic cancer cell to gemcitabine and vice versa.

In the mechanistic studies, we observed no significant additional effect on γ-H_2AX levels for the combination treatment with sunitinib and gemcitabine compared to treatment with gemcitabine alone at all time-points and all combination schedules in PANC-1 and MIA PaCa-2 cell lines. The γ-H_2AX levels decreased significantly after 24 and 48 hours of treatment with all combination schedules compared to its levels at 4 hours ($p < 0.01$; Figure 4.16 B). This suggests that cells were unable to repair DNA damage and underwent

cell death. This result found to be supported by the findings of our apoptosis and cell cycle analysis studies. In both cell lines, PANC-1 and MIA PaCa-2, the two highest doses of gemcitabine and sunitinib resulted in a significant increase of cells in the subG0 population compared to untreated control cells ($p < 0.0001$) at 48 hours time-point, which is indicative of degraded DNA, a hallmark of apoptosis (Teng *et al.*, 2013). In addition, Annexin V analysis indicated that there was a dose- and time- dependent increase in apoptosis in PANC-1 and MIA PaCa-2 cells following combination treatment with gemcitabine and sunitinib compared to gemcitabine treatment alone. A previous study also demonstrated that the combination treatment of pancreatic cancer cells with gemcitabine and sunitinib also had superior proapoptotic activity (Casneuf *et al.*, 2009). In addition, similar to our findings, the apoptotic indices in pancreatic cancer AsPC-1 cells in the control, gemcitabine, sunitinib, gemcitabine plus sunitinib groups were 0.13 ± 0.03, 0.21 ± 0.06, 0.47 ± 0.05 and 0.54 ± 0.01, respectively ($P < 0.00002$ vs. control) (Awasthi, Schwarz and Schwarz, 2011). The least effective combination schedule in the induction of apoptosis in our study was schedule 2; i.e. when gemcitabine was administered after sunitinib. This result was expected, as the schedule 2 combination was the least effective combination schedule in terms of clonogenic survival. These findings can be interpreted by the alterations in cell cycle distribution following this schedule combination treatment. The cell distribution in the S phase, which was reported to be crucial for gemcitabine-induced apoptosis (Shi *et al.*, 2001), was decreased significantly in the highest dose treatment group at 4 and 24 hours post-treatment with schedule 2

combination compared to the untreated cell group in PANC-1 and MIA PaCa-2 cells ($p < 0.01$) in our study. Similar to our findings of antagonistic responses occurred when sunitinib was administered before gemcitabine (schedule 2), a previous study found that pre-incubation of cells with 10 mM of imatinib or dasatinib did not result in an increased response of Mia Paca-2 cells to gemcitabine as compared to masitinib (Figure 2D) (Humbert *et al.*, 2010).

4.4.5 Gemcitabine plus sunitinib plus XBR

For the first time, as far as we aware, we evaluated the cytotoxicity effects of three-treatment combination of gemcitabine plus sunitinib (administered simultaneously as single treatment) administered 48 hours before (schedule 1), after (schedule 2), or simultaneously with (schedule 3) 1 Gy or 2 Gy of XBR on PANC-1 and MIA PaCa-2 cell lines by clonogenic assay and combination index analysis. These cytotoxicity studies were followed by the mechanistic studies (H_2AX detection, cell cycle analysis, and apoptosis) measured at three different time-points (4, 24, and 48 hours). The results were presented in section 4.3.3.

In both PANC-1 and MIA PaCa-2 pancreatic cancer cell lines, exposure to XBR before treatment with gemcitabine plus sunitinib (schedule 2) was the most effective three-treatment combination schedule and induced dose-dependent synergistic responses ($CI < 0.9$) at all tested doses of combination, while schedule 1 combination (in which gemcitabine/sunitinib combination was administered before radiation) resulted in the lowest cytotoxicity and induced

antagonistic responses (CI > 1.1) with all examined doses of gemcitabine/sunitinib and XBR.

Generally, in the current study, γ-H_2AX increased at 4 hours post-exposure to the triple therapy of gemcitabine plus sunitinib and XBR; then it decreased at 24- and 48- hours time-points in both cell lines. Similar to our results, a previous study found that treatment with radiation alone or in combination with gemcitabine caused robust induction of γ-H_2AX by 2 hours in MIA PaCa-2 cells that was resolved to baseline by 24 hours post-radiation (Kausar *et al.*, 2015). Furthermore, we found that the exposure to XBR before incubation of cells with gemcitabine/sunitinib, i.e. schedule 2, caused a dose-dependent significant increase in the γ-H_2AX levels with both XBR doses (1 Gy and 2 Gy) at all examined time-points. Therefore, this anti-tumour effectiveness which was observed with schedule 2 of triple combination therapy can be attributed to the DNA damage. In support to this, it has been reported that the combination treatment of sunitinib and radiotherapy increased the formation of γ-H_2AX at 30 minutes compared to irradiation alone in oesophageal squamous cell carcinoma cells *in vitro* (Ding *et al.*, 2016). It has been reported that the XBR, when combined with sunitinib, decreased the activation of the Akt and Erk pathway and reduced the clonogenic survival in PANC-1 and MIA PaCa-2 cell lines (Kleibeuker, ten Hooven, Verheul, *et al.*, 2015).

Cell cycle analysis and apoptosis detection assays supported the findings of the γ-H_2AX and clonogenic survival results. Schedule 2 combination strategy, in which XBR was given prior to administration of gemcitabine plus sunitinib

treatment, induced apoptosis in a time- and dose- dependent manner in both cell lines, and resulted in a significant cell cycle arrest in the G2/M phase with irradiation with 2 Gy at 4, 24, and 48 hours post-treatment ($p < 0.01$). This arrest was accompanied by a significant decrease in cell distribution in G0/1 and S phases at 4 hours after triple combination treatment ($p < 0.05$).

In conclusion, it can be seen from the two-drug combination treatment that the concurrent administration of gemcitabine with sunitinib was the most effective combination schedule in killing the pancreatic cancer cell lines (PANC-1 and MIA PaCa-2) compared to the treatment with gemcitabine alone. This combination schedule was responsible for the highest DNA damage, measured by elevation of γ-H_2AX expression, and the highest induction of apoptosis in pancreatic cancer cells. Thus, this concurrent administration of gemcitabine and sunitinib was used in our *in vitro* and *in vivo* studies. Moreover, upon the investigation of three-treatment combination on the pancreatic cancer cell in vitro study for the first time, we concluded that the concurrent administration of gemcitabine and sunitinib post cell irradiation (i.e. schedule 3) was the most effective triple combination schedule in terms of clonogenic survival of pancreatic cancer cells. Therefore, we designed our *in vivo* study in accordance with these findings.

CHAPTER 5: In vivo efficacy of gemcitabine, sunitinib, or XBR as single treatment or in combination in nude mice xenografts comprised of PANC-1 pancreatic cancer cells

5.1 Introduction

In the previous study (Chapter 4), the cytotoxic efficacy of novel combination schemes gemcitabine and TKIs (sunitinib or pazopanib) with or without exposure to XBR was reported *in vitro* on PANC-1 and MIA PaCa-2 pancreatic cancer cell lines. The hypothesis of the *in vitro* study stated that the treatment with gemcitabine with TKI (sunitinib or pazopanib) (two-drug) or with TKI plus XBR (three-treatment) combination schedules would result in a synergistic and superior cytotoxic effect in pancreatic cancer cells compared to gemcitabine alone. Generally, this hypothesis was validated, and the combination schedules showed superior efficacy compared to the other arm of the study.

Because the treatment of solid tumour in clinical settings must be based on strong rationale from preclinical studies, this *in vivo* study was conducted due to the promising results of our *in vitro* studies highlighted in chapters 3 and 4. We demonstrated *in vitro*, that the concurrent administration of gemcitabine and sunitinib (schedule 3) was the most effective combination schedule and the exposure to XBR before treatment with gemcitabine plus sunitinib (schedule 2) was the most effective three-treatment combination schedule in both pancreatic cancer cell lines. Therefore, the present *in vivo* work was

designed to mimic these conditions. Thus, for the *in vivo* studies, gemcitabine and sunitinib were administered concurrently, and radiation was applied as a single 5 Gy dose at day 0, before commencing the treatment with the gemcitabine plus sunitinib combination.

Due to time constraints and the poor uptake of MIA PaCa-2 cells as cell xenografts in nude mice, only one pancreatic cancer cell line was able to be analysed *in vivo*.

We hypothesised that combination therapy of gemcitabine plus sunitinib with or without XBR would inhibit pancreatic cancer tumour xenografts growth in nude mice bearing PANC-1 pancreatic cancer cell xenografts model compared to untreated control and cohorts treated with monotherapy.

5.2 Aims

The primary aim of this chapter was to evaluate the effect of novel combination therapy of gemcitabine and sunitinib with or without exposure to XBR on pancreatic cancer xenografts in nude mice.

5.3 Results

Subcutaneous PANC-1 xenografts in six-week-old athymic nude mice were established as described in section 2.13.2 and then treated as described in section 2.13.3. Briefly, 18 days after injection of PANC-1 cells, mice bearing xenograft tumours with a volume of at least 65 mm^3 were randomised into six

treatment groups. The first group consisted of 9 mice and was injected intraperitoneally once a week with 100 µl of PBS as an untreated control. The second group consisted of 8 mice and was treated with 180 mg/kg of gemcitabine alone intraperitoneally once a week. The third group consisted of 8 mice and was treated with 40 mg/kg of sunitinib alone daily via oral gavage. The fourth group consisted of 8 mice and was exposed to 5 Gy single dose XBR alone which was given at day 0 of the experiment. The fifth group (referred as two-drug combination group) consisted of 8 mice and was treated with a combination of 180 mg/kg of gemcitabine (injected intraperitoneally once weekly) and 40 mg/kg of sunitinib (administered orally every day). The last group (referred as three-treatment combination group) consisted of 9 mice and was exposed to 5 Gy single dose XBR at Day 0 then treated with the same dosage regimen of gemcitabine and sunitinib. Doses of gemcitabine and sunitinib were based on the median weekly doses (mg/kg) used in previous *in vivo* studies and shown in Figure 2.3. Appendix A shows a table summarises using gemcitabine in 16 published *in vivo* studies. Radiation dose varies massively between studies in the published literature. Therefore, our laboratory team decided to use 5 Gy as reported in a previous similar study (Tuli *et al.*, 2012).

In order to evaluate the effect of different treatment approaches on pancreatic cancer xenografts in nude mice, we analysed our *in vivo* data in several ways. Firstly, the relative tumour growth was calculated by dividing the tumour volume at the last day by the initial tumour volume for each experimental group i.e. Volume at day x over the volume at day 0 (V_1/V_0). One-way ANOVA then

was used to compare the mean difference of relative tumour volume between treatment groups. This method was used despite its drawbacks, such as ignoring the tumour volume of the control group when measuring the effect of different treatment, because it is one of the most popular methods in similar studies. Secondly, in contrast to the relative tumour growth analysis, the tumour growth inhibition at day 20 (%TGI_{20}), the mean time taken for a two-fold increase in tumour volume (T_2), and the growth delay always consider comparing the tumour volume of the treatment group to the volume from the untreated control group. These analysis methods were described in sections 2.13.4. However, because of several drawbacks of these methods, which will be discussed in detail later in this result section, the analysis of the area under the tumour-time curve was included in this study to draw a clearer conclusion in terms of treatment efficacy on PANC-1 xenografts in nude mice (McCluskey *et al.*, 2012; Hather *et al.*, 2014).

Figure 5.1 shows the effect of gemcitabine, sunitinib, or XBR either alone or in combination on the growth of PANC-1 tumour xenografts (A), and the multiple comparisons (Tukey's test) of the differences in the average relative tumour growths between the treatment groups (B).

A

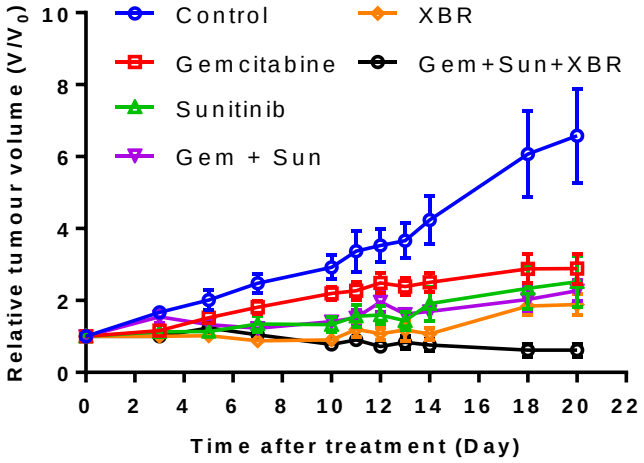

B

Tukey's multiple comparisons test	Diff. in V/V_0 (Mean ± SEM)	Adjusted P-Value
Control vs. Gemcitabine	3.692 ± 1.49	0.0051
Control vs. Sunitinib	4.053 ± 1.55	0.0017
Control vs. Gem + Sun	4.302 ± 1.42	0.0008
Control vs. XBR	4.690 ± 1.42	0.0002
Control vs. Gem + Sun + XBR	5.959 ± 1.32	<0.0001
Gemcitabine vs. Sunitinib	0.361 ± 0.82	0.9991
Gemcitabine vs. Gem + Sun	0.610 ± 0.51	0.9894
Gemcitabine vs. XBR	0.998 ± 0.51	0.9135
Gemcitabine vs. Gem + Sun + XBR	2.267 ± 0.44	0.1961
Sunitinib vs. Gem + Sun	0.249 ± 0.77	0.9999
Sunitinib vs. XBR	0.637 ± 0.76	0.9871
Sunitinib vs. Gem + Sun + XBR	1.907 ± 0.69	0.3714
Gem + Sun vs. XBR	0.388 ± 0.41	0.9987
Gem + Sun vs. Gem + Sun + XBR	1.657 ± 0.34	0.5272
XBR vs. Gem + Sun + XBR	1.269 ± 0.33	0.7745

Figure 5.1 Effect of gemcitabine, sunitinib, or XBR alone or in combination on the growth of PANC-1 xenografts (A). Each treatment group consisted of 8 animals except for the untreated control and triple-therapy groups which were consisted of 9 mice. Mice were treated as described in section 2.13.3. Data are presented in mean ± SD. **(B)** Summary table of differences in V_1/V_0 between treatment groups on the last day of the experiment (day 20) and their corresponding p-values resulted from the Tukey posthoc test which followed a parametric one-way ANOVA test.

The relative tumour growth over the experiment period was calculated by dividing the final average tumour volumes (on Day 20) in each experimental group by their initial volumes on Day 0 (V_1/V_0). Relative volume < 1 indicates tumour shrinkage, and relative volume > 1 indicates tumour growth. The smaller relative tumour volume the more effective the treatment and vice versa.

On the last day of the experiment (Day 20), tumours had achieved a statistically significant reduction in tumour volume only in the three-treatment combination group (i.e group 6) to 0.62 ± 0.55 folds compared to their initial volumes at Day 0. The relative tumour volume in the remaining groups had grown on Day 20 with 6.58 ± 3.93 folds in the control group, 2.88 ± 1.18 folds in gemcitabine alone group, 2.52 ± 2.01 folds in sunitinib alone group, 2.27 ± 0.84 folds in gemcitabine plus sunitinib two-drug combination group, and 1.89 ± 0.80 folds in XBR group, compared to their initial volumes at Day 0 (Table 5.1).

Mean tumour volume differences between the treatment groups and Tukey's multiple comparison tests, following one-way ANOVA, are shown in table B from Figure 5.1. It can be observed that the mean tumour volume of mice in the untreated control group (i.e. group 1; PBS only) was statistically significantly higher than those in all five treatment groups ($p < 0.01$). This indicates that the treatment of PANC-1 xenograft tumours with gemcitabine, sunitinib, or XBR either as single or in combination treatment imposed more favourable cytotoxic effect than untreated controls.

However, there was no statistically significant difference in relative tumour volume (V_1/V_0) between the remaining five treatment groups ($p > 0.05$). Therefore, combination treatment with gemcitabine and sunitinib either without XBR (two-drug combination) or with XBR (three-treatment combination) had no additional benefit on PANC-1 xenograft tumours compared to single treatment with gemcitabine, sunitinib, or XBR alone.

Table 5.1 Relative tumour growth amongst the treatment groups on the last day of the experiment (day 20). Gem = Gemcitabine; Sun = Sunitinib; SD = Standard deviation; Triple therapy = Gemcitabine plus sunitinib plus XBR.

Relative tumour growth at Day 20	Control	Gem	Sun	Gem+Sun	XBR	Triple therapy
Mean	6.58	2.88	2.52	2.27	1.89	0.62
SD	3.93	1.18	2.01	0.84	0.80	0.55

Tumour growth inhibition at day 20 (%TGI_{20}), the mean time taken for a two-fold increase in tumour volume (T_2), and the growth delay (described in section 2.13.4) were calculated for each mouse (Table 5.2). In contrast to the relative tumour growth, these analysis approaches (TGI, T_2, and growth delay) compared the parameter of interest from the treatment group to the untreated control group.

It can be observed that the highest growth inhibition, compared to the untreated control group, resulted from triple therapy (72.95%), followed by sunitinib and single radiotherapy (61.6% and 52.4%, respectively). Of note, combination therapy of gemcitabine plus sunitinib caused lower tumour growth inhibition (23.88%) than either monotherapy.

From another angle of efficacy analysis, the time required for tumours to double in volume (T_2) and the growth delay in the treatment groups, compared to the untreated controls, were calculated (Table 5.2). Tumour volumes reached 200% of the initial volume fastest in the control group (6.11 ± 2.8 days), followed by the two single chemotherapies, and slowest by single radiotherapy (14.5 ± 2.6 days).

The growth delay was calculated as T – C; where T and C are times in days for mean tumour volume in the treated (T) and control (C) groups to reach 200% of the initial tumour volume and shown in (Table 5.2).

Table 5.2 Time to two-fold increase in tumour volumes, tumour growth inhibition (%TGI), and the growth delay in PANC-1 xenografts after 20 days of treatment.

Treatment group	TGI_{20} (%)	Time to 2-fold tumour (T_2)	Growth delay (days)
Control	00.00%	6.11 ± 2.80	0
Gemcitabine	38.11%	8.13 ± 2.30	2.02 ± 1.6
Sunitinib	61.55%	12.0 ± 4.34	5.89 ± 3.32
Gem + Sun	23.88%	13.5 ± 5.68	7.39 ± 4.94
XBR	52.36%	14.5 ± 2.56	8.39 ± 1.13
Gem + Sun + XBR	72.95%	13.7 ± 0.71	7.59 ± 2.71

While these measures (TGI, T_2, and the growth delay) are easy to implement and interpret, they have their limitations. In particular, the measures are inefficient, as they do not make use of any data collected before the final day of treatment. Another problem is that the measure is biased because animals are usually sacrificed when the tumour volume exceeds 16 mm in diameter. If this occurs before the end of the study, these animals will be excluded from the analysis. However, in the current study, the animals that were euthanized because of rapid tumour growth before the termination of the experiment, the tumour volume was extrapolated from the time of euthanasia, in order to overcome this source of bias. The second source of bias occurs when tumours in the control group (which are usually larger than those in the treatment group) experience a differential slowing of their growth rate relative to tumours in treatment group because of nutrient- and oxygen-limiting conditions (Hather *et al.*, 2014). Therefore, the area under the time-volume curve was employed in this study as a robust measure of treatment effectiveness amongst the treatment groups.

Figure 5.2 shows the calculated mean area under the time-volume curve of each mouse in each experimental group. The lower AUC the more effective treatment regimen. It can be observed that there was no significant difference between AUC in the gemcitabine group compared to the untreated control group. The remaining treatment groups showed significantly lower AUC compared to the control group ($p < 0.05$), with a higher difference seen in the single radiotherapy and the triple therapy group ($p < 0.001$). However, there was no significant difference in the AUC between the five treatment groups (p

> 0.05). This result partially supports our hypothesis that the combination therapy of gemcitabine plus sunitinib with or without XBR would inhibit pancreatic cancer tumour xenografts growth in nude mice pancreatic cancer model compared to untreated control and cohorts treated with monotherapy.

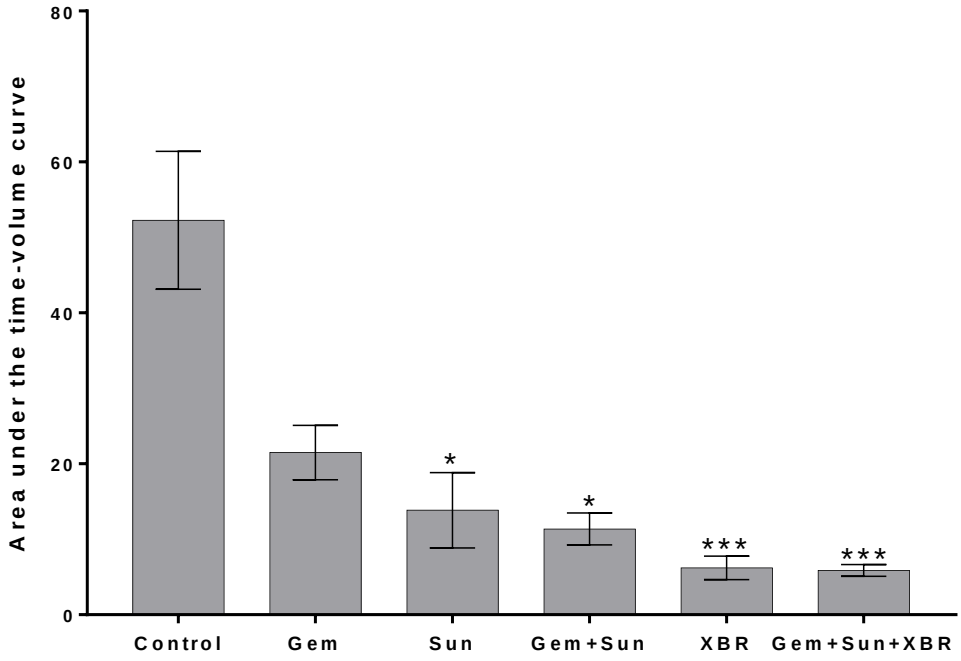

Figure 5.2 The average of the area under the tumour volume curves of each mouse over the experimental time amongst the six treatment groups. Statistical analysis was carried out using a nonparametric one-way ANOVA Kruskal-Wallis test followed by Dunn's multiple comparisons tests to compare the differences in the mean rank of the AUC between the treatment groups. Data are means and SDs of eight or nine independent determinations. *P<0.5 and ***P<0.001 compared to the PBS-treated control group.

5.4 Discussion

The combination of gemcitabine and sunitinib has been studied both *in vitro* and *in vivo* in pancreatic ductal adenocarcinoma xenograft models (Awasthi, Schwarz and Schwarz, 2011). We found from *in vitro* studies in the previous two chapters (chapters 3 and 4), that pancreatic ductal adenocarcinoma cell lines (PANC-1 and MIA PACA-2) showed significantly greater growth inhibition following administration of the combination of gemcitabine and tyrosine kinase inhibitor (sunitinib) as compared to either agent alone.

In the present *in vivo* study, after 18 days of PANC-1 cell injection, nude mice bearing tumours of volumes of at least 65 mm^3 were randomised into six treatment groups as described in section 2.13.3 and the first paragraph of the results part (section 5.3). Due to time constraints and the poor uptake of MIA PaCa-2 cells as cell xenografts in nude mice, only one pancreatic cancer cell line was able to be analysed *in vivo*.

On the last day of the experiment (Day 20), tumours had achieved a statistically significant reduction in tumour volume only in the three-treatment combination group (i.e group 6) to 0.62 ± 0.55 folds compared to their initial volumes at Day 0. Tumours in the remaining groups had grown on Day 20 with 6.58 ± 3.93 folds in the control group, 2.88 ± 1.18 folds in gemcitabine alone group, 2.52 ± 2.01 folds in sunitinib alone group, 2.27 ± 0.84 folds in gemcitabine plus sunitinib two-drug combination group, and 1.89 ± 0.80 folds in XBR group, compared to their initial volumes at Day 0 (Table 5.1). The

relative mean tumour volume of mice in the control group at day 20 was significantly higher than those in the treatment groups ($p < 0.01$) and Tukey's multiple comparison tests revealed that, apart from controls, there was no significant difference in the relative tumour volume between the other five treatment groups.

Gemcitabine, when administered alone, decreased the relative tumour growth significantly to 2.88 fold (TGI_{20} = 38.11%) compared to 6.58 fold in PBS treated controls (p = 0.0051), and delayed the time taken for a two-fold increase in tumour volume (T_2) to 8.13 days compared to 6.11 days in controls. In addition to gemcitabine's cytotoxic action against DNA synthesis in cancer cells, several in vivo studies have demonstrated gemcitabine, when delivered at standard doses, also has an effect on angiogenesis with this antiangiogenic activity acting against nascent tumour-supporting microvasculature which leads to an overall antimetastatic effect (Lee *et al.*, 2000; Amoh *et al.*, 2006). However, there was no significant difference between the area under the tumour curve (AUC) in the gemcitabine group compared to PBS treated controls in our *in vivo* study. Several previous studies found that gemcitabine when administered at doses between 50 and 100 mg/kg twice a week did not affect the tumour growth in pancreatic cancer xenograft studies, whereas the maximum-tolerated dose (MTDG; 150 mg/kg twice weekly) was effective (Yokoi *et al.*, 2005; Olive *et al.*, 2009; Olson *et al.*, 2011). Contradictory to the findings of Laquente *et al.* (2008), Tran Cao *et al.* (2010) found that metronomic daily dosing of gemcitabine at 1 mg/kg/d had inferior activity against the growth of primary pancreatic cancer xenografts than MTDG (Tran

Cao *et al.*, 2010). However, based on the median of gemcitabine doses in similar previous *in vivo* studies, mice in the present experiment was treated with 180 mg/kg once a week. The modest anti-tumour effect of gemcitabine may involve the demonstration that gemcitabine fails to accumulate in pancreatic cancer tumour due to the abundant desmoplastic stromal compartment in mice similar to human tumours (Chu *et al.*, 2007). For our study, this modest efficacy of gemcitabine could be related also to the lower dose regimen used in the experiment compared to the maximum-tolerated dose of gemcitabine reported in the literature.

Angiogenesis plays a critical role in the progression of primary and metastatic pancreatic cancer (Awasthi, Schwarz and Schwarz, 2011). Several antiangiogenic agents have been studied in experimental pancreatic cancer models, including anti-vascular endothelial growth factor (VEGF) agents like bevacizumab, resulted in limited survival benefit both when used alone and in combination with gemcitabine (Ko *et al.*, 2008). Sunitinib is a multi-target RTK inhibitor with antiangiogenic and anti-tumour activity (Abrams *et al.*, 2003; Mendel *et al.*, 2003; O'Farrell *et al.*, 2003).

We found from the present *in vivo* study that the relative tumour volume in sunitinib monotherapy group was significantly lower than those in the control group (difference in V_1/V_0 = 4.05 ± 1.55; p = 0.0017) and sunitinib alone inhibited the tumour growth by 61.6% compared to controls. In contrast to our findings from *in vitro* studies, sunitinib was more effective than gemcitabine in this *in vivo* study in terms of tumour growth inhibition, T_2, and AUC. For time

constraint, we did not conducted any post-mortem tumour histology in order to invistigate the effect of sunitinib on the angiogenesis or microvessel density in pancreatic cancer xenografts. However, we suggest that this profound efficacy of sunitinib in our in vivo study can be attributed to the major mechanism of anti-tumour activity of sunitinib, which involves a reduction of microvessel density and inhibition of angiogenesis process (Chow and Eckhardt, 2007), and these components are not applicable in the *in vitro* model (Casneuf *et al.*, 2009).

However, in other reported studies, sunitinib as a monotherapy or in combination with gemcitabine had no impact on tumour growth in pancreatic cancer in genetically engineered mouse models (GEMM) (Olson *et al.*, 2011) and in pancreatic orthotopic human tumours models (MIA PaCa-2 cells) (Tran Cao *et al.*, 2010). However, sunitinib reduced the frequency of metastasis, delayed the onset of ascites, and was associated with a significant, even though a modest effect on survival (Tran Cao *et al.*, 2010). Even though tyrosine kinase inhibitors, including sunitinib, found to inhibit the key component of the pancreatic cancer stroma, such as the fibroblast and endothelial cells (Awasthi *et al.*, 2014), it has been reported that the cytotoxic efficacy of sunitinib may be inhibited by the pancreatic niche in pancreatic ductal adenocarcinoma tumours (Martinez-Bosch *et al.*, 2016). To enhance the anti-tumour efficacy of sunitinib in pancreatic ductal adenocarcinoma, previous studies suggested co-administration of either anti-fibrotic drugs to penetrate the fibrous capsule around the tumour (Martinez-Bosch *et al.*, 2016),

or nab-paclitaxel to deplete the stroma and improve the permeability of sunitinib and gemcitabine into tumour cells (Hoffman and Bouvet, 2015).

In contrast to our *in vitro* findings, combination therapy of gemcitabine plus sunitinib caused lower tumour growth inhibition (23.88%) than either monotherapy in the animal model. These results also contradicted the findings of a phase I trial of sunitinib and gemcitabine in patients with advanced solid tumours, including pancreatic ductal adenocarcinoma (n = 10 of 33), in which this combination was well-tolerated and had significant clinical activity (Brell *et al.*, 2012). Similar to this result, a previous study, which investigated whether the combination of gemcitabine and sunitinib would lead to an enhanced response compared to single-agent gemcitabine in the pancreatic cancer model, found that the combination of gemcitabine plus sunitinib had no added benefit compared to gemcitabine alone (Olson *et al.*, 2011). These studies differ from our study design, in which both chemotherapy and TKI were administered concurrently, Olson and his colleagues (Olson *et al.*, 2011) initialised sunitinib treatment a week before gemcitabine administration to allow for potential vessel normalisation and drug delivery, as has been suggested in the application of antiangiogenic therapy (Jain, 2001). This discrepancy in treatment approaches between our study and Olson's, however, showed no major impact on anti-tumour efficacy in both experiments. Moreover, hypoxia, which is reported to be increased as a consequence of reduced vascularization following sunitinib treatment (Kleibeuker, ten Hooven, Castricum, *et al.*, 2015), plays an important role in pancreatic cancer cells resistance to gemcitabine through the activation of PI3K/Akt/NF-kB signalling

pathways that regulate cell proliferation, angiogenesis, and apoptosis (Yokoi and Fidler, 2004). Furthermore, the metronomic dose of gemcitabine (1 mg/kg daily, METG) in combination with oral gavage sunitinib (40 mg/kg daily) had a significant inhibitory effect on primary tumour growth compared to control ($p = 0.03$) but not to gemcitabine alone (Tran Cao *et al.*, 2010). METG or sunitinib alone had no inhibitory effect on primary tumour growth compared to control (Tran Cao *et al.*, 2010). In addition, there was no difference in anti-tumour activity between gemcitabine administered at maximum-tolerated dose alone and in combination with daily oral sunitinib (Tran Cao *et al.*, 2010). Furthermore, Awasthi *et al.* (2011) observed a modest efficacy of combination therapy of gemcitabine and sunitinib in a murine pancreatic cancer model, but this combination failed to reduce the proliferation beyond levels achieved by sunitinib alone (Awasthi, Schwarz and Schwarz, 2011). Moreover, in a recent meta-analysis of 3,401 elderly pancreatic cancer patients from six randomized controlled trials, the author found that combined conventional chemotherapy significantly improves OS in comparison with gemcitabine alone (HR 0.73, $p = 0.016$), while gemcitabine plus targeted agents do not improve OS (HR 1.02, $p = 0.83$) when compared with gemcitabine alone (Jin, Teng and Li, 2018). Finally, all these discussed studies data mirror results emerging from human trials; hence in a phase II trial, the combination of gemcitabine plus sunitinib was not superior in locally advanced or metastatic pancreatic ductal adenocarcinoma compared to gemcitabine alone in regard to efficacy but was associated with more toxicity (Bergmann *et al.*, 2015).

However, in other reported studies, the metronomic dose of gemcitabine in combination with sunitinib significantly prolonged median overall survival (44 days) compared with control or either regimen alone ($P < 0.05$) in orthotopic pancreatic cancer tumour grafts (Tran Cao *et al.*, 2010). It has been reported that gemcitabine efficacy was enhanced when tumour blood perfusion increased when administered in combination with an inhibitor of the hedgehog signalling pathway (Olive *et al.*, 2009). Therefore, it was suggested that the reduced blood flow, in concomitant with a reduction in vessel density, following an angiogenesis inhibitor, sunitinib, in combination with gemcitabine may diminish the beneficial effect of gemcitabine (Olson *et al.*, 2011). On the other hand, a previous *in vivo* study demonstrated that adding sunitinib to gemcitabine or radiotherapy (XBR) had a superior proapoptotic effect and was found to intensify the anti-tumour effect of either therapy alone in a murine model of pancreatic cancer PANC-2 xenografts (Casneuf *et al.*, 2009). The authors attributed efficacy of sunitinib in the animal model to the capability of this agent to modulate circulating VEGF pathway biomarkers like VEGF, placenta growth factor (PlGF) and EGF (Casneuf *et al.*, 2009). They also suggested that it is possible that apoptosis and cytotoxic damage to tumour cells caused by conventional chemotherapeutics like gemcitabine, might have been exacerbated through inhibition of tumour-supporting stroma and blood vessels by sunitinib (Casneuf *et al.*, 2009).

Despite the confirmed antiangiogenic activity of sunitinib and gemcitabine, the anti-tumour activity of these agents either alone or in combination in pancreatic cancer still disappointing. Olson *et al.* (2011) suggested that these findings

revealed the striking properties of pancreatic tumours (Olson *et al.*, 2011). The authors suggested that the reduced blood perfusion appears to be a component of disease progression in at least a fraction of pancreatic cancer tumours (Olson *et al.*, 2011). Another explanation involves the fact that antiangiogenic treatment induces destruction of immature and inefficient vessels and promotes maturation of the remaining vessels (Jain, 2003). Further to this, Olson *et al.* (2011) suggested that the modest efficacy of anti-angiogenic agents and the ability of pancreatic cancer tumours to continue progressing following a further therapeutic reduction in vascular density and functionality may highlight their apparently limited dependence on the hallmark capability of angiogenesis (Olson *et al.*, 2011).

For the first time, to the best of our knowledge, we evaluated the anti-tumour efficacy of a triple combination of gemcitabine, sunitinib, and XBR in pancreatic cancer animal model. We found no previous study investigated this combination regimen in pancreatic ductal adenocarcinoma animal model before. Casneuf *et al.* (2009) treated murine mice bearing a PANC02 pancreatic tumour xenograft with gemcitabine, sunitinib, radiotherapy, or a combination of radiation or gemcitabine with sunitinib (Casneuf *et al.*, 2009). In another study, orthotopic fluorescent human pancreatic cancer xenografts were treated with gemcitabine on a low-dose metronomic schedule (1 mg/kg daily) or a MTDG (150 mg/kg twice weekly) schedule with or without sunitinib (Tran Cao *et al.*, 2010). In the third study, SCID-NOD (severe combined immune deficiency, non-obese diabetic) mice aged 6–8 weeks were injected with pancreatic cancer AsPC-1 cells then treated intraperitoneally with PBS

(control), gemcitabine (100 mg/kg, twice weekly) or sunitinib (40 mg/kg for the first week, then 20 mg/kg for the second week five times weekly), either alone or in combination for 2 weeks (Awasthi, Schwarz and Schwarz, 2011). Besides, 9.5-week-old pancreatic ductal adenocarcinoma genetically engineered mouse models (GEMMs) were given either 40 mg/kg sunitinib or vehicle via oral gavage for 4 weeks. Gemcitabine was administered to 10.5-week-old mice at 150 or 75 mg/kg twice weekly for 3 weeks. For sunitinib plus gemcitabine combination therapy, mice received sunitinib beginning at 9.5 weeks and gemcitabine beginning at 10.5 weeks (Olson *et al.*, 2011). Finally, several other *in vivo* studies investigated the efficacy of gemcitabine in combination with radiation (Mason *et al.*, 1999; Pauwels *et al.*, 2005; Shen *et al.*, 2015), or sunitinib with radiation (Cuneo *et al.*, 2008) in pancreatic ductal adenocarcinoma models.

The triple combination therapy of gemcitabine plus sunitinib plus XBR in the current *in vivo* study was the most effective treatment approach hence it shrank the relative tumour volume to 0.62 fold of its initial volume at day 0 (TGI_{20} = 72.95%) compared to 6.58 folds in controls ($p < 0.0001$), delayed the time taken for a two-fold increase in tumour volume (T_2) to 13.7 days compared to 6.11 days in control mice, and decreased the AUC significantly compared to control group ($p < 0.001$).

It has been reported in the literature that tumour growth delay enhanced only when sunitinib treatment was initiated after the completion of fractionated radiation therapy (Brooks *et al.*, 2012). In our study, this was also the case; we

exposed mice in the triple therapy group to 5 Gy XBR on the first day of the experiment before commencing gemcitabine or sunitinib treatment. This suggests that sunitinib may be acting on the irradiated tumour stroma and suppressing its ability to sustain regrowth of the irradiated tumour rather than by radiosensitizing during radiation (Brooks *et al.*, 2012).

However, there was no significant difference in the AUC between the triple therapy and the remaining treatment groups. Of note, all mice in this treatment group were euthanised two days before the end of the experiment (day 18) because of 20% weight loss relative to the initial body weight. We could not determine the cause of the sudden weight loss in those mice treated with triple therapy. This weight loss could be drug-related toxicity. All three agents, gemcitabine (Braakhuis *et al.*, 1995; Fields *et al.*, 2000; Chen *et al.*, 2006; Tran Cao *et al.*, 2010), sunitinib (Hu *et al.*, 2016; Maraz *et al.*, 2018), and radiation (Lees, 1999; Munshi *et al.*, 2003; Hill *et al.*, 2011), were reported to cause weight loss in animal model and human. Casneuf *et al.* (2009) reported that treatment used alone or in combination did not cause drug-related deaths or weight loss of >15% (Casneuf *et al.*, 2009). The doses of sunitinib used in Casneuf's study was identical to ours (40 mg/kg) and the total dose of gemcitabine was 180 mg/kg in both studies, but it was divided into three smaller doses (60 mg/kg) in the first study. But the radiation dose used in Casneuf's study was 5 times higher than ours. This could weaken the possibility that this toxicity was mainly attributed to XBR dose used in our *in vivo* study (5 Gy; single dose). However, Casneuf's study did not investigate these agents as triple therapy. So, it could be there was a synergistic weight

loss side-effect in mice following the triple therapy. Finally, there is a logical possibility that the observed weight loss in this group may be correlated with the relative tumour volume which shrank to 0.62 folds. Other combination treatment in our study (Table 5.1) and Casneuf's study (Casneuf *et al.*, 2009) could not shrink tumour volumes in treated mice.

In conclusion, based on the *in vivo* results, we believe that the combination of gemcitabine with sunitinib and radiation offers a promising approach for treating pancreatic ductal adenocarcinoma in the clinic. However, lowering dosing of all three agents is warranted to decrease the unfavourable side effects while maintaining anti-tumour activity.

CHAPTER 6: General discussion, conclusion, and future work

Pancreatic cancer represents the seventh leading cause of cancer mortality globally (Bray *et al.*, 2018), and despite the advances in cancer therapy over the last two decades, its prognosis is still poor and survival rate among patients with pancreatic cancer for five years is less than 5% (Keane *et al.*, 2014). This can be attributed to late-stage diagnosis, early metastasis, high local recurrence risk and resistance to conventional chemotherapy (Awasthi, Schwarz and Schwarz, 2011).

Gemcitabine is considered the gold standard and the historical first-line treatment for patients with pancreatic ductal adenocarcinomas. However, it mediates only a marginal clinical benefit both when administered alone and in combination with other conventional chemotherapy agents or targeted therapy agents.

Therefore, this project investigated, for the first time, novel triple combinations and treatment schedule strategies of gemcitabine plus repurposed TKI angiogenesis inhibitor (sunitinib or pazopanib) plus external beam radiation in pancreatic cancer preclinical *in vitro* and *in vivo*. We hypothesised that these novel combination strategies would improve anti-tumour efficacy in pancreatic cancer models and in the clinic compared to single or double therapies.

This hypothesis was partially validated from the *in vitro* and the *in vivo* studies. When we investigated the anti-tumour activity of pazopanib for the first time in pancreatic ductal adenocarcinoma, we found that pazopanib offered no additional benefit when combined with gemcitabine. Thus, this part of the hypothesis was not validated. However, our novel combination strategies with lower doses of gemcitabine, sunitinib, and XBR resulted in greater anticancer efficacy than either treatment alone. The concurrent administration of gemcitabine and sunitinib (two-drug schedule 3 combination) and when administered after completing the radiotherapy (three-treatment schedule 2 combination) showed a synergistic effect and was found to be the most effective combination strategy in the treatment of pancreatic cancer. Furthermore, our three-treatment combination strategy in the *in vivo* pancreatic cancer xenograft model was the only combination approach which was able to shrink the tumour in nude mice while other treatment strategies only delayed the tumour growth.

However, the prompt significant weight loss side effect observed in the experimental mice invokes doubts about the safety of this combination strategy. Therefore, the question of whether this novel combination approach will beneficially improve pancreatic cancer therapy in the clinical settings remains open.

Nevertheless, the major results and conclusions of this project were based on a single cell line study in a xenograft setting, which knowing that the clinical tumours are expected to represent a wide spectrum of genetic heterogeneity

that may limit the presence of the susceptibility parameters necessary to mediate this combination benefit (Awasthi, Schwarz and Schwarz, 2011). Moreover, pancreatic tumour microenvironment may affect the results of the *in vivo* experiment. For instance, it has been reported that the probability of metastasis for orthotopically implanted tumours is higher than ectopic (subcutaneous; as per our *in vivo* work) ones (Rezaee and Abdollahi, 2017). Therefore, it would be suggested to use genetically engineered mouse models (GEMMs) to investigate our well-established combination strategies in pancreatic cancer therapy. Although tumours in GEMMs may not reflect the full spectrum of heterogeneity and diversity seen in human tumours, they are likely to be well suited to evaluate drugs that target the tumour microenvironment, because critical signalling axes between cancer cells and stroma are not skewed by interspecies differences (Olson *et al.*, 2011).

Although targeted therapy has failed to improve outcomes in pancreatic cancer patients, or because of this failure, considerable efforts are being made to identify new treatments that can make significant differences for pancreatic cancer patients. Clinical research continues to focus on targeting specific mutations seen in patients with pancreatic cancer through oral monoclonal antibodies (for example, ipilimumab, atezolizumab, pembrolizumab, tremelimumab, nivolumab, durvalumab, and APX005M), small molecular inhibitors, immunotherapy, and alternative formulations of conventional cytotoxic agents (Adel, 2019). Furthermore, Trifluridine/tipiracil (TAS-102) is a combination of a fluorinated thymidine analogue, trifluridine, and a thymidine phosphorylase inhibitor, tipiracil hydrochloride, at a molar ratio of 2:1 (Adel, 2019).

TAS-102 is approved in the US for patients with refractory metastatic colon cancer and is currently being studied in combination with liposomal irinotecan in metastatic pancreatic cancer (Adel, 2019).

Altogether, even in well-designed animal experiments, the differences between humans and animal components may weaken the translatability of data (Rezaee and Abdollahi, 2017). Therefore, our findings in this project would be considered to offer a promising approach for treating pancreatic ductal adenocarcinoma in the clinic.

APPENDICES

Appendix A Using gemcitabine in cancer animal models.

Cell-Line	Mice Type	Gem Dose	Frequency	Gemcitabine	Duration	Route	Study
PANC-1	Female NCr nude mice (6-7 weeks old)	0.5µg/g /day	Daily	GEM in DMSO	26 Days	I.P	(Zheng *et al.*, 2012)
PANC-1	Male BALB/c-nu/nu nude mice aged 4-6 weeks and weighing 18-22 g	25 or 50 mg/kg	Single-dose?	Gem in Saline	Observe after 30 days	I.V (tail)	(Shen *et al.*, 2015)
PANC-1	Athymic nude male mice, 6 to 8 weeks old	200 µL, 120 mg/kg	Every 5 days	HCL in Saline	20 Days	I.V (femoral)	(Li *et al.*, 2013)
PANC-1	Six-week-old, male, athymic, BaLB/c nu/nu mice	125 mg/kg	Every 3 days	Gem in Saline	9 times	I.P	(Guo *et al.*, 2012)
PANC-1, BxPC-3 and CFPAC-1	BALB/c nude mice	25 mg/kg/d; dissolved in PBS	Daily	Gem in PBS	16 days	I.V (caudal)	(Zhi *et al.*, 2015)
MIA PaCa-2	CD nu/nu male mice [Abstract only]	120mg/kg	Every 3 days	-	4 times	??	(Azzariti *et al.*, 2010)
MIA PaCa-2	Male Nog-SCID mice (7 weeks old)	50 mg/kg	Twice/Wk	Gem in Saline	4 Weeks	I.P	(Hermine *et al.*, 2010)
Panc-2	4-to-6 week-old male HsdOla/MF1 mice (16-20 gr body weight)	60 mg/kg	3 times/wk	-	Days 1,4,7	I.P	(Casneuf *et al.*, 2009)

Cell-Line	Mice Type	Gem Dose	Frequency	Gemcitabine	Duration	Route	Study
BxPC- 3-luc	5-6 weeks old female Nu/Nu mice	100 mg/kg	Weekly	Gem in Saline		I.P	(D'Aronzo *et al.*, 2015)
BxPC-3	Male nude BALB/c mice, 6–8 weeks old,	100 mg/ kg	Twice/Wk	Gem in PBS	21 days	I.P	(Wang *et al.*, 2010)
Metastatic L3.6pl	Male athymic nude mice (NCI-nu) (8–10 weeks old)	125 mg/kg	Twice/Wk	Gem in Saline	35 days	I.P	(Solorzano *et al.*, 2003)
COLO 357 and L3.6pl	Female nude mice (ICR-SCID) (4-6 weeks old)	80 mg/kg	Every other day		10 days	I.V	(Banerjee *et al.*, 2005)
HPAC and Capan-1	Male 5-week-old BALB-nu/ nu mice	20 mg/kg	Weekly		Day 1, 8, 15	I.V	(Furugaki *et al.*, 2010)
CFPAC-1	Female athymic BALB/c nu/nu mice (age, 4-5 weeks; weight, 15-16 g)	50 mg/kg	Twice/week		4 Weeks	I.P	(Shi *et al.*, 2016)
DAN-G	6-week-old, female, athymic, BALB/c nu/nu mice	125 mg/kg	Twice/Wk		30 days	I.P	(Ziske *et al.*, 2004)
SW1990 and SW1990/GR	4-week-old BALB/c female nude mice	150 mg/kg	Twice/Wk		28 Days	I.P	(Cai *et al.*, 2013)
USCS	Athymic nu/nu nude mice, 4–6 weeks old	100 mg/kg	Weekly		Twice	I.P	(Igarashi *et al.*, 2017)

REFERENCES

Abou-Alfa, G. K. *et al.* (2006) 'Randomized phase III study of exatecan and gemcitabine compared with gemcitabine alone in untreated advanced pancreatic cancer', *Journal of Clinical Oncology*. American Society of Clinical Oncology, 24(27), pp. 4441–4447.

Abrams, T. J. *et al.* (2003) 'Preclinical evaluation of the tyrosine kinase inhibitor SU11248 as a single agent and in combination with "standard of care" therapeutic agents for the treatment of breast cancer', *Molecular Cancer Therapeutics*, 2(10), pp. 1011 LP – 1021. Available at: http://mct.aacrjournals.org/content/2/10/1011.abstract.

Abratt, R. P. *et al.* (1994) 'Efficacy and safety profile of gemcitabine in non-small-cell lung cancer: a phase II study.', *Journal of Clinical Oncology*, 12(8), pp. 1535–1540.

Achiwa, H. *et al.* (2004) 'Determinants of sensitivity and resistance to gemcitabine: The roles of human equilibrative nucleoside transporter 1 and deoxycytidine kinase in non-small cell lung cancer', *Cancer science*. Wiley Online Library, 95(9), pp. 753–757.

Adel, N. (2019) 'Current treatment landscape and emerging therapies for pancreatic cancer.', *The American Journal of Managed Care*, 25(1 Suppl), pp. S3–S10.

Affram, K. *et al.* (2015) 'In vitro and in vivo antitumor activity of gemcitabine loaded thermosensitive liposomal nanoparticles and mild hyperthermia in pancreatic cancer', *International journal of advanced research*, 3(10), pp. 859–874. doi: 10.14440/jbm.2015.54.A.

Affram, K., Udofot, O. and Agyare, E. (2015) 'Cytotoxicity of gemcitabine-loaded thermosensitive liposomes in pancreatic cancer cell lines.', *Integrative cancer science and therapeutics*, 2(2), pp. 133–142. doi: 10.15761/ICST.1000128.

Ahn, H. K. *et al.* (2013) 'Phase II study of pazopanib monotherapy in metastatic gastroenteropancreatic neuroendocrine tumours', *British journal of cancer*. Nature Publishing Group, 109(6), pp. 1414–1419.

Al-Mefty, O. *et al.* (1990) 'The long-term side effects of radiation therapy for

benign brain tumors in adults', *Journal of neurosurgery*. Journal of Neurosurgery Publishing Group, 73(4), pp. 502–512.

American Cancer Society (no date) *What is Pancreatic Cancer?* Available at: https://www.cancer.org/cancer/pancreatic-cancer/about/what-is-pancreatic-cancer.html (Accessed: 6 October 2016).

Amoh, Y. *et al.* (2006) 'Dual-color imaging of nascent blood vessels vascularizing pancreatic cancer in an orthotopic model demonstrates antiangiogenesis efficacy of gemcitabine', *Journal of Surgical Research*. Elsevier, 132(2), pp. 164–169.

Arlt, A. *et al.* (2003) 'Role of NF-κB and Akt/PI3K in the resistance of pancreatic carcinoma cell lines against gemcitabine-induced cell death', *Oncogene*. Nature Publishing Group, 22(21), p. 3243.

Arora, S. *et al.* (2011) 'Honokiol arrests cell cycle, induces apoptosis, and potentiates the cytotoxic effect of gemcitabine in human pancreatic cancer cells', *PLoS ONE*, 6(6). doi: 10.1371/journal.pone.0021573.

Ashburn, T. T. and Thor, K. B. (2004) 'Drug repositioning: identifying and developing new uses for existing drugs', *Nature reviews Drug discovery*. Nature Publishing Group, 3(8), p. 673.

ATCC (2012) *SOP: Thawing, Propagation and Cryopreservation of NCI-PBCF-CRL1469 (PANC-1)*. Manassas.

Awasthi, N. *et al.* (2014) 'Antitumor activity of nintedanib (BIBF 1120), a triple angiokinase inhibitor, in combination with gemcitabine in experimental pancreatic cancer', *Cancer Research*, 74(19). doi: 10.1158/1538-7445.am2014-1025.

Awasthi, N., Schwarz, M. A. and Schwarz, R. E. (2011) 'Antitumour activity of sunitinib in combination with gemcitabine in experimental pancreatic cancer', *HPB*. Elsevier, 13(9), pp. 597–604.

Azzariti, A. *et al.* (2010) '34 Azd1152 Plus Gemcitabine for Pancreas Cancer Treatment: in Vitro and in Vivo Study', *Cancer Treatment Reviews*, 36, p. S105. doi: 10.1016/S0305-7372(10)70060-8.

Balagamwala, E. H. *et al.* (2013) 'Introduction to radiotherapy and standard teletherapy techniques', in *Ophthalmic Radiation Therapy*. Karger Publishers,

pp. 1–14.

Banerjee, S. *et al.* (2005) ‘Molecular evidence for increased antitumor activity of gemcitabine by genistein in vitro and in vivo using an orthotopic model of pancreatic cancer’, *Cancer Research*, 65(19), pp. 9064–9072. doi: 10.1158/0008-5472.CAN-05-1330.

Barendsen, G. W. (1997) ‘Parameters of linear-quadratic radiation dose-effect relationships: dependence on LET and mechanisms of reproductive cell death’, *International journal of radiation biology*. Taylor & Francis, 71(6), pp. 649–655.

Barton-Burke, M. (1999) ‘Gemcitabine: A pharmacologic and clinical overview’, *Cancer Nursing*, 22(2), pp. 176–183. doi: 10.1097/00002820-199904000-00011.

Baskar, R. *et al.* (2012) ‘Cancer and radiation therapy: current advances and future directions’, *International journal of medical sciences*. Ivyspring International Publisher, 9(3), p. 193.

Beauchamp, R. D. *et al.* (1990) ‘Expression of and response to growth regulatory peptides by two human pancreatic carcinoma cell lines’, *Pancreas*, 5(4), pp. 369–380.

Bergmann, L. *et al.* (2015) ‘A prospective randomised phase-II trial with gemcitabine versus gemcitabine plus sunitinib in advanced pancreatic cancer: A study of the CESAR Central European Society for Anticancer Drug Research-EWIV’, *European Journal of Cancer*, 51(1), pp. 27–36. doi: 10.1016/j.ejca.2014.10.010.

Berlin, J. D. *et al.* (2002) ‘Phase III study of gemcitabine in combination with fluorouracil versus gemcitabine alone in patients with advanced pancreatic carcinoma: Eastern Cooperative Oncology Group Trial E2297’, *Journal of Clinical Oncology*. American Society of Clinical Oncology, 20(15), pp. 3270–3275.

Bertuzzi, A. *et al.* (1997) ‘Cell loss and the concept of potential doubling time’, *Cytometry*, 29(1), pp. 34–40. doi: 10.1002/(SICI)1097-0320(19970901)29:1<34::AID-CYTO3>3.0.CO;2-D.

Bhutia, Y. D. *et al.* (2011) ‘CNT1 expression influences proliferation and chemosensitivity in drug-resistant pancreatic cancer cells’, *Cancer research*. AACR, 71(5), pp. 1825–1835.

Biankin, A. V *et al.* (2012) 'Pancreatic cancer genomes reveal aberrations in axon guidance pathway genes', *Nature*. Nature Publishing Group, 491(7424), p. 399.

Binenbaum, Y., Na'ara, S. and Gil, Z. (2015) 'Gemcitabine resistance in pancreatic ductal adenocarcinoma', *Drug Resistance Updates*, 23, pp. 55–68. doi: 10.1016/j.drup.2015.10.002.

Bisht, S., Feldmann, G. and Brossart, P. (2013) 'Pharmacokinetics and pharmacodynamics of sunitinib for the treatment of advanced pancreatic neuroendocrine tumors', *Expert Opinion on Drug Metabolism & Toxicology*, 9(6), pp. 777–788. doi: 10.1517/17425255.2013.791281.

Blackford, A. *et al.* (2009) 'SMAD4 gene mutations are associated with poor prognosis in pancreatic cancer', *Clinical cancer research*. AACR, 15(14), pp. 4674–4679.

Blackstock, A. W. *et al.* (2003) 'Cancer and leukemia group B (CALGB) 89805: phase II chemoradiation trial using gemcitabine in patients with locoregional adenocarcinoma of the pancreas.', *International journal of gastrointestinal cancer*, 34(2–3), pp. 107–116.

Blumenthal, G. M. *et al.* (2012) 'FDA Approval Summary: Sunitinib for the Treatment of Progressive Well-Differentiated Locally Advanced or Metastatic Pancreatic Neuroendocrine Tumors', *The Oncologist*, 17(8), pp. 1108–1113. doi: 10.1634/theoncologist.2012-0044.

Bodoky, G. *et al.* (2012) 'A phase II open-label randomized study to assess the efficacy and safety of selumetinib (AZD6244 [ARRY-142886]) versus capecitabine in patients with advanced or metastatic pancreatic cancer who have failed first-line gemcitabine therapy', *Investigational New Drugs*, 30(3), pp. 1216–1223. doi: 10.1007/s10637-011-9687-4.

Bolderson, E. *et al.* (2009) 'Recent advances in cancer therapy targeting proteins involved in DNA double-strand break repair', *Clinical Cancer Research*. AACR, 15(20), pp. 6314–6320.

Bonnier, F. (2015) 'Cell viability assessment using the Alamar blue assay : A comparison of 2D and 3D cell culture models', *Toxicology in Vitro*, 29, pp. 124–131. doi: 10.1016/j.tiv.2014.09.014.

Borja-Cacho, D. *et al.* (2008) 'Molecular targeted therapies for pancreatic cancer.', *American journal of surgery*. NIH Public Access, 196(3), pp. 430–41.

doi: 10.1016/j.amjsurg.2008.04.009.

Bosetti, C. *et al.* (2014) 'Diabetes, antidiabetic medications, and pancreatic cancer risk: an analysis from the International Pancreatic Cancer Case-Control Consortium', *Annals of Oncology*, 25(10), pp. 2065–2072.

Braakhuis, B. J. *et al.* (1995) 'Schedule-dependent antitumor effect of gemcitabine in in vivo model system.', in *Seminars in oncology*, pp. 42–46.

Bramhall, S. R. *et al.* (2002) 'A double-blind placebo-controlled, randomised study comparing gemcitabine and marimastat with gemcitabine and placebo as first line therapy in patients with advanced pancreatic cancer', *British Journal of Cancer*. Nature Publishing Group, 87(2), pp. 161–167. doi: 10.1038/sj.bjc.6600446.

Bray, F. *et al.* (2018) 'Global cancer statistics 2018: GLOBOCAN estimates of incidence and mortality worldwide for 36 cancers in 185 countries', *CA: a cancer journal for clinicians*. Wiley Online Library, 68(6), pp. 394–424.

Brell, J. M. *et al.* (2012) 'Phase i trial of sunitinib and gemcitabine in patients with advanced solid tumors', *Cancer Chemotherapy and Pharmacology*, 70(4), pp. 547–553. doi: 10.1007/s00280-012-1936-5.

Brooks, C. *et al.* (2012) 'Preclinical evaluation of sunitinib, a multi-tyrosine kinase inhibitor, as a radiosensitizer for human prostate cancer', *Radiation Oncology*, 7(1), p. 154. doi: 10.1186/1748-717X-7-154.

Bucci, M. K., Bevan, A. and Roach III, M. (2005) 'Advances in radiation therapy: conventional to 3D, to IMRT, to 4D, and beyond', *CA: a cancer journal for clinicians*. Wiley Online Library, 55(2), pp. 117–134.

Burris, H. A. 3rd *et al.* (1997) 'Improvements in survival and clinical benefit with gemcitabine as first-line therapy for patients with advanced pancreas cancer: a randomized trial', *Journal of clinical oncology*. New York, NY: Grune & Stratton, c1983-, 15(6), pp. 2403–2413.

Burris, H. A. and Hurtig, J. (2010) 'Radiation recall with anticancer agents', *The oncologist*. AlphaMed Press, 15(11), pp. 1227–1237.

Cai, B. *et al.* (2013) 'miRNA-181b increases the sensitivity of pancreatic ductal adenocarcinoma cells to gemcitabine in vitro and in nude mice by targeting BCL-2', *Oncology Reports*, 29(5), pp. 1769–1776. doi: 10.3892/or.2013.2297.

Canadian Cancer Society (no date) *Anatomy and physiology of the pancreas*. Available at: http://www.cancer.ca/en/cancer-information/cancer-type/pancreatic/anatomy-and-physiology (Accessed: 6 October 2016).

Cancer Research UK (no date a) *Breast cancer mortality statistics*. Available at: https://www.cancerresearchuk.org/health-professional/cancer-statistics/statistics-by-cancer-type/breast-cancer/mortality (Accessed: 20 July 2019).

Cancer Research UK (no date b) *Cancer Statistics for the UK*. Available at: https://www.cancerresearchuk.org/health-professional/cancer-statistics-for-the-uk (Accessed: 20 July 2019).

Cancer Research UK (no date c) *Lifetime risk of cancer*. Available at: https://www.cancerresearchuk.org/health-professional/cancer-statistics/risk/lifetime-risk (Accessed: 20 July 2019).

Cancer Research UK (no date d) *Pancreatic cancer statistics*. Available at: https://www.cancerresearchuk.org/health-professional/cancer-statistics/statistics-by-cancer-type/pancreatic-cancer.

Carmichael, J. *et al.* (1996) 'Phase II study of gemcitabine in patients with advanced pancreatic cancer', *British journal of cancer*. Nature Publishing Group, 73(1), p. 101.

Casneuf, V. F. *et al.* (2009) 'Antiangiogenic versus cytotoxic therapeutic approaches in a mouse model of pancreatic cancer: An experimental study with a multitarget tyrosine kinase inhibitor (sunitinib), gemcitabine and radiotherapy', *Oncology Reports*, 22(1), pp. 105–113. doi: 10.3892/or_00000412.

Casper, E. S. *et al.* (1994) 'Phase II trial of gemcitabine (2, 2′-difiuorodeoxycytidine) in patients with adenocarcinoma of the pancreas', *Investigational new drugs*. Springer, 12(1), pp. 29–34.

Chakraborty, A. and Trivedi, V. (2015) 'Streamlining the drug discovery process through repurposing of clinically approved drugs', *Austin J Biotechnol Bioeng*, 2(3), p. 1047.

Chari, S. T. *et al.* (2005) 'Probability of pancreatic cancer following diabetes: A population-based study', *Gastroenterology*, 129(2), pp. 504–511. doi: 10.1016/j.gastro.2005.05.007.

Chari, S. T. *et al.* (2008) 'Pancreatic cancer–associated diabetes mellitus: prevalence and temporal association with diagnosis of cancer', *Gastroenterology*. Elsevier, 134(1), pp. 95–101.

Chen, P. *et al.* (2006) 'In-vitro and in-vivo anti-cancer activity of a novel gemcitabine–cardiolipin conjugate', *Anti-cancer drugs*. LWW, 17(1), pp. 53–61.

Chen, Y.-W. *et al.* (2011) 'Proteomic analysis of gemcitabine-induced drug resistance in pancreatic cancer cells', *Molecular BioSystems*. Royal Society of Chemistry, 7(11), pp. 3065–3074.

Chen, Y. *et al.* (2013) 'Combined radiochemotherapy in patients with locally advanced pancreatic cancer: A meta-analysis', *World Journal of Gastroenterology*, 19(42), pp. 7461–7471. doi: 10.3748/wjg.v19.i42.7461.

Chong, C. R. and Sullivan Jr, D. J. (2007) 'New uses for old drugs', *Nature*. Nature Publishing Group, 448(7154), p. 645.

Chou, T. C. and Talalay, P. (1984) 'Quantitative analysis of dose-effect relationships: the combined effects of multiple drugs or enzyme inhibitors', *Advances in Enzyme Regulation*. England, 22(C), pp. 27–55. doi: 10.1016/0065-2571(84)90007-4.

Chow, L. Q. M. and Eckhardt, S. G. (2007) 'Sunitinib: From rational design to clinical efficacy', *Journal of Clinical Oncology*, 25(7), pp. 884–896. doi: 10.1200/JCO.2006.06.3602.

Chu, G. C. *et al.* (2007) 'Stromal biology of pancreatic cancer', *Journal of cellular biochemistry*. Wiley Online Library, 101(4), pp. 887–907.

Cieslak, J. A. *et al.* (2015) 'Manganoporphyrins and ascorbate enhance gemcitabine cytotoxicity in pancreatic cancer', *Free Radical Biology and Medicine*, 83, pp. 227–237. doi: 10.1016/j.freeradbiomed.2015.02.018.

Ciric, E. and Sersa, G. (2010) 'Radiotherapy in combination with vascular-targeted therapies', *Radiology and Oncology*, 44(2), pp. 66–78. doi: 10.2478/v10019-010-0025-9.

Cohen, M. H. *et al.* (2007) 'FDA drug approval summary: bevacizumab plus FOLFOX4 as second-line treatment of colorectal cancer', *The oncologist*. AlphaMed Press, 12(3), pp. 356–361.

Colucci, G. *et al.* (2010) 'Randomized phase III trial of gemcitabine plus cisplatin compared with single-agent gemcitabine as first-line treatment of patients with advanced pancreatic cancer: the GIP-1 study', *Journal of Clinical Oncology*. American Society of Clinical Oncology, 28(10), pp. 1645–1651.

Cook, D. *et al.* (2014) 'Lessons learned from the fate of AstraZeneca's drug pipeline: a five-dimensional framework', *Nature reviews Drug discovery*. Nature Publishing Group, 13(6), p. 419.

Craveiro, R. B. *et al.* (2014) 'In comparative analysis of multi-kinase inhibitors for targeted medulloblastoma therapy pazopanib exhibits promising *in vitro* and *in vivo* efficacy', *Oncotarget*, 5(16), pp. 7149–7161. doi: 10.18632/oncotarget.2240.

Cuneo, K. C. *et al.* (2008) 'SU11248 (Sunitinib) Sensitizes Pancreatic Cancer to the Cytotoxic Effects of Ionizing Radiation', *International Journal of Radiation Oncology Biology Physics*. Elsevier, 71(3), pp. 873–879. doi: 10.1016/j.ijrobp.2008.02.062.

Cunningham, D. *et al.* (2009) 'Phase III randomized comparison of gemcitabine versus gemcitabine plus capecitabine in patients with advanced pancreatic cancer', *Journal of Clinical Oncology*. American Society of Clinical Oncology, 27(33), pp. 5513–5518.

Van Cutsem, E. *et al.* (2004) 'Phase III Trial of Gemcitabine Plus Tipifarnib Compared With Gemcitabine Plus Placebo in Advanced Pancreatic Cancer', *Journal of Clinical Oncology*, 22(8), pp. 1430–1438. doi: 10.1200/JCO.2004.10.112.

D'Aronzo, M. *et al.* (2015) 'Fasting cycles potentiate the efficacy of gemcitabine treatment in in vitro and in vivo pancreatic cancer models', *Oncotarget*, 6(21), pp. 18545–18557.

Dai, Y. and Grant, S. (2010) 'New insights into checkpoint kinase 1 in the DNA damage response signaling network', *Clinical Cancer Research*, 16(2), pp. 376–383. doi: 10.1158/1078-0432.CCR-09-1029.

Danovi, S. A., Wong, H. H. and Lemoine, N. R. (2008) 'Targeted therapies for pancreatic cancer', *British Medical Bulletin*. Narnia, 87(1), pp. 97–130. doi: 10.1093/bmb/ldn027.

Delaney, G. *et al.* (2005) 'The role of radiotherapy in cancer treatment: estimating optimal utilization from a review of evidence-based clinical

guidelines', *Cancer: Interdisciplinary International Journal of the American Cancer Society*. Wiley Online Library, 104(6), pp. 1129–1137.

Desai, J. *et al.* (2006) 'Hypothyroidism after sunitinib treatment for patients with gastrointestinal stromal tumors', *Annals of internal medicine*. Am Coll Physicians, 145(9), pp. 660–664.

Dillhoff, M. and Bloomston, M. (2018) 'How to Treat Resectable Disease', in *Current and Emerging Therapies in Pancreatic Cancer*. Springer, pp. 171–182.

Ding, Y. Q. *et al.* (2016) 'Sunitinib modulates the radiosensitivity of esophageal squamous cell carcinoma cells in vitro', *Diseases of the Esophagus*, 29(8), pp. 1144–1151. doi: 10.1111/dote.12440.

Dobbins, M., Decorby, K. and Choi, B. C. K. (2013) 'The Association between Obesity and Cancer Risk: A Meta-Analysis of Observational Studies from 1985 to 2011', *ISRN Preventive Medicine*, 2013, pp. 1–16. doi: 10.5402/2013/680536.

Duell, E. J. *et al.* (2009) 'Menstrual and reproductive factors and pancreatic cancer in the SEARCH program of the IARC', *Cancer Causes & Control*. Springer, 20(9), p. 1757.

Duong, H. Q. *et al.* (2012) 'Aldehyde dehydrogenase 1A1 confers intrinsic and acquired resistance to gemcitabine in human pancreatic adenocarcinoma MIA PaCa-2 cells', *International Journal of Oncology*, 41(3), pp. 855–861. doi: 10.3892/ijo.2012.1516.

Duong, H. Q. *et al.* (2014) 'Combination of dasatinib and gemcitabine reduces the ALDH1A1 expression and the proliferation of gemcitabine-resistant pancreatic cancer MIA PaCa-2 cells', *International Journal of Oncology*, 45(6), pp. 2132–2138. doi: 10.3892/ijo.2014.2357.

Eaby-sandy, B., Grande, C. and Viale, P. H. (2012) 'Dermatologic Toxicities in Epidermal Growth Factor Receptor and Multikinase Inhibitors', *Journal of the Advanced Practitioner in Oncology PAMELA HALLQUIST VIALE*, 3, pp. 138–150. Available at: https://www.ncbi.nlm.nih.gov/pmc/articles/PMC4093313/pdf/jadp-03-138.pdf (Accessed: 21 May 2017).

Van Engeland, M. *et al.* (1998) 'Annexin V-affinity assay: a review on an apoptosis detection system based on phosphatidylserine exposure', *Cytometry: The Journal of the International Society for Analytical Cytology*.

Wiley Online Library, 31(1), pp. 1–9.

Evans, D. B. *et al.* (2008) ‘Preoperative gemcitabine-based chemoradiation for patients with resectable adenocarcinoma of the pancreatic head’, *Journal of Clinical Oncology*. American Society of Clinical Oncology, 26(21), pp. 3496–3502.

Everhart, J. (1995) ‘Diabetes mellitus as a risk factor for pancreatic cancer. A meta-analysis’, *JAMA: The Journal of the American Medical Association*, 273(20), pp. 1605–1609. doi: 10.1001/jama.273.20.1605.

Faivre, S. *et al.* (2007) ‘Molecular basis for sunitinib efficacy and future clinical development’, *Nature reviews Drug discovery*. Nature Publishing Group, 6(9), p. 734.

Feakins, R. M. (2016) ‘Obesity and metabolic syndrome: pathological effects on the gastrointestinal tract’, *Histopathology*. Wiley Online Library, 68(5), pp. 630–640.

Fenton MS, Marion KM, Salem AK, Hogen R, Naeim F, H. J. (2010) ‘Sunitinib inhibits MEK/ERK and SAPK/ JNK pathways and increases sodium/iodide symporter expression in papillary thyroid cancer’, *Thyroid*, 20(9), pp. 965–974. doi: 10.1089/ thy.2010.0008.

Ferlay, J. *et al.* (2010) ‘Estimates of worldwide burden of cancer in 2008: GLOBOCAN 2008’, *International Journal of Cancer*. 2011/02/26, 127(12), pp. 2893–2917. doi: 10.1002/ijc.25516.

Ferlay, J., Partensky, C. and Bray, F. (2016) ‘More deaths from pancreatic cancer than breast cancer in the EU by 2017’, *Acta Oncologica*. Taylor & Francis, 55(9–10), pp. 1158–1160.

Fernandez, E. *et al.* (1995) ‘Menstrual and reproductive factors and pancreatic cancer risk in women’, *International journal of cancer*. Wiley Online Library, 62(1), pp. 11–14.

Fields, M. T. *et al.* (2000) ‘Radiosensitization produced in vivo by once-vs. twice-weekly 2′ 2′-difluoro-2′-deoxycytidine (gemcitabine)’, *International Journal of Radiation Oncology* Biology* Physics*. Elsevier, 47(3), pp. 785–791.

Foo, W. C. and Wang, H. (2017) ‘Pathology and Molecular Pathology of Pancreatic Cancer BT - Pathology and Epidemiology of Cancer’, in Loda, M.

et al. (eds). Cham: Springer International Publishing, pp. 489–509. doi: 10.1007/978-3-319-35153-7_26.

Fountzilas, G., Lim, L. O. and Yunis, A. A. (1984) 'Sensitivity of human pancreatic carcinoma cell line (MIA PaCa-2) to Bisantrene and Theprubicin in vitro', *In vitro*. Springer, 20(9), pp. 685–691.

Franke, A. J. *et al.* (2015) 'The role of radiation therapy in pancreatic ductal adenocarcinoma in the neoadjuvant and adjuvant settings', in *Seminars in oncology*. Elsevier, pp. 144–162.

Franken, N. A. P. *et al.* (2001) 'Radiosensitization by bromodeoxyuridine and hyperthermia: analysis of linear and quadratic parameters of radiation survival curves of two human tumor cell lines', *Journal of radiation research*. OUP, 42(2), pp. 179–190.

Franken, N. A. P. *et al.* (2006) 'Clonogenic assay of cells in vitro', *Nature Protocols*, 1(5), pp. 2315–2319. doi: 10.1038/nprot.2006.339.

Freelove, R. and Walling, A. D. (2006) 'Pancreatic cancer: diagnosis and management', *Am Fam Physician*, 73(3), pp. 485–492.

Fryer, R. A. *et al.* (2011) 'Mechanisms underlying gemcitabine resistance in pancreatic cancer and sensitisation by the iMiD™ lenalidomide', *Anticancer Research*, 31(11), pp. 3747–3756. doi: 0250-7005/2011.

Furugaki, K. *et al.* (2010) 'Antitumor activity of erlotinib in combination with gemcitabine in in vitro and in vivo models of KRAS-mutated pancreatic cancers', *Oncology Letters*, 1(2), pp. 231–235. doi: 10.3892/ol_00000041.

Galmarini, C. M. *et al.* (2002) 'Expression of a non-functional p53 affects the sensitivity of cancer cells to gemcitabine', *International journal of cancer*. Wiley Online Library, 97(4), pp. 439–445.

Ghadirian, P. *et al.* (1991) 'Reported family aggregation of pancreatic cancer within a population-based case-control study in the Francophone community in Montreal, Canada', *International Journal of Pancreatology*. Springer, 10(3–4), pp. 183–196.

Giardiello, F. M. *et al.* (1987) 'Increased risk of cancer in the Peutz–Jeghers syndrome', *New England Journal of Medicine*. Mass Medical Soc, 316(24), pp. 1511–1514.

Giovannetti, E. *et al.* (2006) 'Transcription analysis of human equilibrative nucleoside transporter-1 predicts survival in pancreas cancer patients treated with gemcitabine', *Cancer research*. AACR, 66(7), pp. 3928–3935.

Giroux, V. *et al.* (2006) 'p8 Is a New Target of Gemcitabine in Pancreatic Cancer Cells', *Clinical Cancer Research*, 12(1), pp. 235–241. doi: 10.1158/1078-0432.CCR-05-1700.

Goggins, M. *et al.* (1996) 'Germline BRCA2 gene mutations in patients with apparently sporadic pancreatic carcinomas', *Cancer research*. AACR, 56(23), pp. 5360–5364.

Goldstein, D. A. *et al.* (2016) 'Cost description of chemotherapy regimens for the treatment of metastatic pancreas cancer', *Medical Oncology*, 33(5), p. 48. doi: 10.1007/s12032-016-0762-8.

Graham, G. J. and Freshney, M. G. (2000) 'CFU-A assay for measurement of the antiproliferative effects of chemokines on murine early hemopoietic progenitors.', *Methods in molecular biology (Clifton, N.J.)*. United States, 138, pp. 179–189. doi: 10.1385/1-59259-058-6:179.

De Gramont, A. and Van Cutsem, E. (2005) 'Investigating the potential of bevacizumab in other indications: metastatic renal cell, non-small cell lung, pancreatic and breast cancer', *Oncology*. Karger Publishers, 69(Suppl. 3), pp. 46–56.

Grande, E. *et al.* (2014) 'Pazopanib activity in pancreatic neuroendocrine tumors (pNETs)', *Journal of Clinical Oncology*, 32(15).

Grosse, J. *et al.* (2014) 'Mechanisms of apoptosis in irradiated and sunitinib-treated follicular thyroid cancer cells', *Apoptosis*. Springer, 19(3), pp. 480–490.

Gruber, J. *et al.* (1996) '2',2'-Difluorodeoxycytidline (Gemcitabine) Induces Apoptosis in Myeloma Cell Lines Resistant to Steroids and 2-Chlorodeoxyadenosine (2-Cda)', *Stem Cells*, 14(3), pp. 351–362. doi: 10.1002/stem.140351.

Guo, H. C. *et al.* (2012) 'Emodin potentiates the antitumor effects of gemcitabine in PANC-1 pancreatic cancer xenograft model in vivo via inhibition of inhibitors of apoptosis', *International Journal of Oncology*, 40(6), pp. 1849–1857. doi: 10.3892/ijo.2012.1389.

Gupta, S. C. *et al.* (2013) 'Cancer drug discovery by repurposing: teaching new tricks to old dogs', *Trends in pharmacological sciences*. Elsevier, 34(9), pp. 508–517.

Gupta, S. and El-Rayes, B. F. (2008) 'Small molecule tyrosine kinase inhibitors in pancreatic cancer', *Biologics*. Dove Press, 2(4), pp. 707–715. Available at: http://www.ncbi.nlm.nih.gov/entrez/query.fcgi?cmd=Retrieve&db=PubMed&dopt=Citation&list_uids=19707451 (Accessed: 24 May 2017).

Haas, B. *et al.* (2016) 'Is sunitinib a Narrow Therapeutic Index Drug? - A systematic review and in vitro toxicology-analysis of Sunitinib vs. Imatinib in cells from different tissues', *Regulatory Toxicology and Pharmacology*, 77, pp. 25–34. doi: 10.1016/j.yrtph.2016.02.010.

Hahn, S. A. *et al.* (1996) 'DPC4, a candidate tumor suppressor gene at human chromosome 18q21. 1', *Science*. American Association for the Advancement of Science, 271(5247), pp. 350–353.

Hall, J. S. *et al.* (2014) 'Investigation of radiosensitivity gene signatures in cancer cell lines', *PloS one*. Public Library of Science, 9(1), pp. e86329–e86329. doi: 10.1371/journal.pone.0086329.

Hamed, S. S., Straubinger, R. M. and Jusko, W. J. (2013) 'Pharmacodynamic modeling of cell cycle and apoptotic effects of gemcitabine on pancreatic adenocarcinoma cells', *Cancer Chemotherapy and Pharmacology*, 72(3), pp. 553–563. doi: 10.1007/s00280-013-2226-6.

Hanahan, D. and Weinberg, R. A. (2000) 'The hallmarks of cancer', *cell*. Elsevier, 100(1), pp. 57–70.

Hanahan, D. and Weinberg, R. A. (2011) 'Hallmarks of cancer: the next generation', *cell*. Elsevier, 144(5), pp. 646–674.

Hare, J. I. *et al.* (2017) 'Challenges and strategies in anti-cancer nanomedicine development: an industry perspective', *Advanced drug delivery reviews*. Elsevier, 108, pp. 25–38.

Harrington, K. J. (2016) 'The biology of cancer', *Medicine*, 44(1), pp. 1–5. doi: http://dx.doi.org/10.1016/j.mpmed.2015.10.005.

Hashimoto, D. *et al.* (2015) 'Staging laparoscopy leads to rapid induction of chemotherapy for unresectable pancreatobiliary cancers', *Asian journal of*

endoscopic surgery. Wiley Online Library, 8(1), pp. 59–62.

Hasinoff, B. B., Patel, D. and O'Hara, K. A. (2008) 'Mechanisms of Myocyte Cytotoxicity Induced by the Multiple Receptor Tyrosine Kinase Inhibitor Sunitinib', *Molecular Pharmacology*, 74(6), pp. 1722–1728. doi: 10.1124/mol.108.050104.

Hather, G. *et al.* (2014) 'Growth Rate Analysis and Efficient Experimental Design for Tumor Xenograft Studies', *Cancer Informatics*, 13(Suppl 4), p. 65. doi: 10.4137/CIN.S13974.

Hefferin, M. L. and Tomkinson, A. E. (2005) 'Mechanism of DNA double-strand break repair by non-homologous end joining', *DNA repair*. Elsevier, 4(6), pp. 639–648.

Heinemann, V. *et al.* (2006) 'Randomized phase III trial of gemcitabine plus cisplatin compared with gemcitabine alone in advanced pancreatic cancer', *J Clin Oncol*, 24(24), pp. 3946–3952.

Heinemann, V. *et al.* (2007) 'Increased survival using platinum analog combined with gemcitabine as compared to single-agent gemcitabine in advanced pancreatic cancer: pooled analysis of two randomized trials, the GERCOR/GISCAD intergroup study and a German multicenter study', *Annals of oncology*. Oxford University Press, 18(10), pp. 1652–1659.

Heinemann, V. *et al.* (2008) 'Meta-analysis of randomized trials: evaluation of benefit from gemcitabine-based combination chemotherapy applied in advanced pancreatic cancer', *BMC cancer*. BioMed Central, 8(1), p. 82. doi: 10.1186/1471-2407-8-82.

Hennig, R. *et al.* (2002) 'Staging laparoscopy and its indications in pancreatic cancer patients', *Digestive surgery*. Karger Publishers, 19(6), pp. 484–488.

Herman, J. M. *et al.* (2013) 'Randomized phase III multi-institutional study of TNFerade biologic with fluorouracil and radiotherapy for locally advanced pancreatic cancer: final results', *Journal of Clinical Oncology*. American Society of Clinical Oncology, 31(7), p. 886.

Herman, J. M. *et al.* (2015) 'Phase 2 multi-institutional trial evaluating gemcitabine and stereotactic body radiotherapy for patients with locally advanced unresectable pancreatic adenocarcinoma', *Cancer*. Wiley Online Library, 121(7), pp. 1128–1137.

Hermine, O. *et al.* (2010) 'Masitinib Combined with Standard Gemcitabine Chemotherapy: In Vitro and In Vivo Studies in Human Pancreatic Tumour Cell Lines and Ectopic Mouse Model', *Figshare*, 5(3). doi: 10.1371/journal.pone.0009430.

Herrmann, R. *et al.* (2007) 'Gemcitabine plus capecitabine compared with gemcitabine alone in advanced pancreatic cancer: a randomized, multicenter, phase III trial of the Swiss Group for Clinical Cancer Research and the Central European Cooperative Oncology Group', *Journal of Clinical Oncology*. American Society of Clinical Oncology, 25(16), pp. 2212–2217.

Hesler, R. A. *et al.* (2016) 'TGF-beta-induced stromal CYR61 promotes resistance to gemcitabine in pancreatic ductal adenocarcinoma through downregulation of the nucleoside transporters hENT1 and hCNT3', *Carcinogenesis*, 37(11), pp. 1041–1051. doi: 10.1093/carcin/bgw093.

Hill, A. *et al.* (2011) 'Associations between nutritional status, weight loss, radiotherapy treatment toxicity and treatment outcomes in gastrointestinal cancer patients', *Clinical nutrition*. Elsevier, 30(1), pp. 92–98.

Von Hoff, D. D. *et al.* (2013) 'Increased Survival in Pancreatic Cancer with nab-Paclitaxel plus Gemcitabine', *New England Journal of Medicine*, 369(18), pp. 1691–1703. doi: 10.1056/NEJMoa1304369.

Hoffman, R. M. and Bouvet, M. (2015) 'Nanoparticle albumin-bound-paclitaxel: a limited improvement under the current therapeutic paradigm of pancreatic cancer'. Taylor & Francis.

Hong, S. P. *et al.* (2009) 'CD44-positive cells are responsible for gemcitabine resistance in pancreatic cancer cells', *International journal of cancer*. Wiley Online Library, 125(10), pp. 2323–2331.

Horii, A. *et al.* (2015) 'Human cancer cells acquire chemoresistance to gemcitabine mainly through loss-of-function mutations in the DCK gene'. AACR.

Hruban, R. H. *et al.* (2010) 'Update on familial pancreatic cancer', *Advances in surgery*. NIH Public Access, 44, p. 293.

Hu, J. *et al.* (2016) 'In vitro and in vivo evaluation of targeted sunitinib-loaded polymer microbubbles against proliferation of renal cell carcinoma', *Journal of Ultrasound in Medicine*, 35(3), pp. 589–597. doi: 10.7863/ultra.14.10038.

Huang, P. *et al.* (1991) 'Action of 2′, 2′-difluorodeoxycytidine on DNA synthesis', *Cancer research*. AACR, 51(22), pp. 6110–6117.

Humbert, M. *et al.* (2010) 'Masitinib combined with standard gemcitabine chemotherapy: In vitro and in vivo studies in human pancreatic tumour cell lines and ectopic mouse model', *PLoS ONE*, 5(3). doi: 10.1371/journal.pone.0009430.

Hung, S. W. *et al.* (2015) 'Defective hCNT1 transport contributes to gemcitabine chemoresistance in ovarian cancer subtypes: overcoming transport defects using a nanoparticle approach', *Cancer letters*. Elsevier, 359(2), pp. 233–240.

Huxley, R. *et al.* (2005) 'Type-II diabetes and pancreatic cancer: a meta-analysis of 36 studies.', *British journal of cancer*, 92(11), pp. 2076–83. doi: 10.1038/sj.bjc.6602619.

Idachaba, S. *et al.* (2019) 'A Review of Pancreatic Cancer: Epidemiology, Genetics, Screening, and Management', *Open Access Macedonian Journal of Medical Sciences*, 7(4), pp. 663–671. doi: 10.3889/oamjms.2019.104.

Igarashi, K. *et al.* (2017) 'High Efficacy of Pazopanib on an Undifferentiated Spindle-Cell Sarcoma Resistant to First-Line Therapy Is Identified With a Patient-Derived Orthotopic Xenograft (PDOX) Nude Mouse Model', *Journal of Cellular Biochemistry*. Wiley-Blackwell, 118(9), pp. 2739–2743. doi: 10.1002/jcb.25923.

Infante, J. R. *et al.* (2014) 'A randomised, double-blind, placebo-controlled trial of trametinib, an oral MEK inhibitor, in combination with gemcitabine for patients with untreated metastatic adenocarcinoma of the pancreas', *European Journal of Cancer*, 50(12), pp. 2072–2081. doi: 10.1016/j.ejca.2014.04.024.

Iodice, S. *et al.* (2008) 'Tobacco and the risk of pancreatic cancer: a review and meta-analysis', *Langenbeck's archives of surgery*. Springer, 393(4), pp. 535–545. doi: 10.1007/s00423-007-0266-2.

Ishiwata, T. *et al.* (2012) 'Enhanced expression of fibroblast growth factor receptor 2 IIIc promotes human pancreatic cancer cell proliferation', *American Journal of Pathology*, 180(5), pp. 1928–1941. doi: 10.1016/j.ajpath.2012.01.020.

Izzedine, H. *et al.* (2007) 'Sunitinib malate', *Cancer Chemotherapy and*

Pharmacology, 60(3), pp. 357–364. doi: 10.1007/s00280-006-0376-5.

Jacobs, E. J. *et al.* (2010) 'Family history of cancer and risk of pancreatic cancer: a pooled analysis from the Pancreatic Cancer Cohort Consortium (PanScan)', *International journal of cancer*. Wiley Online Library, 127(6), pp. 1421–1428.

Jain, R. K. (2001) 'Normalizing tumor vasculature with anti-angiogenic therapy: a new paradigm for combination therapy', *Nature medicine*. Nature Publishing Group, 7(9), pp. 987–989.

Jain, R. K. (2003) 'Molecular regulation of vessel maturation', *Nature medicine*. Nature Publishing Group, 9(6), pp. 685–693.

Jee, S. H. (2005) 'Fasting Serum Glucose Level and Cancer Risk in Korean Men and Women', *Jama*, 293(2), p. 194. doi: 10.1001/jama.293.2.194.

Jennings, R. E. *et al.* (2015) 'Human pancreas development', *Development*, 142(18), pp. 3126 LP – 3137. doi: 10.1242/dev.120063.

Jin, J. M., Teng, C. B. and Li, T. (2018) 'Combination therapy versus gemcitabine monotherapy in the treatment of elderly pancreatic cancer: a meta-analysis of randomized controlled trials', *Drug Design Development and Therapy*, 12, pp. 475–480. doi: 10.2147/dddt.s156766.

Jones, S. *et al.* (2008) 'Core signaling pathways in human pancreatic cancers revealed by global genomic analyses', *science*. American Association for the Advancement of Science, 321(5897), pp. 1801–1806.

El Kaffas, A. *et al.* (2014) 'Sunitinib effects on the radiation response of endothelial and breast tumor cells', *Microvascular research*. Elsevier, 92, pp. 1–9.

Kalyan, A. *et al.* (2015) 'A phase I multicenter study of the combination of temozolomide and pazopanib in advanced pancreatic neuroendocrine tumors (PNET)', *Journal of Clinical Oncology*, 33(3).

Kausar, T. *et al.* (2015) 'Sensitization of Pancreatic Cancers to Gemcitabine Chemoradiation by WEE1 Kinase Inhibition Depends on Homologous Recombination Repair', *Neoplasia*, 17(10), pp. 757–766. doi: 10.1016/j.neo.2015.09.006.

Kazuno, H. *et al.* (2005) 'Possible antitumor activity of 1-(3-C-ethynyl-β-d-ribo-pentofuranosyl) cytosine (ECyd, TAS-106) against an established gemcitabine (dFdCyd)-resistant human pancreatic cancer cell line', *Cancer science*. Wiley Online Library, 96(5), pp. 295–302.

Keane, M. G. *et al.* (2014) 'Sociodemographic trends in the incidence of pancreatic and biliary tract cancer in UK primary care', *PLoS ONE*, 9(9). doi: 10.1371 /journal.pone.0108498.

Keisner, S. V and Shah, S. R. (2011) 'Pazopanib', *Drugs*, 71(4), pp. 443–454. doi: 10.2165/11588960-000000000-00000.

Kelsen, D. P. *et al.* (1997) 'Pain as a predictor of outcome in patients with operable pancreatic carcinoma', *Surgery*. Elsevier, 122(1), pp. 53–59.

Kim, B. *et al.* (2015) 'Therapeutic implications for overcoming radiation resistance in cancer therapy', *International journal of molecular sciences*. Multidisciplinary Digital Publishing Institute, 16(11), pp. 26880–26913.

Kim, S. T. *et al.* (2014) 'Pazopanib, a Novel Multitargeted Kinase Inhibitor, Shows Potent In Vitro Antitumor Activity in Gastric Cancer Cell Lines with FGFR2 Amplification', *Molecular Cancer Therapeutics*, 13(11), pp. 2527–2536. doi: 10.1158/1535-7163.MCT-14-0255.

Kindler, H. L. *et al.* (2007) 'A double-blind, placebo-controlled, randomized phase III trial of gemcitabine (G) plus bevacizumab (B) versus gemcitabine plus placebo (P) in patients (pts) with advanced pancreatic cancer (PC): A preliminary analysis of Cancer and Leukemia Group B (CALGB', *Journal of Clinical Oncology*. American Society of Clinical Oncology, 25(18_suppl), p. 4508.

Kleibeuker, E. A., ten Hooven, M. A., Verheul, H. M., *et al.* (2015) 'Combining radiotherapy with sunitinib: lessons (to be) learned', *Angiogenesis*, 18(4), pp. 385–395. doi: 10.1007/s10456-015-9476-3.

Kleibeuker, E. A., ten Hooven, M. A., Castricum, K. C., *et al.* (2015) 'Optimal treatment scheduling of ionizing radiation and sunitinib improves the antitumor activity and allows dose reduction', *Cancer medicine*. Wiley Online Library, 4(7), pp. 1003–1015.

Ko, A. H. *et al.* (2008) 'A phase II study evaluating bevacizumab in combination with fixed-dose rate gemcitabine and low-dose cisplatin for metastatic pancreatic cancer: Is an anti-VEGF strategy still applicable?', *Investigational*

New Drugs, 26(5), pp. 463–471. doi: 10.1007/s10637-008-9127-2.

Koong, A. C. *et al.* (2004) 'Phase I study of stereotactic radiosurgery in patients with locally advanced pancreatic cancer', *International Journal of Radiation Oncology* Biology* Physics*. Elsevier, 58(4), pp. 1017–1021.

Krishna, K. *et al.* (2015) 'Modified gemcitabine and nab-paclitaxel in patients with metastatic pancreatic cancer (MPC): A single-institution experience.', in *Journal of Clinical Oncology*, pp. 366–366. doi: 10.1200/jco.2015.33.3_suppl.366.

Kroep, J. R. *et al.* (2000) 'Sequence dependent effect of paclitaxel on gemcitabine metabolism in relation to cell cycle and cytotoxicity in non-small-cell lung cancer cell lines', *British Journal of Cancer*, 83(8), pp. 1069–1076. doi: 10.1054/bjoc.2000.1399.

Kufe, D. W. *et al.* (1980) 'Correlation of cytotoxicity with incorporation of ara-C into DNA.', *Journal of Biological Chemistry*. ASBMB, 255(19), pp. 8900–8997.

Kulke, M. H. *et al.* (2017) 'The efficacy and safety of sunitinib in patients with advanced well-differentiated pancreatic neuroendocrine tumors', *Journal of Clinical Oncology*, 35(4 Supplement 1), p. 435. Available at: http://meetinglibrary.asco.org/record/139403/abstract%0Ahttp://ovidsp.ovid.com/ovidweb.cgi?T=JS&PAGE=reference&D=emexa&NEWS=N&AN=618087346.

Kuo, L. J. and Yang, L.-X. (2008) 'Gamma-H2AX - a novel biomarker for DNA double-strand breaks.', *In vivo (Athens, Greece)*. Greece, 22(3), pp. 305–309.

Kwekkeboom, D. J. (2015) 'Pazopanib: A new drug for pancreatic neuroendocrine tumours', *The Lancet Oncology*, 16(6), pp. 606–607. doi: 10.1016/S1470-2045(15)70200-7.

Laquente, B. *et al.* (2008) 'Antiangiogenic effect of gemcitabine following metronomic administration in a pancreas cancer model', *Molecular Cancer Therapeutics*. AACR, 7(3), pp. 638–647.

Larsson, S. C., Orsini, N. and Wolk, A. (2007) 'Body mass index and pancreatic cancer risk: a meta-analysis of prospective studies', *International journal of cancer*. Wiley Online Library, 120(9), pp. 1993–1998. doi: 10.1002/ijc.22535.

Lawrence, T. S. *et al.* (1996) 'Radiosensitization of pancreatic cancer cells by

2′, 2′-difluoro-2′-deoxycytidine', *International Journal of Radiation Oncology* Biology* Physics*. Elsevier, 34(4), pp. 867–872.

Lea, D. E. *et al.* (1942) 'The mechanism of the induction by radiation of chromosome aberrations in Tradescantia', *Journal of genetics*. Indian Academy of Sciences Bengaluru, 44(02–03).

Lee, C. J., Dosch, J. and Simeone, D. M. (2008) 'Pancreatic cancer stem cells', *Journal of clinical oncology*. American Society of Clinical Oncology, 26(17), pp. 2806–2812.

Lee, N. C. *et al.* (2000) 'Antimetastatic efficacy of adjuvant gemcitabine in a pancreatic cancer orthotopic model', *Clinical & experimental metastasis*. Springer, 18(5), pp. 379–384.

Lees, J. (1999) 'Incidence of weight loss in head and neck cancer patients on commencing radiotherapy treatment at a regional oncology centre.', *European journal of cancer care*, 8(3), pp. 133–136.

Li, D. and Abbruzzese, J. L. (2010) 'New Strategies in Pancreatic Cancer: Emerging Epidemiological and Therapeutic Concepts', *Clinical Cancer Research*, 16(17), pp. 4313–4318. doi: 10.1158/1078-0432.CCR-09-1942.New.

Li, H. *et al.* (2017) 'Inhibition of Neddylation Modification Sensitizes Pancreatic Cancer Cells to Gemcitabine', *Neoplasia*, 19(6), pp. 509–518. doi: 10.1016/j.neo.2017.04.003.

Li, J. *et al.* (2013) 'Gemcitabine-loaded albumin nanospheres (GEM-ANPs) inhibit PANC-1 cells in vitro and in vivo', *Nanoscale Research Letters*, 8(1), pp. 1–9. doi: 10.1186/1556-276X-8-176.

Lieber, M. *et al.* (1975) 'Establishment of a continuous tumor-cell line (PANC-1) from a human carcinoma of the exocrine pancreas', *International journal of cancer*. Wiley Online Library, 15(5), pp. 741–747.

Lin, P.-W. *et al.* (2005) 'Pancreaticoduodenectomy for pancreatic head cancer: PPPD versus Whipple procedure.', *Hepato-gastroenterology*, 52(65), pp. 1601–4. Available at: http://www.ncbi.nlm.nih.gov/pubmed/16201125 (Accessed: 17 July 2019).

Liu, Y. *et al.* (2016) 'Periostin promotes the chemotherapy resistance to

gemcitabine in pancreatic cancer', *Tumor Biology*, 37(11), pp. 15283–15291. doi: 10.1007/s13277-016-5321-6.

Liubavičiute, A. *et al.* (2015) 'Evaluation of low-dose proton beam radiation efficiency in MIA PaCa-2 pancreatic cancer cell line vitality and H2AX formation', *Medicina (Lithuania)*, 51(5), pp. 302–306. doi: 10.1016/j.medici.2015.10.002.

Löbrich, M. and Kiefer, J. (2006) 'Assessing the likelihood of severe side effects in radiotherapy', *International journal of cancer*. Wiley Online Library, 118(11), pp. 2652–2656.

Lomax, M. E., Folkes, L. K. and O'neill, P. (2013) 'Biological consequences of radiation-induced DNA damage: relevance to radiotherapy', *Clinical oncology*. Elsevier, 25(10), pp. 578–585.

Louvet, C. *et al.* (2005) 'Gemcitabine in combination with oxaliplatin compared with gemcitabine alone in locally advanced or metastatic pancreatic cancer: results of a GERCOR and GISCAD phase III trial', *Journal of Clinical Oncology*. American Society of Clinical Oncology, 23(15), pp. 3509–3516.

Lovelock, J. E. and Bishop, M. W. H. (1959) 'Prevention of freezing damage to living cells by dimethyl sulphoxide', *Nature*. Nature Publishing Group, 183(4672), p. 1394.

Lowenfels, A. B. *et al.* (1993) 'Pancreatitis and the Risk of Pancreatic Cancer', *New England Journal of Medicine*, 328(20), pp. 1433–1437. doi: 10.1056/NEJM199305203282001.

Lowenfels, A. B. *et al.* (1997) 'Hereditary pancreatitis and the risk of pancreatic cancer', *Journal of the National Cancer Institute*. Oxford University Press, 89(6), pp. 442–446.

Lowenfels, A. B. and Maisonneuve, P. (2002) 'Epidemiologic and etiologic factors of pancreatic cancer', *Hematol Oncol Clin North Am*, 16(36), pp. 1–16. doi: http://dx.doi.org/10.1016/S0889-8588(01)00003-X.

Lowery, M. A. *et al.* (2011) 'An emerging entity: pancreatic adenocarcinoma associated with a known BRCA mutation: clinical descriptors, treatment implications, and future directions', *The oncologist*. AlphaMed Press, 16(10), pp. 1397–1402.

Luo, J. *et al.* (2001) 'Pancreatic cancer cell-derived vascular endothelial growth factor is biologically active in vitro and enhances tumorigenicity in vivo', *International Journal of Cancer*, 92(3), pp. 361–369. doi: 10.1002/ijc.1202.

Lyros, O. *et al.* (2010) 'Analysis of anti-proliferative and chemosensitizing effects of sunitinib on human esophagogastric cancer cells: Synergistic interaction with vandetanib via inhibition of multi-receptor tyrosine kinase pathways', *International journal of cancer*. Wiley Online Library, 127(5), pp. 1197–1208.

M. P. Curado *et al.* (2007) 'Cancer incidence in five continents, Volume IX', *IARC Scientific Publications*.

Ma, J. *et al.* (2017) 'Ku70 inhibits gemcitabine-induced DNA damage and pancreatic cancer cell apoptosis', *Biochemical and Biophysical Research Communications*, 484(4), pp. 746–752. doi: 10.1016/j.bbrc.2017.01.146.

Maeda, J. *et al.* (2016) 'Intrinsic Radiosensitivity and Cellular Characterization of 27 Canine Cancer Cell Lines', *PloS one*. Public Library of Science, 11(6), pp. e0156689–e0156689. doi: 10.1371/journal.pone.0156689.

Magnino, A. *et al.* (2005) 'Phase II trial of primary radiation therapy and concurrent chemotherapy for patients with locally advanced pancreatic cancer', *Oncology*. Karger Publishers, 68(4–6), pp. 493–499.

Mahalingam, D. *et al.* (2011) 'Targeting PIM kinase enhances the activity of sunitinib in renal cell carcinoma', *British journal of cancer*. Nature Publishing Group, 105(10), p. 1563.

Makohon-Moore, A. and Iacobuzio-Donahue, C. A. (2016) 'Pancreatic cancer biology and genetics from an evolutionary perspective', *Nature Reviews Cancer*, 16(9), pp. 553–565. doi: 10.1038/nrc.2016.66.

Mallik, S. and Karandish, F. (2016) 'Biomarkers and Targeted Therapy in Pancreatic Cancer', *Biomarkers in Cancer*. Libertas Academica, 8, p. 27. doi: 10.4137/BIC.S34414.

Maraz, A. *et al.* (2018) 'Dose escalation can maximize therapeutic potential of sunitinib in patients with metastatic renal cell carcinoma', *BMC Cancer*. BioMed Central Ltd., 18(1). doi: 10.1186/s12885-018-4209-9.

Martinez-Bosch, N. *et al.* (2016) 'The pancreatic niche inhibits the

effectiveness of sunitinib treatment of pancreatic cancer', *Oncotarget*, 7(30), pp. 48265–48279. doi: 10.18632/oncotarget.10199.

Mason, K. A. *et al.* (1999) 'Maximizing therapeutic gain with gemcitabine and fractionated radiation', *International Journal of Radiation Oncology* Biology* Physics*. Elsevier, 44(5), pp. 1125–1135.

Matsuoka, T. and Yashiro, M. (2016) 'Molecular targets for the treatment of pancreatic cancer: Clinical and experimental studies', *World Journal of Gastroenterology*. Baishideng Publishing Group Co., Limited, 22(2), pp. 776–789. doi: 10.3748/wjg.v22.i2.776.

Matthews, D. J. *et al.* (2007) 'Pharmacological abrogation of S-phase checkpoint enhances the anti-tumor activity of gemcitabine in vivo', *Cell cycle*. Taylor & Francis, 6(1), pp. 104–110.

McCluskey, A. G. *et al.* (2012) 'Inhibition of Poly(ADP-Ribose) Polymerase Enhances the Toxicity of 131I-Metaiodobenzylguanidine/Topotecan Combination Therapy to Cells and Xenografts That Express the Noradrenaline Transporter', *Journal of Nuclear Medicine*, 53(7), pp. 1146–1154. doi: 10.2967/jnumed.111.095943.

McGinn, C. J., Shewach, D. S. and Lawrence, T. S. (1996) 'Radiosensitizing nucleosides', *JNCI: Journal of the National Cancer Institute*. Oxford University Press, 88(17), pp. 1193–1203.

McIntyre, L. J. and Kim, Y. S. (1984) 'Effects of sodium butyrate and dimethylsulfoxide on human pancreatic tumor cell lines.', *European Journal of Cancer & Clinical Oncology*, 20(2), pp. 265–71. Available at: http://www.ncbi.nlm.nih.gov/pubmed/6200329 (Accessed: 18 December 2017).

Meershoek, E. *et al.* (2005) 'Late Side Effects of Short-Course Preoperative Radiotherapy Combined With Total Mesorectal Excision for Rectal Cancer: Increased Bowel Dysfunction in Irradiated Patients-A Dutch Late Side Effects of Short-Course Preoperative Radiotherapy Combined With Tot', *Article in Journal of Clinical Oncology*, 23, pp. 6199–6206. doi: 10.1200/JCO.2005.14.779.

Mendel, D. B. *et al.* (2003) 'In vivo antitumor activity of SU11248, a novel tyrosine kinase inhibitor targeting vascular endothelial growth factor and platelet-derived growth factor receptors: determination of a pharmacokinetic/pharmacodynamic relationship', *Clinical Cancer Research*.

AACR, 9(1), pp. 327–337.

Meryman, H. T. (2007) ‘Cryopreservation of living cells: principles and practice’, *Transfusion*. John Wiley & Sons, Ltd (10.1111), 47(5), pp. 935–945. doi: 10.1111/j.1537-2995.2007.01212.x.

Midha, S., Chawla, S. and Garg, P. K. (2016) ‘Modifiable and non-modifiable risk factors for pancreatic cancer: A review’, *Cancer Letters*, 381(1), pp. 269–277. doi: http://dx.doi.org/10.1016/j.canlet.2016.07.022.

Mimeault, M. *et al.* (2005) ‘Recent advances on the molecular mechanisms involved in pancreatic cancer progression and therapies’, *Pancreas*. LWW, 31(4), pp. 301–316.

Mini, E. *et al.* (2006) ‘Cellular pharmacology of gemcitabine’, *Annals of oncology*. Oxford University Press, 17(suppl_5), pp. v7–v12.

Montano, R. *et al.* (2013) ‘Sensitization of human cancer cells to gemcitabine by the Chk1 inhibitor MK-8776: Cell cycle perturbation and impact of administration schedule in vitro and in vivo’, *BMC Cancer*, 13. doi: 10.1186/1471-2407-13-604.

Montano, R. *et al.* (2017) ‘Cell cycle perturbation induced by gemcitabine in human tumor cells in cell culture, xenografts and bladder cancer patients: implications for clinical trial designs combining gemcitabine with a Chk1 inhibitor’, *Oncotarget*, 8(40), pp. 67754–67768. doi: 10.18632/oncotarget.18834.

Moore, M. J. *et al.* (2007) ‘Erlotinib plus gemcitabine compared with gemcitabine alone in patients with advanced pancreatic cancer: A phase III trial of the National Cancer Institute of Canada Clinical Trials Group’, *Journal of Clinical Oncology*, 25(15), pp. 1960–1966. doi: 10.1200/JCO.2006.07.9525.

Morgan, M. A. and Lawrence, T. S. (2015) ‘Molecular pathways: overcoming radiation resistance by targeting DNA damage response pathways’, *Clinical Cancer Research*. AACR, 21(13), pp. 2898–2904.

Mosmann, T. (1983) ‘Rapid colorimetric assay for cellular growth and survival: application to proliferation and cytotoxicity assays’, *J Immunol.Methods*, 65(0022–1759), pp. 55–63. doi: https://doi.org/10.1016/0022-1759(83)90303-4.

Motulsky, H. J. (no date) *Equation: log(inhibitor) vs. normalized response -- Variable slope*. Available at: https://www.graphpad.com/guides/prism/7/curve-fitting/index.htm?reg_dr_inhibit_normalized_variable.htm (Accessed: 20 March 2017).

Motzer, R. J. *et al.* (2013) 'Pazopanib versus sunitinib in metastatic renal-cell carcinoma', *New England Journal of Medicine*. Mass Medical Soc, 369(8), pp. 722–731.

Motzer, R. J. *et al.* (2014) 'Overall Survival in Renal-Cell Carcinoma with Pazopanib versus Sunitinib', *New England Journal of Medicine*, 370(18), pp. 1769–1770. doi: 10.1056/NEJMc1400731.

Munshi, A. *et al.* (2003) 'Weight loss during radiotherapy for head and neck malignancies: what factors impact it?', *Nutrition and cancer*. Taylor & Francis, 47(2), pp. 136–140.

Nakamura, K. *et al.* (2014) 'Recent advances in radiation oncology: intensity-modulated radiotherapy, a clinical perspective', *International journal of clinical oncology*. Springer, 19(4), pp. 564–569.

National Cancer Intelligence Network and Cancer Research UK (2009) *Cancer Incidence and Survival by Major Ethnic Group, England, 2002-2006*. Available at: http://www.ncin.org.uk/view?rid=75.

National Institute for Health and Care Excellence (NICE) (2001) *Guidance on the use of gemcitabine for the treatment of pancreatic cancer*. Available at: https://www.nice.org.uk/guidance/TA25 (Accessed: 17 August 2019).

Nordh, S., Ansari, D. and Andersson, R. (2014) 'hENT1 expression is predictive of gemcitabine outcome in pancreatic cancer: A systematic review', *World Journal of Gastroenterology*, 20(26), pp. 8482–8490. doi: 10.3748/wjg.v20.i26.8482.

Nosengo, N. (2016) 'Can you teach old drugs new tricks?', *Nature News*, 534(7607), p. 314.

O'brien, J. *et al.* (2000) 'Investigation of the Alamar Blue (resazurin) fluorescent dye for the assessment of mammalian cell cytotoxicity', *European journal of biochemistry*. Wiley Online Library, 267(17), pp. 5421–5426.

O'Farrell, A.-M. *et al.* (2003) 'SU11248 is a novel FLT3 tyrosine kinase inhibitor

with potent activity in vitro and in vivo', *Blood, The Journal of the American Society of Hematology*. American Society of Hematology Washington, DC, 101(9), pp. 3597–3605.

Ochs, K. and Kaina, B. (2000) 'Apoptosis induced by DNA Damage O-Methylguanine is Bcl-2 and Caspase-9/3 regulated and Fas/Caspase-8 independent', *Cancer research*. AACR, 60(20), pp. 5815–5824.

Oettle, H. *et al.* (2005) 'A phase III trial of pemetrexed plus gemcitabine versus gemcitabine in patients with unresectable or metastatic pancreatic cancer', *Annals of Oncology*. Oxford University Press, 16(10), pp. 1639–1645.

Ohhashi, S. *et al.* (2008) 'Down-regulation of deoxycytidine kinase enhances acquired resistance to gemcitabine in pancreatic cancer', *Anticancer research*. International Institute of Anticancer Research, 28(4B), pp. 2205–2212.

Olive, K. P. *et al.* (2009) 'Inhibition of Hedgehog signaling enhances delivery of chemotherapy in a mouse model of pancreatic cancer', *Science*. American Association for the Advancement of Science, 324(5933), pp. 1457–1461.

Olson, P. *et al.* (2011) 'Imaging guided trials of the angiogenesis inhibitor sunitinib in mouse models predict efficacy in pancreatic neuroendocrine but not ductal carcinoma', *Proceedings of the National Academy of Sciences*, 108(49), pp. E1275–E1284. doi: 10.1073/pnas.1111079108.

Omura, N. *et al.* (2008) 'Genome-wide profiling at methylated promoters in pancreatic adenocarcinoma', *Cancer biology & therapy*. Taylor & Francis, 7(7), pp. 1146–1156.

Ono, H., Basson, M. D. and Ito, H. (2015) 'PTK6 Potentiates Gemcitabine-Induced Apoptosis by Prolonging S-phase and Enhancing DNA Damage in Pancreatic Cancer', *Molecular Cancer Research*, 13(8), pp. 1174–1184. doi: 10.1158/1541-7786.mcr-15-0034.

Overholser, J. P. *et al.* (2000) 'Epidermal growth factor receptor blockade by antibody IMC-C225 inhibits growth of a human pancreatic carcinoma xenograft in nude mice', *Cancer*. Wiley Online Library, 89(1), pp. 74–82.

Pauwels, B. *et al.* (2002) 'The role of cell cycle effects in the radiosensitizing mechanism of gemcitabine', *Proceedings of the American Association for Cancer Research Annual Meeting*, 43, p. 648.

Pauwels, B. *et al.* (2003) 'Cell cycle effect of gemcitabine and its role in the radiosensitizing mechanism in vitro', *International Journal of Radiation Oncology Biology Physics*, 57(4), pp. 1075–1083. doi: 10.1016/S0360-3016(03)01443-3.

Pauwels, B. *et al.* (2005) 'Combined modality therapy of gemcitabine and radiation', *The oncologist*. AlphaMed Press, 10(1), pp. 34–51.

Pellegata, N. S. *et al.* (1994) 'K-ras and p53 gene mutations in pancreatic cancer: ductal and nonductal tumors progress through different genetic lesions.', *Cancer research*, 54(6), pp. 1556–60. Available at: http://www.ncbi.nlm.nih.gov/pubmed/8137263 (Accessed: 20 April 2017).

Philip, P. A. *et al.* (2010) 'Phase III study comparing gemcitabine plus cetuximab versus gemcitabine in patients with advanced pancreatic adenocarcinoma: Southwest oncology group-directed intergroup trial S0205', *Journal of Clinical Oncology*, 28(22), pp. 3605–3610. doi: 10.1200/JCO.2009.25.7550.

Ping, S.-Y., Wu, C.-L. and Yu, D.-S. (2012) 'Sunitinib can enhance BCG mediated cytotoxicity to transitional cell carcinoma through apoptosis pathway', in *Urologic Oncology: Seminars and Original Investigations*. Elsevier, pp. 652–659.

Plummer, R. *et al.* (2013) 'A Phase i study of pazopanib in combination with gemcitabine in patients with advanced solid tumors', *Cancer Chemotherapy and Pharmacology*, 71(1), pp. 93–101. doi: 10.1007/s00280-012-1982-z.

Plunkett, W. *et al.* (1996) 'Gemcitabine: preclinical pharmacology and mechanisms of action', *Semin Oncol*, 23(5 Suppl 10), pp. 3–15. doi: 0093-7754/96/2305-1015.

Pollom, E. L. *et al.* (2014) 'Single-versus multifraction stereotactic body radiation therapy for pancreatic adenocarcinoma: outcomes and toxicity', *International Journal of Radiation Oncology* Biology* Physics*. Elsevier, 90(4), pp. 918–925.

Poon, C. *et al.* (2015) 'Self-assembled nanoscale coordination polymers carrying oxaliplatin and gemcitabine for synergistic combination therapy of pancreatic cancer', *Journal of controlled release*. Elsevier, 201, pp. 90–99.

Poplin, E. *et al.* (2006) 'Phase III trial of gemcitabine (30-minute infusion) versus gemcitabine (fixed-dose rate infusion) versus gemcitabine plus

oxaliplatin (GEMOX) in patients with advanced pancreatic cancer', *J. Clin. Oncol*, 24, p. 933.

Preston-Martin, S. (1991) 'Evaluation of the evidence that tobacco-specific nitrosamines (TSNA) cause cancer in humans', *Critical reviews in toxicology*. Taylor & Francis, 21(4), pp. 295–298.

Pushpakom, S. *et al.* (2019) 'Drug repurposing: progress, challenges and recommendations', *Nature Reviews Drug Discovery*. Nature Publishing Group, 18(1), p. 41.

Qiao, Z. *et al.* (2013) 'Chidamide, a novel histone deacetylase inhibitor, synergistically enhances gemcitabine cytotoxicity in pancreatic cancer cells', *Biochemical and Biophysical Research Communications*, 434(1), pp. 95–101. doi: 10.1016/j.bbrc.2013.03.059.

Raimondi, S. *et al.* (2010) 'Pancreatic cancer in chronic pancreatitis; Aetiology, incidence, and early detection', *Best Practice and Research: Clinical Gastroenterology*. 2010/06/01, 24(3), pp. 349–358. doi: 10.1016/j.bpg.2010.02.007.

Rampersad, S. N. (2012) 'Multiple applications of alamar blue as an indicator of metabolic function and cellular health in cell viability bioassays', *Sensors (Switzerland)*. 2012/11/01, 12(9), pp. 12347–12360. doi: 10.3390/s120912347.

Ranieri, G. *et al.* (2014) 'Pazopanib a tyrosine kinase inhibitor with strong anti-angiogenetic activity: a new treatment for metastatic soft tissue sarcoma', *Crit Rev Oncol Hematol*, 89(2), pp. 322–329. doi: 10.1016/j.critrevonc.2013.08.012.

Rao, A. D. *et al.* (2016) 'Patient-reported outcomes of a multicenter phase 2 study investigating gemcitabine and stereotactic body radiation therapy in locally advanced pancreatic cancer', *Practical radiation oncology*. Elsevier, 6(6), pp. 417–424.

Raymond, E. *et al.* (2011) 'Sunitinib Malate for the Treatment of Pancreatic Neuroendocrine Tumors', *New England Journal of Medicine*, 364(11), pp. 501–513. doi: 10.1056/NEJMoa1003825.

Reni, M. *et al.* (2005) 'Gemcitabine versus cisplatin, epirubicin, fluorouracil, and gemcitabine in advanced pancreatic cancer: a randomised controlled multicentre phase III trial', *The Lancet. Oncology*, 6(6), pp. 369–376. doi:

10.1016/S1470-2045(05)70175-3.

Rezaee, R. and Abdollahi, M. (2017) ‘The importance of translatability in drug discovery’. Taylor & Francis.

Riall, T. S. *et al.* (2005) ‘Pancreaticoduodenectomy with or without distal gastrectomy and extended retroperitoneal lymphadenectomy for periampullary adenocarcinoma--part 3: update on 5-year survival’, *Journal of Gastrointestinal Surgery*, 9(9), pp. 1191–206. doi: 10.1016/j.gassur.2005.08.034.

Rini, B. I. *et al.* (2007) ‘Hypothyroidism in patients with metastatic renal cell carcinoma treated with sunitinib’, *Journal of the National Cancer Institute*. Oxford University Press, 99(1), pp. 81–83.

Rivenson, A. *et al.* (1988) ‘Induction of lung and exocrine pancreas tumors in F344 rats by tobacco-specific and Areca-derived N-nitrosamines’, *Cancer research*. AACR, 48(23), pp. 6912–6917.

Rivera, F. *et al.* (2009) ‘Treatment of advanced pancreatic cancer: from gemcitabine single agent to combinations and targeted therapy.’, *Cancer treatment reviews*, 35(4), pp. 335–9. doi: 10.1016/j.ctrv.2008.11.007.

Roberts, N. J. *et al.* (2012) ‘ATM mutations in patients with hereditary pancreatic cancer’, *Cancer discovery*. AACR, 2(1), pp. 41–46.

Rocha Lima, C. M. *et al.* (2004) ‘Irinotecan plus gemcitabine results in no survival advantage compared with gemcitabine monotherapy in patients with locally advanced or metastatic pancreatic cancer despite increased tumor response rate’, *Journal of Clinical Oncology*. American Society of Clinical Oncology, 22(18), pp. 3776–3783.

Rockwell, S. and Grindey, G. B. (1992) ‘Effect of 2′, 2′-difluorodeoxycytidine on the viability and radiosensitivity of EMT6 cells in vitro’, *Oncology Research Featuring Preclinical and Clinical Cancer Therapeutics*. Cognizant Communication Corporation, 4(4–5), pp. 151–155.

Roeske, J. C. *et al.* (2007) ‘Characterization of the theorectical radiation dose enhancement from nanoparticles’, *Technology in Cancer Research and Treatment*, 6(5), pp. 395–401. doi: 10.1177/153303460700600504.

Rosati, L. M. *et al.* (2018) ‘Novel Radiotherapy Modalities’, in *Current and Emerging Therapies in Pancreatic Cancer*. Springer, pp. 323–348.

Saiki, Y. and Horii, A. (2014) ‘Molecular pathology of pancreatic cancer’, *Pathology International*. John Wiley & Sons, Ltd (10.1111), 64(1), pp. 10–19. doi: 10.1111/pin.12114.

Sainato, A. *et al.* (2015) ‘Safety and effectiveness of the combination of single chemotherapeutic agent (gemcitabine) with radiotherapy in radically resected pancreatic adenocarcinoma’, *European Journal of Cancer*, 51, pp. S418–S418. doi: 10.1016/s0959-8049(16)31171-6.

Saito, Y. *et al.* (2012) ‘Sunitinib induces apoptosis in pheochromocytoma tumor cells by inhibiting VEGFR2/Akt/mTOR/S6K1 pathways through modulation of Bcl-2 and BAD’, *American Journal of Physiology-Endocrinology and Metabolism*. American Physiological Society Bethesda, MD, 302(6), pp. E615–E625.

Sakorafas, G. H., Tsiotou, A. G. and Tsiotos, G. G. (2000) ‘Molecular biology of pancreatic cancer; oncogenes, tumour suppressor genes, growth factors, and their receptors from a clinical perspective’, *Cancer Treat Rev*, 26(1), pp. 29–52. doi: 10.1053/ctrv.1999.0144.

Sancar, A. *et al.* (2004) ‘Molecular mechanisms of mammalian DNA repair and the DNA damage checkpoints’, *Annual review of biochemistry*. Annual Reviews 4139 El Camino Way, PO Box 10139, Palo Alto, CA 94303-0139, USA, 73(1), pp. 39–85.

Sarkar, F. H., Banerjee, S. and Li, Y. (2007) ‘Pancreatic cancer: pathogenesis, prevention and treatment’, *Toxicology and applied pharmacology*. Elsevier, 224(3), pp. 326–336.

Sawai, H. *et al.* (2005) ‘The G691S RET polymorphism increases glial cell line–derived neurotrophic factor–induced pancreatic cancer cell invasion by amplifying mitogen-activated protein kinase signaling’, *Cancer research*. AACR, 65(24), pp. 11536–11544.

Scaltriti, M. and Baselga, J. (2006) ‘The epidermal growth factor receptor pathway: a model for targeted therapy’, *Clinical Cancer Research*. AACR, 12(18), pp. 5268–5272.

Scheidegger, S. *et al.* (2013) ‘Using state variables to model the response of tumour cells to radiation and heat: a novel multi-hit-repair approach’, *Computational and mathematical methods in medicine*. Hindawi, 2013.

Schellenberg, D. *et al.* (2008) ‘Gemcitabine chemotherapy and single-fraction

stereotactic body radiotherapy for locally advanced pancreatic cancer', *International Journal of Radiation Oncology* Biology* Physics*. Elsevier, 72(3), pp. 678–686.

Schellenberg, D. *et al.* (2011) 'Single-fraction stereotactic body radiation therapy and sequential gemcitabine for the treatment of locally advanced pancreatic cancer', *International Journal of Radiation Oncology* Biology* Physics*. Elsevier, 81(1), pp. 181–188.

Schenk, M. *et al.* (2001) 'Familial risk of pancreatic cancer', *Journal of the National Cancer Institute*. Oxford University Press, 93(8), pp. 640–644.

Sclafani, F. *et al.* (2015) 'Management of metastatic pancreatic cancer: Current treatment options and potential new therapeutic targets', *Crit Rev Oncol Hematol*, 95(3), pp. 318–36. doi: http://dx.doi.org/10.1016/j.critrevonc.2015.03.008.

Seeger, R. C. *et al.* (1985) 'Association of multiple copies of the N-myc oncogene with rapid progression of neuroblastomas', *New England Journal of Medicine*. Mass Medical Soc, 313(18), pp. 1111–1116.

Seiler, C. A. *et al.* (2005) 'Randomized clinical trial of pylorus-preserving duodenopancreatectomy versus classical Whipple resection—long term results', *British Journal of Surgery: Incorporating European Journal of Surgery and Swiss Surgery*. Wiley Online Library, 92(5), pp. 547–556.

Sellam, F. *et al.* (2015) 'Delayed diagnosis of pancreatic cancer reported as more common in a population of North African young adults', *Journal of gastrointestinal oncology*. AME Publishing Company, 6(5), pp. 505–510. doi: 10.3978/j.issn.2078-6891.2015.051.

Shaib, W. L. and El-Rayes, B. F. (2018) 'Molecularly Targeted Therapies in Pancreatic Cancer BT', in Bekaii-Saab, T. and El-Rayes, B. (eds) *Current and Emerging Therapies in Pancreatic Cancer*. Cham: Springer International Publishing, pp. 219–233. doi: 10.1007/978-3-319-58256-6_12.

Sharma, N. K. *et al.* (2015) 'Evaluation of low-dose fractionated radiation therapy as a chemopotentiator of gemcitabine in advanced pancreatic cancer: results from an international multi-institutional phase II trial', *Journal of Radiation Oncology*, 4(4), pp. 401–409. doi: 10.1007/s13566-015-0213-8.

Shen, Z. T. *et al.* (2015) 'Effects of gemcitabine on radiosensitization, apoptosis, and Bcl-2 and Bax protein expression in human pancreatic cancer

xenografts in nude mice', *Genetics and Molecular Research*, 14(4), pp. 15587–15596. doi: 10.4238/2015.December.1.10.

Shewach, D. S. *et al.* (1994) 'Metabolism of 2′, 2′-difluoro-2′-deoxycytidine and radiation sensitization of human colon carcinoma cells', *Cancer research*. AACR, 54(12), pp. 3218–3223.

Shi, C., Hruban, R. H. and Klein, A. P. (2009) 'Familial pancreatic cancer', *Archives of pathology & laboratory medicine*, 133(3), pp. 365–374.

Shi, Y. *et al.* (2016) 'Inhibitory effect of metformin combined with gemcitabine on pancreatic cancer cells in vitro and in vivo', *Molecular Medicine Reports*, 14(4), pp. 2921–2928. doi: 10.3892/mmr.2016.5592.

Shi, Y. and Massagué, J. (2003) 'Mechanisms of TGF-β signaling from cell membrane to the nucleus', *cell*. Elsevier, 113(6), pp. 685–700.

Shi, Z. *et al.* (2001) 'S-Phase arrest by nucleoside analogues and abrogation of survival without cell cycle progression by 7-hydroxystaurosporine', *Cancer Research*. AACR, 61(3), pp. 1065–1072.

Shukla, S. *et al.* (2009) 'Sunitinib (Sutent, SU11248), a small-molecule receptor tyrosine kinase inhibitor, blocks function of the ATP-binding cassette (ABC) transporters P-glycoprotein (ABCB1) and ABCG2', *Drug Metabolism and Disposition*, 37(2), pp. 359–365. doi: 10.1124/dmd.108.024612.

Siegel, R. L., Miller, K. D. and Jemal, A. (2016) 'Cancer statistics, 2016', *CA: A Cancer Journal for Clinicians*, 66(1), pp. 7–30. doi: 10.3322/caac.21332.

Siegel, R. L., Miller, K. D. and Jemal, A. (2018) 'Cancer statistics, 2018.', *CA: a cancer journal for clinicians*, 68(1), pp. 7–30. doi: 10.3322/caac.21442.

Slack, J. M. (1995) 'Developmental biology of the pancreas', *Development*, 121(6), pp. 1569 LP – 1580. Available at: http://dev.biologists.org/content/121/6/1569.abstract.

Slater, E. P. *et al.* (2010) 'PALB2 mutations in European familial pancreatic cancer families', *Clinical genetics*. Wiley Online Library, 78(5), pp. 490–494.

De Snoo, F. A. *et al.* (2008) 'Increased risk of cancer other than melanoma in CDKN2A founder mutation (p16-Leiden)-positive melanoma families', *Clinical Cancer Research*. AACR, 14(21), pp. 7151–7157.

Sohn, T. A. *et al.* (2000) 'Resected adenocarcinoma of the pancreas—616 patients: results, outcomes, and prognostic indicators', *Journal of gastrointestinal surgery*. Elsevier, 4(6), pp. 567–579.

Solorzano, C. C. *et al.* (2003) 'Administration of optimal biological dose and schedule of interferon ?? combined with gemcitabine induces apoptosis in tumor-associated endothelial cells and reduces growth of human pancreatic carcinoma implanted orthotopically in nude mice', *Clinical Cancer Research*, 9(5), pp. 1858–1867. Available at: http://clincancerres.aacrjournals.org/content/clincanres/9/5/1858.full.pdf.

Sonpavde, G. and Hutson, T. E. (2007) 'Pazopanib: A novel multitargeted tyrosine kinase inhibitor', *Current Oncology Reports*, 9(2), pp. 115–119. doi: 10.1007/s11912-007-0007-2.

Sorensen, A. *et al.* (2012) 'In Vivo Evaluation of a Cancer Therapy Strategy Combining HSV1716-Mediated Oncolysis with Gene Transfer and Targeted Radiotherapy', *Journal of Nuclear Medicine*, 53(4), pp. 647–654. doi: 10.2967/jnumed.111.090886.

Sorokin, M. *et al.* (2018) 'Acquired resistance to tyrosine kinase inhibitors may be linked with the decreased sensitivity to X-ray irradiation', *Oncotarget*, 9(4). doi: 10.18632/oncotarget.23700.

Sperti, C. *et al.* (1996) 'Survival after resection for ductal adenocarcinoma of the pancreas', *British Journal of Surgery*. Wiley Online Library, 83(5), pp. 625–631.

Spratlin, J. *et al.* (2004) 'The absence of human equilibrative nucleoside transporter 1 is associated with reduced survival in patients with gemcitabine-treated pancreas adenocarcinoma', *Clinical Cancer Research*. AACR, 10(20), pp. 6956–6961.

Sternberg, C. N. *et al.* (2013) 'A randomised, double-blind phase III study of pazopanib in patients with advanced and/or metastatic renal cell carcinoma: Final overall survival results and safety update', *European Journal of Cancer*, 49(6), pp. 1287–1296. doi: 10.1016/j.ejca.2012.12.010.

Stocks, T. *et al.* (2009) 'Blood glucose and risk of incident and fatal cancer in the metabolic syndrome and cancer project (Me-Can): Analysis of six prospective cohorts', *PLoS Medicine*, 6(12), p. e1000201. doi: 10.1371/journal.pmed.1000201.

Strittmatter, S. M. (2014) ‘Overcoming drug development bottlenecks with repurposing: old drugs learn new tricks’, *Nature medicine*. Cellular Neuroscience, Neurodegeneration and Repair Program, Departments of Neurology and Neurobiology, Yale University School of Medicine, New Haven, Connecticut, USA.: Nature Publishing Group, 20(6), pp. 590–591. doi: http://dx.doi.org/10.1038/nm.3595.

Sultana, A. *et al.* (2007) ‘Meta-analyses of chemotherapy for locally advanced and metastatic pancreatic cancer’, *Journal of Clinical Oncology*, 25(18), pp. 2607–2615. doi: 10.1200/jco.2006.09.2551.

Sun, J. *et al.* (2012) ‘The multi-targeted kinase inhibitor Sunitinib induces apoptosis in colon cancer cells via PUMA’, *Cancer Research*, 72(8 Supplement), pp. 860–860. doi: 10.1158/1538-7445.AM2012-860.

Sun, M. *et al.* (2014) ‘Re: Pazopanib versus sunitinib in metastatic renal-cell carcinoma’, *European Urology*, 65(5), pp. 1014–1015. doi: 10.1016/j.eururo.2013.12.042.

Taeger, J. *et al.* (2011) ‘Targeting FGFR/PDGFR/VEGFR Impairs Tumor Growth, Angiogenesis, and Metastasis by Effects on Tumor Cells, Endothelial Cells, and Pericytes in Pancreatic Cancer’, *Molecular Cancer Therapeutics*, 10(11), pp. 2157–2167. doi: 10.1158/1535-7163.MCT-11-0312.

Tamm, E. P. *et al.* (2003) ‘Diagnosis, staging, and surveillance of pancreatic cancer’, *American Journal of Roentgenology*. American Roentgen Ray Society, 180(5), pp. 1311–1323. doi: 10.2214/ajr.180.5.1801311.

Targeted Molecular Therapy – Abramson Cancer Center (no date). Available at: https://www.pennmedicine.org/cancer/navigating-cancer-care/treatment-types/targeted-therapy (Accessed: 21 July 2019).

Teng, C. L. J. *et al.* (2013) ‘Effector mechanisms of sunitinib-induced G1 cell cycle arrest, differentiation, and apoptosis in human acute myeloid leukaemia HL60 and KG-1 cells’, *Annals of Hematology*, 92(3), pp. 301–313. doi: 10.1007/s00277-012-1627-7.

Thoennissen, N. H. *et al.* (2009) ‘Cucurbitacin B induces apoptosis by inhibition of the JAK/STAT pathway and potentiates antiproliferative effects of gemcitabine on pancreatic cancer cells’, *Cancer Research*, 69(14), pp. 5876–5884. doi: 10.1158/0008-5472.CAN-09-0536.

Thottassery, J. V. (2006) ‘c-Abl-independent p73 stabilization during

gemcitabine- or 4'-thio- -D-arabinofuranosylcytosine-induced apoptosis in wild-type and p53-null colorectal cancer cells', *Molecular Cancer Therapeutics*, 5(2), pp. 400–410. doi: 10.1158/1535-7163.MCT-05-0409.

Tonato, M., Mosconi, A. M. and Martin, C. (1995) 'Safety profile of gemcitabine.', *Anti-Cancer Drugs*, 6, pp. 27–32.

Tran Cao, H. S. *et al.* (2010) 'Metronomic Gemcitabine in Combination with Sunitinib Inhibits Multisite Metastasis and Increases Survival in an Orthotopic Model of Pancreatic Cancer', *Molecular Cancer Therapeutics*, 9(7), pp. 2068–2078. doi: 10.1158/1535-7163.MCT-10-0201.

Tran, K. T. C. *et al.* (2004) 'Pylorus preserving pancreaticoduodenectomy versus standard Whipple procedure: a prospective, randomized, multicenter analysis of 170 patients with pancreatic and periampullary tumors', *Annals of surgery*. Lippincott, Williams, and Wilkins, 240(5), p. 738.

Tribius, S. and Bergelt, C. (2011) 'Intensity-modulated radiotherapy versus conventional and 3D conformal radiotherapy in patients with head and neck cancer: is there a worthwhile quality of life gain?', *Cancer treatment reviews*. Elsevier, 37(7), pp. 511–519.

Tuli, R. *et al.* (2012) 'Development of a novel preclinical pancreatic cancer research model: bioluminescence image-guided focal irradiation and tumor monitoring of orthotopic xenografts', *Translational oncology*. 2012/04/01. Neoplasia Press Inc., 5(2), pp. 77–84. doi: 10.1593/tlo.11316.

UK, P. C. and Pancreatic Cancer UK (2016) 'Nab-paclitaxel (Abraxane®)', 2016`(10 October 2016). Available at: http://www.pancreaticcancer.org.uk/abraxane.

Veldeman, L. *et al.* (2008) 'Evidence behind use of intensity-modulated radiotherapy: a systematic review of comparative clinical studies', *The lancet oncology*. Elsevier, 9(4), pp. 367–375.

Vermes, I. *et al.* (1995) 'A novel assay for apoptosis flow cytometric detection of phosphatidylserine expression on early apoptotic cells using fluorescein labelled annexin V', *Journal of immunological methods*. Elsevier, 184(1), pp. 39–51.

Vogelstein, B. and Kinzler, K. (2004) 'Cancer genes and the pathways they control', *Nature Medicine*, 10(8), pp. 789–799. doi: 10.1038/nm1087.

Vogelstein, B., Lane, D. and Levine, A. J. (2000) 'Surfing the p53 network', *Nature*. Nature Publishing Group, 408(6810), p. 307.

Waddell, N. *et al.* (2015) 'Whole genomes redefine the mutational landscape of pancreatic cancer', *Nature*. Nature Publishing Group, 518(7540), p. 495.

Wahi, M. M. *et al.* (2009) 'Reproductive factors and risk of pancreatic cancer in women: a review of the literature', *Annals of epidemiology*. Elsevier, 19(2), pp. 103–111.

Wang, J., Wang, H. and Qian, H. (2018) 'Biological effects of radiation on cancer cells', *Military Medical Research*. BioMed Central, 5(1), p. 20.

Wang, S.-L. *et al.* (2018) 'Identification of unique microRNAs associated with pancreatic cancer radioresistance using deep sequencing', *Translational Cancer Research; Vol 7, No 4 (August 2018): Translational Cancer Research*.

Wang, S. J. *et al.* (2010) 'Dihydroartemisinin inactivates NF-κB and potentiates the anti-tumor effect of gemcitabine on pancreatic cancer both in vitro and in vivo', *Cancer Letters*, 293(1), pp. 99–108. doi: 10.1016/j.canlet.2010.01.001.

Wang, Y.-T. *et al.* (2016) 'Association between alcohol intake and the risk of pancreatic cancer: a dose–response meta-analysis of cohort studies', *BMC Cancer*. London: BioMed Central, 16(1), p. 212. doi: 10.1186/s12885-016-2241-1.

Wang, Y. *et al.* (2015) 'The Histone Deacetylase Inhibitor Valproic Acid Sensitizes Gemcitabine-Induced Cytotoxicity in Gemcitabine-Resistant Pancreatic Cancer Cells Possibly Through Inhibition of the DNA Repair Protein Gamma-H2AX', *Targeted Oncology*, 10(4), pp. 575–581. doi: 10.1007/s11523-015-0370-0.

Whipple, A. O. (1942) 'Present-day surgery of the pancreas', *New England Journal of Medicine*. Mass Medical Soc, 226(13), pp. 515–526.

Whitcomb, D. C. *et al.* (1996) 'Hereditary pancreatitis is caused by a mutation in the cationic trypsinogen gene', *Nature genetics*. Nature Publishing Group, 14(2), p. 141.

Wiedmer, T. *et al.* (2017) 'Autophagy inhibition improves sunitinib efficacy in pancreatic neuroendocrine tumors via a lysosome-dependent mechanism', *Molecular cancer therapeutics*. AACR, 16(11), pp. 2502–2515.

Witkiewicz, A. K. *et al.* (2015) 'Whole-exome sequencing of pancreatic cancer defines genetic diversity and therapeutic targets', *Nature communications*. Nature Publishing Group, 6, p. 6744.

Wolpin, B. M. *et al.* (2009) 'Oral mTOR inhibitor everolimus in patients with gemcitabine-refractory metastatic pancreatic cancer', *Journal of Clinical Oncology*, 27(2), pp. 193–198. doi: 10.1200/JCO.2008.18.9514.

Wood, L. D., Adsay, N. V. and Hruban, R. H. (2013) 'Molecular Pathology of Pancreatic Cancer BT - Molecular Surgical Pathology', in Cheng, L. and Eble, J. N. (eds) *Pathology and Epidemiology of Cancer*. New York, NY: Springer New York, pp. 17–42. doi: 10.1007/978-1-4614-4900-3_2.

World Health Organisation (2016) *Cancer*. Available at: http://www.who.int/cancer/en/.

World Health Organization, W. (2014) *World Cancer Report*. Edited by S. BW and W. CW. International Agency for Research on Cancer. doi: 10.1017/S0020860400079146.

Xia, B. T., Kim, Y. and Ahmad, S. A. (2018) 'The Management of Locally Advanced Nonmetastatic Pancreas Cancer', in *Current and Emerging Therapies in Pancreatic Cancer*. Springer, pp. 183–204.

Xie, C. and Plunkett, W. (1995) 'Metabolism and actions of 2-chloro-9-(2-deoxy-2-fluoro-β-D-arabinofuranosyl)-adenine in human lymphoblastoid cells', *Cancer research*. AACR, 55(13), pp. 2847–2852.

Xu, J. *et al.* (2014) 'PIM kinases: an overview in tumors and recent advances in pancreatic cancer', *Future Oncology*. Future Medicine, 10(5), pp. 865–876.

Yang, F. *et al.* (2010) 'Sunitinib induces apoptosis and growth arrest of medulloblastoma tumor cells by inhibiting STAT3 and AKT signaling pathways', *Molecular Cancer Research*. AACR, 8(1), pp. 35–45.

Yasuda, A. *et al.* (2006) 'The stem cell factor/c-kit receptor pathway enhances proliferation and invasion of pancreatic cancer cells', *Molecular Cancer*, 5(February). doi: 10.1186/1476-4598-5-46.

Yee, K. W. H. *et al.* (2004) 'Synergistic effect of SU11248 with cytarabine or daunorubicin on FLT3 ITD–positive leukemic cells', *Blood*. Am Soc Hematology, 104(13), pp. 4202–4209.

Yellu, M., Kamireddy, C. and Olowokure, O. O. (2018) 'Pancreatic Cancer Epidemiology and Environmental Risk Factors', in *Current and Emerging Therapies in Pancreatic Cancer*. Springer, pp. 1–22.

Yeo, C. J. *et al.* (1997) 'Six hundred fifty consecutive pancreaticoduodenectomies in the 1990s: pathology, complications, and outcomes.', *Annals of surgery*. Lippincott, Williams, and Wilkins, 226(3), p. 248.

Yeo, C. J. *et al.* (2002) 'Pancreaticoduodenectomy with or without distal gastrectomy and extended retroperitoneal lymphadenectomy for periampullary adenocarcinoma, part 2: Randomized controlled trial evaluating survival, morbidity, and mortality', in *Annals of Surgery*. doi: 10.1097/00000658-200209000-00012.

Yokoi, K. *et al.* (2005) 'Simultaneous inhibition of EGFR, VEGFR, and platelet-derived growth factor receptor signaling combined with gemcitabine produces therapy of human pancreatic carcinoma and prolongs survival in an orthotopic nude mouse model', *Cancer research*. AACR, 65(22), pp. 10371–10380.

Yokoi, K. and Fidler, I. J. (2004) 'Hypoxia Increases Resistance of Human Pancreatic Cancer Cells to Apoptosis Induced by Gemcitabine', *Clinical Cancer Research*, 10(7), pp. 2299–2306. doi: 10.1158/1078-0432.CCR-03-0488.

Yong, K. J. *et al.* (2013) 'Sensitization of tumor to 212Pb radioimmunotherapy by gemcitabine involves initial abrogation of G2 arrest and blocked DNA damage repair by interference with Rad51', *International Journal of Radiation Oncology Biology Physics*, 85(4), pp. 1119–1126. doi: 10.1016/j.ijrobp.2012.09.015.

Yoon, C. Y. *et al.* (2011) 'Sunitinib malate synergistically potentiates anti-tumor effect of gemcitabine in human bladder cancer cells', *Korean Journal of Urology*, 52(1), pp. 55–63. doi: 10.4111/kju.2011.52.1.55.

Yunis, A. A., Arimura, G. K. and Russin, D. J. (1977) 'Human pancreatic carcinoma (mia paca-2) in continuous culture: Sensitivity to asparaginase', *International Journal of Cancer*. United States, 19(1), pp. 128–135. doi: 10.1002/ijc.2910190118.

Zhan, H. *et al.* (2015) 'Pancreatic cancer stem cells: new insight into a stubborn disease', *Cancer letters*. Elsevier, 357(2), pp. 429–437.

Zhang, H.-P. *et al.* (2010) ‘Effect of sunitinib combined with ionizing radiation on endothelial cells’, *Journal of radiation research*. Journal of Radiation Research Editorial Committee, p. 1012210178.

Zheng, X. *et al.* (2012) ‘Effects of 12-O-tetradecanoylphorbol-13-acetate in combination with gemcitabine on Panc-1 pancreatic cancer cells cultured in vitro or Panc-1 tumors grown in immunodeficient mice’, *International Journal of Oncology*, 41(6), pp. 2269–2275. doi: 10.3892/ijo.2012.1651.

Zhi, X. *et al.* (2015) ‘OSI-027 inhibits pancreatic ductal adenocarcinoma cell proliferation and enhances the therapeutic effect of gemcitabine both <i>in vitro</i> and <i>in vivo</i>’, *Oncotarget*, 6(28), pp. 26230–26241. doi: 10.18632/oncotarget.4579.

Zhou, J. and Du, Y. (2012) ‘Acquisition of resistance of pancreatic cancer cells to 2-methoxyestradiol is associated with the upregulation of manganese superoxide dismutase’, *Molecular cancer research : MCR*. 2012/04/30, 10(6), pp. 768–777. doi: 10.1158/1541-7786.MCR-11-0378.

Ziske, C. *et al.* (2004) ‘Retroviral IFN-α Gene Transfer Combined with Gemcitabine Acts Synergistically via Cell Cycle Alteration in Human Pancreatic Carcinoma Cells Implanted Orthotopically in Nude Mice’, *Journal of Interferon & Cytokine Research*, 24(8), pp. 490–496. doi: 10.1089/1079990041689647.